STUDIES IN THE MODELLING AND SIMULATION OF THE HUMAN CARDIOVASCULAR SYSTEM WITH APPLICATION TO THE EFFECTS OF DRUGS

by

HENRY EDWARD PULLEN

A thesis submitted for the
degree of Doctor of Philosophy
at The City University

Department of Systems Science
The City University

March 1976

CONTENTS

LIST OF TABLES

LIST OF ILLUSTRATIONS

ACKNOWLEDGEMENTS

I am very grateful to my principal supervisor, Professor L. Finkelstein (Department of Systems Science, The City University), for his considerable help and guidance throughout the project.

I also wish to thank the following individuals :

Dr. D. [redacted] (Royal College of Surgeons of England) for originally suggesting the specific project and for his helpful advice and constant interest throughout.

Prof. [redacted] (Charing Cross Hospital Medical School) for initially interesting the Department of Systems Science in circulatory problems.

Dr. R. [redacted] (The Wellcome Research Laboratories) for supplying me with much useful information on drug effects.

Prof. [redacted] (University of California) for very helpful discussions on cardiovascular dynamics.

Dr. M. [redacted] (Charing Cross Hospital Medical School) for his helpful comments and provision of a great deal of information.

Finally, thanks are due to The City University for providing me with a Research Studentship for one year of the work.

ABSTRACT

A pulsatile mathematical model of the human cardiovascular system suitable for the study of short-term haemodynamics was developed. The circulatory fluid mechanics section of this model was based on lumped parameter approximations with linear arterial segments, nonlinear venous segments and time-varying compliance pumping in the four heart chambers. Neural control was added in the form of a mathematical description of the aortic arch and carotid sinus baroreceptors and central nervous regulation of heart rate, peripheral resistance, myocardial contractility and venous tone. The model was intended for the study of haemodynamics following the injection of a cardiovascular agent so a mathematical description of the injection, transport, action and breakdown of a single drug was included making the overall model of order 61.

The model was implemented as a digital computer simulation and reasons for the choice of simulation technique, programming language and numerical method were presented. Attention was given to techniques for computing a steady state solution and also the treatment of constrained state variables, differentiation and algebraic loops.

The digital simulation was validated by comparison with data from humans and comparable animals. Essential features of significant variables were checked and the model was subjected to tests such as orthostasis, blood volume changes, the Valsalva manoeuvre and cardiac pacing. In these respects the model performed realistically. In the pacing tests, the cardiac output changed very little and so a remarkably close linear relationship between stroke volume and heart period was found. The beat-by-beat estimation of total peripheral resistance from mean arterial pressure and cardiac output was found to be unreliable during rapid transients.

When injections of methoxamine, isoprenaline and noradrenaline were simulated, realistic responses were obtained. In the case of noradrenaline, venoconstriction had to be included to obtain the bradycardia observed in practice. It was concluded that the model had an explanatory usefulness and potential as a cardiovascular agent design aid in pharmacology.

LIST OF PRINCIPAL SYMBOLS USED

a	elastance (reciprocal compliance)
A	cross-sectional area
b	variable associated with myocardial contractility control
B	baroreceptor output
C	compliance
d	variable associated with venous tone control
f	frequency
F	flow
g	acceleration due to gravity
G	hydrostatic pressure difference
h	integration step length
k	constant
ℓ	length
L	inertance
m	mass
M	injected mass
n	number of g's of acceleration
P	pressure
q	variable associated with peripheral resistance control
r	radial coordinate
R	resistance
t	time
T	duration or period
u	variable associated with heart rate control
v	velocity
V	volume

ω	concentration
x	variable associated with time-varying compliance generation
y	variable associated with respiration
z	longitudinal coordinate
α	constant
θ	angular coordinate
μ	kinematic viscosity
ϱ	density
σ	variable associated with drug effects
τ	time constant
ϕ	angle between the axis of a segment and a perpendicular to the direction of gravitational force
$\mathcal{L}$	Laplace transform

LIST OF PRINCIPAL SUBSCRIPTS USED

Compartmental subscripts (after Beneken & Dewit, 1967) :-

AA	Abdominal arteries	LA	Left atrium
AO1	Ascending aorta	LV	Left ventricle
AO2	Aortic arch	PA	Pulmonary arteries
AO3	Thoracic aorta	PV	Pulmonary veins
AV	Abdominal veins	RA	Right atrium
CA	Leg arteries	RV	Right ventricle
CV	Leg veins	SVC	Superior vena cava
IA	Intestinal arteries	UA	Head and arm arteries
IV	Intestinal veins	UV	Head and arm veins
IVC	Inferior vena cava		

Other subscripts :-

ABD	Abdomen	LEG	Legs
BRONC	Bronchial	LUNG	Lungs
CC	Critical closure	MAX	Maximum
COR	Coronary	MIN	Minimum
D	Diastolic	N	Normal
H	Heart	R	Respiratory
HEAD	Head and arms	S	Systolic
IE	Inhalation-exhalation	TH	Thorax
INT	Intestinal	T	Total
		U	Unstressed

CHAPTER 1
INTRODUCTION

1.1 Organisation of the thesis

This thesis is concerned with the modelling and simulation of the human cardiovascular system with application to the effects of cardiovascular agents.

In chapter 1, the objectives of cardiovascular modelling and simulation are given and the subject is briefly reviewed. The remaining chapters progress in a logical manner.

In chapters 2 to 4, the system to be simulated is analysed and mathematical models are produced. Chapter 2 describes the formulation of a lumped parameter model of the uncontrolled circulatory system. The modelling of central nervous control mechanisms is described in chapter 3. For the complete model to be of use in the study of drug effects, the modelling of the injection, transport and local actions of a particular drug must be included. This is presented in chapter 4.

Having constructed the complete mathematical model, the equations have to be solved by computer. The techniques and problems of digital computer solution are described in chapter 5. When it is verified that the digital implementation provides an acceptably accurate numerical solution of the mathematical model, it is necessary to investigate the validity of the model. The digital simulation is subjected to a variety of tests and results from the simulation are compared with results in the literature obtained from equivalent physiological experiments. This validation process is presented in chapter 6.

The suitably validated model can be used to predict the overall action of a drug from the combined local effects of the drug and this application is described for 3 different drugs in chapter 7.

Various suggestions for future work are presented in chapter 8 and the main conclusions are given in chapter 9.

The appendices include the complete set of equations of the mathematical model and also the complete FORTRAN simulation program listing.

Assumptions and approximations are stated in each chapter as the

sections of the model are developed. The tables and figures associated with the chapters are presented at the end of the respective chapters.

A knowledge of elementary cardiovascular physiology is assumed in this work - an introduction to the required physiology is given by Green (1972).

1.2 General objectives of cardiovascular modelling

The cardiovascular system is the main transport system of the body. Nutrients are transported to the tissues, waste products are transported from the tissues and also various substances are transported from organ to organ by the bloodstream. Neural and humoral control mechanisms enable the system to adapt to a changing environment.

Mathematical modelling and computer simulation of the cardiovascular system and its controls has the following objectives :

(1) A clearer picture of the system is provided which improves knowledge, insight and understanding.

(2) Observed relationships between system variables are described in a compact, precise, quantitative way. Idealisations, assumptions, approximations and omissions are clearly recorded in symbolic form. In these respects, mathematical models are superior to purely conceptual or mental models of the cardiovascular system.

(3) The formal approach of mathematical modelling may assist the cardiovascular researcher by revealing areas of uncertainty or weak knowledge and useful experiments may be suggested.

(4) An appropriate computer simulation can function as a general purpose "test bed" and can be subjected to conditions that would be difficult or dangerous to attempt in the human. All variables are directly accessible and the effect of any parameter change can be studied with ease.

(5) A compact, high speed computer simulation that can function faster than "real time" would be useful for estimation, prediction and control applications in a clinical or surgical environment.

(6) Hypotheses (e.g. concerning the structure of a subsystem) which are expressible in mathematical form can be tested in the computer simulation.

(7) From the standpoint of control theory and systems science, the

study of the cardiovascular control mechanisms may lead to improved methods of structuring and organising complex multivariable nonlinear control systems in engineering and other applications.

(8) A useful exchange of ideas and technology can occur between workers in the biological and non-biological fields.

(9) A range of interesting and challenging problems arise in the areas of computer science, numerical analysis and mathematics in this type of modelling and simulation exercise.

(10) Computer simulations of the human cardiovascular system can be of educational value to students of biomedical engineering and medicine.

Naturally, it is important to keep in mind the approximations mentioned in item (2) and to realise that the model is only valid for the physiological conditions for which it was originally constructed and validated. Any extrapolations or predictions made using the model have to be interpreted with necessary caution.

1.3 Specific objectives in the work described

The central objective of the work was to produce a pulsatile mathematical model and computer simulation of the controlled cardiovascular system of a normal, resting, conscious, average human suitable for the study of short-term haemodynamics. The longer term mechanisms were therefore excluded (e.g. capillary fluid shifts, stress relaxation, baroreceptor adaptation, etc.).

The aim was to make the model sufficiently detailed and comprehensive for the study of short-term pharmacokinetics (i.e. drug effects with the major dynamics complete within 2 or 3 minutes) and to use the model to study the overall effects of an injected drug assuming a number of simultaneous actions of the circulating drug at specific sites.

The construction of a comprehensive model implies a large set of algebraic and differential equations which leads to the problem of excessive digital computer time or excessive analog computer equipment. The model therefore had to be of manageable size and was required to take into account the accessibility, turnaround time and processing speed of available computers. The simplest models of subsystems

that were adequate for the purpose had to be used and fine detail was to be included only where it was essential for realistic dynamics.

1.4 Techniques that have been used to model and simulate the cardiovascular system

The flow of blood through tapered, branching, elastic vessels may be described accurately by very large sets of nonlinear, time-varying, partial differential equations. These equations are virtually impossible to deal with analytically and may be very difficult to handle by other techniques. Simplifications therefore are frequently made so that an analytical or computational solution is possible.

Fluid mechanical modelling is usually based on cause-effect considerations and the laws of hydrodynamics are applied. In the case of central nervous control mechanisms, the complex systems involved are not amenable to analysis based on physical laws and so empirical, phenomenological or black-box models are developed which have approximately correct input-output relations. Static or dynamic empirical models are normally designed to fit available data in the most compact mathematical form and do not usually reflect the true internal structure and cause-effect relationships within the system. Predictions made using such models have to be interpreted therefore with caution.

The numerical values of constants in models based on physical laws can be calculated directly from the results of experiments performed on animals and humans. Constants in the empirical models are normally obtained by adjustment of the model parameters to achieve a best fit of the equations to data from physiological experiments using an appropriate performance criterion (e.g. least squares).

1.4.1 Types of circulatory fluid mechanics model

Cardiovascular models may be classified broadly as either lumped parameter or distributed parameter.

In the lumped parameter approach, the system is modelled as a collection of linked segments, each segment functioning effectively as an elastic reservoir (windkessel). In each segment, the properties of a length of blood vessel or collection of blood vessels are concentrated at a point and infinite wave velocity within the segment

is assumed. These models are characterised by ordinary differential equations relating pressures, flows and volumes in the lumped parameter segments. Such models are used mainly in studies of the overall cardiovascular system when fine detail of wave propagation in individual blood vessels is not required.

In the distributed parameter approach, the continuous spatial variation of the properties of blood vessels and the finite wave velocity are taken into account. This type of model consists of partial differential equations describing the variation of pressure and flow in space and time and is used typically in studies of transmission phenomena in arteries.

Lumped parameter modelling is clearly far more approximate than distributed parameter modelling but as the number of windkessels is increased and each segment is made smaller the accuracy of the lumped parameter results approaches that of the distributed parameter results.

1.4.2 Simulation techniques employed

Circulatory models have been implemented in a variety of forms :

(1) Hydraulic models - These employ liquid-filled flexible tubes and are rarely used due to problems of construction and the difficulties of making changes.

(2) Graphical solutions - These are applicable only in fairly simple cases.

(3) Analytical solutions - Usually it is only linear or linearised models that can be solved directly because there are no mathematical tools available for the general solution of nonlinear ordinary or partial differential equations at present. A computational solution may be preferable for high order linear models because of the labour involved in an analytical solution.

(4) Electrical network analogs - The analogy between pressure and voltage and between flow and current enables electrical analogs of large lumped parameter systems to be constructed cheaply. However these analogs are inflexible and are required to operate on a greatly compressed time-scale to avoid very large inductance and capacitance values.

(5) Computer simulations - Analog, hybrid and digital computers provide the greatest operational convenience and have been used extensively in cardiovascular simulation. The analog computer is

a truly parallel processor and gives a real-time or faster-than-real-time solution of large dynamic models with acceptable accuracy for biological work. The conventional digital computer, while much slower than the analog computer for large models, does have considerable advantages in terms of documentation, debugging, information storage and general flexibility. The digital computer can also handle complex nonlinearities and solve extremely large models which would otherwise require enormous quantities of analog computer equipment. The hybrid computer combines some of the advantages of the two types of machine and has been used frequently in cardiovascular work with, for example, fast dynamics simulated in the analog machine and slow dynamics in the digital machine.

The mathematical model described in this report is implemented as a digital computer simulation primarily because of the size of the model and the limited analog equipment available.

1.5 A consideration of some detailed computer simulations of the cardiovascular system

Numerous attempts have been made to model the cardiovascular system in part and in whole. Noordergraaf (1969), Beneken (1972) and Talbot & Gessner (1973) have given reviews of some of the models that have been used.

As the author has already reviewed the literature on cardiovascular modelling and simulation elsewhere (Pullen, 1970), a comprehensive literature survey is not given here. Instead, three specific examples are used to illustrate the principal approaches employed in recent high order computer simulations of the human cardiovascular system and the applicability of these approaches in the present work is evaluated.

The degree of detail in the examples given can be judged to some extent by the order of the mathematical system i.e. the number of first order differential equations required when the model is expressed in state space form or equivalently the number of integrators required in an analog computer implementation.

1.5.1 Beneken & Dewit (1967)

This model consists of a pulsatile mathematical description of the controlled human circulatory system suitable for the study of short-term haemodynamics. A lumped parameter approach is used and the fluid mechanical system is modelled using 19 segments. Various control mechanisms are added to this basic model and the complete equation set (of order 36) is solved by analog computer to give pressures and flows with acceptable time-courses.

The model responds reasonably well to Valsalva manoeuvres and blood volume reduction tests. Details of the subsystems and their respective orders are given in table 1.1 . Beneken & Dewit's model is discussed in some detail by Talbot & Gessner (1973). and is used as an illustration of systems physiology (i.e. physiology from the viewpoint of systems science). The circulatory fluid mechanics model of chapter 2 is based on the mathematical description of Beneken & Dewit .

1.5.2 Guyton, Coleman & Granger (1972)

These authors have developed a non-pulsatile lumped parameter model of the uncontrolled circulation to which has been added a number of short-term and long-term control mechanisms. As the model is used to study overall circulatory behaviour, the black-box approach is applied extensively and minute detail is missing in many of the subsystems.

The 18 subsystems (given in table 1.2) lead to an equation set of order 37 which is solved by digital computer. Time constants in the model vary from 0.005 min (in the haemodynamic circuit) to 57600 min (for hypertrophy effects in the heart). Results from simulated experiments agree closely with results from equivalent animal or human experiments.

1.5.3 Auslander, Lobdell & Chong (1972)

Auslander (1968) developed an interesting and quite different approach to distributed parameter simulation on a digital computer which dispenses with numerical solution of differential equations completely. The basic element used in the simulation is the ideal, uniform, dispersionless, lossless transmission line (or bilateral delay line).

A discrete-time model is formulated by keeping track of waves (travelling undisturbed along lines) only as they pass through specified points and only at specified times. A common delay time, Δt , is chosen for the system and each line is then divided into segments each having a delay time equal to Δt . The state vector at $t+\Delta t$ is found by multiplying the state vector at t by a generalised scattering matrix.

The cardiovascular system structure is presented in bond-graph notation as a network of lines (representing ideal transmission lines) and nodes (representing junctions at which scattering, partial reflection or partial transmission can occur). A convenient linked data-block structure is set up in the digital computer memory to represent the graph topology.

There is no direct comparison of system order with the examples of sections 1.5.1 and 1.5.2 because an ideal time delay corresponds to an infinite order system. This very detailed model involves 208 ideal transmission line elements (see table 1.3) and has been used in ballistocardiographic studies.

1.5.4 Applicability of existing computer simulations to the present work

An evaluation of the approaches described previously reveals that there is no single existing model which is suitable in all respects for the study of short-term pharmacokinetics associated with injections of cardiovascular agents within the terms of section 1.3 .

For various reasons, including analog computer equipment limitations and the need for flexibility and convenience, a digital simulation is employed. The distributed parameter models, although providing fine detail, require excessive digital computer time. In the lumped parameter models, the number of segments can be chosen to give

(a) acceptable computer time
(b) adequate spatial representation
(c) the required accuracy

The model is intended for the study of short-term phenomena so pulsatility cannot be excluded and it may be of significance in the pharmacokinetics especially in view of the presence of nonlinearities in the system.

Of the existing pulsatile lumped parameter models, the circulatory fluid mechanics description of Beneken & Dewit (1967) is the most suitable but does not include pharmacokinetics and some central nervous control mechanisms. There was therefore a requirement for a new mathematical model based partly on existing mathematical descriptions of particular subsystems and partly on new or modified subsystem models developed by the author where no suitable model could be found in the literature.

1.6 Units employed

Where applicable, variables are expressed in terms of Medical Units (using mmHg, ml, sec). This is to be consistent with a large section of the literature on physiology and biomedical engineering and to facilitate communication with physiologists.

Variables expressed in Medical Units in this report are as follows :

Variable	Medical Unit
Pressure	mmHg
Flow	ml sec^{-1}
Volume	ml
Compliance	ml $mmHg^{-1}$
Elastance	mmHg ml^{-1}
Resistance	mmHg sec ml^{-1}
Inertance	mmHg sec^2 ml^{-1}

Elsewhere, CGS units (also employed in the literature on physiology) are used. Conversion between Medical Units and CGS units makes use of the equivalence :

$$1 \text{ mmHg} = 1332 \text{ gm cm}^{-1} \text{ sec}^{-2}$$

1.7 Conclusion

Reasons for cardiovascular modelling and simulation in general have been presented. The aim is to improve knowledge and understanding, to evaluate alternative hypotheses expressible in mathematical form and to estimate or predict cardiovascular variables.

Cardiovascular models are frequently implemented as computer simulations because of the power and flexibility offered by computer systems. Some examples of recent computer simulations of the human cardiovascular system have been given in this chapter.

A specific objective of the work is the development of a detailed pulsatile model of short-term haemodynamics and pharmacokinetics to study the effects of an injected cardiovascular agent. No single existing model possesses all the required attributes and so it is necessary to develop a composite model. This model, which is implemented as a digital simulation, includes new mathematical descriptions developed by the author.

SUBSYSTEM	ORDER	SUBSYSTEM	ORDER
19-SEGMENT CIRCULATORY FLUID MECHANICS MODEL	29	PERIPHERAL RESISTANCE CONTROL	1
HEART RATE CONTROL	3	CAPILLARY PRESSURE & BLOOD VOLUME CONTROL	1
INTERVAL-STRENGTH RELATION OF HEART MUSCLE	1	INFLUENCE OF CORONARY FLOW ON HEART PERFORMANCE	1
TOTAL ORDER = 36			

TABLE 1.1 SUBSYSTEMS IN THE MODEL OF BENEKEN & DEWIT (1967)

SUBSYSTEM	ORDER	SUBSYSTEM	ORDER	SUBSYSTEM	ORDER
CIRCULATORY DYNAMICS	5	ANGIOTENSIN CONTROL	1	NON-MUSCLE OXYGEN DELIVERY	2
VASCULAR STRESS RELAXATION	1	ALDOSTERONE CONTROL	1	NON-MUSCLE, NON-RENAL LOCAL BLOOD FLOW CONTROL	3
CAPILLARY MEMBRANE DYNAMICS	2	A. D. H. CONTROL	2	AUTONOMIC CONTROL	2
TISSUE FLUIDS, PRESSURES & GEL	4	THIRST AND DRINKING	0	HEART RATE & STROKE VOLUME	0
ELECTROLYTES & CELL WATER	4	KIDNEY DYNAMICS & EXCRETION	0	RED CELLS AND VISCOSITY	2
PULMONARY DYNAMICS & FLUIDS	2	MUSCLE BLOOD FLOW CONTROL & P_{O_2}	3	HEART HYPERTROPHY OR DETERIORATION	3
TOTAL ORDER = 37					

TABLE 1.2 SUBSYSTEMS IN THE MODEL OF GUYTON, COLEMAN & GRANGER (1972)

SUBSYSTEM	NUMBER OF ELEMENTS	SUBSYSTEM	NUMBER OF ELEMENTS
63 SYSTEMIC ARTERIAL VESSELS	110	11 PULMONARY VESSELS	11
53 SYSTEMIC VEINS	65	PULMONARY CAPILLARY BEDS	2
16 SYSTEMIC CAPILLARY BEDS	16	2 ATRIA & 2 VENTRICLES	4
TOTAL NUMBER OF IDEAL TRANSMISSION LINE ELEMENTS = 208			

TABLE 1.3 IDEAL TRANSMISSION LINE ELEMENTS IN THE MODEL OF AUSLANDER, LOBDELL & CHONG (1972)

CHAPTER 2

A MATHEMATICAL MODEL OF CIRCULATORY FLUID MECHANICS

This chapter describes the construction of a mathematical model of the blood-vascular system of an average human. The methods used to model particular regions of the circulation are described in the following sections. The complete set of equations of the circulatory fluid mechanics model is given in Appendix 1.

In general, the flow of blood through the complex network of branching, elastic, tapered vessels in the cardiovascular system is described in distributed parameter terms by a large set of simultaneous nonlinear time-varying partial differential equations. Certain simplifications have to be made to obtain a computationally tractable solution.

If laminar flow through a single blood vessel is considered and blood is assumed to be homogeneous, incompressible and Newtonian, the Navier-Stokes and continuity equations of hydromechanics can be applied. In cylindrical coordinates, assuming no external forces, these are as follows (given by Brower et al.,1969) :

$$\frac{\partial v_z}{\partial t} + v_r \frac{\partial v_z}{\partial r} + \frac{v_\theta}{r} \frac{\partial v_z}{\partial \theta} + v_z \frac{\partial v_z}{\partial z} - \mu \left[\frac{\partial^2 v_z}{\partial r^2} + \frac{1}{r} \frac{\partial v_z}{\partial r} + \frac{1}{r^2} \frac{\partial^2 v_z}{\partial \theta^2} + \frac{\partial^2 v_z}{\partial z^2} \right] = -\frac{1}{\rho} \frac{\partial P}{\partial z} \qquad ---(2.1a)$$

$$\frac{\partial v_r}{\partial t} + v_r \frac{\partial v_r}{\partial r} + \frac{v_\theta}{r} \frac{\partial v_r}{\partial \theta} - \frac{v_\theta^2}{r} + v_z \frac{\partial v_r}{\partial z} - \mu \left[\frac{\partial^2 v_r}{\partial r^2} + \frac{1}{r} \frac{\partial v_r}{\partial r} - \frac{v_r}{r^2} + \frac{1}{r^2} \frac{\partial^2 v_r}{\partial \theta^2} + \frac{2}{r^2} \frac{\partial v_\theta}{\partial \theta} + \frac{\partial^2 v_r}{\partial z^2} \right] = -\frac{1}{\rho} \frac{\partial P}{\partial r} \qquad ---(2.1b)$$

$$\frac{\partial v_\theta}{\partial t} + v_r \frac{\partial v_\theta}{\partial r} + \frac{v_\theta}{r} \frac{\partial v_\theta}{\partial \theta} + \frac{v_r v_\theta}{r} + v_z \frac{\partial v_\theta}{\partial z} - \mu \left[\frac{\partial^2 v_\theta}{\partial r^2} + \frac{1}{r} \frac{\partial v_\theta}{\partial r} - \frac{v_\theta}{r^2} + \frac{1}{r^2} \frac{\partial^2 v_\theta}{\partial \theta^2} + \frac{2}{r^2} \frac{\partial v_r}{\partial \theta} + \frac{\partial^2 v_\theta}{\partial z^2} \right] = -\frac{1}{\rho r} \frac{\partial P}{\partial \theta} \qquad ---(2.1c)$$

$$\frac{\partial v_r}{\partial r} + \frac{v_r}{r} + \frac{1}{r}\frac{\partial v_\theta}{\partial \theta} + \frac{\partial v_z}{\partial z} = 0 \qquad ---(2.1d)$$

where z, r and θ are longitudinal, radial and angular coordinates respectively, t is time, v is the fluid velocity and ρ and μ are fluid density and kinematic viscosity respectively.

Further simplifying assumptions (e.g. axial symmetry, negligible nonlinear terms, etc.) lead to hydromechanical equations similar to the transmission line equations encountered in electrical engineering.

The ordinary differential equations of a lumped parameter model may be derived from the simplified distributed parameter representation of eqns. (2.1) by a process of spatial discretisation which is a standard method for the numerical solution of partial differential equations (Smith, 1969). Alternatively, each lumped segment may be chosen to represent a particular collection of blood vessels and the properties of the vessels are concentrated at a point within the segment. The pressure, compliance, resistance and inertance within a segment may be regarded as values spatially averaged over the length of the original blood vessels e.g. for a segment representing a blood vessel of length ℓ ,

$$P(t) = \frac{1}{\ell}\int_0^\ell P(z,t)\,dz \qquad ---(2.2a)$$

$$C = \frac{1}{\ell}\int_0^\ell C(z)\,dz \qquad ---(2.2b)$$

$$R = \frac{1}{\ell}\int_0^\ell R(z)\,dz \qquad ---(2.2c)$$

$$L = \frac{1}{\ell}\int_0^\ell L(z)\,dz \qquad ---(2.2d)$$

In the simplest cases the lumped parameter model consists of a collection of linked elastic reservoirs. Beneken (1965) used this approach to develop an approximate 8-segment description of the uncontrolled circulation.

The static pressure-volume curve for a typical lumped parameter segment is only slightly curved in the normal operating range and is

approximated by the tangent at the operating point (fig. 2.1). With constant compliance (C_1) the equation relating transmural pressure (P_1) and volume (V_1) is then :

$$P_1 = \frac{1}{C_1}(V_1 - V_{u1}) \quad , \quad V_1 \geq V_{u1} \qquad ---(2.3)$$

where V_{u1} is the unstressed volume. It is possible for the transmural pressure to become negative if $V_1 < V_{u1}$. In this situation, the effective compliance (C_1) is likely to change especially if the vessel is collapsible (as in certain venous segments). The constraint $V_1 \geq 0$ has to be applied - this is equivalent to specifying that the compliance becomes zero at zero volume which corresponds to the real physical situation.

Considering two connected segments (fig. 2.2), the laminar Poiseuille flow (F_{12}) through the viscous resistance (R_{12}) between the segments is :

$$F_{12} = \frac{1}{R_{12}}(P_1 - P_2) \qquad ---(2.4)$$

From continuity considerations, it is necessary that :

$$\frac{dV_1}{dt} = F_{01} - F_{12} \qquad ---(2.5)$$

The three equations (2.3), (2.4) and (2.5) characterise a typical segment in the simplest of lumped parameter models.

2.1 Selection of a structure for the circulatory fluid mechanics model

As the study described in this report concerns the overall controlled cardiovascular system, fine detail of wave propagation is not essential and a lumped parameter representation is acceptable provided that :

(a) there is sufficient spatial detail to be of use in blood transport studies.

(b) the dynamic performance of the model is realistic for a variety of test conditions (including satisfactory time-courses of pressures, flows and volumes in each segment).

(c) the representation is sufficiently economical in mathematical terms so that severe computational problems do not arise.

A circulatory fluid mechanics structure which is most suitable for the present work and which satisfies the above conditions is the

19-segment lumped parameter description of Beneken & Dewit (1967). The interconnections of segments in this description are shown in fig. 2.3 with arrows indicating the direction of blood flow. In adopting this model, the subscript notation used by Beneken & Dewit to identify the segments is retained and, where applicable, the same numerical values of hydromechanical constants are used. These constants derive from the results of physiological experiments on humans and comparable animals recorded in the literature. The model is constructed for an "average human" who is considered to have a blood volume of 4544 ml (8 pints).

In using the circulatory fluid mechanics model described in the original paper of Beneken & Dewit (1967) the author has made changes and has added further explanations and calculations where these are considered necessary.

2.2 A model of the heart

This section gives an approximate mathematical description of cardiac hydromechanics. The heart is viewed as a set of four separate unidirectional pumps and so any direct mechanical effects on one chamber due to the wall motion of an adjacent chamber are excluded. Also the detailed shapes of the atria and ventricles are not taken into account.

2.2.1 The timing of events in the cardiac cycle

The cardiac cycle is assumed to commence at the onset of atrial systole. The durations of activities in the heart that are required for an approximate description of cardiac hydromechanics are :

(a) the duration of atrial systole (T_{AS})
(b) the time between the onset of atrial systole and the onset of ventricular systole (T_{AV})
(c) the duration of ventricular systole (T_{VS})

Beneken & Dewit (1967) have obtained linear algebraic approximations relating T_{AS}, T_{AV} and T_{VS} to the heart period T_H based on a study of electrocardiogram (ECG) data. These approximations are in satisfactory agreement with data from ECG analyses given by Rushmer (1970, p.372).

The interval T_{AS} is assumed to be the time between the beginning

of the P-wave and the R-wave (i.e. the P-R interval) of the ECG and is approximately related to T_H by :

$$T_{AS} = 0.1 + 0.09\,T_H \qquad ---(2.6)$$

The interval T_{AV} is assumed to be the sum of the time for the atrial muscle contraction wave to travel from the sinoatrial node to the atrioventricular (AV) node and the time for the contraction wave to travel from the AV node down the AV bundle (bundle of His) to the apex of the heart. The P-Q interval of the ECG represents this time which is related to T_{AS} by the approximation :

$$T_{AV} = T_{AS} - 0.04 \qquad ---(2.7)$$

The duration of ventricular systole (T_{VS}) is taken as the Q-T interval of the ECG and is related to T_H by the approximation :

$$T_{VS} = 0.16 + 0.2\,T_H \qquad ---(2.8)$$

Once the cardiac cycle has been initiated the cardiac muscle is refractory to any stimuli. This is incorporated by ensuring that the value of T_H (and hence T_{AS}, T_{AV} and T_{VS}) at the start of the cycle remains unchanged until the cycle has been completed.

Assuming a normal heart rate of 75 bpm, the heart period (T_H) is 0.8 sec and the intervals calculated from the above equations are :

$T_{AS} = 0.172$ sec $T_{AV} = 0.132$ sec $T_{VS} = 0.32$ sec

2.2.2 The pumping action of the four heart chambers

The pumping action in the lumped parameter representations of the atria and ventricles is approximated by using the "compliance pumping" approach developed by Beneken (1965). Instead of the fixed compliances used in the passive arterial segments, time-varying elastances (reciprocal compliances) provide a representation of the active contraction. The equation relating pressure (P), volume (V) and the elastance function $[a(t)]$ is :

$$P = a(t)[V - V_u] \qquad ---(2.9)$$

where V_u is the unstressed volume.

An important consequence of this approximate description is that Starling's "Law of the Heart" (Green, 1972 ; p.46) is obeyed because any increase in end-diastolic ventricular volume in one cycle leads to

a higher systolic pressure in the next cycle which in turn results in a greater stroke volume.

The time-courses of the four elastances are shown in fig. 2.4. Both atria are assumed to contract simultaneously and similarly both ventricles are assumed to contract simultaneously. Beneken (1965,p.21) has pointed out that the actual shape of the systolic portion of each elastance waveform is not critical provided that the maximum and minimum elastance values remain unchanged. This assertion is confirmed in the validation tests of chapter 6. For convenience, a half-sinusoidal systolic waveform is used in each case.

The minimum elastance value (a_D) is calculated from eqn. (2.9) using corresponding diastolic pressure and volume values. Similarly, the maximum elastance value (a_S) is calculated using corresponding systolic pressure and volume values as follows :

$$a_D = \frac{P_D}{V_D - V_u} \qquad ---(2.10)$$

$$a_S = \frac{P_S}{V_S - V_u} \qquad ---(2.11)$$

The elastance waveforms are generated by introducing a variable u which is the elapsed time measured from the start of the cardiac cycle ($0 \leq u \leq T_H$). The following two functions are introduced :

$$x_3 = \begin{cases} \sin\left(\frac{\pi u}{T_{AS}}\right) , & 0 \leq u < T_{AS} \\ 0 , & u \geq T_{AS} \end{cases} \qquad ---(2.12)$$

$$x_5 = \begin{cases} 0 , & u \leq T_{AV} \\ \sin\left[\frac{\pi}{T_{VS}}(u - T_{AV})\right] , & T_{AV} < u < (T_{AV} + T_{VS}) \\ 0 , & u \geq (T_{AV} + T_{VS}) \end{cases} \qquad ---(2.13)$$

The elastance functions for the four heart chambers are then given by :

$$a_{RA} = x_3(a_{RAS} - a_{RAD}) + a_{RAD} \qquad ---(2.14)$$

$$a_{RV} = x_5(a_{RVS} - a_{RVD}) + a_{RVD} \qquad ---(2.15)$$

$$a_{LA} = x_3(a_{LAS} - a_{LAD}) + a_{LAD} \qquad ---(2.16)$$

$$a_{LV} = x_5(a_{LVS} - a_{LVD}) + a_{LVD} \qquad ---(2.17)$$

The elapsed time u is generated in the computer program by using an integrator with unity input to generate a ramp function with unit slope, the output being reset to zero at the end of each cardiac cycle.

2.2.3 The atria

For the atria, the maximum and minimum elastance values (a_{RAS}, a_{LAS}, a_{RAD}, a_{LAD}) are those specified by Beneken & Dewit (1967) and are given in Appendix 2.

For the right atrium, the equations are :

$$P_{RA} = a_{RA}(t)\left[V_{RA} - V_{URA}\right] \qquad ---(2.18)$$

$$\frac{dV_{RA}}{dt} = F_I - F_{RARV} \quad , \; V_{RA} \geq 0 \qquad ---(2.19)$$

$$F_{RARV} = \begin{cases} \dfrac{P_{RA} - P_{RV}}{R_{RARV}} & , \; P_{RA} > P_{RV} \\ 0 & , \; P_{RA} \leq P_{RV} \end{cases} \qquad ---(2.20)$$

$$F_I = F_{SVCRA} + F_{IVCRA} + F_{BRONC} + F_{COR} \qquad ---(2.21)$$

Equation (2.20) approximates the action of the tricuspid valve with R_{RARV} being the resistance of the fully opened valve. The quantity F_I in equation (2.21) represents the total inflow of the right atrium. The effect of contraction of the right atrial inlet (which assists the pumping action) is taken into account by modifying the separate right atrial inflows appropriately. The basic flows through the coronary and bronchial vascular beds are given by :

$$F_{COR} = \frac{P_{AO1} - P_{RA}}{R_{COR}} \qquad ---(2.22)$$

$$F_{BRONC} = \frac{P_{AO3} - P_{RA}}{R_{BRONC}} \qquad ---(2.23)$$

R_{COR} and R_{BRONC} have large numerical values (in both cases 12 mmHg sec ml^{-1} is assumed) which are much greater than the resistance introduced by the contracted atrial inlet and so the effect of right atrial inlet contraction on F_{COR} and F_{BRONC} is not included.

However, for the blood flow from the inferior and superior venae cavae, the segmental fluidic resistances are quite small (R_{IVC} =0.015

and R_{SVC} =0.06 mmHg sec ml^{-1} respectively). The inlet contraction is therefore likely to have a significant effect on the flows F_{IVCRA} and F_{SVCRA}. The effect is approximated by computing a particular inflow assuming no right atrial inlet contraction and then decreasing the magnitude to one-tenth if the flow is reversed due to increased right atrial pressure. If F_9 and F_{10} are the computed flows from the inferior vena cava and superior vena cava into the right atrium respectively assuming no contraction, then

$$F_{IVCRA} = \begin{cases} F_9, & F_9 \geq 0 \\ 0.1F_9, & F_9 < 0 \end{cases} \qquad ---(2.24)$$

$$F_{SVCRA} = \begin{cases} F_{10}, & F_{10} \geq 0 \\ 0.1F_{10}, & F_{10} < 0 \end{cases} \qquad ---(2.25)$$

In each case this is equivalent to increasing the total resistance to backflow by 10 times.

For the left atrium, the equations are :

$$P_{LA} = a_{LA}(t)\left[V_{LA} - V_{ULA}\right] \qquad ---(2.26)$$

$$\frac{dV_{LA}}{dt} = F_{PVLA} - F_{LALV} \quad , V_{LA} \geq 0 \qquad ---(2.27)$$

$$F_{LALV} = \begin{cases} \dfrac{P_{LA} - P_{LV}}{R_{LALV}} & , P_{LA} > P_{LV} \\ 0 & , P_{LA} \leq P_{LV} \end{cases} \qquad ---(2.28)$$

Equation (2.28) approximates the action of the mitral valve with R_{LALV} being the resistance of the fully opened valve.

The effect of left atrial inlet contraction (which assists the pumping action) is taken into account by computing the left atrial inflow from the pulmonary veins segment assuming no contraction (F_3) and then decreasing the magnitude to one-tenth if the flow is reversed due to increased left atrial pressure i.e.

$$F_{PVLA} = \begin{cases} F_3, & F_3 \geq 0 \\ 0.1F_3, & F_3 < 0 \end{cases} \qquad ---(2.29)$$

As in the right atrial case, this is equivalent to increasing the total resistance to backflow by 10 times.

2.2.4 The ventricles

The ventricular diastolic and systolic elastances are calculated using eqns. (2.10) and (2.11) of section 2.2.2. Beneken (1965) calculated that a_{LVS} =1.5 and a_{RVS} =0.3 but omitted the atria and compensated for their absence by increasing the diastolic compliances of the ventricles. The recalculated diastolic values for this model are

$$a_{LVD} = \frac{10}{150} = 0.067 \quad mm\,Hg\; m\ell^{-1}$$

$$a_{RVD} = \frac{6.8}{150} = 0.046 \quad mm\,Hg\; m\ell^{-1}$$

The pumping action in both ventricles is represented by :

$$P_{RV} = a_{RV}(t)\left[V_{RV} - V_{uRV}\right] \qquad ---(2.30)$$

$$P_{LV} = a_{LV}(t)\left[V_{LV} - V_{uLV}\right] \qquad ---(2.31)$$

From continuity considerations, we have that :

$$\frac{dV_{RV}}{dt} = F_{RARV} - F_{RVPA}\;,\; V_{RV} \geq 0 \qquad ---(2.32)$$

$$\frac{dV_{LV}}{dt} = F_{LALV} - F_{LVAOI}\;,\; V_{LV} \geq 0 \qquad ---(2.33)$$

The dynamics associated with the pulmonary and aortic valves has to be examined more carefully because the blood is subjected to considerable acceleration at these locations and moves with high velocity in the following vessels.

The equations used by Beneken & Dewit (1967) for the pulmonary and aortic valves are as follows :

$$P_{RV} - P_{PA} = R_{RVPA}F_{RVPA} + L_{RV}\frac{dF_{RVPA}}{dt} + \frac{\rho}{2}\left[\frac{F_{RVPA}}{A_{PA}}\right]^2,\; F_{RVPA} \geq 0 \qquad ---(2.34)$$

$$P_{LV} - P_{AOI} = R_{LVAOI}F_{LVAOI} + L_{LV}\frac{dF_{LVAOI}}{dt} + \frac{\rho}{2}\left[\frac{F_{LVAOI}}{A_{AOI}}\right]^2,\; F_{LVAOI} \geq 0 \qquad ---(2.35)$$

The constraints associated with the two equations correspond to the actions of the pulmonary and aortic valves in ensuring unidirectional blood flow.

The first term on the right hand side of each equation corresponds to the pressure drop caused by the viscous properties of blood. With

$R_{RVPA} = R_{LVAO} = 0.003$ mmHg sec ml^{-1} and an instantaneous flow rate of 500 ml sec^{-1}, the pressure drop across an open valve due to viscous resistance is 1.5 mmHg which is small compared to the contribution of the other terms.

The second term on the right hand side of eqn. (2.34) and (2.35) accounts for the inertia of a blood column assumed to have a length equal to the inner radius of the ventricle and a diameter equal to the diameter of the outflow vessel.

The final term on the right hand side of eqn. (2.34) and (2.35) represents the pressure drop originating from the fact that the outflow vessel has a cross-sectional area much smaller than the cross-sectional area of the corresponding ventricle. In including this term, Beneken & Dewit (1967) have applied Bernoulli's theorem (the law of variation of pressure along a stream line) to the efflux of a liquid through a small orifice in a large containing vessel (Newman & Searle, 1952 ; p. 364). Steady state conditions are assumed to exist once the flow is established, blood is considered to be incompressible and viscous forces have been shown above to be insignificant. Thus the application of Bernoulli's theorem can be justified.

A complication arises in the application of Bernoulli's theorem because the ejected blood is constrained to flow in a curved elastic artery. In the lumped parameter representation here, the cross-sectional areas A_{PA} and A_{AO} have to represent the effective values over the pulmonary artery and ascending aorta segments taking into account the curvature of the vessels. These area values are not given by Beneken & Dewit (1967) and so they are calculated in Appendix 5. Further approximations involved in the formulation of eqns. (2.34) and (2.35) are :

(a) Turbulence and also flow disturbances originating at the valves are ignored despite the high blood velocity.

(b) The vessel diameters are assumed constant over their length. This is an acceptable approximation over the relatively short distances involved.

(c) In practice, when a liquid flows freely from a small orifice in a containing vessel, the jet cross-section contracts to a minimum value (the contracted vein) after which it increases. This phenomenon is ignored due to the constraints of the outflow vessels.

The actual cross-sectional area of the aortic valve orifice was obtained by averaging figures from several publications. Guyton (1971, p.218) gives the cross-sectional area of the aorta as 2.5 cm^2 corresponding to a diameter of 1.785 cm. The average aortic blood velocity is given as 33 cm sec^{-1} so assuming an average flow rate of 100 ml sec^{-1}, the average aortic cross-sectional area works out as 3 cm^2 corresponding to a diameter of 1.955 cm. Davies (1967, p.774) gives the aortic diameter as 3 cm at the heart and 1.75 cm at the end of the aorta. The aortic orifice diameter is given as a little over 2.5 cm (Davies, 1967 ; p.758). Rushmer (1970, p.493) states that the aortic valve orifice has a normal area of 2.5-3.5 cm^2 which corresponds to a diameter range of 1.785-2.111 cm. On the basis of these figures, an aortic valve orifice diameter of 1.9 cm was assumed (cross-sectional area 2.835 cm^2). After performing the calculations described in Appendix 5 using this value, the effective cross-sectional area for use in eqns. (2.34) and (2.35) is 1.539 cm^2 (effective diameter = 1.4 cm). The same value is used for both the aortic and pulmonary valves.

The magnitude of the blood velocity when the instantaneous flow rate is 500 ml sec^{-1} is

$$v_{AOI} = \frac{F_{LVAOI}}{A_{AOI}} = \frac{500}{1.539} = 325 \ cm\ sec^{-1}$$

The corresponding pressure drop is then

$$\frac{1}{2}\rho v_{AOI}^2 = \frac{1}{2}\left(\frac{1.06}{1332}\right)(325)^2 = 42 \ mm\ Hg$$

This pressure drop is quite substantial and indicates that the detailed consideration of effective areas above is justified especially as the area is squared in the Bernoulli terms.

2.2.5 Coronary flow

Pulsatile coronary blood flow is governed by the time-course of the aortic pressure P_{AOI} and the time-course of the resistance to flow which varies during the cardiac cycle due to compression of the coronary vessels by the contracting heart (Rushmer, 1970 ; p.274). The detailed time-course of coronary flow is not of immediate interest in the model so the resistance R_{COR} is assumed constant and the flow is defined by :

$$F_{COR} = \frac{P_{AOI} - P_{RA}}{R_{COR}} \qquad ---(2.36)$$

As the coronary vessel compression occurs only during systole and

as about 10% of the cardiac output normally flows through the coronary circulation, the maximum error in the cardiac output due to the constant coronary resistance approximation occurs if the coronary flow actually ceases completely during systole and will be about $10(T_{VS}/T_H)\%$ or about 4% at 75 bpm. Rushmer (1970, p.274) points out that significant coronary flow in fact occurs during systole so if a systolic doubling of the coronary resistance is assumed, the maximum error in cardiac output due to the constant resistance assumption will be about 2% at 75 bpm. Thus the approximation is not too severe.

As only short-term haemodynamics are considered, the modelling of metabolic deficit development is excluded. Myocardial oxygen consumption and autoregulation mechanisms are not introduced.

2.3 A model of the systemic arteries

In modelling the arteries of the systemic or greater circulation, inertia effects have to be included due to the rapid acceleration of the blood. Also the wall viscoelasticity and geometrical and elastic taper have to be taken into account.

The equations used by Beneken & Dewit (1967) to describe a typical arterial segment (numbered 2 here, with adjacent segments numbered 1 and 3) are as follows :

$$P_1 - P_2 = R_{12} F_{12} + L_{12} \frac{dF_{12}}{dt} \qquad ---(2.37)$$

$$\frac{dV_2}{dt} = F_{12} - F_{23} \quad , \quad V_2 \geq 0 \qquad ---(2.38)$$

$$P_2 = \frac{1}{C_2}(V_2 - V_{u2}) + R_2' \frac{dV_2}{dt} \qquad ---(2.39)$$

$$C_2 R_2' = 0.04 \qquad ---(2.40)$$

The inertance (L_{12}), resistance (R_{12}) and compliance (C_2) of each segment have been determined by Beneken & Dewit (1967) from the literature by averaging the vascular dimensions and properties of all the blood vessels represented by the segment. Numerical values used in the computer simulation are given in Appendix 2.

Equation (2.37) follows directly from the linearised Navier-Stokes equations and accounts for resistance to flow and the inertia of the blood in segment 2. In the above lumped parameter representation, the resistance (R_{12}) and inertance (L_{12}) of arterial segment 2 are located in the connection between segment 1 and segment 2. It is assumed that R_{12} and L_{12} stay constant in arteries as the systolic to diastolic diameter change is perhaps only 5%. Dick et al (1968) performed tests on dogs using a superposition method which indicated that nonlinearities are fairly small in the canine arterial system. It is assumed that nonlinearities can be neglected in the human arterial system.

The arterial wall material exhibits such phenomena as frequency-dependent Young's modulus, stress relaxation, creep and hysteresis (Westerhof & Noordergraaf, 1970). However a reasonable approximation to account for the properties of the arterial wall is the assumption of a linear, isotropic, Newtonian, viscoelastic material in which stress depends linearly on both strain and strain-rate. In the lumped parameter representation of eqn. (2.39) :

P_2 is equivalent to stress

$(V_2 - V_{u2})$ is equivalent to strain

$\frac{dV_2}{dt}$ is equivalent to strain rate

$\frac{1}{C_2}$ is equivalent to wall elasticity

and R_2' is equivalent to wall viscosity

This is the so-called Maxwell model of viscoelasticity which can be thought of in mechanical terms as a series combination of a spring and a dashpot or in electrical terms as a capacitor and a resistor in series.

Following Beneken & Dewit (1967), the time constant $C_2 R_2'$ is taken as 0.04 sec for all systemic arterial segments as in eqn. (2.40). The importance of the wall viscosity in the model to ensure an approximately correct input impedance of the systemic circulation is discussed in chapter 6.

A linear electrical analog of the systemic circulation model showing the connections of the arterial segments is given in fig. 2.5. This corresponds to the connections of systemic segments in the block diagram of fig. 2.3. The electrical circuit makes use of the analogies between pressure and voltage, flow and current, volume and charge, viscous resistance and electrical resistance, inertance and inductance and compliance and capacitance.

The electrical analog is used to check the input impedance of the systemic circulation model in one of the validation tests described in chapter 6. The nonlinearities of the venous segments (discussed in section 2.5) are not included in the electrical analog of fig. 2.5 and instead resistances and compliances of venous segments are set to their normal values. k_β is the viscoelastic time constant (normally 0.04 sec). The FORTRAN program used to compute the input impedance is given in Appendix 6.

2.4 A model of the systemic vascular beds

In the systemic circulation, the main resistance to flow is offered by the very small blood vessels (arterioles, capillaries and venules) in the various vascular beds. If the blood flow through a vascular bed is assumed to be laminar because of the low blood velocity and if the resistance is assumed constant for the present, the blood flow is proportional to the pressure drop across the vascular bed.

In the 19-segment model of Beneken & Dewit (1967), the resistances of the vascular beds are represented by six lumped arteriovenous resistances. Blood flows through the various beds are given by the following equations :

$$F_{UAUV} = \frac{P_{UA} - P_{UV}}{R_{HEAD}} \qquad ---(2.41)$$

$$F_{COR} = \frac{P_{AO1} - P_{RA}}{R_{COR}} \qquad ---(2.42)$$

$$F_{BRONC} = \frac{P_{AO3} - P_{RA}}{R_{BRONC}} \qquad ---(2.43)$$

$$F_{INIV} = \frac{P_{IA} - P_{IV}}{R_{INT}} \qquad ---(2.44)$$

$$F_{AAAV} = \frac{P_{AA} - P_{AV}}{R_{ABD}} \qquad ---(2.45)$$

$$F_{CACV} = \frac{P_{CA} - P_{CV}}{R_{LEG}} \qquad ---(2.46)$$

In the controlled cardiovascular model, R_{BRONC} , R_{INT} , R_{ABD} and R_{LEG} are under central nervous control and circulating vasoactive substances can influence the arteriovenous resistances. The modelling of these effects is discussed in chapters 3 and 4. The locations of the arteriovenous resistances in a linear electrical analog of the systemic circulation are indicated in fig. 2.5.

2.5 A model of the systemic veins

Unlike the arteries, veins are highly compliant, collapsible, large-capacity vessels with relatively low transmural pressures and nonlinear modelling has to be applied to obtain an adequate representation. This is especially necessary in situations where large volume changes occur in certain venous segments e.g. during simulated haemorrhages or tilt-table experiments.

When a venous segment collapses, the effective compliance and resistance change . Following Snyder & Rideout (1969), the compliance is considered to be a piecewise linear function of volume with the compliance increasing to 20 times its normal value when the transmural pressure becomes negative i.e. when the volume becomes less than the unstressed value V_u (see fig. 2.6).

Inertia effects are neglected due to the low blood acceleration and also wall viscosity effects are not considered significant in the short time-scale of the model so that equations relating pressure and volume for a segment numbered 2 are :

$$P_2 = \frac{1}{C_2}\left[V_2 - V_{u2}\right] \qquad ---(2.47)$$

$$\text{where} \quad C_2 = \begin{cases} C_{2N} , & V_2 > V_{u2} \\ 20\,C_{2N} , & V_2 \leq V_{u2} \end{cases} \qquad ---(2.48)$$

The usual continuity requirements are defined by the equation :

$$\frac{dV_2}{dt} = F_{12} - F_{23} \quad , \quad V_2 \geq 0 \qquad ---(2.49)$$

If the volume of a vessel of fixed length decreases, the effective radius will decrease and the resistance to flow will increase. Considering a straight vessel with a circular cross-section of radius r connecting segments numbered 2 and 3, laminar Poiseuille flow is

given by

$$F_{23} = K_A (P_2 - P_3) r^4 \qquad ---(2.50)$$

where k_A is a constant.

Due to the lumped parameter representation, the volume of the vessel is concentrated in segment 2 and is given by

$$V_2 = K_B r^2 \qquad ---(2.51)$$

where k_B is a constant.

Eliminating r between eqns. (2.50) and (2.51) gives

$$F_{23} = K_C (P_2 - P_3) V_2^2 \qquad ---(2.52)$$

where $K_C = \frac{K_A}{K_B^2}$

In this model, the constant k_C can be related to the fixed fluidic resistance (R_{23}) assumed by Beneken & Dewit (1967) for each of their linear venous segments. If it is assumed that when $V_2 = V_{u2}$,

$$F_{23} = \frac{P_2 - P_3}{R_{23}} \qquad ---(2.53)$$

then from eqns. (2.52) and (2.53),

$$K_C = \frac{1}{R_{23} V_{u2}^2} \qquad ---(2.54)$$

Equations (2.52) and (2.54) are considered to apply to a collection of blood vessels rather than a single vessel provided that all the vessels change their dimensions proportionately. These equations provide an approximation for pressure-flow relations in uncollapsed and collapsed vessels. Clearly $F_{23} \to 0$ as $V_2 \to 0$ in equation (2.52) so the approximation is not unreasonable.

2.5.1 Venous valves

Valves at various locations in the venous system ensure unidirectional blood flow. In the circulatory fluid mechanics model of Beneken & Dewit (1967), a venous valve is included between the segments representing leg veins and abdominal veins and this valve obstructs backflow completely. This can be described mathematically by computing the flow between the segments assuming no valve present (F_8) and then defining

$$F_{CVAV} = \begin{cases} F_8, & F_8 > 0 \\ 0, & F_8 \leq 0 \end{cases} \qquad ---(2.55)$$

Valves are also associated with the veins of both arms but in this model the veins of the head and arms are lumped together in one segment. The neck veins do not have valves and the flow to the head is assumed to be twice the flow to both arms so, if F_5 is the flow between the segments representing the head and arms veins and the superior vena cava assuming no valves, the effect of the valves in the arm veins is given by :

$$F_{UVSVC} = \begin{cases} F_5 , & F_5 > 0 \\ 0.667 F_5 , & F_5 \leq 0 \end{cases} \qquad \text{--- (2.56)}$$

2.6 A model of the pulmonary circulation

The pulmonary or lesser circulation is represented by two lumped parameter segments, one for the pulmonary arteries and the other for the pulmonary veins.

The equations produced by Beneken & Dewit (1967) to describe the pulmonary arteries are :

$$P_{PA} = \frac{1}{C_{PA}} \left(V_{PA} - V_{UPA} \right) \qquad \text{---(2.57)}$$

$$\frac{dV_{PA}}{dt} = F_{RVPA} - F_{PAPV} \; , \; V_{PA} \geq 0 \qquad \text{---(2.58)}$$

$$F_{PAPV} = \begin{cases} \dfrac{P_{PA} - P_{PV}}{R_{LUNG}} , & P_{PV} > P_{CC} \\ \dfrac{P_{PA} - P_{CC}}{R_{LUNG}} , & P_{PV} \leq P_{CC} \end{cases} \qquad \text{---(2.59)}$$

Equation (2.57) is the normal pressure-volume relation for a constant compliance elastic reservoir. In the lumped representation, inertia effects in the pulmonary arteries are incorporated in the equations for the preceding right ventricle segment and so an inertance does not appear in eqn. (2.57). In eqn. (2.59), the pressure-flow relation in the pulmonary vascular bed is dependent on the value of pulmonary venous pressure (P_{PV}) relative to a critical closing pressure (P_{CC}) which is about 7 mm Hg. In mathematical terms, this accounts approximately for the critical closure of the pulmonary capillaries.

The pulmonary veins are represented by a segment which has equations similar to those for the systemic veins segments described

in section 2.5 with the addition of the atrial inlet contraction discussed in section 2.2.3 (eqn. 2.29). The equations for the pulmonary veins segment are :

$$P_{PV} = \frac{1}{C_{PV}} (V_{PV} - V_{UPV}) \qquad ---(2.60)$$

$$C_{PV} = \begin{cases} C_{PVN}, & V_{PV} > V_{UPV} \\ 20\, C_{PVN}, & V_{PV} \leq V_{UPV} \end{cases} \qquad ---(2.61)$$

$$\frac{dV_{PV}}{dt} = F_{PAPV} - F_{PVLA} \;, \; V_{PV} \geq 0 \qquad ---(2.62)$$

$$F_3 = \frac{(P_{PV} - P_{LA})\, V_{PV}^2}{R_{PVLA}\, V_{UPV}^2} \qquad ---(2.63)$$

$$F_{PVLA} = \begin{cases} F_3, & F_3 \geq 0 \\ 0.1 F_3, & F_3 < 0 \end{cases} \qquad ---(2.64)$$

2.7 A model of respiration

Beneken & Dewit (1967), in their circulatory fluid mechanics model, assume a constant intrathoracic pressure (P_{TH}) of -4 mm Hg and a constant intra-abdominal pressure (P_{ABD}) of +4 mmHg, both pressures being measured relative to atmospheric pressure.

In this work, it was considered useful to illustrate respiratory variation of blood pressure, heart rate, etc. and also to demonstrate the respiratory pump action. Hence cyclic respiration is introduced into the model and is employed in the validation process described in chapter 6.

If T_R is the respiratory period and T_{IE} is the inhalation-exhalation duration then the intrathoracic pressure (P_{TH}) will be at the resting respiratory level for a time ($T_R - T_{IE}$) in each respiratory cycle. If y_2 is the elapsed time measured from the start of the respiratory cycle ($0 \leq y_2 \leq T_R$) then cyclic respiration can be approximated as follows

$$y_1 = \begin{cases} y_2, & 0 \leq y_2 \leq T_{IE} \\ 0, & T_{IE} \leq y_2 \leq T_R \end{cases} \qquad ---(2.65)$$

$$P_{TH} = K_1 + (K_2 - K_1) \sin\left(\frac{\pi y_1}{T_{IE}}\right) \qquad ---(2.66)$$

$$P_{ABD} = K_3 + (K_4 - K_3) \sin\left(\frac{\pi y_1}{T_{IE}}\right) \qquad ---(2.67)$$

The time-courses of these respiratory variables are given in fig. 2.7. The elapsed time y_2 is generated in the computer program by using an integrator with unity input to generate a ramp function with unit slope, the output being reset to zero at the end of each respiratory cycle.

The pressures P_{TH} and P_{ABD} are introduced into 8 equations defining flow across the thoracic or abdominal boundaries (These boundaries are indicated in fig. 2.3). For example, the equation defining flow between the segments representing the thoracic aorta and the abdominal arteries is modified from

$$\frac{dF_{AO3AA}}{dt} = \frac{P_{AO3} - P_{AA} - R_{AA} F_{AO3AA}}{L_{AA}} \qquad ---(2.68)$$

to

$$\frac{dF_{AO3AA}}{dt} = \frac{P_{AO3} + P_{TH} - P_{AA} - P_{ABD} - R_{AA} F_{AO3AA}}{L_{AA}} \qquad ---(2.69)$$

A facility is provided in the digital computer program to switch between the static respiration of Beneken & Dewit (1967) and the cyclic respiration model as required.

2.8 A model of orthostasis

The effects of gravity on the columns of blood in the cardiovascular system are included in the model so that it is possible to simulate the dynamics which occur during a passive tilt from a previously resting, recumbent position. The circulatory response to orthostasis provides a useful test of the compensatory mechanisms in the complete controlled cardiovascular model and is discussed further in the validation tests of chapter 6. The muscle pump action, which occurs due to contraction of skeletal muscle and which aids venous return when an individual stands upright, is not incorporated.

The approach used by Snyder & Rideout (1969) is employed. Pressure generators are included between various segments to represent the effective hydrostatic pressure differences over the corresponding

lengths of blood vessels.

Let g = acceleration due to gravity
ϱ = density of blood
n = number of g's of acceleration (normally 1)
ℓ = effective segment length for the lumped parameter representation
ϕ = angle between the axis of the segment and a perpendicular to the direction of gravitational force.

then the hydrostatic pressure difference is given by

$$G = n g \varrho \ell \sin\phi \qquad \text{---(2.70)}$$

The hydrostatic pressure generators are assigned to arteries and veins in such a way that the sum of hydrostatic pressures round any closed circulatory loop is zero.

The pressure generators are introduced at the locations shown in fig. 2.8 and the equations defining flow at these locations are modified appropriately. For example, eqn. (2.69) defining flow between the segments representing the thoracic aorta and the abdominal arteries (with respiratory effects included) is modified to

$$\frac{dF_{AO3AA}}{dt} = \frac{P_{AO3} + P_{TH} - P_{AA} - P_{ABD} - R_{AA} F_{AO3AA} + G_{AO3AA}}{L_{AA}} \qquad \text{---(2.71)}$$

where

$$G_{AO3AA} = n g \varrho \ell_{AO3AA} \sin\phi \qquad \text{---(2.72)}$$

A facility is provided in the digital computer program to switch orthostasis on or off as required.

2.9 Calculation of mean arterial pressure, stroke volume, cardiac output and total systemic resistance

Mean values of aortic pressure and flow are important in cardiovascular physiology and their calculation is necessary here to enable results from the model to be compared with results in the literature on circulatory physiology.

The stroke volume (SV) and mean arterial pressure (MAP) may be obtained on a beat-by-beat basis by integration of the left ventricular outflow and the aortic pressure over one cardiac cycle. If t_1 is the time at which a cardiac cycle starts and T_H is the heart period then

$$(MAP) = \frac{1}{T_H} \int_{t_1}^{t_1+T_H} P_{AOI}\, dt \qquad ---(2.73)$$

$$(SV) = \int_{t_1}^{t_1+T_H} F_{LVAOI}\, dt \qquad ---(2.74)$$

The values of (MAP) and (SV) obtained from eqns. (2.73) and (2.74) are available only at the end of each cardiac cycle. The cardiac output (CO) or mean aortic flow on a beat-by-beat basis can be calculated from

$$(CO) = \frac{(SV)}{T_H} \qquad ---(2.75)$$

The resistance of the network of blood vessels in the real systemic circulation is referred to as the peripheral resistance. In this model, the resistance to flow between the left ventricle and the right atrium offered by the 13 systemic segments is referred to as the total systemic resistance.

An estimated total systemic resistance (ETSR) can be obtained on a beat-by-beat basis from

$$(ETSR) = \frac{(MAP)}{(CO)} \qquad ---(2.76)$$

An electrical analog of the network of resistances to flow in the model is given in fig. 2.9. The true total systemic resistance (TTSR) at any instant can be obtained by calculation of the input resistance of the electrical analog. This calculation is included in the digital computer program. The resistances of venous segments are volume-dependent and the lumped resistances of vascular beds will become variable when central nervous control of peripheral resistance and pharmacokinetics are introduced. Fig. 2.9 therefore includes these effects. The equations for the calculation of (TTSR) are given in Appendix 1.

The estimate (ETSR) obtained from equation (2.76) is correct when the system is in a pulsatile steady state. However, during transient dynamics, (ETSR) may differ considerably from (TTSR). This assertion is proved theoretically in appendix 8 for a simple reduced model of the systemic circulation and is verified for the complete model by comparing (ETSR) with (TTSR) during tests on the digital simulation described in chapters 6 and 7.

In the literature on cardiovascular research, peripheral

resistance is usually calculated using eqn. (2.76) with time-averaging of aortic pressure and flow over one or more cardiac cycles or the smoothing of pressure and flow signals by low-pass filtering. In most of the results obtained from the digital simulation in chapters 6 and 7, (ETSR) is presented rather than (TTSR) to enable comparison with equivalent results from experiments on animals and humans described in the literature.

2.10 Conclusion

A pulsatile 19-segment lumped parameter model of the uncontrolled human blood circulation suitable for the study of short-term haemodynamics has been presented. The model is based on the work of Beneken & Dewit (1967) with the following principal additions and modifications by the author :

(a) Detailed consideration of flow through the aortic and pulmonary valves.
(b) Nonlinear modelling of venous segments.
(c) Cyclic respiration
(d) Detailed consideration of the beat-by-beat estimation of peripheral resistance from mean arterial pressure and cardiac output.

The basic model is of order 27 and another 4 integrators are required for cyclic respiration, beating of the heart and the calculation of mean arterial pressure and stroke volume. The model provides a qualitatively adequate description of the circulatory fluid mechanics and has sufficient spatial detail without being of excessively high order which would cause computational problems.

The complete set of equations for the circulatory fluid mechanics model is given in Appendix 1. The values of all the constants and initial conditions used are given in Appendix 2.

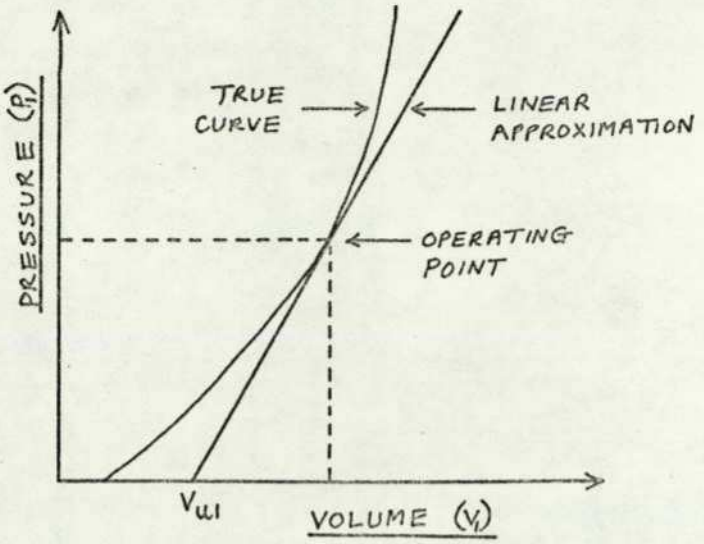

FIG. 2.1 STATIC PRESSURE-VOLUME RELATIONSHIP FOR A TYPICAL SEGMENT

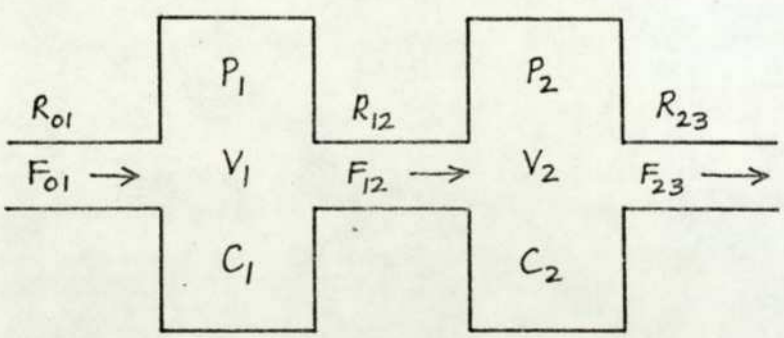

FIG. 2.2 TWO TYPICAL ADJOINING LUMPED PARAMETER SEGMENTS

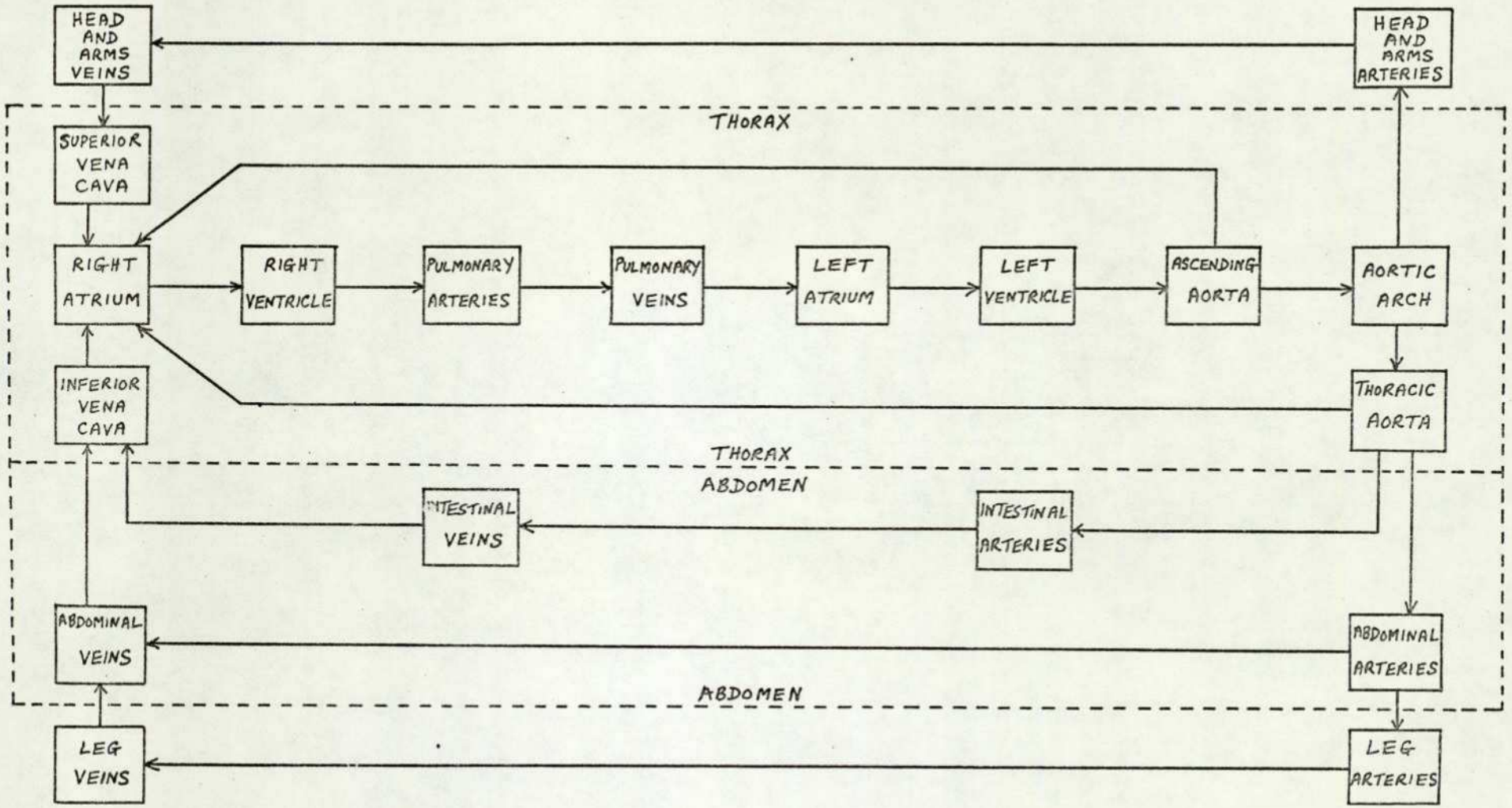

FIG. 2.3 INTERCONNECTION OF SEGMENTS IN THE CIRCULATORY FLUID MECHANICS MODEL OF BENEKEN & DEWIT (1967)

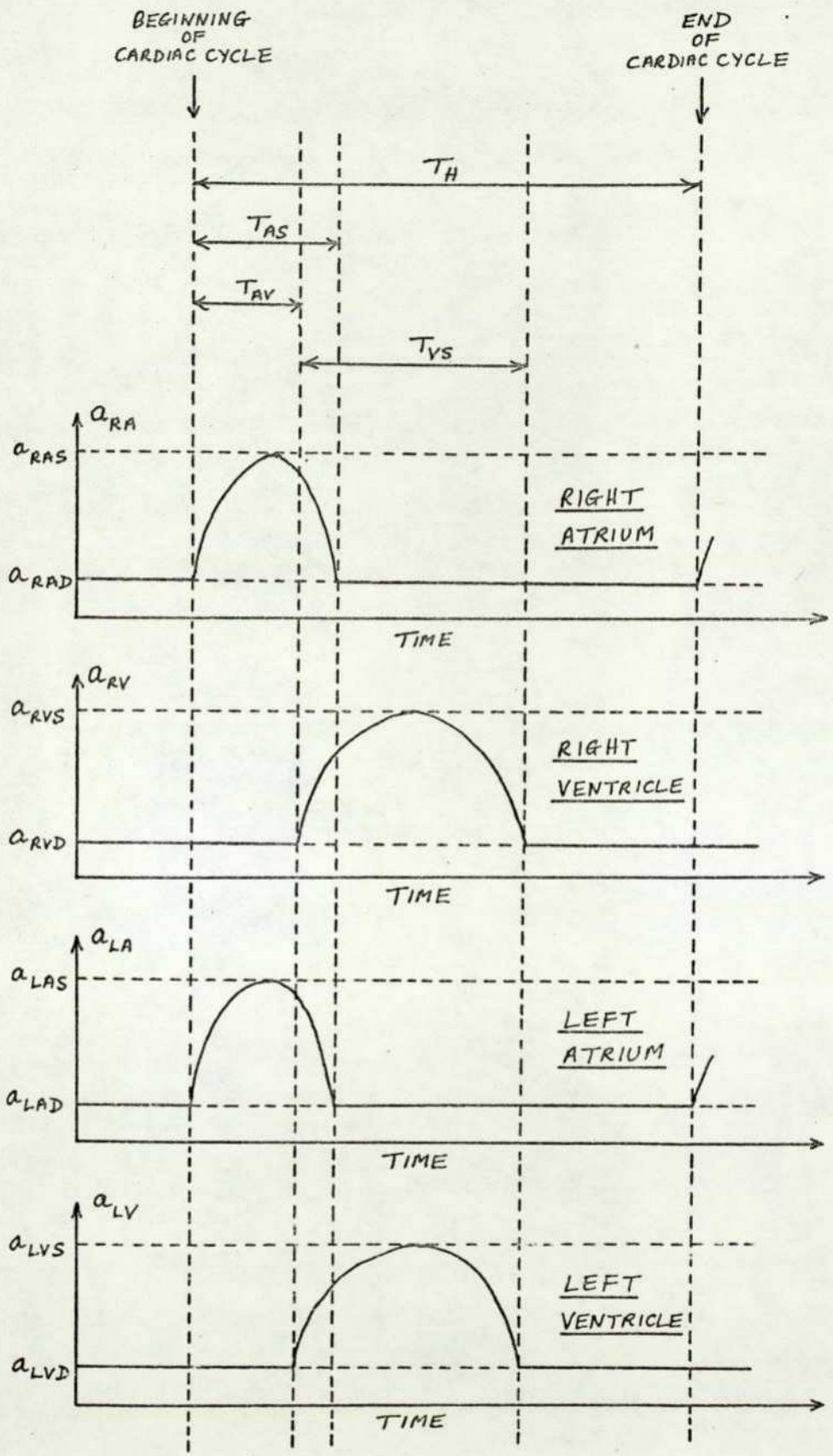

FIG. 2.4 ELASTANCES OF THE FOUR HEART CHAMBERS

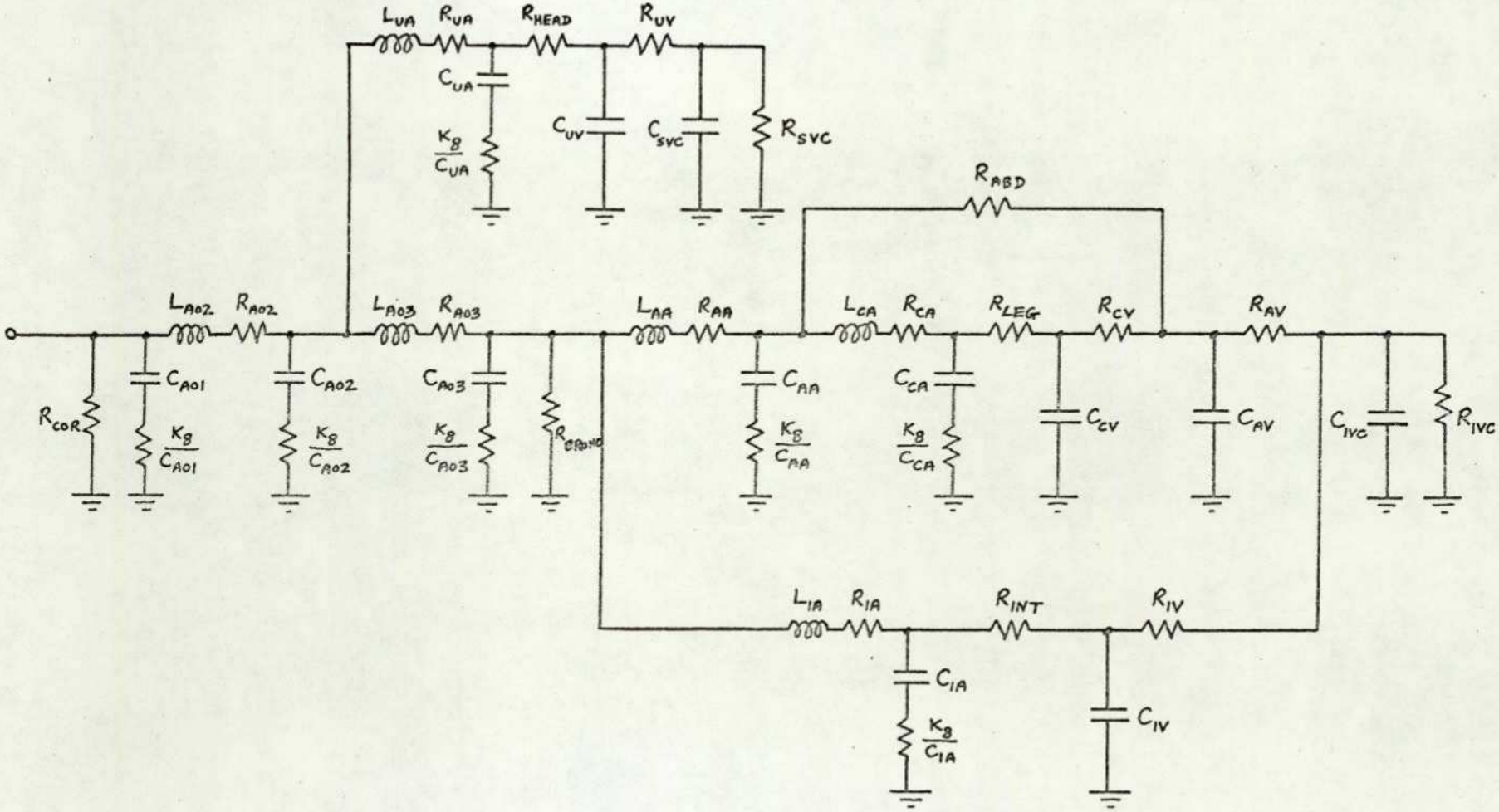

FIG. 2.5 LINEAR ELECTRICAL ANALOG OF THE SYSTEMIC CIRCULATION

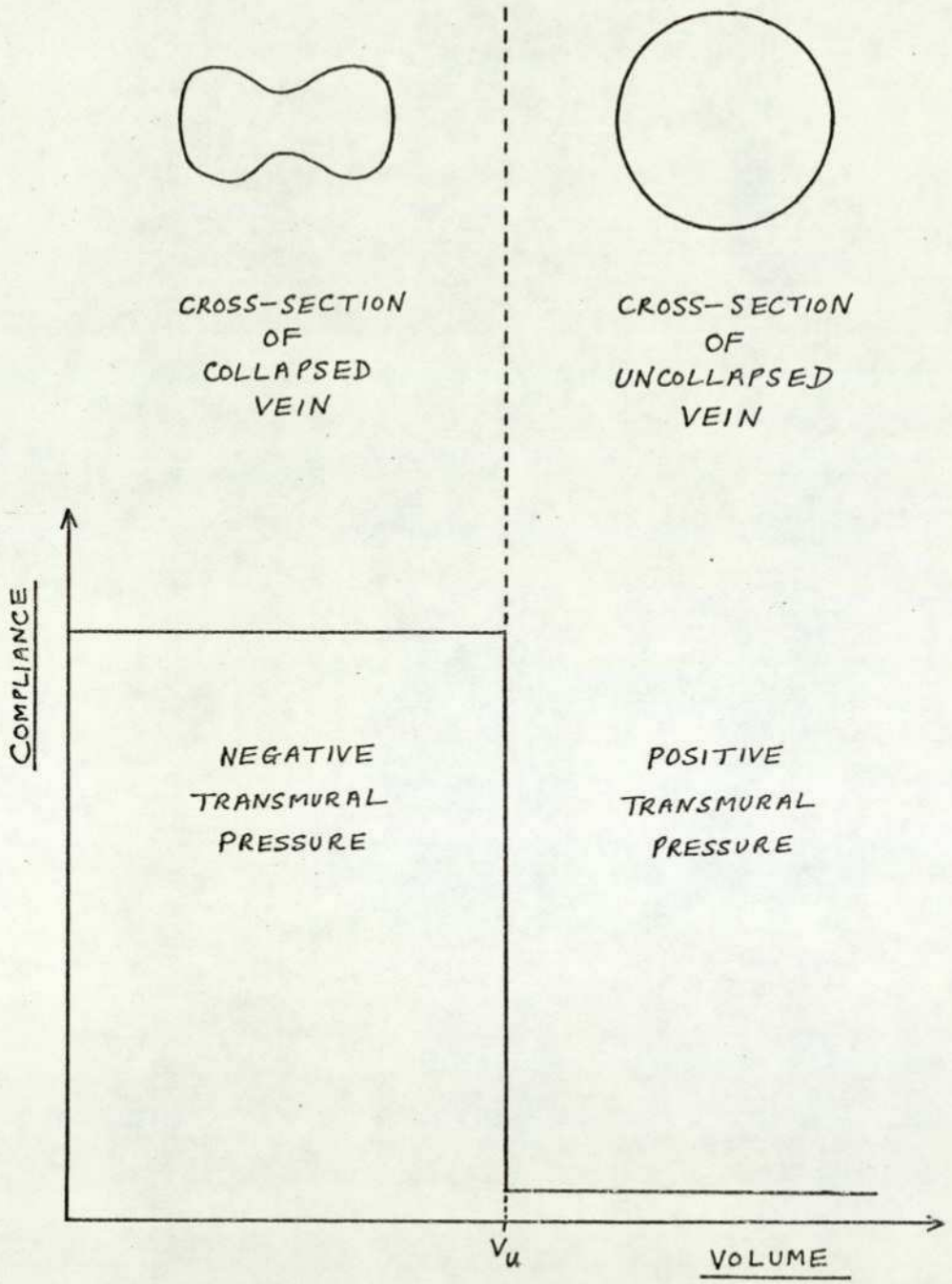

FIG. 2.6 PIECEWISE LINEAR APPROXIMATION FOR THE COMPLIANCE OF A VENOUS SEGMENT

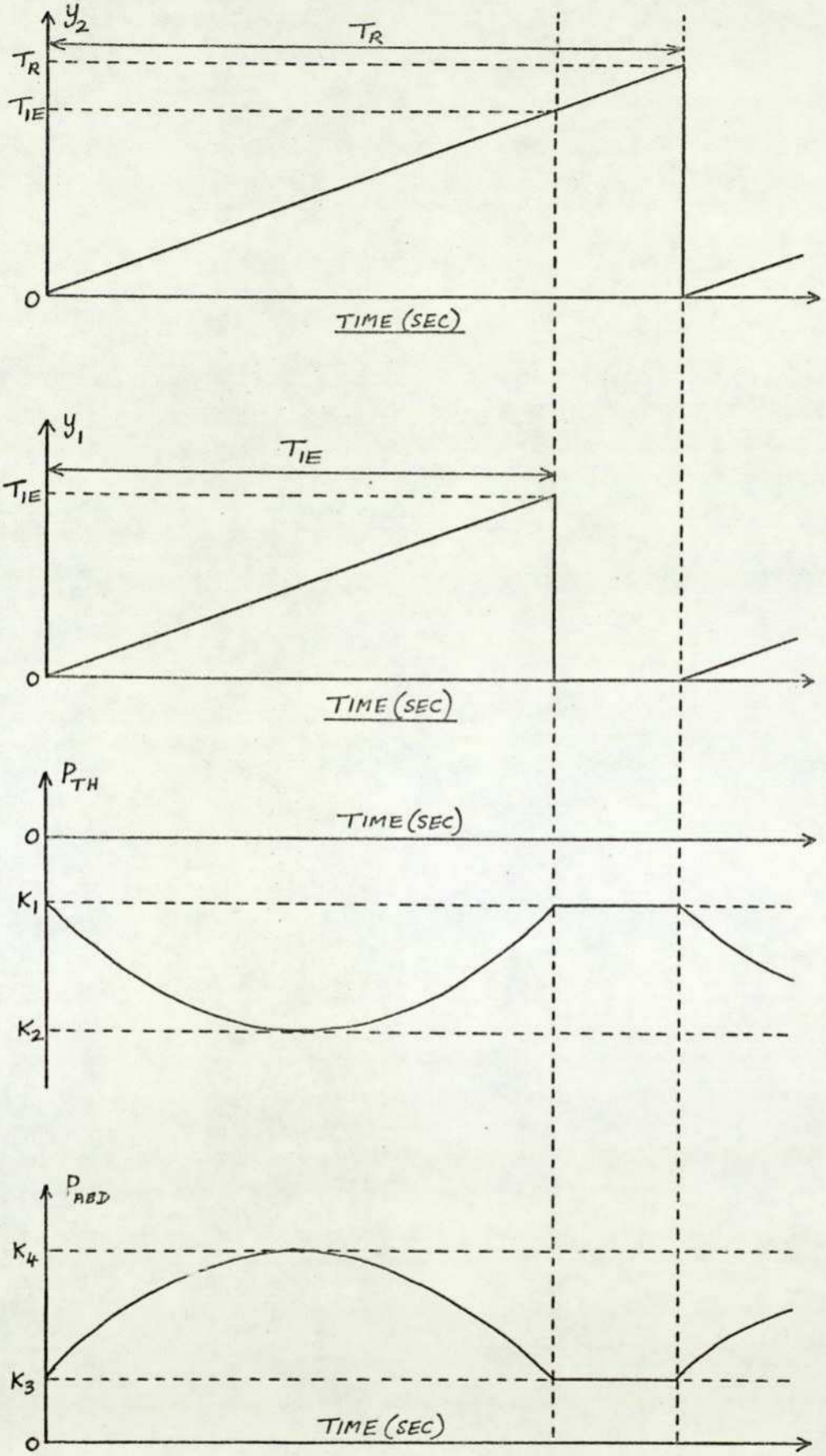

FIG. 2.7 TIME-COURSES OF VARIABLES IN THE CYCLIC RESPIRATION MODEL

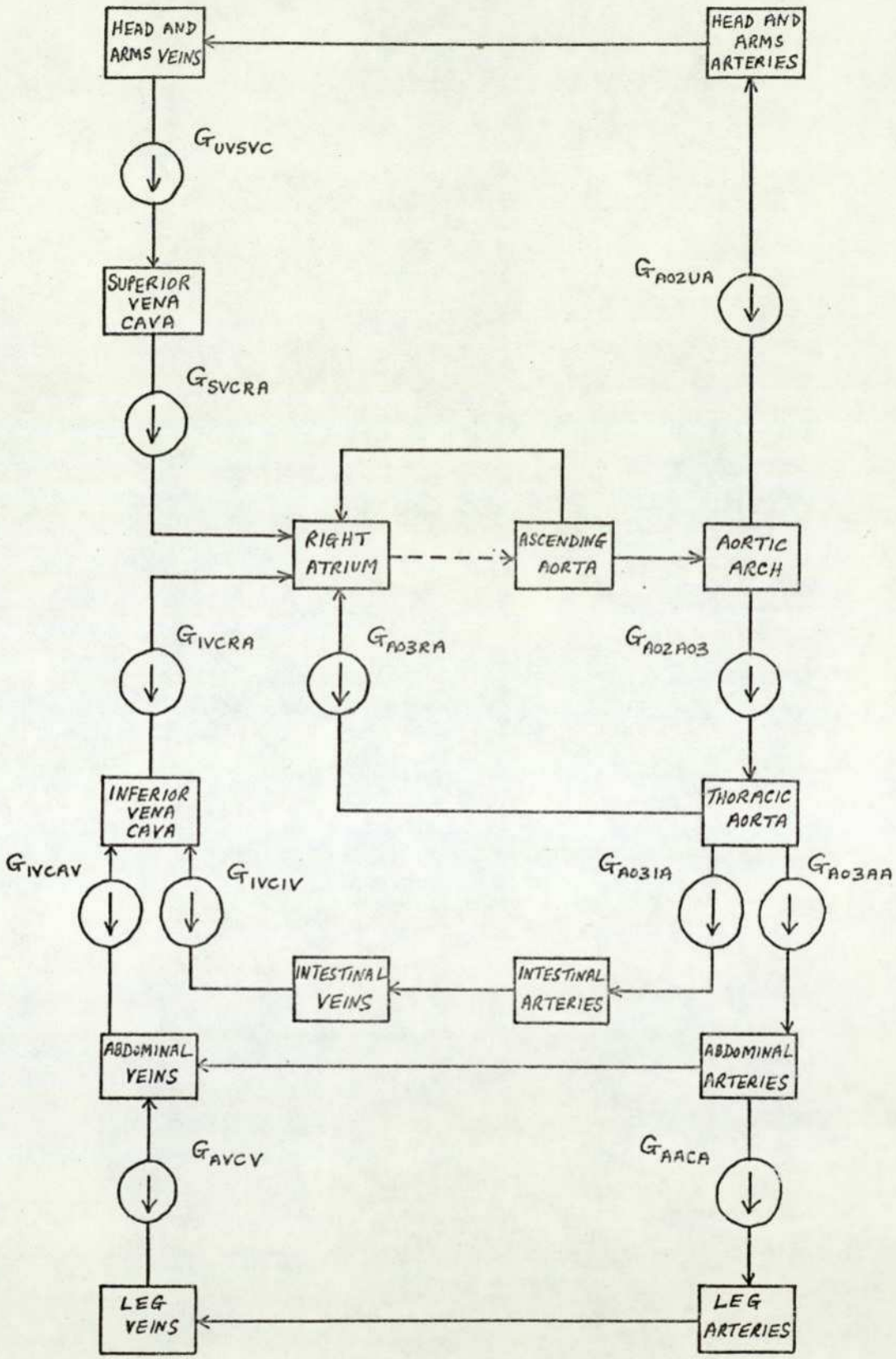

FIG. 2.8 LOCATIONS OF HYDROSTATIC PRESSURE GENERATORS TO SIMULATE ORTHOSTASIS

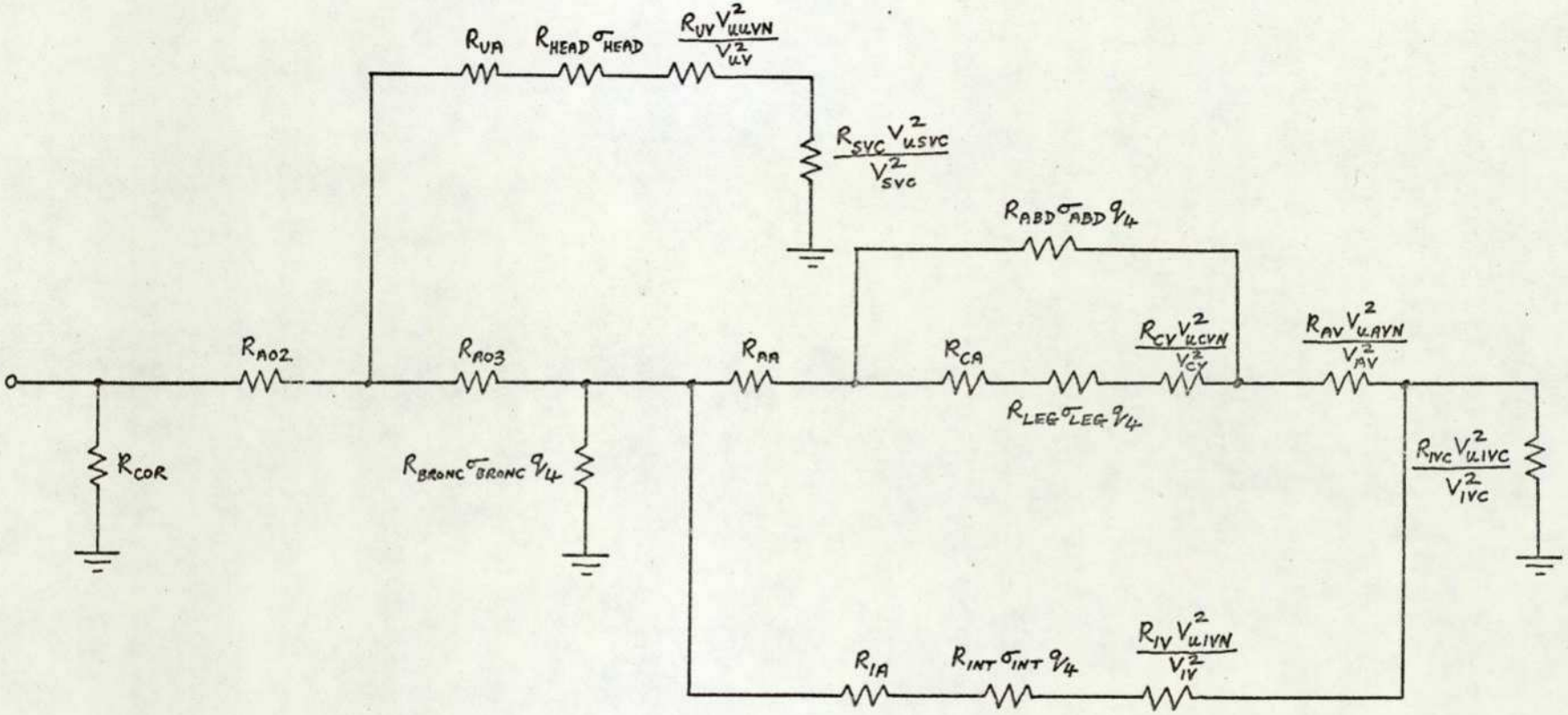

FIG. 2.9 ELECTRICAL ANALOG USED TO CALCULATE TRUE TOTAL SYSTEMIC RESISTANCE.

CHAPTER 3

A MATHEMATICAL MODEL OF NEURAL CONTROL

Neural and humoral control mechanisms enable the cardiovascular system to adapt to a changing environment. This chapter describes the mathematical representation of central nervous control mechanisms which are included in the model of short-term haemodynamics and pharmacokinetics.

The transport in the bloodstream of numerous internally secreted chemical substances which affect the cardiovascular system is ignored in the model (e.g. the renin-angiotensin-aldosterone system) because most of these humoral effects have time constants much longer than the short time-scale (0-2 minutes) of the present model. Any short-term humoral control actions are considered to augment the central nervous control actions and so are not included (e.g. the catecholamines noradrenaline and adrenaline which are secreted by the adrenal medulla and which augment the activity of the sympathetic nervous system).

Local autoregulatory mechanisms help to adjust blood flow through particular tissues to meet the local metabolic needs of those tissues and such mechanisms are important during periods of biological demand. The model considered here applies to a relaxed, resting human and so local autoregulatory mechanisms are not included.

Central nervous control is achieved in the cardiovascular system by variation of parameters - in particular heart rate, peripheral resistance, myocardial contractility and venous tone. Central nervous input information on the blood pressures at various locations is provided by the pressure-sensitive baroreceptors, the principal receptors being located in the aortic arch and carotid sinus regions. Neural control of the four previously mentioned parameters (viz. heart rate, peripheral resistance, myocardial contractility and venous tone) is included in the model because, in simulating the injection of a cardiovascular agent, cooperative or competitive interactions can occur at certain sites between the neural control and the drug action.

The activity of the cardiac and vasomotor centres in the medulla can be influenced by the higher centres of the cerebral cortex in the normal, conscious human. These effects are ignored as the model applies to a relaxed, resting human who is assumed to be in a permanently calm state of mind.

In the mathematical description of circulatory fluid mechanics given in chapter 2, the modelling is based primarily on the application of physical laws and principles. The central nervous system is an extremely complex system consisting of millions of interconnected neurones and each neurone can be regarded as a nonlinear dynamic system. It is not appropriate therefore to apply physical laws in the mathematical formulation. Instead, suitable empirical or "black box" dynamic models with approximately correct input-output relations have to be constructed.

There is a high degree of accuracy in the control of blood pressure and also spontaneous and broadly repetitive fluctuations of blood pressure can occur at a frequency differing from that of respiration. Because nonlinear control systems using bang-bang or on-off control can also show a high degree of control accuracy and can exhibit limit cycles in the controlled variable, Hyndman (1970) suggested simple empirical models of central nervous control mechanisms incorporating bang-bang actions. This approach is used here in the models for control of peripheral resistance, myocardial contractility and venous tone.

3.1 The baroreceptor system

The baroreceptor reflexes are important short-term negative feedback mechanisms for the regulation of blood pressure. The principal baroreceptors are located in the aortic arch and carotid sinus regions and afferent nerve impulses pass from these regions to the medulla. If the blood pressure rises, the impulse activity increases and there is greater inhibition of sympathetic centres and stimulation of parasympathetic centres in the brain. This leads to a decreased discharge of sympathetic impulses and an increased discharge of parasympathetic impulses throughout the body. The resulting effects (e.g. slowing of the heart and arteriolar vasodilatation) tend to limit the original rise in blood pressure. If the blood pressure falls, the opposite effects occur (e.g. acceleration of the heart and arteriolar vasoconstriction) and the original fall of blood pressure is limited. Mathematical models of the aortic arch and carotid sinus baroreceptors are given below.

When arterial pressure is increased to a new level and remains at that level for long periods, the baroreceptors are strongly stimulated

at first but then they adapt to the new level of pressure and lose their excess stimulation in the process. This adaptation (or "resetting") mechanism is ignored in the model as only short-term phenomena are considered.

The baroreceptor reflex response depends on the net effect of all the baroreceptor impulses arriving at the brain. The firing frequency of each baroreceptor nerve fibre is known to depend on the blood pressure level and its first time-derivative. Katona et al (1967) developed a highly simplified empirical model in which the net effect at the brain of all the baroreceptor impulses was characterised by a single "input function" (B_1). B_1 was computed from the systolic pressure (P_S) and the diastolic pressure (P_D) in one cardiac cycle as follows :

$$B_o = \frac{P_S + P_D}{2} + K_A(P_S - P_D) - K_B \qquad ---(3.1)$$

$$B_1 = \begin{cases} B_o , & B_o > 0 \\ 0 , & B_o \leq 0 \end{cases} \qquad ---(3.2)$$

In eqn. (3.1), the term $\frac{P_S + P_D}{2}$ gives an approximation for the mean arterial pressure and the term $K_A(P_S - P_D)$, which is proportional to the pulse pressure, reflects the sensitivity of the baroreceptors to the positive time-derivative of pressure. The constant K_B represents a steady state threshold pressure below which baroreceptor firing does not occur. Equation (3.2) ensures that the input function does not become negative which would correspond to a physically meaningless negative firing rate.

In Katona's model, B_1 is a constant for each cardiac cycle. In reality, the baroreceptor impulse activity is not steady throughout the cardiac cycle but occurs in bursts with the main activity during systole. Katona's model is therefore modified here to include the high speed dynamics occurring within the cardiac cycle. In addition, separate representations of the aortic arch and carotid sinus baroreceptors are incorporated because the blood pressures in these regions may differ considerably when large intrathoracic pressure changes occur e.g. during a Valsalva manoeuvre.

For each baroreceptor area, the following equations apply :

$$S_A = \begin{cases} \frac{dP}{dt} , & \frac{dP}{dt} > 0 \\ 0 , & \frac{dP}{dt} \leq 0 \end{cases} \qquad ---(3.3)$$

$$\frac{dS_B}{dt} = \frac{P - S_B}{\tau_1} \qquad ---(3.4)$$

$$\frac{dS_C}{dt} = \frac{S_A - S_C}{\tau_2} \qquad ---(3.5)$$

$$S_D = S_B + K_C S_C - K_D \qquad ---(3.6)$$

$$B_2 = \begin{cases} S_D , & S_D > 0 \\ 0 , & S_D \leq 0 \end{cases} \qquad ---(3.7)$$

Equation (3.3) represents the unidirectional rate sensitivity of the baroreceptors. The positive time-derivative of pressure (s_A) is passed through a first-order low-pass filter (eqn. 3.5) with a very short time constant (τ_2) to give a dynamic estimate (S_C) of the positive pressure derivative. A dynamic mean pressure estimate (S_B) is obtained by passing the pressure through a first-order low-pass filter (eqn. 3.4) with a longer time constant (τ_1). The linear combination of the mean and derivative estimates (eqn. 3.6) together with the constraint that firing rate must be positive (eqn. 3.7) gives the output function (B_2) for an individual baroreceptor area. Fig. 3.1 gives a block diagram representation of an individual baroreceptor model.

The threshold pressure K_B in eqn. (3.1) is given by Beneken & Dewit (1967) as 40 mmHg so K_D in eqn. (3.6) is set to 40 mmHg. Beneken & Dewit (1967) give the constant K_A of eqn. (3.1) as 1.5 and so for a normal pulse pressure of 40 mmHg, $K_A(P_S - P_D)$ has a value of 60. This value represents the average contribution of the positive pressure derivative term over one cardiac cycle. To estimate K_C in eqn. (3.6), it is assumed that the average value of $K_C S_C$ over one cardiac cycle is also 60 i.e.

$$\frac{1}{T_H}\int_{t_1}^{t_1+T_H} K_C S_C \, dt = 60$$

giving

$$K_C = \frac{60\,T_H}{\int_{t_1}^{t_1+T_H} S_C \, dt} \qquad ---(3.8)$$

For normal heart rate and blood pressure the value of K_C is calculated from eqn. (3.8) to be approximately 1.0 .

The effective input for the central nervous system is assumed to be a static function of the output of the carotid sinus baroreceptors (B_{UA}) and the aortic arch baroreceptors (B_{AOZ}) i.e.

$$B = f(B_{UA}, B_{AOZ}) \qquad ---(3.9)$$

A further assumption is made that the function of eqn. (3.9) can be approximated satisfactorily by linearisation about an operating point to give the following weighted sum :

$$B = \alpha B_{UA} + (1-\alpha) B_{AOZ} \qquad ---(3.10)$$

where α is a constant in the range $0 \leq \alpha \leq 1$. This formulation of the effective CNS input function is illustrated in fig. 3.2 .

Dampney et al.(1971) investigated the relative steady state gains of the carotid sinus and aortic arch baroreceptor systems in dogs by observing the effect on hindlimb vascular resistance when one baroreceptor area was stimulated and the other was eliminated. The ratio of the gain of the carotid sinus system to the gain of the aortic arch system was found to be 2.22:1.06 . It is assumed that this result applies approximately to the gain ratio in the human system so α is set to 0.7 in eqn. (3.10).

Beneken & Dewit (1967) used Katona's approach (eqns. 3.1 & 3.2) to represent the combined effect of the baroreceptors in the aortic arch and carotid sinus regions. P_S was replaced by a linear combination of systolic pressures in the two regions and P_D was replaced by a similar linear combination of diastolic pressures in the two regions. This approach cannot be applied when the rapid dynamics within the cardiac cycle are considered because the individual baroreceptor models are nonlinear and the principle of superposition is not applicable.

3.2 Central nervous control of heart rate

The mathematical model of heart rate control is based on work by Katona et al.(1967). Katona performed experiments on chloralose-anaesthetised dogs in which a balloon was inflated in the thoracic aorta to obstruct blood flow and changes in blood pressure and heart rate were observed. From a study of the experimental results, a two-region dynamic empirical model was formulated and the parameters were determined by least-squares fitting techniques. It is assumed

here that this model is applicable to an unanaesthetised human.

For blood pressures above normal, the central nervous input function B is greater than a threshold value K_E and heart rate responses are relatively large and fast and mainly of vagal (cardioinhibitory) origin. In this region (region A), Katona found that the heart period increased faster than it decreased i.e. the response was asymmetric. The dynamics of region A are approximated by a first order system and the features of the response are described by the following equations :

$$u_A = \begin{cases} (B - K_E) , & B > K_E \\ 0 , & B \leq K_E \end{cases} \qquad ---(3.11)$$

$$u_B = \begin{cases} 1.5 , & \frac{du_A}{dt} > 0 \\ 4.5 , & \frac{du_A}{dt} \leq 0 \end{cases} \qquad ---(3.12)$$

$$\frac{du_C}{dt} = \frac{u_A - u_C}{u_B} \qquad ---(3.13)$$

For blood pressures below normal, the input function B is generally less than the threshold value K_E and heart rate responses are relatively small and slow and mainly of sympathetic (cardioaccelerator) origin. In this region (region B), the dynamics are approximated by a second order system and described by the following equations :

$$u_D = \begin{cases} K_E , & B > K_E \\ B , & B \leq K_E \end{cases} \qquad ---(3.14)$$

$$\frac{du_E}{dt} = \frac{u_D - u_E}{\tau_3} \qquad ---(3.15)$$

$$\frac{du_F}{dt} = \frac{u_E - u_F}{\tau_4} \qquad ---(3.16)$$

The overall response of the controller is obtained by forming a linear combination of the outputs in regions A and B :

$$u_G = K_F (u_C + u_F) \qquad ---(3.17)$$

The quantity u_G in eqn. (3.17) represents a continuously varying estimate of heart period for use in the next cardiac cycle.

Heart rates above about 200 bpm are on the verge of fibrillation in man. Also heart rates below about 30 bpm are incompatible with

viable homeostasis and so the heart rate (f_H) in the model is limited to a range $30 \leq f_H \leq 200$ bpm. The following constraint on the estimated heart period is therefore added to Katona's basic model :

$$u_H = \begin{cases} 2.0, & u_G \geq 2.0 \\ u_G, & 0.3 < u_G < 2.0 \\ 0.3, & u_G \leq 0.3 \end{cases} \qquad ---(3.18)$$

A block diagram of the heart rate controller based on equations (3.11) to (3.18) is given in fig. 3.3 .

The heart period to be used for the next cardiac cycle (T_H) is obtained by sampling the continuously varying u_H at the end of the current cardiac cycle. The value of T_H then stays constant during the cardiac cycle because the heart is refractory to further stimuli until the cycle is complete.

The values of constants and initial conditions used in this model are given in Appendix 2. The numerical values given by Katona are employed because, as Beneken & Dewit (1967) pointed out, it is difficult to predict in which direction any changes of parameter should be made in nonlinear control systems such as this.

A facility is provided in the digital computer program to switch between the neural control of heart rate and a fixed preset heart rate. The latter is used in the simulation of pacing experiments.

3.3 Central nervous control of peripheral resistance

Smooth muscle in the walls of the arterioles is normally in a state of partial contraction due to sympathetic tone originating from the medullary vasomotor centre. A reduction of sympathetic activity (e.g. resulting from a rise in blood pressure) leads to vasodilatation and a decrease of peripheral resistance. Conversely, an increase of sympathetic activity (e.g. resulting from a fall in blood pressure) leads to vasoconstriction and an increase of peripheral resistance. A mathematical model of peripheral resistance control must approximate these effects satisfactorily.

In view of the high degree of accuracy in the control of blood pressure and the occurrence of spontaneous very low frequency oscillations in blood pressure, Hyndman (1970) suggested that empirical models of central nervous control should incorporate bang-bang or on-off control actions. In applying this approach to

peripheral resistance control, Hyndman used the input function B which represented all the systemic arterial baroreceptor activity. The output of the controller was a time-varying peripheral resistance R. Hyndman's peripheral resistance controller may be described by the following equations :

$$q = \begin{cases} 0.5 , & B > K_E \\ 1.5 , & B \leq K_E \end{cases} \qquad ---(3.19)$$

$$\frac{\mathcal{L}(R)}{\mathcal{L}(q)} = \frac{(1+7.95s)\, e^{-1.5s}}{(1+4s)\,(1+20s)} \qquad ---(3.20)$$

The bang-bang action represented by eqn. (3.19) occurs when the input function B crosses the threshold value K_E (normally 80) which is used in the heart rate controller of Katona et al.(1967) described in section 3.2 .

Equation (3.20) gives the transfer function of the linear part of the controller. It is seen that the second order system has time constants of 4 sec and 20 sec respectively and that a time delay of 1.5 sec is incorporated. Hyndman obtained these numerical values by analysis of data from experiments in which digital blood flow was observed after pressing the neck in the carotid sinus region of a conscious man.

In adapting Hyndman's representation to the mathematical model here, certain changes are made. The time-domain description of the modified version is as follows :

$$q_A = \begin{cases} 0.6 , & B > K_E \\ 1.4 , & B \leq K_E \end{cases} \qquad ---(3.21)$$

$$\frac{dq_B}{dt} = \frac{q_A - q_B}{4} \qquad ---(3.22)$$

$$\frac{dq_C}{dt} = \frac{q_A - q_C}{20} \qquad ---(3.23)$$

$$q_D = 0.75\, q_C + 0.25\, q_B \qquad ---(3.24)$$

A block diagram representation of these relationships is given in fig. 3.4 . The output (q_D) in eqn. (3.24) is a dimensionless quantity which multiplies the normal values of arteriovenous resistance in the bronchial, intestinal, abdominal and leg vascular beds in the model.

Equations (2.43) to (2.46) in section 2.4 of chapter 2 become modified with the introduction of peripheral resistance control as follows :

$$F_{BRONC} = \frac{P_{AO3} - P_{RA}}{q_D \, R_{BRONC}} \qquad ---(3.25)$$

$$F_{IAIV} = \frac{P_{IA} - P_{IV}}{q_D \, R_{INT}} \qquad ---(3.26)$$

$$F_{AAAV} = \frac{P_{AA} - P_{AV}}{q_D \, R_{ABD}} \qquad ---(3.27)$$

$$F_{CACV} = \frac{P_{CA} - P_{CV}}{q_D \, R_{LEG}} \qquad ---(3.28)$$

Other systemic vascular beds are assumed to be uninfluenced by central nervous control. The pulmonary vasculature is known to be highly non-reactive to both neural and humoral control (Rushmer, 1970 ; p.165) and so is also excluded from peripheral resistance control in the model.

The bang-bang values of eqn. (3.21) give a maximum variation of resistance in any controlled vascular bed of $\pm 40\%$ and result in q_D having a normal steady state value of about 1.0 .

Equations (3.22) to (3.24) represent a parallel decomposition of the original transfer function of Hyndman, omitting the time delay. By transforming these equations to the complex frequency domain using Laplace transforms, the transfer function relating q_D to q_A is

$$\frac{\mathcal{L}(q_D)}{\mathcal{L}(q_A)} = \frac{(1+8s)}{(1+4s)(1+20s)} \qquad ---(3.29)$$

The time delay of 1.5 sec in Hyndman's model is ignored for two reasons :

(a) Hyndman states that the average time from the onset of neck pressure to the onset of the digital flow response is approximately 1.5 sec . Consider a Heaviside unit step input to the transfer function of eqn. (3.29) i.e. $q_A = H(t)$. The output after 1.5 sec is given by

$$(q_D)_{t=1.5} = 0.75\left(1 - e^{-1.5/20}\right) + 0.25\left(1 - e^{-1.5/4}\right) = 0.13$$

This means that after 1.5 sec only 13% of the input change would be observable at the output. Such a small change would only just

be observable within the limits of experimental error so the "delay" observed by Hyndman cannot be distinguished clearly from the lag in the response of the transfer function itself. The numerical values are of course very approximate anyway.

(b) A pure time delay adds considerably to the computation time in the digital simulation due to the storage and retrieval of previous values and the interpolation between previous values.

A facility is provided in the digital computer program to switch between the neural control of peripheral resistance (q_D variable) and fixed, normal values of arteriovenous resistances (q_D=1.0).

3.4 Central nervous control of myocardial contractility

The heart muscle has sympathetic innervation and increased sympathetic activity in the medullary centres (e.g. as a result of a fall in blood pressure) results in a positive inotropic response i.e. more powerful contraction of the ventricular musculature. There is no universally agreed measure of the contractile state of the heart and several myocardial contractility measures are in current use (e.g. maximum rate of change of left ventricular outflow, maximum rate of change of left ventricular pressure, etc.).

The equation relating pressure, volume and elastance in the lumped parameter representation of a heart chamber is as follows :

$$P = a(t)[V - V_u] \qquad ---(3.30)$$

In this model, the systolic elastance is used as a myocardial contractility measure and is given by

$$a_s = \left(\frac{dP}{dV}\right)_{max} \qquad ---(3.31)$$

This is a reasonable measure because both maximum pressure and maximum rate of change of pressure increase as a_s is increased. Tests on the digital simulation described in chapters 6 and 7 confirm that systolic elastance is an acceptable measure of contractility when compared with other commonly used measures in the same tests.

Hyndman (1970) developed a simple first order dynamic empirical model of left ventricular contractility control which, like the peripheral resistance control described in section 3.3, employed bang-bang or on-off control. The input of Hyndman's model is the input

function B which represents the general systemic baroreceptor activity and the output is the left ventricular systolic elastance.

Adapting Hyndman's approach to the model here, the equations describing the myocardial contractility controller are :

$$b_A = \begin{cases} 0.6, & B > K_E \\ 1.4, & B \leq K_E \end{cases} \qquad ---(3.32)$$

$$\frac{db_B}{dt} = \frac{b_A - b_B}{10} \qquad ---(3.33)$$

A block diagram of the controller is given in fig. 3.5 .

In eqn. (3.32) the input function B is compared with the threshold K_E which is used in the heart rate controller of Katona et al. (1967) described in section 3.2. The bang-bang levels are chosen so that the maximum variation of b_B is $\pm 40\%$ and the steady state value of b_B is approximately 1.0 . Equation (3.33) represents a first order system with a time constant of 10 sec which was determined by Hyndman from analysis of data in the physiology literature.

The output b_B in eqn. (3.33) is a dimensionless variable which multiplies the normal systolic elastances in all four heart chambers. Equations (2.14) to (2.17), defining the elastance functions of the four heart chambers, are modified as follows :

$$a_{RA} = x_3\left[b_B a_{RAS} - a_{RAD}\right] + a_{RAD} \qquad ---(3.34)$$

$$a_{RV} = x_5\left[b_B a_{RVS} - a_{RVD}\right] + a_{RVD} \qquad ---(3.35)$$

$$a_{LA} = x_3\left[b_B a_{LAS} - a_{LAD}\right] + a_{LAD} \qquad ---(3.36)$$

$$a_{LV} = x_5\left[b_B a_{LVS} - a_{LVD}\right] + a_{LVD} \qquad ---(3.37)$$

Beneken & Dewit (1967) included a direct relationship between heart rate and myocardial contractility in their model. However, Noble et al. (1966) pointed out that, in the physiological range in conscious dogs, changing heart rate has little, if any, effect on myocardial contractility. There is a possibility that any direct positive inotropic effect of increasing heart rate could be counteracted by a reflex negative inotropic effect due to sympathetic

outflow reduction as a result of the blood pressure rise induced by the increased heart rate. Despite this, a direct relationship is not incorporated in the model.

Hyndman (1970) tested a simplified 11th order circulatory fluid mechanics model incorporating the above first order control of left ventricular contractility and found that this reflex was insignificant in comparison with the venous tone reflex. He therefore excluded the left ventricular contractility reflex from any further work. Nevertheless, myocardial contractility control is included in the model described here for the following reasons :

(a) The model used here is considerably more detailed than that used by Hyndman and it is not certain that the contractility reflex will be insignificant in this case, either alone or in combination with other reflexes.

(b) The model is intended ultimately to study the effects of circulating drugs including those with inotropic actions and there is a possibility of significant cooperation or competition between the neural control action and the drug action

A facility is provided in the digital computer program for switching between neural control of myocardial contractility (b_B variable) and fixed, normal values of systolic elastances ($b_B = 1$).

3.5 Central nervous control of venous tone

Venous or venomotor tone refers to the active constriction or dilation of venules caused by variations of arterial pressure and mediated through the sympathetic nervous system. Following a suggestion of Snyder & Rideout (1969), it is assumed that changes of venous tone result in changes of the unstressed volumes and compliances of lumped parameter venous segments.

As in the peripheral resistance and myocardial contractility control systems, Hyndman (1970) assumed that bang-bang or on-off control was appropriate for central nervous control of venous tone. Adapting Hyndman's version for the model here, the equations are as follows :

$$d_A = \begin{cases} 0.7 , & B > K_E \\ 1.6 , & B \leq K_E \end{cases} \qquad ---(3.38)$$

$$\frac{dd_B}{dt} = \frac{d_A - d_B}{14} \qquad ---(3.39)$$

$$d_C = K_G d_B + (1 - K_G) \qquad ---(3.40)$$

$$d_D = K_H d_B + (1 - K_H) \qquad ---(3.41)$$

A block diagram of the controller is given in fig. 3.6 . The input function B (representing the general systemic baroreceptor activity) is compared with the threshold K_E which is used in the heart rate controller of Katona et al. (1967) described in section 3.2 . In eqn. (3.38), the bang-bang levels are adjusted so that the maximum variation of the compliance or unstressed volume in a controlled segment is about $\pm 40\%$ and the steady state value of d_B is about 1.0 . Following Hyndman (1970) the linear part of the controller is a first order system with a time constant of 14 sec as in eqn. (3.39).

The compliances in controlled segments are divided by the dimensionless variable d_C in eqn. (3.40) and the unstressed volumes are divided by the variable d_D of eqn. (3.41). Division is required in this case to ensure that the control system exhibits negative feedback. If the blood pressure rises, venous tone will decrease and the venous compliance and unstressed volume will increase thus lowering the venous pressure. This will result in reduced venous return and reduced cardiac output so that the original blood pressure rise will be limited.

The constants K_G and K_H in eqns. (3.40) and (3.41) respectively control the percentage deviation of d_C and d_D from the normal value of 1.0 .

Equations (2.47) and (2.48) for a typical systemic venous segment are modified in the following manner for controlled venous segments :

$$V_{u2} = \frac{V_{u2N}}{d_D} \qquad ---(3.42)$$

$$P_2 = \frac{d_C}{C_2}\left[V_2 - V_{u2}\right] \qquad ---(3.43)$$

$$C_2 = \begin{cases} C_{2N}, & V_2 > V_{u2} \\ 20\,C_{2N}, & V_2 \leq V_{u2} \end{cases} \qquad ---(3.44)$$

In the model, sympathetic innervation is assumed only in the head and arms veins, intestinal veins, abdominal veins and leg veins segments.

A facility is provided in the digital computer program for switching between neural control of venous tone (d_c , d_D variable) and fixed, normal values of compliance and unstressed volume ($d_c = d_D = 1$).

3.6 Conclusion

Empirical models of the aortic arch and carotid sinus baroreceptors and the central nervous control of heart rate, peripheral resistance, myocardial contractility and venous tone have been presented in this chapter. These models are based on the work of Katona (1967) and Hyndman (1970) with the following principal additions and modifications by the author :

(a) Separate aortic arch and carotid sinus baroreceptors
(b) Pulsatile baroreceptor dynamics
(c) Adaptation of the controllers to the 19-segment circulatory fluid mechanics model.

The overall neural control model is of order 11 and provides a compact and satisfactory representation of central nervous control mechanisms for use with the circulatory fluid mechanics and pharmacokinetics models. The adequacy of the neural control models will be assessed in the validation tests on the complete model described in chapter 6.

The complete set of equations of the neural control model is given in Appendix 1 and the numerical values of constants and initial conditions are given in Appendix 2.

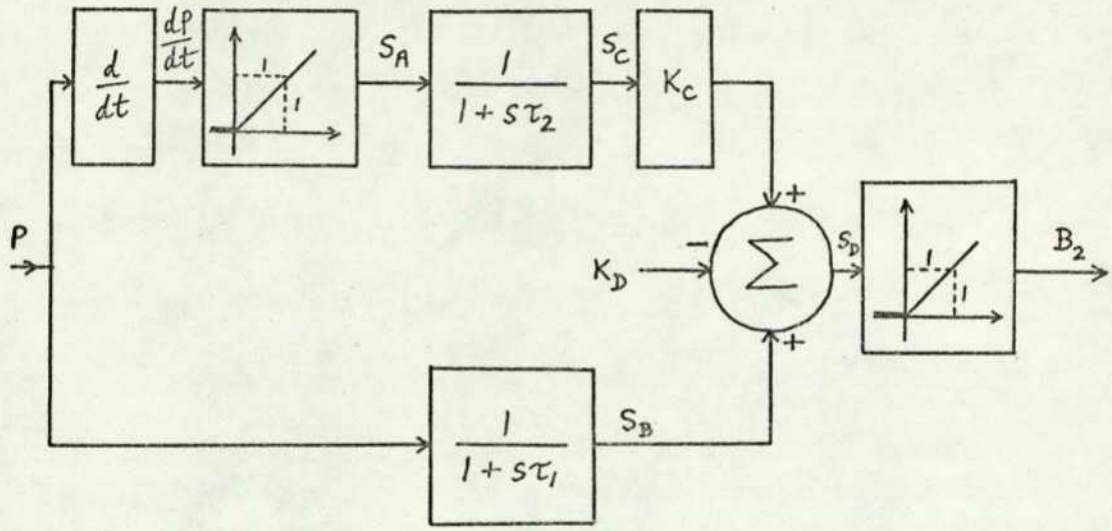

FIG. 3.1 BLOCK DIAGRAM OF AN INDIVIDUAL BARORECEPTOR MODEL

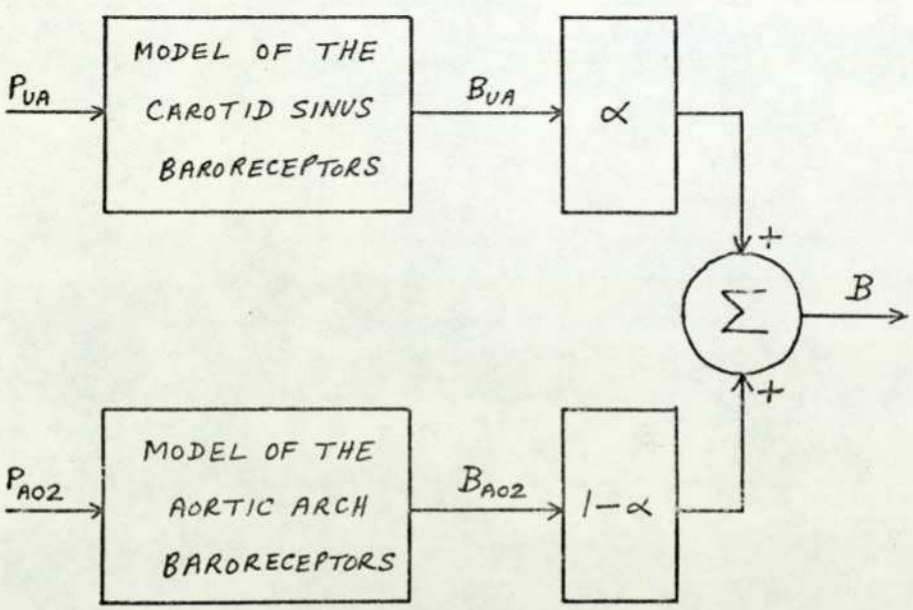

FIG. 3.2 LINEAR COMBINATION OF BARORECEPTOR OUTPUTS TO GIVE THE CNS INPUT FUNCTION (B)

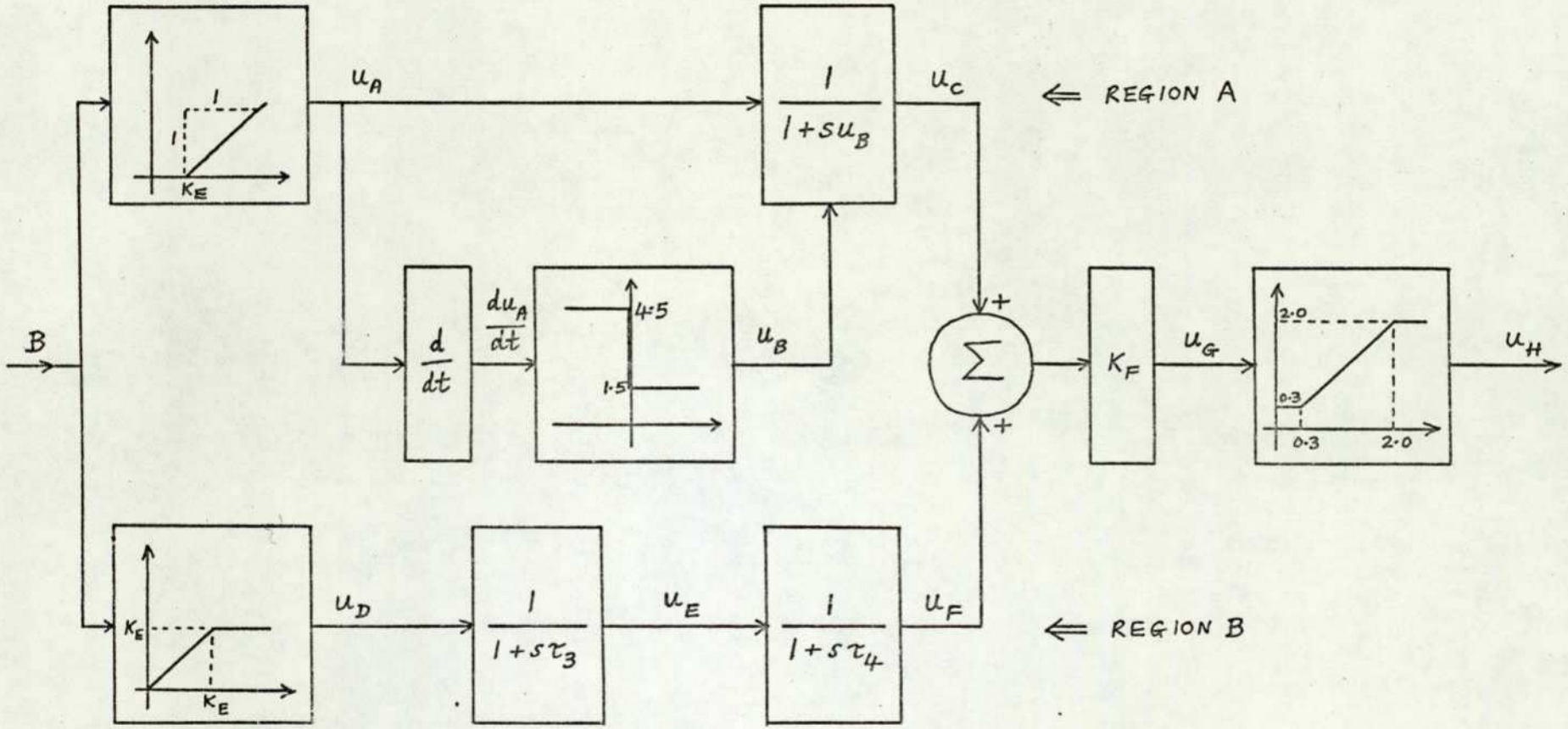

FIG. 3.3 BLOCK DIAGRAM OF THE HEART RATE CONTROLLER BASED ON THE MODEL OF KATONA ET AL (1967)

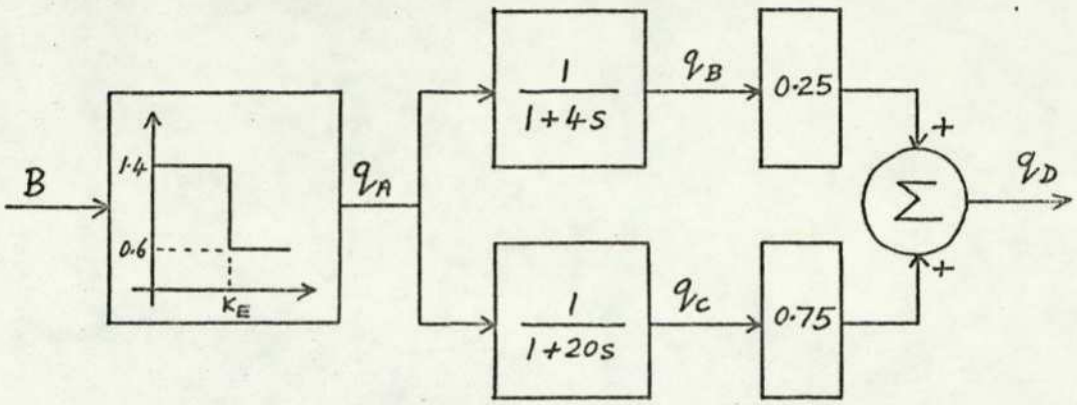

FIG. 3.4 BLOCK DIAGRAM OF THE PERIPHERAL RESISTANCE CONTROLLER

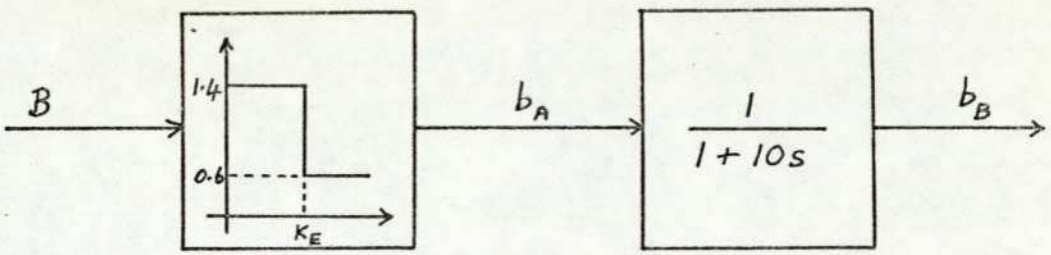

FIG. 3.5 BLOCK DIAGRAM OF THE MYOCARDIAL CONTRACTILITY CONTROLLER

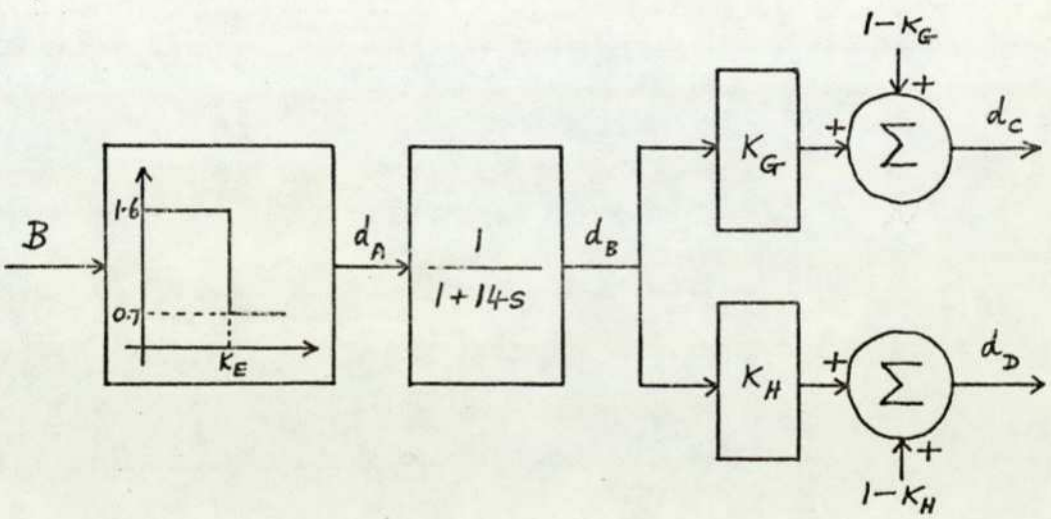

FIG. 3.6 BLOCK DIAGRAM OF THE VENOUS TONE CONTROLLER

CHAPTER 4

A MATHEMATICAL MODEL OF PHARMACOKINETICS

The complete model is to be used for the study of short-term pharmacokinetics i.e. the effects of an injected drug in which the major dynamics are complete within two or three minutes. This chapter describes an appropriate mathematical model of the injection, transport and action of a single drug which can be combined with the circulatory fluid mechanics model of chapter 2 and the neural control model of chapter 3.

4.1 A model of drug transport

A method for representing the blood transport of a chemical substance which is applicable to lumped parameter models is the "multiple modelling" technique of Beneken & Rideout (1968). In this method, segments of a slave transport model are coupled to the corresponding segments of the master blood circulation model so that transport flow is proportional to concentration in the transport model multiplied by flow in the circulation model.

Referring to fig. 4.1, the mathematical description is formulated in the following way :

The mass inflow of the nth segment is $\omega_{n-1,n} F_{n-1,n}$ where

$$\omega_{n-1,n} = \begin{cases} \omega_{n-1} , & F_{n-1,n} > 0 \\ \omega_n , & F_{n-1,n} \leq 0 \end{cases} \qquad ---(4.1)$$

The variable $\omega_{n-1,n}$ is the concentration appropriate to the direction of flow between the (n-1)th and nth segments.

The mass outflow of the nth segment is similarly $\omega_{n,n+1} F_{n,n+1}$ where

$$\omega_{n,n+1} = \begin{cases} \omega_n , & F_{n,n+1} > 0 \\ \omega_{n+1} , & F_{n,n+1} \leq 0 \end{cases} \qquad ---(4.2)$$

The rate of change of mass in the nth segment is given by

$$\frac{dm_n}{dt} = \omega_{n-1,n} F_{n-1,n} - \omega_{n,n+1} F_{n,n+1} , \; m_n \geq 0 \qquad --(4.3)$$

The concentration within the rth lumped segment is simply the mass per unit volume i.e.

$$\omega_r = \frac{m_r}{V_r} \qquad ---(4.4)$$

It is desirable that the model should simulate the transport delay which occurs before the arrival of the drug at a site distant from the point of injection. By considering a special case, it may be demonstrated that as the number of segments used to represent a given length of blood vessel is increased, a closer and closer approximation to a pure delay is obtained.

Suppose the flow F is constant and unidirectional and each segment has an identical volume V. If the total volume of blood in the vessel considered is V_T and if N segments are used, the volume of each segment is

$$V = \frac{V_T}{N} \qquad ---(4.5)$$

Applying equations (4.1) to (4.4), the differential equation for the nth segment is

$$\frac{dm_n}{dt} = \frac{F}{V}\left(m_{n-1} - m_n\right) \qquad ---(4.6)$$

Taking Laplace transforms of eqn. (4.6) and rearranging :

$$\frac{\mathcal{L}(m_n)}{\mathcal{L}(m_{n-1})} = \frac{1}{1 + s\left(\frac{V}{F}\right)} \qquad ---(4.7)$$

Each segment therefore corresponds to a first order lag with a time constant of $\frac{V}{F}$ sec.

Applying eqn. (4.7) to each segment in turn, multiplying the resulting equations together and substituting for V using eqn. (4.5):

$$\frac{\mathcal{L}(m_N)}{\mathcal{L}(m_o)} = \frac{1}{\left(1 + \frac{s V_T}{NF}\right)^N} \qquad ---(4.8)$$

For an infinite number of segments, each of infinitesimal length, eqn. (4.8) becomes

$$\frac{\mathcal{L}(m_\infty)}{\mathcal{L}(m_o)} = \frac{1}{\lim_{N\to\infty}\left(1 + \frac{sV_T}{NF}\right)^N} = e^{-s\left(\frac{V_T}{F}\right)} \qquad ---(4.9)$$

which, in transfer function terms, corresponds to a pure delay of $\frac{V_T}{F}$ sec between the entry of the drug into the blood vessel and its exit from the vessel. The above equations are analogous to those obtained in the analysis of an electrical transmission line with distributed resistance and capacitance.

The circulatory fluid mechanics model described in chapter 2 has 19 segments so the slave transport model will also have 19 segments. The accuracy of representation in this case is investigated in one of the validation tests described in chapter 6.

The incorporation of genuine transport delays in the digital simulation is considered unsuitable because there are 24 links between the 19 segments and the flow is variable in each case so that 24 variable time delays would be required which would impose an intolerable computational burden.

In the digital computer program, a facility is provided to switch out all the equations concerned with drug transport if these are not required in order to save computing time (e.g. in some of the validation tests described in chapter 6)

4.1.1 Drug injection

The time taken to complete an injection is assumed to be very short compared with the time constants of the transport dynamics in the model and the volume of the injection is assumed to be negligible compared with the volume of the segment being injected.

If the mass of drug contained in the injection is M then an injection into the nth segment at time t_I may be modelled quite simply by introducing a Dirac delta-function in eqn. (4.3) as follows :

$$\frac{dm_n}{dt} = M\,\delta(t-t_I) + \omega_{n-1,n}\,F_{n-1,n} - \omega_{n,n+1}\,F_{n,n+1} \qquad ---(4.10)$$

An average human is assumed to weigh 70 kg so if the dosage of the drug is Δ μg per kg of body weight, the injected mass will be

$$M = 70\Delta \ \mu g$$

The delta function in eqn. (4.10) is implemented in the digital simulation by increasing the mass m_n by M units at time $t = t_I$. Normally, m_n will be zero prior to the injection and t_I will be zero.

4.1.2 Drug breakdown and absorption

As an injected drug moves round the circulatory system, the drug will be absorbed or transformed chemically. The effective concentration of the drug will decrease with time due to the breakdown

or absorption as well as decreasing because of dilution resulting from distribution throughout the blood volume.

An approximation is made in the model that the rate of change of mass due to breakdown is proportional to the remaining mass of drug in a segment and that the time constant for breakdown (τ_B) is identical in all segments. τ_B depends on the properties of the injected drug and a typical value is 30 sec.

Equation (4.3) is modified in the following manner :

$$\frac{dm_n}{dt} = \omega_{n-1,n} F_{n-1,n} - \omega_{n,n+1} F_{n,n+1} - \frac{m_n}{\tau_B} \qquad ---(4.11)$$

As t increases, the sum of the drug masses in all segments, $\sum_{n=1}^{19} m_n$, decays exponentially to zero in this formulation. If breakdown or absorption does not occur ($\tau_B = \infty$), the injected drug mass M will eventually become uniformly distributed throughout the total blood volume V_T so that the concentrations in each segment of the model will tend to $\frac{M}{V_T}$.

4.2 A model of drug action

It is necessary to simulate the actions of the injected drug at specific sites in the circulation. The selected parameters to be influenced by the circulating drug are those already influenced by central nervous control viz. heart rate, peripheral resistance, myocardial contractility and venous tone. This choice encompasses the actions of a wide range of cardiovascular agents.

In the models of neural control described in chapter 3, simultaneous changes were assumed in all the variables under control of a particular central nervous controller e.g. all the arteriovenous resistances changed together in proportion under the influence of the peripheral resistance controller. In the case of a circulating drug, the agent arrives at different sites at different times because of transport delays and so the drug action at each site has to be modelled separately.

Consider a general circulatory parameter R which is subject to a combination of instantaneous neural and humoral influence. Let σ_N be a dimensionless variable corresponding to neural control action which is equal to 1.0 in the absence of neural control and deviates from 1.0

in the presence of neural control (as in the peripheral resistance, myocardial contractility and venous tone controllers described in chapter 3). Let σ_D be a dimensionless variable corresponding to drug action which is also equal to 1.0 in the absence of drug effects and deviates from 1.0 when drug effects are present. A mathematically compact and convenient empirical relationship which represents the combined neural and humoral influences on R is :

$$R = R_N \sigma_N \sigma_D \qquad ---(4.12)$$

where R_N is the normal value of the parameter R.

It is assumed that the change in R at a particular location depends on the drug concentration (ω) at that location and that the effect is instantaneous. If σ_N is regarded as constant for this analysis and if R increases as ω increases, a linearised relationship between R and ω implies that

$$\sigma_D = 1 + K\omega \qquad ---(4.13)$$

where K is a positive constant which determines the sensitivity of R to a given change in ω . Equation (4.13) is strictly applicable only to small values of ω but is extended here to all values of ω .

If R decreases as ω increases then σ_D could become negative for large ω in eqn.(4.13) which would result in a physically meaningless negative parameter R . To avoid this difficulty and also to provide a more realistic asymptotic approach of σ_D to zero with increasing ω , the following equation is used if R and ω change in opposite directions :

$$\sigma_D = \frac{1}{1 + K\omega} \qquad ---(4.14)$$

If the right hand side of eqn.(4.14) is expanded as a power series in ω and small values of ω are considered so that ω^2 and higher order terms are negligible, eqn.(4.14) reduces to

$$\sigma_D = 1 - K\omega \qquad ---(4.15)$$

Thus eqn.(4.14) has a similar linear characteristic to eqn.(4.13) for small ω .

In the digital computer program, a facility is provided for switching between eqns.(4.13) and (4.14) depending on whether a positive or negative drug action is required. Alternatively the drug action can be switched off altogether if necessary.

The application of the above empirical approach to specific locations of drug action is now considered.

4.2.1 Effect on heart rate

In the mathematical description, a chronotropic drug action is achieved by modifying the output of the heart rate controller in eqn.(3.17) as follows :

$$u_G = K_F \bar{\sigma}_H (u_C + u_F) \qquad ---(4.16)$$

where $\bar{\sigma}_H$ depends on the drug concentration in the vicinity of the sinoatrial node in the right atrium :

$$\bar{\sigma}_H = \begin{cases} 1 + \bar{\sigma}_2 \omega_{RA} & , \text{ bradycardia} \\ \dfrac{1}{1 + \bar{\sigma}_2 \omega_{RA}} & , \text{ tachycardia} \end{cases} \qquad ---(4.17)$$

The constant $\bar{\sigma}_2$ determines the sensitivity of the heart period to changes in drug concentration.

4.2.2 Effect on peripheral resistance

Vasoconstriction or vasodilatation produced by the drug action is implemented by modifying the equations describing flow through vascular beds. Equations (3.25) to (3.28) are changed as follows :

$$F_{BRONC} = \frac{P_{AO3} - P_{RA}}{q_D \bar{\sigma}_{BRONC} R_{BRONC}} \qquad ---(4.18)$$

$$F_{IAIV} = \frac{P_{IA} - P_{IV}}{q_D \bar{\sigma}_{INT} R_{INT}} \qquad ---(4.19)$$

$$F_{AAAV} = \frac{P_{AA} - P_{AV}}{q_D \bar{\sigma}_{ABD} R_{ABD}} \qquad ---(4.20)$$

$$F_{CACV} = \frac{P_{CA} - P_{CV}}{q_D \bar{\sigma}_{LEG} R_{LEG}} \qquad ---(4.21)$$

Also eqn.(2.41) is modified as overleaf.

$$F_{UAUV} = \frac{P_{UA} - P_{UV}}{\sigma_{HEAD} R_{HEAD}} \qquad ---(4.22)$$

Each σ variable introduced in eqns.(4.18) to (4.22) depends on the concentration of the drug in the preceding arterial segment in each case. Thus

$$\sigma_{BRONC} = \begin{cases} 1 + \sigma_I \omega_{AO3}, & \text{vasoconstriction} \\ \dfrac{1}{1 + \sigma_I \omega_{AO3}}, & \text{vasodilatation} \end{cases} \qquad ---(4.23)$$

$$\sigma_{INT} = \begin{cases} 1 + \sigma_I \omega_{IA}, & \text{vasoconstriction} \\ \dfrac{1}{1 + \sigma_I \omega_{IA}}, & \text{vasodilatation} \end{cases} \qquad ---(4.24)$$

$$\sigma_{ABD} = \begin{cases} 1 + \sigma_I \omega_{AA}, & \text{vasoconstriction} \\ \dfrac{1}{1 + \sigma_I \omega_{AA}}, & \text{vasodilatation} \end{cases} \qquad ---(4.25)$$

$$\sigma_{LEG} = \begin{cases} 1 + \sigma_I \omega_{CA}, & \text{vasoconstriction} \\ \dfrac{1}{1 + \sigma_I \omega_{CA}}, & \text{vasodilatation} \end{cases} \qquad ---(4.26)$$

$$\sigma_{HEAD} = \begin{cases} 1 + \sigma_I \omega_{UA}, & \text{vasoconstriction} \\ \dfrac{1}{1 + \sigma_I \omega_{UA}}, & \text{vasodilatation} \end{cases} \qquad ---(4.27)$$

The constant σ_I determines the sensitivity of the arteriovenous resistances to changes in drug concentration and is assumed to be the same for all vascular beds.

4.2.3 Effect on myocardial contractility

An inotropic drug action is represented in the model by modifying eqns.(3.34) to (3.37) giving the elastance functions of each of the heart chambers :

$$a_{RA} = x_3 \left[b_B \sigma_{RA} a_{RAS} - a_{RAD} \right] + a_{RAD} \qquad ---(4.28)$$

$$a_{RV} = x_5 \left[b_B \sigma_{RV} a_{RVS} - a_{RVD} \right] + a_{RVD} \qquad ---(4.29)$$

$$a_{LA} = x_3 \left[b_B \sigma_{LA} a_{LAS} - a_{LAD} \right] + a_{LAD} \qquad ---(4.30)$$

$$a_{LV} = x_5 \left[b_B \sigma_{LV} a_{LVS} - a_{LVD} \right] + a_{LVD} \qquad ---(4.31)$$

Each σ^- variable in eqns.(4.28) to (4.31) depends on the concentration of the drug in the corresponding heart chamber :

$$\sigma_{RA} = \begin{cases} 1 + \sigma_3^- \omega_{RA} & , \text{ positive inotropy} \\ \dfrac{1}{1 + \sigma_3^- \omega_{RA}} & , \text{ negative inotropy} \end{cases} \qquad ---(4.32)$$

$$\sigma_{RV} = \begin{cases} 1 + \sigma_3^- \omega_{RV} & , \text{ positive inotropy} \\ \dfrac{1}{1 + \sigma_3^- \omega_{RV}} & , \text{ negative inotropy} \end{cases} \qquad ---(4.33)$$

$$\sigma_{LA}^- = \begin{cases} 1 + \sigma_3^- \omega_{LA} & , \text{ positive inotropy} \\ \dfrac{1}{1 + \sigma_3^- \omega_{LA}} & , \text{ negative inotropy} \end{cases} \qquad ---(4.34)$$

$$\sigma_{LV}^- = \begin{cases} 1 + \sigma_3^- \omega_{LV} & , \text{ positive inotropy} \\ \dfrac{1}{1 + \sigma_3^- \omega_{LV}} & , \text{ negative inotropy} \end{cases} \qquad ---(4.35)$$

The constant σ_3^- determines the sensitivity of the individual systolic elastances to changes in drug concentration and is assumed to be the same for each heart chamber.

4.2.4 Effect on venous properties

Venoconstriction or venodilatation produced by the circulating drug is represented in the model by modifying the compliances and unstressed volumes of venous segments.

Considering a typical venous segment under central nervous control, eqns.(3.42) and (3.43) are changed in the following way :

$$V_{u2} = \frac{V_{u2N}}{d_D \sigma_u^-} \qquad ---(4.36)$$

$$P_2 = \frac{d_c \sigma_c^-}{C_2}\left[V_2 - V_{u2}\right] \qquad ---(4.37)$$

For venous segments not subject to central nervous control, the equations are similar to (4.36) and (4.37) except that $d_c = d_D = 1$.

The variables σ_u^- and σ_c^- represent the effect of the drug on the unstressed volume and compliance respectively and depend on the drug concentration in the venous segment (ω_V) as follows :

$$\sigma_u^- = \begin{cases} 1 + \sigma_4^- \omega_V & , \text{ venoconstriction} \\ \dfrac{1}{1 + \sigma_4^- \omega_V} & , \text{ venodilatation} \end{cases} \qquad ---(4.38)$$

$$\sigma_c^- = \begin{cases} 1 + \sigma_5^- \omega_V & , \text{ venoconstriction} \\ \dfrac{1}{1 + \sigma_5^- \omega_V} & , \text{ venodilatation} \end{cases} \qquad ---(4.39)$$

The constant σ_4 determines the sensitivity of the venous unstressed volume to changes in drug concentration. Likewise, the constant σ_5 determines the sensitivity of the venous compliance to changes in the drug concentration. Each constant is assumed to be the same in all venous segments.

As the effects on veins are not considered important for the types of cardiovascular agent studied, the above drug effect model is not included as an integral part of the digital simulation program. However it is found necessary to introduce drug-induced venous changes in the particular case of noradrenaline and this is discussed further in chapter 7.

4.3 Conclusion

A model of the injection, transport, action and breakdown of a single cardiovascular agent has been presented in this chapter. The "multiple modelling" technique is used to represent drug transport and new empirical algebraic models of drug-induced changes in heart rate, peripheral resistance, myocardial contractility and venous properties are employed.

In combination with the previously described models of circulatory fluid mechanics and neural control, the pharmacokinetics model provides an adequate and computationally manageable mathematical tool for the study of cardiovascular dynamics following the injection of a drug with specified properties.

The complete set of equations for the 19th order pharmacokinetics model is given in Appendix 1. The values of all the constants and initial conditions used are given in Appendix 2.

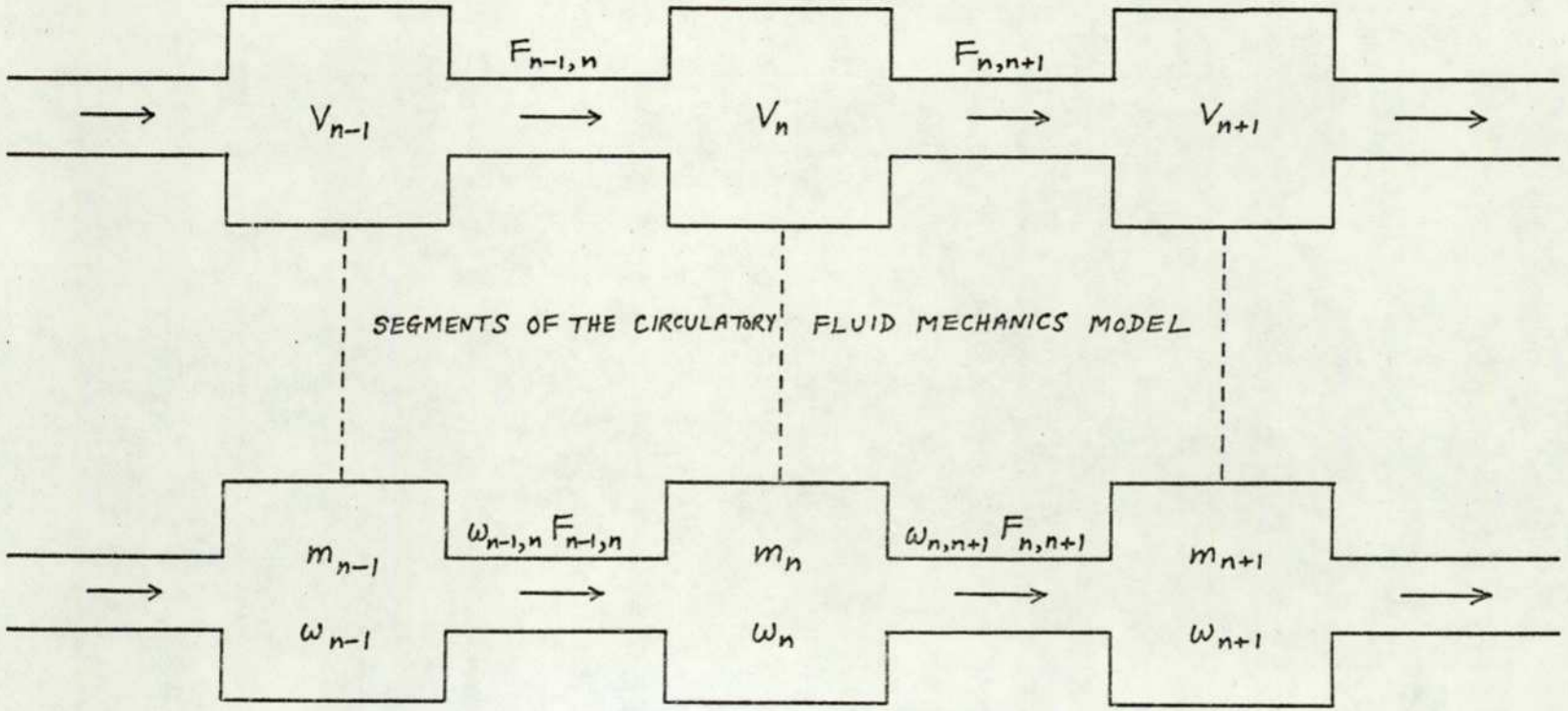

FIG. 4.1 BLOCK DIAGRAM TO ILLUSTRATE THE MULTIPLE MODELLING TECHNIQUE OF BENEKEN & RIDEOUT (1968)

CHAPTER 5

DEVELOPMENT OF A DIGITAL SIMULATION

Having developed mathematical models of circulatory fluid mechanics, neural control and pharmacokinetics, the equations have to be solved in order that the complete model can be validated and subsequently used to study the effects of drugs. This chapter deals with a digital computer solution of the mathematical model and examines the problems that arise in implementation and the methods used to solve these problems.

5.1 Selection of a suitable simulation technique

When the various sections of the model are assembled (fig. 5.1), it is found that the mathematical description consists of 61 first order differential equations and 159 algebraic equations (table 5.1). An analytical solution is clearly neither practical (due to the number of equations) nor possible (due to the nonlinearities in the system). In selecting a suitable simulation technique, the following interrelated factors have to be considered :

(1) Speed of solution
(2) Accuracy of results
(3) Flexibility
(4) Convenience in use
(5) Accessibility
(6) Cost

In view of the large number of equations in the model and also the large number of runs required for testing, validation and experimental work, the speed of solution is the primary consideration.

Of the alternative methods outlined in section 1.4.2, a computer solution provides the best approach particularly in terms of the flexibility required during model development.

The analog computer provides the fastest solution due to the truly parallel processing operation which makes the solution speed independent of the problem size. The speed of solution can be increased if necessary by the process of time-scaling. A disadvantage of the analog computer when solving very large systems of equations is the large amount of equipment required. In the case of the present model,

an analog computer with 61 integrators and capable of handling 159 algebraic equations was not available and so this approach had to be abandoned.

The hybrid computer attempts to combine the advantages of the digital and analog machines and can function at very high speeds using the parallel processing capability of the analog computer. Mawson (1975) has indicated that a typical advanced hybrid computing system can operate about 40 times faster than a CDC 7600 computer or about 6 times faster than the ILLIAC IV machine (Slotnick, 1971). Again, due to the large number of equations in the model, a hybrid computer with a suitably large analog machine was not available and so the advantages of this approach could not be pursued.

A digital computer solution was the only alternative method remaining. The widely available serial digital computer enables very large nonlinear, time-varying problems to be solved, gives considerable flexibility, avoids the amplitude scaling problems of analog computing and can give very accurate results. However, serial digital solution of large models can be extremely slow and any increase in required accuracy or number of equations to be solved results in an increase of program execution time. Therefore, in developing a digital simulation program, it is necessary to

(1) select the fastest of accessible machines.
(2) choose the lowest acceptable accuracy for the computed solution (taking into account the generally low accuracy of physiological data)
(3) select a numerical method giving the fastest solution of the differential equations for a specified accuracy.
(4) choose a high level programming language and its associated compiler giving efficient object code.
(5) employ efficient programming techniques.

These points are considered in the following sections.

5.2 Selection of a suitable digital computer and programming language

Continuous system simulation languages (CSSLs) enable mathematical models to be implemented quickly with a high probability of first-run success for the following reasons :

(1) A variable-step-length integration routine is usually incorporated which automatically solves the differential equations to a specified accuracy.

(2) Such languages are often block- or equation-oriented so that the source program retains the structure or format of the original mathematical model.

(3) Some continuous system simulation languages have an equation sorting routine which enables the program statements to be placed in any order thus providing great flexibility.

These features were included in the MIMIC language (Chu, 1969) which was used for the initial development of the model on a CDC 6600 computer. However, MIMIC ceased to be available in the early part of the work and so a study was made of the available digital computers and programming languages to decide the best approach for continued work on the model.

To obtain a rough estimate of the speed of different computer and programming language combinations, a simple test algorithm was constructed for the numerical solution of the well-known nonlinear second-order differential equation of van der Pol :

$$\frac{d^2x}{dt^2} + \varepsilon(x^2-1)\frac{dx}{dt} + x = 0 \qquad ---(5.1)$$

with $\varepsilon = 1$, $x(0) = 2$, and $\frac{dx}{dt}(0) = 0$. The classical fourth-order Runge-Kutta process (Gear, 1971 ; p.35) was used with a fixed step length of 0.001 sec and results were printed every 0.1 sec with the algorithm terminating at $t = 30$ sec . The algorithm was implemented on a variety of machines using various programming languages with similar types of program statement in each version. The fastest combination of those tested was the CDC 7600 computer with the FTN extended FORTRAN IV optimising compiler (OPT=2) requiring about 0.8 sec execution time.

The CDC 7600 machine was fairly accessible via a remote job entry system and the FORTRAN IV language was well supported on this machine and on most other machines so that software portability was ensured. In addition a large number of software packages for the numerical solution of ordinary differential equations were written in FORTRAN IV and could be used.

Despite the fact that writing the simulation program in FORTRAN IV involved detailed consideration of the integration routine to be

employed and careful ordering of the statements representing the mathematical model, full control over the internal events of the simulation program was ensured which was missing in the MIMIC programs.

In converting from the non-procedural language MIMIC to the procedural language FORTRAN IV the listing of the Function Language Program produced by the MIMIC compiler was very useful. The Function Language Program is an intermediate program in tabular form involving MIMIC functions sorted into the correct order for the built-in integration routine to handle. The ordering of these functions provided a guide to the ordering of statements in the FORTRAN IV program.

Debugging and testing after conversion to FORTRAN IV was greatly facilitated by the development of an interactive version of the simulation program for use at the terminal of a time-sharing system. A control segment was added to the basic simulation program to enable any variable to be inspected at any stage of execution, to enable rapid changes to be made to constants or variables and to permit short reruns of the dynamic simulation. The time-sharing system was based on an ICL 1905E computer which was considerably slower than the CDC 7600 computer (the above van der Pol test algorithm using the XFAE extended FORTRAN IV compiler with TRACE level 0 required about 100 sec execution time). In addition the elapsed time at a terminal was considerably longer than the execution time because the processor power was shared amongst the terminals in use. Despite these disadvantages, the interactive version of the simulation program greatly accelerated the debugging process.

After completing the debugging phase, the interactive control segment was removed and replaced by an executive control segment for the subsequent full length runs using the CDC 7600 computer.

5.3 Selection of a numerical method for solving the differential equations

Most numerical methods for the solution of ordinary differential equations require the Nth order mathematical model to be expressed as a set of N simultaneous first order differential equations i.e. in state space form. This approach is used in the cardiovascular simulation which includes a subroutine for calculating the derivatives

of the 61 state variables. The application of the numerical method leads to a system of N recurrence relations which may be single-step or multi-step and explicit or implicit. The Nth order state vector is computed at successive integration steps starting from a predefined initial state vector.

The approximations in the numerical method introduce a local truncation error at each step which must be controlled to obtain acceptable accuracy. The truncation error can be reduced by decreasing the step length but this increases the execution time of the program to reach a given value of the independent variable t . In the present model, an accuracy of about 2% is considered adequate for the computed results as physiological data, with which the results from the model will be compared, are not normally accurate to better than 2% . Thus to reduce program execution time, the step length used was the largest permissible consistent with numerical stability and an accuracy of about 2% .

To ensure that the truncation errors are kept at an acceptably small level at all times, an integration routine with automatic step length adjustment can be used. Gear (1971, p.233) has suggested that a variable-step-length Runge-Kutta method is generally superior to other methods when low accuracy is required. Thus the approach initially adopted in the FORTRAN IV implementation was the use of the variable-step-length Runge-Kutta-Merson process (Gear, 1971 ; p.85).

Using the Merson process with the pharmacokinetics section of the model "switched on" (i.e. all 61 first order differential equations being solved), the simulation program required 81 sec execution time on the CDC 7600 computer to reach t=100 sec in the solution with a relative accuracy of 2% . With the pharmacokinetics section "switched off" (i.e. only 42 first order differential equations being solved), 56 sec execution time was required. It was desirable to reduce the execution time further to obtain a faster turnaround time on the CDC 7600 computer and so the nature of the equations being solved was examined more closely.

5.3.1 The treatment of stiff equations

Careful examination of the differential equations of the cardiovascular model reveals that the system exhibits "stiffness" i.e. has very large time constants (e.g. 20 sec in the peripheral resistance controller) in combination with extremely small time constants (e.g.

about 2 ms in the case of ventricular ejection dynamics).

A requirement for the numerical stability of the classical fourth order Runge-Kutta process (Gear, 1971 ; p.210) is that

$$h < 2.8\,\tau_{MIN} \qquad ---(5.2)$$

where h is the integration step length and τ_{MIN} is the smallest time constant of the system. In a stiff system this leads to the highly undesirable computational situation of having to integrate numerically over a long range always using an extremely small step length and thus requiring excessive computing time. Some special numerical methods have been developed for the solution of highly stiff systems (e.g. Gear, 1971 ; p.158) but these do not provide a significant reduction in execution time compared with the variable-step-length Runge-Kutta methods when low accuracy is required (Gear, 1971 ; p.233).

In the cardiovascular model, the smallest "time constants" are in fact variable because the differential equations relating to flow through the pulmonary and aortic valves are nonlinear. From eqns. (2.34) and (2.35), the effective "time constants" in each case are :

$$\tau_{RVPA} = \frac{L_{RV}}{R_{RVPA} + \left(\frac{\rho}{2A_{PA}^2}\right) F_{RVPA}} \qquad ---(5.3)$$

$$\tau_{LVAOI} = \frac{L_{LV}}{R_{LVAOI} + \left(\frac{\rho}{2A_{AOI}^2}\right) F_{LVAOI}} \qquad ---(5.4)$$

It is seen that each "time constant" is dependent on the corresponding ventricular outflow. Table 5.2 shows the values of these "time constants" for various peak flow rates. During ventricular diastole, the outflows are zero and the aortic valve and pulmonary valve "time constants" are 73.33 ms and 60.00 ms respectively. For a peak flow rate of say 500 ml sec^{-1} , these "time constants" reduce to 2.53 ms and 2.07 ms respectively. Each "time constant" has its minimum value for only a brief period in each cardiac cycle when the flow reaches its maximum value.

Euler's method (Gear, 1971 ; p.10) is the simplest numerical method for solving differential equations but is not normally used because the truncation error per step is very large and extremely small steps are necessary for satisfactory accuracy. The requirement for the stability of Euler's method (Gear, 1971 ; p.210) is that

$$h < 2\tau_{MIN} \qquad \text{---(5.5)}$$

If Euler's method is used in the cardiovascular simulation, a fixed step length of 0.5 ms will satisfy the stability requirement of eqn.(5.5) for flow rates up to 1000 ml sec^{-1} and will be considerably less than the smallest effective "time constant" during most of the cardiac cycle thus providing reasonable accuracy.

When tested in the digital simulation, it was found that the results using Euler's method agreed to within 3% with accurate results obtained using the variable-step-length Runge-Kutta-Merson method (with the relative accuracy of the Merson method set to 0.01%). Additionally the full 61st order model required 56 sec execution time on the CDC 7600 computer to reach t=100 sec in the solution. With the pharmacokinetics model "switched off", the 42nd order model required only 39 sec execution time on the same machine.

As the accuracy of the Euler results was acceptable and the execution time was reduced by a factor of 1.45, the Euler solution was used for all the remaining work. The simulation program listed in Appendix 3 includes the Euler integration subroutine.

Rounding errors were shown to be insignificant in the results by transferring the program from the CDC 7600 computer to the ICL 1905E computer. A single precision floating point number in the CDC 7600 has 47 significant binary digits equivalent to about 14 significant decimal digits whereas a single precision floating point number in the ICL 1905E has 37 significant binary digits equivalent to about 11 significant decimal digits. The results obtained from the two machines agreed to better than 0.1% over a complete run from t=0 to t=100 sec indicating that the effect of cumulative rounding errors was negligible.

5.4 Evaluation of techniques for computing a steady state solution directly

If the full transient pulsatile dynamics of the cardiovascular model are required, the only applicable digital technique is the numerical solution of the differential equations starting at t=0 sec .

A dynamic model in state space form may be represented by

$$\dot{\underline{x}} = \underline{f}(\underline{x}, t) \qquad \text{---(5.6)}$$

where $\underline{x}$ is a state vector, the dot denotes differentiation with respect to time t and $\underline{f}$ is a vector function. The normal procedure for obtaining a nonperiodic steady state solution of a dynamic model is to set the derivatives of the state vector, $\dot{\underline{x}}$, to zero in eqn.(5.6) and to solve the set of equations

$$\lim_{t \to \infty} \underline{f}(\underline{x}, t) = 0 \qquad \text{---(5.7)}$$

This procedure is not applicable if the steady state is periodic e.g. if the system has a periodic forcing function or if the system has a stable limit cycle. In this case, the steady state solution may be obtained by computing the solution from t=0 sec for a sufficiently long time until the transients have decayed to a negligible level.

In cardiovascular modelling, the steady state is frequently of interest in predictive work when the long-term effect of an intervention or parameter change is required. The following special features of cardiovascular modelling may be of use in the development of new methods to compute the steady state solution directly :

(1) The steady state of the cardiovascular system is periodic.
(2) The results are required to an accuracy of only about 2% .
(3) In a clinical situation, it is often only the maxima, minima or mean values of variables that are of interest.

Methods which are intended to take advantage of these features are discussed in the following subsections, the aim being to obtain a considerable reduction of execution time over the conventional numerical solution method. The applicability of the suggested methods is discussed in section 5.4.4 .

5.4.1 A truncated Fourier series method

As the steady state is periodic in the cardiovascular model, the application of Fourier series methods is suggested.

If a truncated Fourier series representation is assumed for the r th state variable, x_r , with harmonics up to the N_rth retained to give acceptable accuracy then

$$x_r = \frac{a_{or}}{2} + \sum_{n=1}^{N_r} a_{nr} \cos\left(\frac{2\pi n t}{T}\right) + \sum_{n=1}^{N_r} b_{nr} \sin\left(\frac{2\pi n t}{T}\right) \qquad \text{---(5.8)}$$

where T is the period in the steady state.

There are $2N_r+1$ unknown Fourier coefficients in eqn.(5.8) so that, for the present cardiovascular model, the total number of Fourier coefficients to be determined (N_A) will be

$$N_A = 2\sum_{r=1}^{61} N_r + 61 \qquad ---(5.9)$$

Substitution of the truncated Fourier series representation of eqn.(5.8) for each state variable into the cardiovascular model and comparison of the coefficients of all the sine, cosine and constant terms will lead to a set of N_A nonlinear algebraic and transcendental equations.

5.4.2 A sampled data method

An alternative method is the use of a sampled data representation for each periodic state variable. If the r th state variable, x_r , is truncated at the N_rth harmonic then from Shannon's sampling theorem (Shannon, 1949), J_r equispaced samples per cycle will be sufficient to retain all the information of the continuous variable provided that $J_r \geq 2N_r$. The sampled state variable is periodic so that, if K is an integer,

$$x_r\left(\frac{iT}{J_r}\right) = x_r\left(\frac{iT}{J_r} + KT\right), \quad i = 1,2,3,\ldots,J_r \qquad ---(5.10)$$

The continuous state variable x_r may be reconstructed from the sampled data version using the "Cardinal Series" :

$$x_r(t) = \sum_{i=-\infty}^{\infty} x_r\left(\frac{iT}{J_r}\right) \frac{\sin\left(\frac{\pi J_r t}{T} - i\pi\right)}{\left(\frac{\pi J_r t}{T} - i\pi\right)} \qquad ---(5.11)$$

Because of the periodicity of $x_r\left(\frac{iT}{J_r}\right)$ in eqn.(5.10), eqn.(5.11) may be written as

$$x_r(t) = \sum_{i=1}^{J_r} g(i,T,J_r,t)\, x_r\left(\frac{iT}{J_r}\right) \qquad ---(5.12)$$

where

$$g(i,T,J_r,t) = \sum_{s=-\infty}^{\infty} \frac{\sin\left(\frac{\pi J_r t}{T} - i\pi - sJ_r\pi\right)}{\left(\frac{\pi J_r t}{T} - i\pi - sJ_r\pi\right)} \qquad ---(5.13)$$

There are J_r unknown sample values in eqn.(5.12) so that, for the present cardiovascular model, the total number of sample values to be determined will be

$$N_B = \sum_{r=1}^{61} J_r \geq 2 \sum_{r=1}^{61} N_r \qquad ---(5.14)$$

Substitution of the representation of eqn.(5.12) for each state variable into the cardiovascular model will lead to a set of N_B nonlinear algebraic and transcendental equations.

5.4.3 An interval arithmetic method

Frequently only the maxima and minima of variables are of interest in a clinical situation (e.g. systolic pressure and diastolic pressure) so it may be possible to take advantage of this reduced information output requirement in order to reduce execution time when the model is used predictively. A branch of mathematics which appears applicable is Interval Analysis (Moore, 1966).

Consider the closed intervals $[a,b]$ and $[c,d]$ defined by :

$$[a,b] = \{x \mid a \leq x \leq b\} \qquad ---(5.15)$$

$$[c,d] = \{y \mid c \leq y \leq d\} \qquad ---(5.16)$$

then the basic operations of interval arithmetic are given by

$$[a,b] + [c,d] = [a+c, b+d] \qquad ---(5.17)$$

$$[a,b] - [c,d] = [a-d, b-c] \qquad ---(5.18)$$

$$[a,b] \cdot [c,d] = [\min(ac,ad,bc,bd), \max(ac,ad,bc,bd)] \qquad ---(5.19)$$

$$\frac{[a,b]}{[c,d]} = [a,b] \cdot \left[\frac{1}{d}, \frac{1}{c}\right] \quad , 0 \notin [c,d] \qquad ---(5.20)$$

In each case, the arithmetic operation is performed using only the endpoints of the interval and hence the applicability of interval analysis to a solution yielding only maxima and minima.

To illustrate the method, consider the variables $x \in [a,b]$, $y \in [c,d]$, $z \in [e,f]$. The equation

$$x = y + z \qquad ---(5.21)$$

becomes transformed to

$$[a, b] \subset [c+e, d+f] \qquad ---(5.22)$$

Operations of this type can be extended to an Nth order dynamic model to give a set of 2N equations in terms of maxima and minima of state variables in the periodic steady state.

5.4.4 Applicability of the methods

Both the truncated Fourier series method and the sampled data method are highly impractical for the following reasons :

(1) There is much labour involved in manipulating the equations to start with.

(2) Considerable digital computer execution time will be required to obtain a solution of the very large set of nonlinear equations by iterative or optimisation methods.

(3) There is a high probability of encountering the problem of multiple roots in the solution of nonlinear equations.

In the case of the sampled data method, there are the additional difficulties of evaluating the function of eqn.(5.13) for each sample value and also differentiating the same function for substitution in the cardiovascular model.

The interval bounds obtained by applying the basic interval arithmetic operations of eqns.(5.17) to (5.20) to a dynamic model are very conservative and also the distributive law does not always hold for interval arithmetic (Moore, 1966 ; p.9). Thus this method is unsuitable for the cardiovascular model.

All three techniques are unsuitable in the present work so the only practical approach for obtaining a steady state solution is the direct numerical solution of the differential equations starting at t=0 and continuing until the transients have decayed to a negligible level.

5.5 Constraints on state variables

State variables of the model are required to be constrained in the following cases :

(1) In each segment of the circulatory fluid mechanics model, the constraint $V \geq 0$ is applied to the volume. This is equivalent to specifying that the compliance becomes zero at zero volume which corresponds to the real physical situation.

(2) In eqns.(2.34) and (2.35) describing ventricular outflow, the constraints $F_{RVPA} \geq 0$ and $F_{LVAO} \geq 0$ are applied to represent the actions of the pulmonary and aortic valves respectively.

(3) In the pharmacokinetics model, the constraint $m \geq 0$ is applied to each mass so that a physically meaningless negative mass does not arise for example as a result of numerical errors in the program.

If a fixed-step-length integration routine is used, these constraints may be enforced simply by resetting the appropriate state variables to zero whenever they become negative in any integration step. However if a variable-step-length integration routine is used, it is important that the state variables are not changed within the subroutine used to calculate the derivatives or the method will fail. In the latter case, the constraints can be enforced by manipulating the derivatives of state variables rather than the state variables themselves. This approach is used in the simulation program given in Appendix 3 to enable the equations to be solved using either fixed or variable step-length integration routines.

The method is illustrated in the flowchart of fig. 5.2 . Consider a state variable, x , to be constrained to positive values only. If the derivative $\frac{dx}{dt}$ is positive then x will become more positive in the next integration step and so the method will not be required. If however the derivative is negative, there is a possibility of x becoming negative in the following integration step so a limit is placed on the negative slope. The algorithm ensures that the minimum time constant for a decreasing value of x is kept at 5 ms. This ensures that the Euler solution with a fixed step of 0.5 ms remains numerically stable and gives reasonable accuracy while still permitting x to decrease rapidly to zero.

The method is applied to the 19 segmental volumes, the 19 segmental masses and the 2 ventricular outflows in the program.

5.6 The treatment of differentiation

Differentiation is necessary in the models of the aortic arch baroreceptors, the carotid sinus baroreceptors and the neural control of heart rate. If a fixed step-length integration routine is employed, differentiation may be achieved using a suitable difference approximation. However if the integration routine has a variable step-length, the derivative computed in this way will vary considerably as the step-length is automatically changed. This difficulty is avoided in the simulation by replacing the derivative calculation by previously derived algebraic expressions and incorporation of the expressions into the program.

5.6.1 The aortic arch baroreceptors

In eqn.(A1.117) the derivative $S_1 = \frac{dP_{AO2}}{dt}$ is required. Substituting for $\frac{dV_{AO2}}{dt}$ from eqn.(A1.28) in eqn.(A1.31) gives

$$P_{AO2} = \frac{1}{C_{AO2}}(V_{AO2} - V_{uAO2}) + \frac{K_8}{C_{AO2}}\left[F_{AO1AO2} - F_{AO2UA} - F_{AO2AO3}\right] \qquad ---(5.23)$$

Differentiating eqn.(5.23) :

$$S_1 = \frac{1}{C_{AO2}}\frac{dV_{AO2}}{dt} + \frac{K_8}{C_{AO2}}\left[\frac{dF_{AO1AO2}}{dt} - \frac{dF_{AO2UA}}{dt} - \frac{dF_{AO2AO3}}{dt}\right] \qquad ---(5.24)$$

The derivatives on the right hand side of eqn.(5.24) are available from the equations (A1.25),(A1.28),(A1.29) and (A1.30) and thus S_1 can be calculated.

5.6.2 The carotid sinus baroreceptors

In eqn.(A1.123), the derivative $S_6 = \frac{dP_{UA}}{dt}$ is required. If it is assumed that σ_{HEAD} changes much more slowly than P_{UA} in the segment representing the head and arms arteries then the differentiation of eqn.(A4.4) gives

$$S_6 = \frac{\frac{dV_{UA}}{dt} + K_8\left(\frac{dF_{AO2UA}}{dt} + \frac{1}{R_{HEAD}\sigma_{HEAD}}\frac{dP_{UV}}{dt}\right)}{C_{UA} + \frac{K_8}{R_{HEAD}\sigma_{HEAD}}} \qquad ---(5.25)$$

Now d_3 and V_{uUV} change much more slowly than V_{UV} so that an approximation for $\frac{dP_{UV}}{dt}$ obtained by differentiating eqn.(A1.36) is

$$\frac{dP_{UV}}{dt} = \left(\frac{d_3}{C_{UV}}\right)\frac{dV_{UV}}{dt} \qquad ---(5.26)$$

Substituting for $\frac{dP_{UV}}{dt}$ from eqn.(5.26) in eqn.(5.25) gives

$$S_6 = \frac{\frac{dV_{UA}}{dt} + K_8\left(\frac{dF_{AOZUA}}{dt} + \frac{d_3}{C_{UV}R_{HEAD}\sigma_{HEAD}}\frac{dV_{UV}}{dt}\right)}{C_{UA} + \frac{K_8}{R_{HEAD}\sigma_{HEAD}}} \qquad ---(5.27)$$

The derivatives on the right hand side of eqn.(5.27) are available from the equations (A1.29),(A1.32) and (A1.35) and thus S_6 can be calculated.

5.6.3 The heart rate controller

In eqn.(A1.132), the derivative $u_2 = \frac{du_1}{dt}$ is required. Differentiation of eqns.(A1.131) and (A1.127) leads to

$$u_2 = \begin{cases} K_{17}\left[(1-K_{16})\frac{dB_{AOZ}}{dt} + K_{16}\frac{dB_{UA}}{dt}\right] & , B > K_{18} \\ 0 & , B \leq K_{18} \end{cases} \qquad ---(5.28)$$

Differentiation of eqns.(A1.120) and (A1.119) gives

$$\frac{dB_{AOZ}}{dt} = \begin{cases} K_{13}\left(\frac{dS_3}{dt} + K_{14}\frac{dS_4}{dt}\right) & , S_5 > 0 \\ 0 & , S_5 \leq 0 \end{cases} \qquad ---(5.29)$$

Differentiation of eqns.(A1.126) and (A1.125) gives

$$\frac{dB_{UA}}{dt} = \begin{cases} K_{13}\left(\frac{dS_8}{dt} + K_{14}\frac{dS_9}{dt}\right) & , S_{10} > 0 \\ 0 & , S_{10} \leq 0 \end{cases} \qquad ---(5.30)$$

The derivatives on the right hand sides of eqns.(5.29) and (5.30) are available from eqns.(A1.115), (A1.116), (A1.121) and (A1.122) so that $\frac{dB_{AOZ}}{dt}$ and $\frac{dB_{UA}}{dt}$ can be calculated. Substitution of these two derivatives into eqn.(5.28) thus enables u_2 to be calculated.

5.7 The treatment of algebraic loops

When the model was initially implemented using the MIMIC language, a failure occurred in the sorting procedure due to the presence of implicit algebraic relationships referred to as algebraic loops. A nonprocedural language such as MIMIC cannot handle implicit algebraic or transcendental equations directly and a facility is usually provided for solution of these implicit equations at each integration step by an iterative process (e.g. Newton-Raphson method). Unfortunately, the iterative solution of the implicit equations at each step increases the execution time considerably. The difficulty can be avoided if the equations can be initially rearranged to eliminate the algebraic loops.

A useful visual aid in the detection of algebraic or transcendental loops in large models is the dependence diagram. This is a directed graph in which nodes represent variables and branches represent dependence between variables (fig. 5.3). If the dependence diagram is drawn as far as possible in planar graph form, loops become immediately apparent. This was applied to the systemic arterial variables in the model and 6 separate algebraic loops were detected (fig. 5.4). The loops were removed by rearrangement of the relevant equations, details of which are given in appendix 4.

5.8 Structure of the digital simulation program

The program given in appendix 3 is written in FORTRAN IV for the reasons given in section 5.2 . "Standard" FORTRAN IV is used, omitting such extensions as free formats and mixed mode arithmetic, to ensure portability of the program. The compiled program requires about 5K of main memory in the CDC 7600 computer and about 10K of main memory in the ICL 1905E computer.

As there are a large number of constants and variables in the mathematical model, arrays are used rather than separate variable names to make the program listing more compact. The principal arrays in the program are :

X(61) - state variables
D(61) - derivatives of state variables
V(112) - other numerical variables
P(178) - numerical constants
L(14) - logical variables (for control of the simulation)

The details of the array elements and the equivalent variables in the mathematical model are given in appendix 2. The arrays V, P and L are placed in labelled COMMON blocks to reduce the storage requirements. The arrays X and D are kept as subroutine arguments to retain compatibility with certain library routines available on the CDC7600 and ICL1905E computer systems.

The program consists of a main executive control segment together with 8 subprograms. Details of these are given in the following subsections.

5.8.1 Executive control segment

This is the main segment which controls the execution of the simulation program. Its operation is illustrated in the flow diagram of fig. 5.5 . In the version listed in appendix 3, the values of selected variables are printed at the end of each cardiac cycle commencing at $t = 0$ and finishing as soon as the value of t at the end of a cardiac cycle exceeds 100 sec. The program is designed to start in a steady state with all neural controllers "switched on" but with the pharmacokinetics section "switched off" . Any changes to be made (e.g. to simulate an injection of a specific drug or to investigate the effect of a parameter change) are introduced into this segment at the point indicated in the listing of appendix 3.

5.8.2 SUBROUTINE INTEG(D,X,T)

This subroutine performs one step of Euler's method when called by the executive control segment. The current state vector is replaced by the value of the state vector at the next integration step. The derivatives are obtained by a call of the subroutine MODEL. If required, the Euler method can be replaced by another integration procedure such as a Runge-Kutta method.

5.8.3 SUBROUTINE MODEL(D,X,T)

This subroutine computes the derivatives of the state variables (in D) from the current state vector (X) and time (T) using the equations of the mathematical model. It is called by INTEG at each step and also once at $t = 0$ by the executive control segment.

It would normally be desirable to split this subroutine into a number of separate subroutines corresponding to the main sections of

the mathematical model but this was not done for the following reasons :

(1) MODEL is called 200,000 times in each 100 second run using Euler's method with a fixed step-length of 0.5 ms . It is therefore necessary to keep the number of subroutine accesses per call of MODEL to a minimum to improve speed of execution.

(2) The ordering of the statements in MODEL is such that it does not split up into sections in a simple way.

Any calculations that are not required at each integration step have been removed from MODEL and placed in other less frequently called subroutines to obtain faster execution.

5.8.4 SUBROUTINE ODDJOB(D,X,T)

This subroutine performs the following tasks at $t = 0$ and once every cardiac cycle when called by the executive control segment :

(1) calculation of the hydrostatic pressure differences required in orthostasis

(2) injection of a drug when required

(3) setting of the state variables d_2 and b_2 to unity if venous tone control and myocardial contractility control are not required

(4) calculation of the total blood volume

5.8.5 SUBROUTINE CYCLE(D,X,T)

Static and cyclic respiration calculations are performed at each integration step in this subroutine which is called by the executive control segment. The calculations are not included in MODEL because a discontinuity occurs in the state variable y_2 at the end of the respiratory cycle. The subroutine also tests for the end of the cardiac cycle and, when detected, performs the following tasks :

(1) signals the end of the cardiac cycle to the executive control segment

(2) records the systolic pressure, diastolic pressure and stroke volume during the cycle

(3) computes the mean arterial pressure, cardiac output and estimated total systemic resistance.

(4) sets the heart period to the value for the next cycle

(5) calls the subroutine TTSR to obtain the current true total systemic resistance

5.8.6 SUBROUTINE RESULT(D,X,T)

At $t = 0$, this subroutine prints a heading for the table of results. Thereafter values of the selected variables are printed whenever the subroutine is called by the executive control segment. In the version of appendix 3, the variables to be printed are :

t , (MAP) , (SV) , (CO) , T_H , f_H , (ETSR) , $(P_{AOI})_{MAX}$, $(P_{AOI})_{MIN}$

5.8.7 SUBROUTINE PRELIM

To increase the execution speed, any frequently used constant expressions are evaluated once only in this subroutine which is called by the executive control segment at $t = 0$.

5.8.8 SUBROUTINE TTSR(X)

This subroutine computes the true total systemic resistance using equations (A1.105) to (A1.114) in appendix 1. It is called once per cardiac cycle from the subroutine CYCLE.

5.8.9 BLOCK DATA

This subprogram is used by the compiler to initialise all the arrays and variables in labelled COMMON blocks.

The initial values of state variables were computed originally by choosing initial volumes as specified by Beneken & Dewit (1967), setting all masses to zero in the pharmacokinetics model, estimating the values of other state variables and then letting the simulation run until the transients decayed to a negligible level. The values of the state variables at the beginning of a cardiac cycle in the steady state were then recorded and used as the initial values for all future runs.

5.9 Conclusion

An implementation of the 61 first order differential equations and 159 algebraic equations of the cardiovascular model as a digital simulation using FORTRAN IV has been described in this chapter.

The model possesses time-varying stiffness and this property enables a fixed step-length Euler integration method to be used with truncation and rounding errors at an acceptably low level. An examination of alternative methods for computing a steady state solution reveals that direct numerical solution of the equations until the transients die away is the only practical approach in this case. The simulation requires about 56 sec CDC 7600 execution time to reach $t = 100$ sec in the solution.

The problems of implementing constrained state variables, algebraic loops and differentiation in the simulation have been examined and solved satisfactorily.

The numerical values of constants and initial conditions and the identification of variables in the program are given in appendix 2. The listing of the complete simulation program is given in appendix 3.

SECTION	SUBSECTION	NUMBER OF FIRST ORDER DIFFERENTIAL EQUATIONS	NUMBER OF ALGEBRAIC EQUATIONS
CIRCULATORY FLUID MECHANICS MODEL	RIGHT ATRIUM	1	4
	RIGHT VENTRICLE	2	1
	PULMONARY ARTERIES	1	2
	PULMONARY VEINS	1	4
	LEFT ATRIUM	1	3
	LEFT VENTRICLE	2	1
	ASCENDING AORTA	2	2
	AORTIC ARCH	3	1
	HEAD & ARMS ARTERIES	1	2
	HEAD & ARMS VEINS	1	5
	THORACIC AORTA	3	2
	INTESTINAL ARTERIES	1	2
	INTESTINAL VEINS	1	5
	ABDOMINAL ARTERIES	2	2
	ABDOMINAL VEINS	1	5
	LEG ARTERIES	1	2
	LEG VEINS	1	5
	INFERIOR VENA CAVA	1	4
	SUPERIOR VENA CAVA	1	4
	TIME-VARYING COMPLIANCES OF ATRIA & VENTRICLES	1	12
	RESPIRATION	1	3
	CALCULATION OF MAP, SV, CO, ETSR	2	2
	CALCULATION OF TRUE TOTAL SYSTEMIC RESISTANCE	0	10
NEURAL CONTROL MODEL	AORTIC ARCH BARORECEPTORS	2	4
	CAROTID SINUS BARORECEPTORS	2	4
	C.N.S. INPUT FUNCTION	0	1
	C.N.S. CONTROL OF HEART RATE	3	8
	C.N.S. CONTROL OF PERIPHERAL RESISTANCE	2	2
	C.N.S. CONTROL OF MYOCARDIAL CONTRACTILITY	1	1
	C.N.S. CONTROL OF VENOUS TONE	1	3
PHARMACOKINETICS MODEL	DRUG INJECTION, TRANSPORT & BREAKDOWN	19	43
	EFFECT OF DRUG ON HEART RATE	0	1
	EFFECT OF DRUG ON PERIPHERAL RESISTANCE	0	5
	EFFECT OF DRUG ON MYOCARDIAL CONTRACTILITY	0	4
	TOTAL	61	159

TABLE 5.1 NUMBER OF EQUATIONS IN THE DIGITAL COMPUTER IMPLEMENTATION

PEAK FLOW RATE ($ML.SEC^{-1}$)	MINIMUM AORTIC VALVE "TIME CONSTANT" (MS)	MINIMUM PULMONARY VALVE "TIME CONSTANT" (MS)
0	73.33	60.00
50	19.30	15.79
100	11.11	9.093
150	7.803	6.385
200	6.012	4.919
250	4.890	4.001
300	4.121	3.372
350	3.561	2.913
400	3.135	2.565
450	2.800	2.291
500	2.529	2.070
550	2.307	1.887
600	2.120	1.735
650	1.961	1.605
700	1.825	1.493
750	1.706	1.396
800	1.602	1.310
850	1.509	1.235
900	1.427	1.168
950	1.353	1.107
1000	1.287	1.053

TABLE 5.2 AORTIC AND PULMONARY VALVE "TIME CONSTANTS" AT VARIOUS PEAK FLOW RATES (TO ASSESS THE STIFFNESS OF THE MODEL)

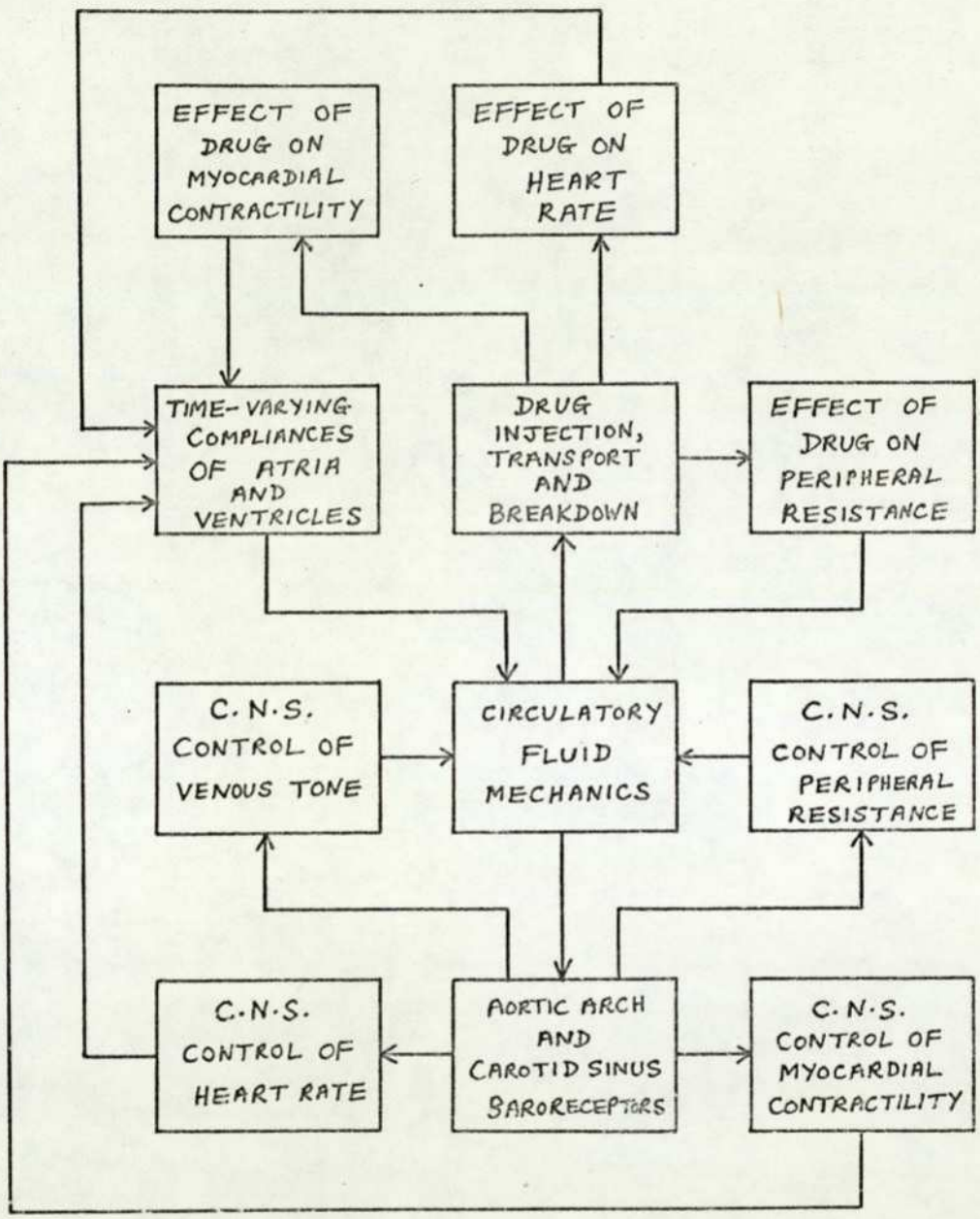

FIG. 5.1 INTERACTIONS BETWEEN SUBSYSTEMS IN THE MODEL

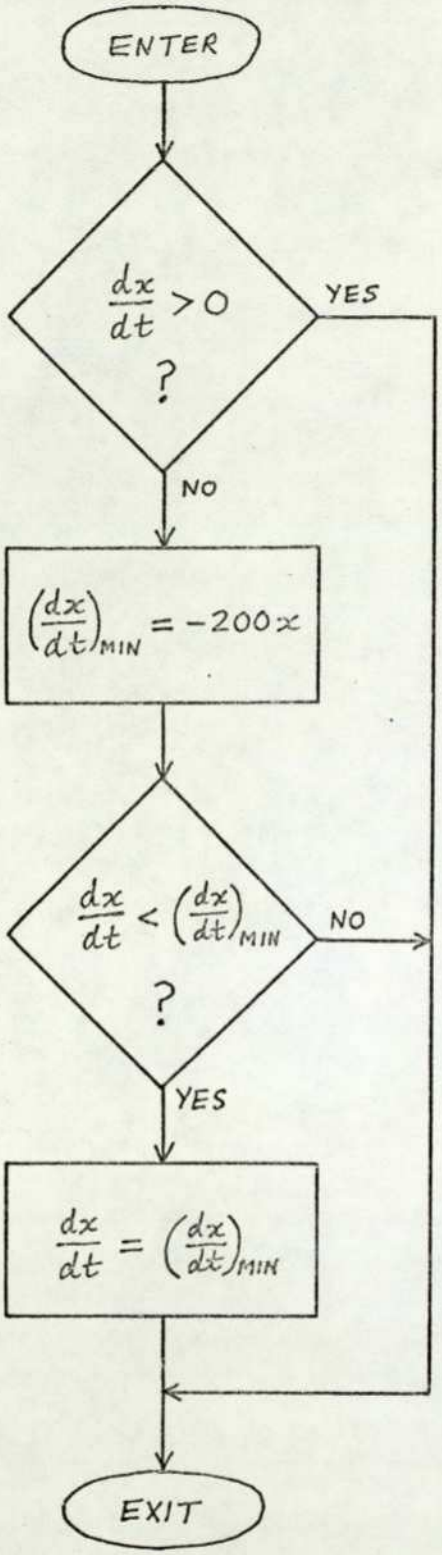

FIG. 5.2 FLOW DIAGRAM ILLUSTRATING THE PROCESS IN THE DERIVATIVE SUBROUTINE WHICH ENSURES THAT THE COMPUTED VOLUME, MASS OR VENTRICULAR OUTFLOW DO NOT BECOME NEGATIVE WHEN USING VARIABLE-STEP-LENGTH INTEGRATION ALGORITHMS

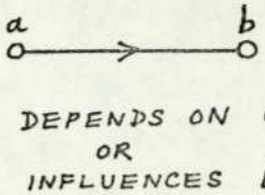

FIG. 5.3 PRINCIPLE OF THE DEPENDENCE DIAGRAM

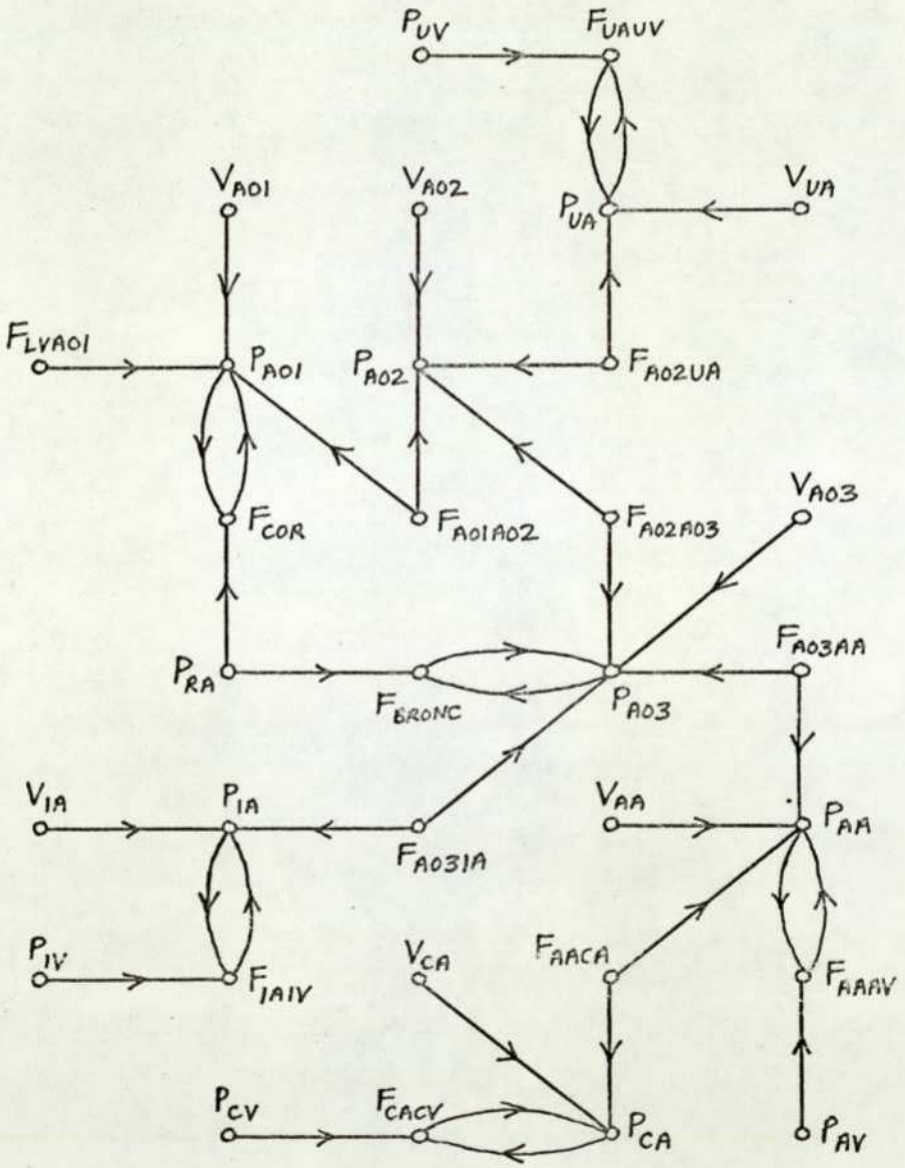

FIG. 5.4 A DEPENDENCE DIAGRAM TO DETECT ALGEBRAIC LOOPS

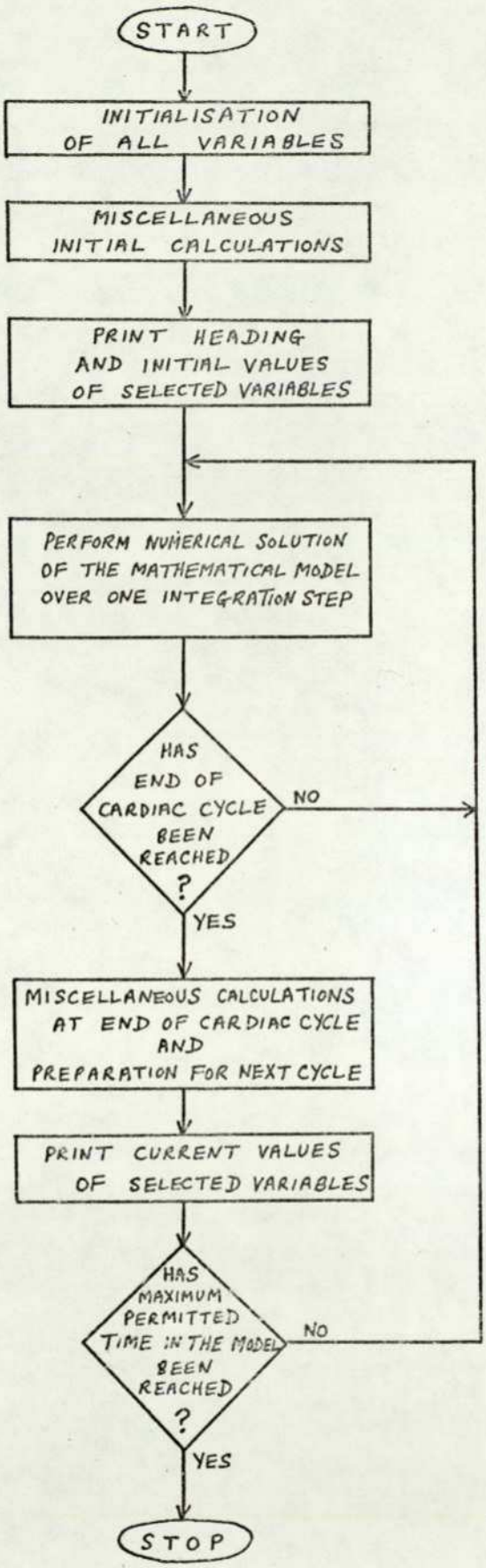

FIG. 5.5 GENERAL FLOW DIAGRAM FOR THE SIMULATION PROGRAM

CHAPTER 6

VALIDATION OF THE DIGITAL SIMULATION

Before investigating the effects of drugs using the digital simulation it is necessary to determine whether the mathematical model and its computer implementation adequately represent the real cardiovascular system. This chapter describes a series of tests performed on the digital simulation to assess the validity of the original mathematical model.

6.1 The validation process

Validation is the process of establishing that the mathematical model truly represents the real system (Crosbie, 1975). Once it is established that the digital simulation correctly represents the mathematical model (by reduction of truncation and rounding errors to an acceptable level and the elimination of programming errors), the validity of the mathematical model can be investigated by performing tests on the digital simulation and comparing the responses of the simulation with results from equivalent tests on the real system.

Due to the considerable physiological variation within the human population and the errors involved in measurements on the cardiovascular system, it is not appropriate to use integral of error-squared, integral of absolute error or similar performance criteria in the comparison of the present model with the real cardiovascular system. Instead, the principal features of the responses are compared and a combination of quantitative and qualitative assessment of validity is made. The magnitudes of variables in the model must lie in the physiological range for a response to be acceptable.

The adequacy of the model has to be assessed on the basis of a limited number of carefully selected tests. A flow diagram showing the iterative nature of the validation procedure is given in fig. 6.1 . If a particular test fails, it is necessary to change the parameters or even the structure of the model and in the case of nonlinear systems it will be necessary to repeat all previous tests because the principle of superposition is not applicable.

The cardiovascular model has been constructed for a conscious human and so it is necessary to select tests which are applicable to conscious humans or comparable conscious animals. Results from anaesthetised humans are inappropriate because of the changes in the control mechanisms which occur during anaesthesia. The principal validation tests applied to the model are orthostasis, blood volume changes, the Valsalva manoeuvre and pacing tests. The responses to these tests are well-known and they are useful in assessing the performance of the circulatory fluid mechanics model and the effectiveness of the neural control mechanisms.

6.2 The checking of magnitudes and waveforms

A preliminary validation procedure that can be performed is the checking of the features of all pressure, flow and volume waveforms and the magnitudes of all variables.

The simulation commences in a steady state and gives the following results :

Mean Arterial Pressure (MAP)	: 109.1 mmHg
Stroke Volume (SV)	: 69.6 ml
Cardiac Output (CO)	: 84.6 ml sec^{-1}
Heart Period (τ_H)	: 0.823 sec
Heart Rate (f_H)	: 72.9 bpm
Estimated Total Systemic Resistance (ETSR)	: 1.29 mmHg sec ml^{-1}
Systolic Pressure ($P_{AOI\ MAX}$)	: 130.9 mmHg
Diastolic Pressure ($P_{AOI\ MIN}$)	: 90.8 mmHg

These values are all within acceptable limits for an average human. The systolic/diastolic pressure ratio is normally quoted as 120/80 (Green, 1972 ; p.54) but a range of pressures may be found in a normal human population and also the pressures tend to increase with age so that the ratio 130.9/90.8 is satisfactory. The pulse pressure of 40.1 mmHg is normal.

The arithmetic mean of the systolic and diastolic pressures is 110.8 mmHg which is close to the mean arterial pressure of 109.1 mmHg. The mean pressure is normally calculated as one-third of the way up from the diastolic pressure to the systolic pressure (Green, 1972 ; p.54 and Rushmer, 1970 ; p.158) but if there is a significant rise in aortic pressure after the dichrotic notch, the pressure waveform is

very roughly triangular and the mean value over one cycle is then the arithmetic mean of the systolic and diastolic values.

The total blood volume in the model should remain constant as the system is closed and there is no mechanism incorporated for producing volume changes. This was verified on a step-by-step and a cycle-by-cycle basis in the tests and the total volume remained constant at 4544 ml (8 pints).

The waveforms of selected transmural pressures during one cardiac cycle are shown in fig. 6.2 . A dichrotic notch (incisura) occurs in the ascending aortic pressure waveform when the aortic valve closes which is a normal feature of this waveform. The change of the pressure waveform with distance from the heart can be seen by comparing P_{AO1} , P_{AO2} , P_{AO3} , P_{AA} and P_{CA} in fig. 6.2 . The peaks of P_{AO1} and P_{CA} occur about 0.15 sec apart and, since the distance between the segments representing the ascending aorta and leg arteries in the average human is roughly 90 cm, this interval corresponds to a pulse wave velocity of about 600 cm sec^{-1} which is approximately the normal value (Green, 1972 ; p.57). This indicates that, despite the lumped parameter approximation, the model exhibits wave propagation phenomena satisfactorily.

The left ventricular pressure waveform (P_{LV}) has a peak value of 177 mmHg whereas the ascending aortic pressure (P_{AO1}) has a maximum value of 131 mmHg. The large difference occurs in the model due to the lumped parameter approximations and the way the ejection dynamics have been modelled. The Bernoulli term contributes significantly at peak flow as explained in section 2.2.4 . The peak left ventricular pressure is normally quoted as being approximately the same as the peak ascending aortic pressure (Green, 1972 ; p.28) but this will only be true when the pressure drop across the opened aortic valve is due to viscous resistance alone. Because of the dynamic nature of the ejection, it is highly likely that significant pressure drops do occur at the opened valve although they would not be as large as obtained here. Similar considerations apply to right ventricular ejection.

The transmural left atrial pressure waveform (P_{LA}) exhibits some correct features although the left atrial segment is mechanically isolated in the model so the effects of ventricular contraction on the atrium do not appear.

The waveforms of selected volumes and flow rates are shown in fig. 6.3 . It is seen that the left and right ventricular outflows decrease rapidly to zero at the end of systole but do not become negative indicating that the slope limiting technique for simulating the aortic and pulmonary valve actions (described in section 5.5) is functioning correctly.

The ventricular volumes have acceptable time-courses and it is seen that the stroke volume of both ventricles is about 70 ml.

The waveforms of pressures in the aortic arch segment and head and arms arteries segment together with the waveform of the C.N.S. input function (B) are shown in fig. 6.4 . The two segmental pressures correspond to the inputs of the aortic arch and carotid sinus baroreceptors respectively. The rapid rise of B at $t = 0.18$ sec reflects the sensitivity of the baroreceptors to the positive pressure derivative.

6.3 The effect of orthostasis

In the normal human, a passive tilt from a recumbent position to an upright position leads to large hydrostatic pressure differences in the system which hinder the return of blood to the heart. To maintain venous return and hence cardiac output, the circulatory system makes prompt compensatory adaptation. Venous tone is increased which causes contraction of the large venous channels , the elevation of central venous pressure and thus an improvement in venous return. If the subject is preparing for walking or other action then skeletal muscle contraction can squeeze the veins and, due to the presence of venous valves, can force blood towards the heart and also improve venous return.

The compensatory action of neural control mechanisms during a simulated head-up tilt in the model is illustrated in fig. 6.5 . The fall in cardiac output is limited to about 6% which is rather less than the 20% or so which occurs in practice (Rushmer, 1970 ; p.211). The initial drop in arterial pressure is limited by reflex vasoconstriction, tachycardia, venoconstriction and positive inotropy.

A return to recumbency from the upright position (fig. 6.5 at $t = 50$ sec) shows, as expected, changes in the opposite direction. However the waveforms differ from the previous case because the

dynamic response is direction-dependent due to the nonlinearities in the system.

The dynamics following a simulated head-down tilt in the model are shown in fig. 6.6. The effect of gravity is to improve venous return in this case so that the cardiac output and blood pressure rise initially. However the rise of blood pressure is limited by reflex peripheral vasodilatation, bradycardia, venodilatation and negative inotropy. The rise in cardiac output is limited to about 6% . As in the head-up tilt case, a return to recumbency shows changes in the opposite direction with an asymmetry of dynamic response.

If the number of g's of acceleration (n) is set to a figure greater than 1 in the model, the effects encountered by astronauts during take-off can be simulated. With a head-up tilt and n = 10 , the cardiac output falls to zero in 7 seconds in the model which is equivalent to the blackout experienced by astronauts positioned with feet trailing on take-off . With a head-down tilt and n = 10 , the blood pressure exceeds 219 mmHg after 7 seconds and the heart rate slows to 30 bpm indicating that this orientation is also highly unsuitable for high g conditions.

The results obtained in the orthostasis tests are in good general agreement with results reported in the literature (Rushmer, 1970 ; p.211 and Green, 1972 ; p.48).

6.4 The effects of blood volume changes

If the blood volume is reduced below normal e.g. following a haemorrhage, the venous capacity is reduced by venoconstriction to compensate for this. If this compensation is incomplete, the venous return and cardiac output are reduced. The falling blood pressure leads to reflex arteriolar vasoconstriction and tachycardia.

If hypervolaemia is induced e.g. by a transfusion of blood, the venous return and cardiac output are increased and the increasing blood pressure leads to reflex arteriolar vasodilatation and bradycardia.

These effects are demonstrated in the model by simulating the sudden removal of 500 ml blood from the head and arms veins segment (fig. 6.7) and by simulating the sudden transfusion of 500 ml blood

into the head and arms veins segment (fig. 6.8).

The effects of blood volume changes on the steady state mean arterial pressure, cardiac output, etc. in the model are shown in fig. 6.9. The heart rate cannot exceed 200 bpm in the model so that if a blood volume of greater than 1200 ml is removed, the heart rate controller can no longer compensate for decreasing blood pressure. For this level of blood volume reduction, the cardiac output in the model is reduced to about one-third of its normal value. At this level, anoxia of the tissues would occur in the real system and surgical shock would ensue. If the anoxia persisted, the shock could eventually become irreversible due to acute cardiac failure. These effects are not incorporated in the present model so that the return of blood volume to a normal value following sustained and severe hypovolaemia leads to the restoration of normal mean arterial pressure, cardiac output, etc.

The response of the model for small blood volume changes is in satisfactory agreement with the response of the real system.

6.5 The effect of a Valsalva manoeuvre

The Valsalva manoeuvre consists of a forced expiration against a closed glottis. The effect is to increase the intrathoracic pressure to a large positive value which temporarily prevents venous blood from entering the thorax. The blood already in the thorax is expelled at a higher pressure than normal so that increased cardiac output initially occurs. However the output then falls since there is no venous return. The heart rate shows a corresponding variation with an initial reflex decrease followed by a compensatory increase to counteract the falling blood pressure. The manoeuvre can only be sustained for a few seconds.

In the model the manoeuvre is simulated by changing P_{TH} and P_{ABD} both to +40 mmHg for a period of 12 seconds (after Beneken & Dewit, 1967) and then setting P_{TH} and P_{ABD} back to their normal values of -4 mmHg and +4 mmHg respectively. The dynamics during the simulated manoeuvre are shown in fig. 6.10 and are in good agreement with results reported in the literature (e.g. Green, 1972 ; p.48). The heart rate response shows an initial fall for about 3 beats and then a continuing rise until the end of the manoeuvre when a further rise for about 3 beats occurs followed by a more rapid fall back to normal heart rate.

The response reveals the asymmetry in the heart rate controller

6.6 The effect of pacing the heart

Noble et al.(1966) have investigated the effect of changing the heart rate on the cardiovascular function of the conscious dog by pacing the heart using an implanted right atrial electrode. It was found that as the heart rate increased, the stroke volume fell and the cardiac output either increased or changed very little. A close linear relationship between stroke volume and heart rate was found over the range studied. It is assumed here that these results can be extended to humans so that comparison with the present model is possible.

In the experiments of Noble et al., the lowest heart rate that could be achieved depended on the spontaneous heart rate since entrainment was only possible with a pacing frequency higher than the spontaneous rate. This limitation does not apply in the model and pacing of the heart can be simulated very simply by switching off the heart rate controller and substituting a fixed preset value of heart period.

Simulated pacing experiments were performed using 23 different values of heart period from 0.3 sec to 1.4 sec in steps of 0.05 sec. In each case, the simulation was allowed to settle to a steady state and the values of heart period, heart rate, mean arterial pressure, stroke volume, cardiac output, estimated total systemic resistance, systolic pressure and diastolic pressure were recorded. The results are shown graphically in figs. 6.11 and 6.12 .

The relationship between stroke volume and heart rate was not linear but the least squares regression of stroke volume (SV ml) on heart rate (HR bpm) gave the following regression line :

$$(SV) = -0.5798\,(HR) + 120.4 \quad , \quad r = 0.9336 \qquad ---(6.1)$$

The correlation coefficient was comparable with values obtained by Noble et al.

More interesting was the remarkably close linear relationship between stroke volume (SV ml) and heart period (HP sec) which gave the following least squares regression line :

$$(SV) = 79.35\,(HP) + 3.183 \quad , \quad r = 0.9988 \qquad ---(6.2)$$

The cardiac output (CO ml sec^{-1}) changed very little with heart rate and since

$$(SV) = (CO)(HP) \qquad ---(6.3)$$

the close linear relationship between (SV) and (HP) was to be expected.

The theoretical descending limb of the cardiac output versus heart rate curve hypothesised by Noble et al. was in fact obtained beyond 109 bpm (fig. 6.11) although the curve was not parabolic. Noble et al. also found that mean arterial pressure always rose whenever cardiac output increased. This was found to be true only for heart rates from 109 bpm up to 200 bpm and from 42 bpm up to 47 bpm. For heart rates from 47 bpm to 109 bpm, the mean arterial pressure in fact fell with increasing cardiac output (fig. 6.12).

The results obtained in these pacing tests are broadly consistent with the results of Noble et al.(1966) indicating a measure of model validity.

6.7 Further tests on the circulatory fluid mechanics model

This section describes a variety of other tests performed to validate further the circulatory fluid mechanics section of the complete model.

6.7.1 The effect of respiration

The previously described tests in sections 6.3 to 6.6 employed a static respiration model with P_{TH} = -4 mmHg and P_{ABD} =+4 mmHg. The "respiratory pump" action (Green, 1972 ; p.48) can be demonstrated with the static respiration model by increasing the magnitude of the negative intrathoracic pressure and showing that the venous return and thus the cardiac output is increased. Results of this test are given in table 6.1 .

If a cyclic respiration model is employed, with P_{TH} varying between -3 mmHg and -6 mmHg and P_{ABD} varying between +3 mmHg and +6 mmHg during the respiratory cycle, the normal respiratory variations of heart rate (sinus arrhythmia), blood pressure, etc. appear. This is illustrated using a respiratory rate of 12 breaths per min. in fig.6.13.

If cyclic respiration is used and the model is also subjected to a head-up tilt, variations of heart rate, blood pressure, etc. appear as in the recumbent case at the frequency of breathing (fig. 6.14). Hyndman (1970) and Hyndman et al.(1971) have suggested that sufficiently low breathing rates will result in an additional low frequency component of about 0.1 Hz appearing in the circulatory variables due to limit cycles in the nonlinear blood pressure control system. This was not observed in the present model over a wide range of respiratory rates in orthostasis or recumbency probably because the effective gains of the nonlinear control systems were insufficient to sustain limit cycles.

6.7.2 The estimation of total systemic resistance

In the average human, if the cardiac output is 5 litres per min. and the mean arterial pressure is 100 mmHg, a normal value for the total peripheral resistance will be

$$\frac{100 \times 60}{5000} = 1.2 \quad \text{mm Hg sec } ml^{-1}$$

The value of the estimated total systemic resistance (ETSR) obtained from the model in a steady state is 1.29 mmHg sec ml^{-1} which is satisfactory. The value of the true total systemic resistance (TTSR) in the steady state is 1.22 mmHg sec ml^{-1} which is acceptably close to the estimated value (ETSR).

It is suggested in section 2.9 and appendix 8 that (ETSR) may differ considerably from the true value (TTSR) during transient dynamics. This is demonstrated in the model by simulating a Valsalva manoeuvre and simultaneously recording (ETSR) and (TTSR) as in fig.6.15. It is seen that the (TTSR) changes very little during the short duration of the manoeuvre (12 sec) which is to be expected because the peripheral resistance controller has time constants of 4 sec and 20 sec. The sudden jumps in (ETSR) at the beginning and end of the manoeuvre cannot reflect changes of (TTSR) because of these time constants. Thus the value of (ETSR) computed from one cardiac cycle is rather an unreliable indicator of peripheral resistance for rapid transient dynamics. A further comparison of (ETSR) and (TTSR) is made during a simulated injection of methoxamine described in chapter 7.

6.7.3 The input impedance of the systemic circulation model

The input impedance of the systemic circulation model is computed from an electrical analog of the systemic circulation (fig.2.5) using a FORTRAN subroutine given in appendix 6.

The modulus and phase angle of the impedance for normal values of parameters are shown in the upper graphs of fig. 6.16. The modulus shows a rapid decrease from the total systemic resistance value of 1.22 mmHg sec ml^{-1} to a minimum value of 0.05 mmHg sec ml^{-1} at 1.8 Hz. Thereafter the modulus gradually increases. The phase angle is negative at low frequencies but becomes zero at about 4.2 Hz and positive above this frequency. These features are in satisfactory agreement with results obtained by Mills et al.(1970) and Noble et al.(1967).

6.7.4 The effect of changing the arterial wall viscoelasticity

The effect of changing the viscoelastic time constant for systemic arterial walls (K_s) on the steady state of the model is shown in table 6.2. It is seen that below the normal value of 0.04 sec the control mechanisms are unable to maintain the blood pressure and stroke volume at normal values. The effect of removing arterial wall viscoelasticity altogether on the input impedance of the systemic circulation model is illustrated in the lower graphs of fig. 6.16 which shows that the modulus and phase angle become highly oscillatory and unrealistic. Thus the viscoelasticity is important in the model to ensure an approximately correct input impedance of the systemic circulation.

6.7.5 The effect of changing the shape of the elastance waveforms

Beneken (1965, p.21) has pointed out that the shape of the systolic portion of the elastance waveform used in the representation of the pumping action of the heart is not critical provided that the maximum and minimum elastance values remain unchanged. This is verified in the present model by investigating the steady state using triangular, rectangular, half-sinusoidal and parabolic elastance waveforms (table 6.3). It is seen that there is very little difference between the half-sinusoidal and parabolic results but, reasonably enough, there are more substantial changes if grossly unrealistic waveforms are used as in the triangular and rectangular cases.

The replacement of the half-sinusoidal waveform by the parabolic

waveform produced a negligible change in the execution time of the program on the CDC 7600 computer so a half-sinusoidal waveform was used for programming convenience.

6.7.6 The effect of changing the diameters of the aortic and pulmonary valves

In table 6.4, the effect of changing the diameters and hence the cross-sectional areas A_{AOI} and A_{PA} of the aortic and pulmonary valves is shown. As expected, the reduction of the diameter to 1.0 cm leads to a significant decrease of stroke volume, cardiac output and mean arterial pressure. The removal of the terms in eqns.(2.34) and (2.35) representing the application of Bernoulli's theorem to ventricular ejection is equivalent to setting the areas A_{AOI} and A_{PA} to infinity and the result in the model is a significant increase of mean arterial pressure, stroke volume and cardiac output coupled with a reflex slowing of the heart. The results with a diameter of 1.4 cm give the most acceptable mean cardiac values.

6.7.7 The systolic elastance as a myocardial contractility measure

In section 3.4, it is suggested that the systolic elastance is an acceptable measure of myocardial contractility for the simplified representation of the heart in this model. This may be confirmed by performing a simulated Valsalva manoeuvre and recording the systolic elastance together with a number of commonly used measures of myocardial contractility (fig. 6.17). It is seen that, for the first four seconds of the manoeuvre, all the measures decrease confirming a negative inotropic action. Thereafter the left ventricular elastance and the isometric time tension index (Siegel & Sonnenblick, 1963) increase while the remaining indices continue to decrease. At the end of the manoeuvre, all the indices tend to increase for the first 2 or 3 seconds following completion. Thereafter, a gradual return of all indices to normal values occurs.

The systolic elastance agrees most closely with the isometric time tension index and, overall, there is a broad general agreement between all the measures indicating decreased contractility during the manoeuvre and recovery following the manoeuvre.

6.8 Further tests on the neural control model

The earlier tests of overall cardiovascular control indicated that the neural controllers were, broadly speaking, functioning correctly. Further specific checks were made to confirm this conclusion.

The bang-bang action in the peripheral resistance, venous tone and myocardial contractility controllers was found to be operating correctly with a period equal to the heart period in the steady state. The central nervous input function (B) was below the threshold K_{18} for about 0.39 sec and above the threshold K_{18} for about 0.44 sec (fig. 6.4).

The constant K_{16} in the model of appendix 1 controls the relative contributions of the aortic arch baroreceptors and carotid sinus baroreceptors to the overall central nervous input function (B). The effect of varying K_{16} on the steady state of the model is shown in table 6.5. It is seen that varying K_{16} has little effect which is to be expected in the steady state because the baroreceptor inputs P_{AO2} and P_{UA} have similar characteristics.

However when P_{AO2} and P_{UA} differ, the effect of changing K_{16} is more significant. This is demonstrated by observing changes in the features of the heart rate response in a Valsalva manoeuvre with changing K_{16} (table 6.6). The results indicate that the response is less realistic if the pressure information is derived almost entirely from one baroreceptor alone so that the value of 0.7 used normally and based on results of Dampney et al.(1971) is acceptable.

6.9 Tests on the pharmacokinetics model

If no breakdown of an injected drug occurs, then a consequence of the formulation of the model is that the sum total of masses in all segments of the slave transport model should remain constant. This was tested and found to be correct in all of the simulated injections in which no breakdown occurred. In this particular case, the injected substance should eventually become distributed throughout the circulation with equal concentration in all segments. This too was confirmed with the ultimate concentration in all segments following a 70 μg injection being 0.0154 $\mu g\ m\ell^{-1}$.

The concentration changes in the head and arms veins segment and

the left ventricle segment following an injection of 70 μg of a neutral substance (i.e. with no action on the cardiovascular system) into the head and arms veins segment at $t = 0$ is shown in fig. 6.18 for various values of the time constant for breakdown/absorption. The time constant used in the drug investigations (τ_q) is 30 sec and this gives an acceptable time-course for the concentration.

The approximate simulation of transport delays in the 19-segment transport model is shown in fig. 6.19 again following an injection of a neutral substance into the head and arms veins segment at $t = 0$.

These results indicate that, despite the approximations of the multiple modelling approach, a satisfactory representation of drug transport is achieved.

6.10 Conclusion

The mathematical model and its digital computer implementation have been validated by a variety of methods described in this chapter.

The waveforms and magnitudes of variables have been checked and the performance of the model has been investigated using orthostasis, blood volume changes, a Valsalva manoeuvre and pacing of the heart. In the pacing tests, the cardiac output changed very little with heart rate so that a very close linear relationship between stroke volume and heart period was obtained.

In the above tests and further subsidiary checks, the model exhibits satisfactory dynamic responses and yields acceptable numerical values. The results indicate that the model is broadly adequate for the intended study of effects following injections of cardiovascular agents.

INTRATHORACIC PRESSURE (MMHG)	0	−4	−7	−10
INTRA-ABDOMINAL PRESSURE (MMHG)	0	+4	+7	+10
MEAN ARTERIAL PRESSURE (MMHG)	102.5	109.1	113.7	119.5
STROKE VOLUME (ML)	61.5	69.6	75.7	83.5
CARDIAC OUTPUT ($ML\ SEC^{-1}$)	79.3	84.6	88.4	93.1
HEART RATE (BEATS PER MIN.)	77.4	72.9	70.1	66.9
ESTIMATED TOTAL SYSTEMIC RESISTANCE ($MMHG\ SEC\ ML^{-1}$)	1.292	1.289	1.286	1.283
SYSTOLIC PRESSURE (MMHG)	123.0	130.9	136.7	143.7
DIASTOLIC PRESSURE (MMHG)	86.3	90.8	94.1	98.0

TABLE 6.1 DEMONSTRATION OF THE RESPIRATORY PUMP ACTION USING A STATIC RESPIRATION MODEL (VALUES GIVEN WERE OBSERVED IN THE STEADY STATE)

VISCOELASTIC TIME CONSTANT OF THE ARTERIAL WALL (SEC)	0.01	0.02	0.04	0.06	0.08
MEAN ARTERIAL PRESSURE (MMHG)	92.1	101.6	109.1	109.6	109.8
STROKE VOLUME (ML)	54.4	62.3	69.6	71.0	72.6
CARDIAC OUTPUT ($ML\ SEC^{-1}$)	76.1	81.1	84.6	84.6	84.4
HEART RATE (BEATS PER MIN.)	84.0	78.1	72.9	71.5	69.8
ESTIMATED TOTAL SYSTEMIC RESISTANCE ($MMHG\ SEC\ ML^{-1}$)	1.210	1.253	1.289	1.295	1.301
SYSTOLIC PRESSURE (MMHG)	109.4	120.1	130.9	134.8	138.6
DIASTOLIC PRESSURE (MMHG)	78.1	85.8	90.8	90.5	89.8

TABLE 6.2 EFFECT OF VARYING THE VISCOELASTIC TIME CONSTANT (K_8) OF THE ARTERIAL WALL ON THE STEADY STATE OF THE MODEL

WAVEFORM OF ELASTANCE FUNCTION	TRIANGULAR	RECTANGULAR	HALF SINUSOID	PARABOLA
MEAN ARTERIAL PRESSURE (MMHG)	104·3	109·0	109·1	109·6
STROKE VOLUME (ML)	63·6	64·3	69·6	70·1
CARDIAC OUTPUT ($ML\ SEC^{-1}$)	79·1	81·5	84·6	85·4
HEART RATE (BEATS PER MIN)	74·5	76·0	72·9	73·1
ESTIMATED TOTAL SYSTEMIC RESISTANCE ($MMHG\ SEC\ ML^{-1}$)	1·320	1·338	1·289	1·284
SYSTOLIC PRESSURE (MMHG)	133·9	148·1	130·9	130·5
DIASTOLIC PRESSURE (MMHG)	87·5	91·4	90·8	91·3

TABLE 6.3 EFFECT OF VARYING THE WAVEFORM OF THE ELASTANCE FUNCTION ON THE STEADY STATE OF THE MODEL (MAXIMUM AND MINIMUM ELASTANCE VALUES UNCHANGED)

DIAMETER OF AORTIC VALVE OR PULMONARY VALVE ORIFICE (CM)	1·0	1·4	∞
MEAN ARTERIAL PRESSURE (MMHG)	100·6	109·1	113·3
STROKE VOLUME (ML)	51·2	69·6	84·4
CARDIAC OUTPUT ($ML\ SEC^{-1}$)	76·5	84·6	89·2
HEART RATE (BEATS PER MIN)	89·6	72·9	63·5
ESTIMATED TOTAL SYSTEMIC RESISTANCE ($MMHG\ SEC\ ML^{-1}$)	1·315	1·289	1·270
SYSTOLIC PRESSURE (MMHG)	114·4	130·9	154·1
DIASTOLIC PRESSURE (MMHG)	87·7	90·8	90·6

TABLE 6.4 EFFECT OF VARYING THE DIAMETER OF THE AORTIC VALVE AND PULMONARY VALVE ORIFICES ON THE STEADY STATE OF THE MODEL

RELATIVE CONTRIBUTION OF THE CAROTID SINUS BARORECEPTOR OUTPUT TO THE CENTRAL NERVOUS INPUT FUNCTION (K_{16})	0·1	0·3	0·5	0·7	0·9
MEAN ARTERIAL PRESSURE (MMHG)	107·6	108·0	108·4	109·1	110·0
STROKE VOLUME (ML)	67·4	67·5	68·1	69·6	70·2
CARDIAC OUTPUT ($ML\ SEC^{-1}$)	84·0	84·3	84·4	84·6	85·1
HEART RATE (BEATS PER MIN)	74·8	74·9	74·3	72·9	72·8
ESTIMATED TOTAL SYSTEMIC RESISTANCE ($MMHG\ SEC\ ML^{-1}$)	1·281	1·282	1·284	1·289	1·293
SYSTOLIC PRESSURE (MMHG)	129·2	129·5	130·0	130·9	132·0
DIASTOLIC PRESSURE (MMHG)	89·9	90·2	90·5	90·8	91·6

TABLE 6.5 EFFECT ON THE STEADY STATE OF THE MODEL OF VARYING THE RELATIVE CONTRIBUTION OF THE CAROTID SINUS BARORECEPTOR OUTPUT TO THE CENTRAL NERVOUS INPUT FUNCTION (K_{16})

RELATIVE CONTRIBUTION OF THE CAROTID SINUS BARORECEPTOR OUTPUT TO THE CNS INPUT FUNCTION (K_{16})	HEART RATE IN THE BEAT BEFORE THE START OF THE MANOEUVRE	MINIMUM HEART RATE DURING THE MANOEUVRE	HEART RATE IN THE BEAT BEFORE THE END OF THE MANOEUVRE	MAXIMUM HEART RATE FOLLOWING THE MANOEUVRE
0·1	74·8	74·3	99·8	102·1
0·3	74·9	73·8	96·4	101·0
0·5	74·3	71·7	92·5	100·1
0·7	72·9	69·0	91·6	101·4
0·9	72·8	67·4	91·3	105·2

TABLE 6.6 EFFECT ON CERTAIN FEATURES OF THE HEART RATE RESPONSE IN A VALSALVA MANOEUVRE OF VARYING THE RELATIVE CONTRIBUTION OF THE CAROTID SINUS BARORECEPTOR OUTPUT TO THE CENTRAL NERVOUS INPUT FUNCTION (K_{16})

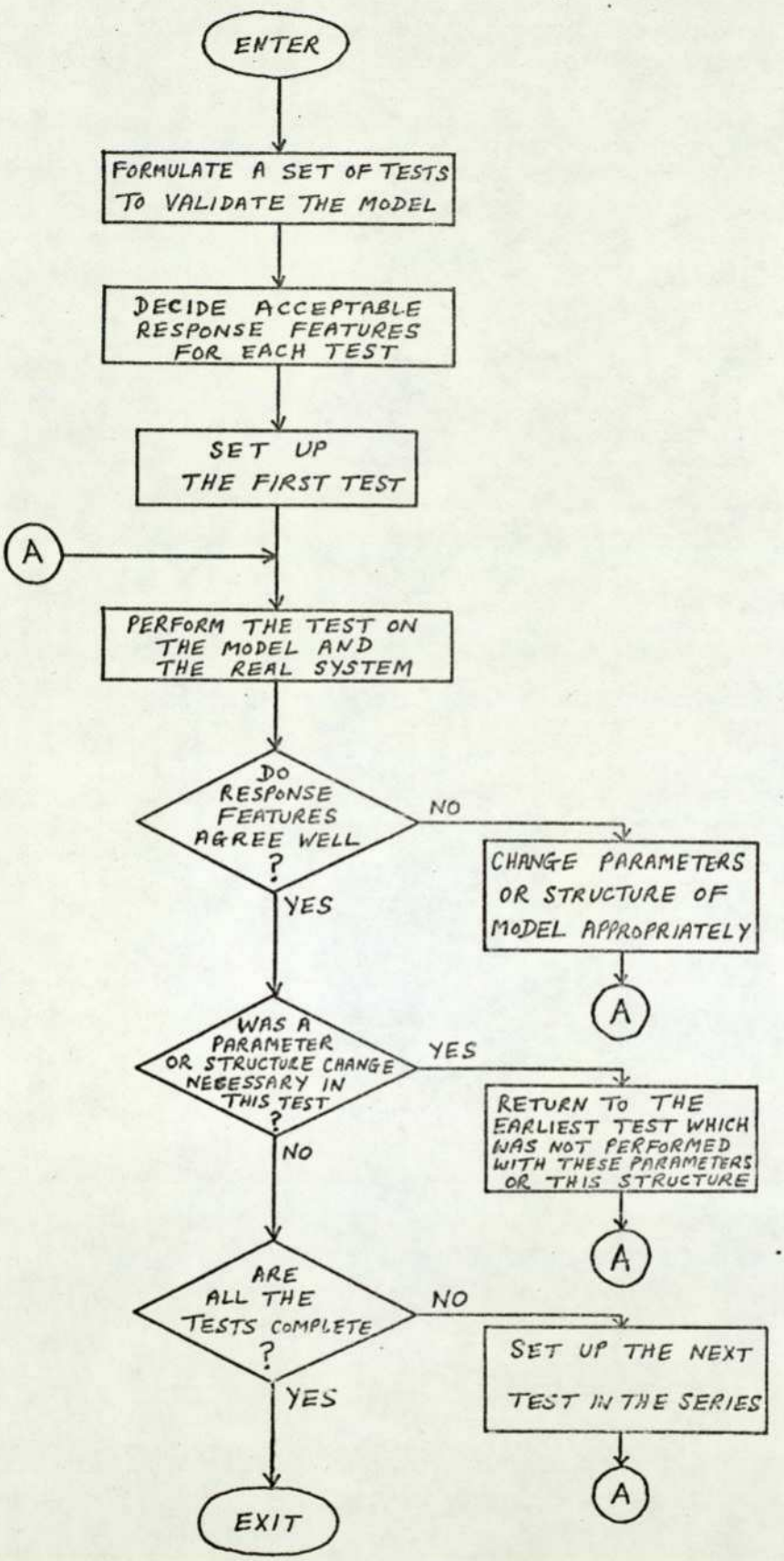

FIG. 6.1 FLOW DIAGRAM OF A VALIDATION PROCEDURE FOR NONLINEAR MODELS BASED ON THE COMPARISON OF FEATURES.

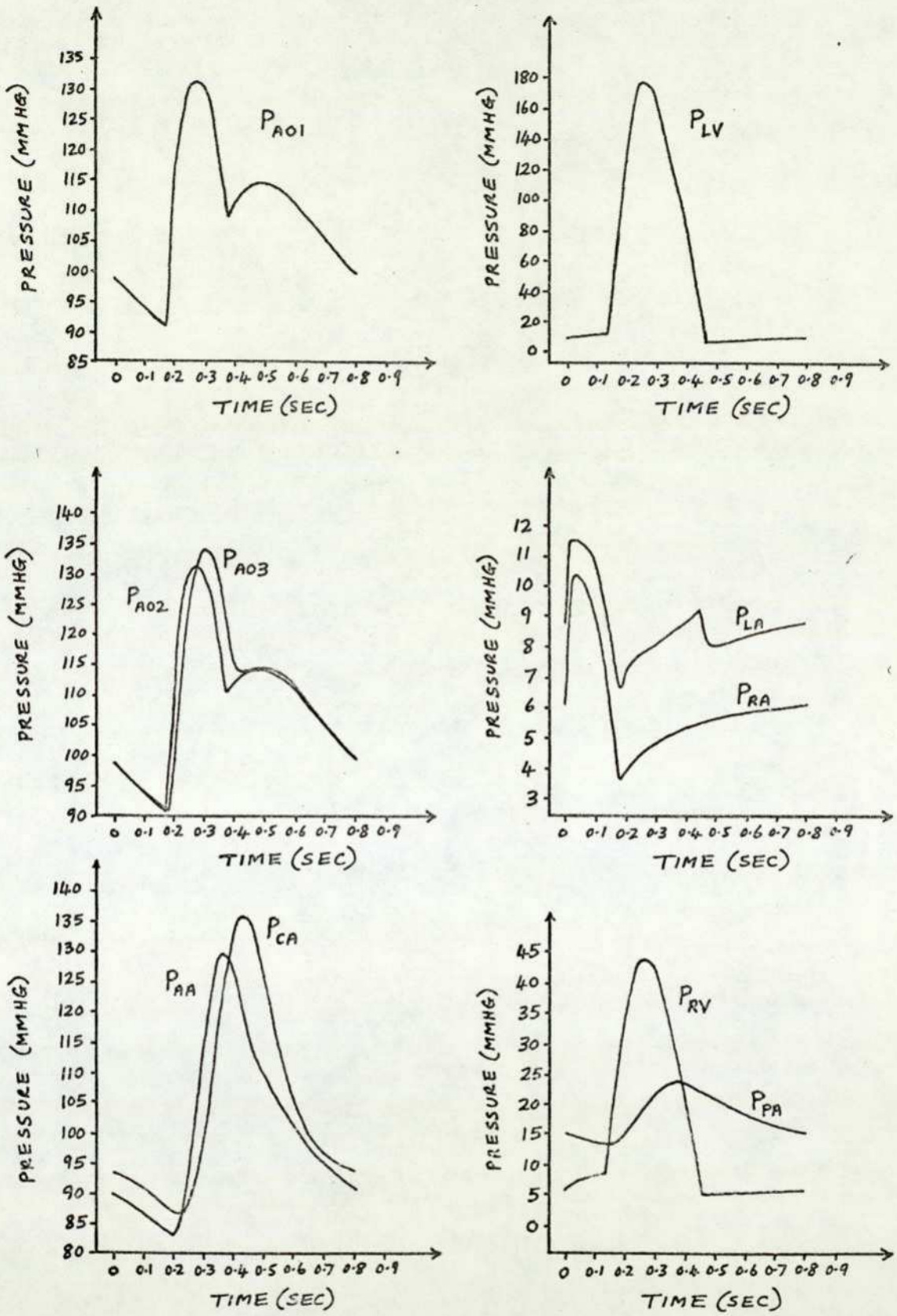

FIG. 6.2 WAVEFORMS OF SELECTED PRESSURES DURING ONE CARDIAC CYCLE IN THE STEADY STATE.

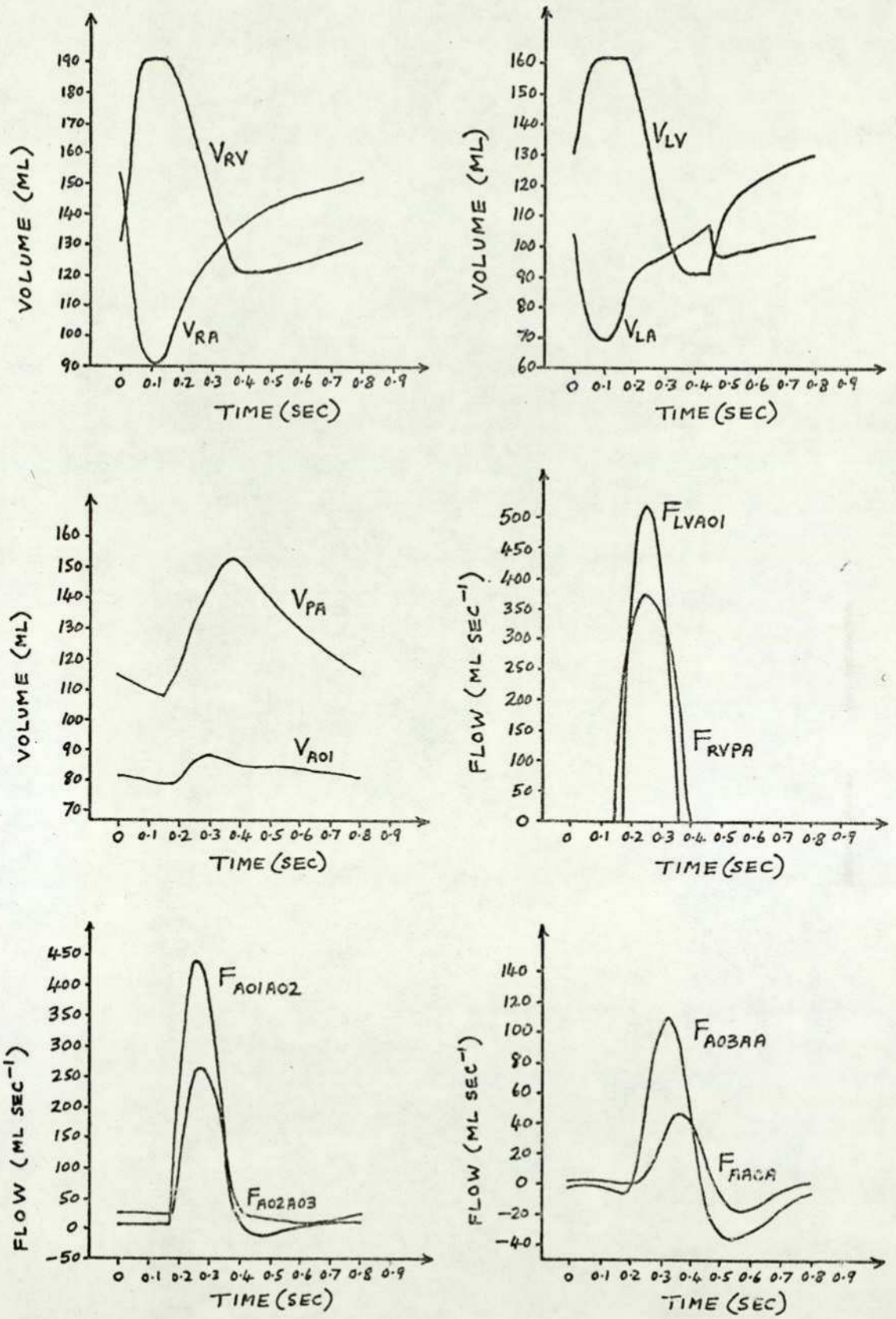

FIG. 6.3 WAVEFORMS OF SELECTED VOLUMES AND FLOWS DURING ONE CARDIAC CYCLE IN THE STEADY STATE

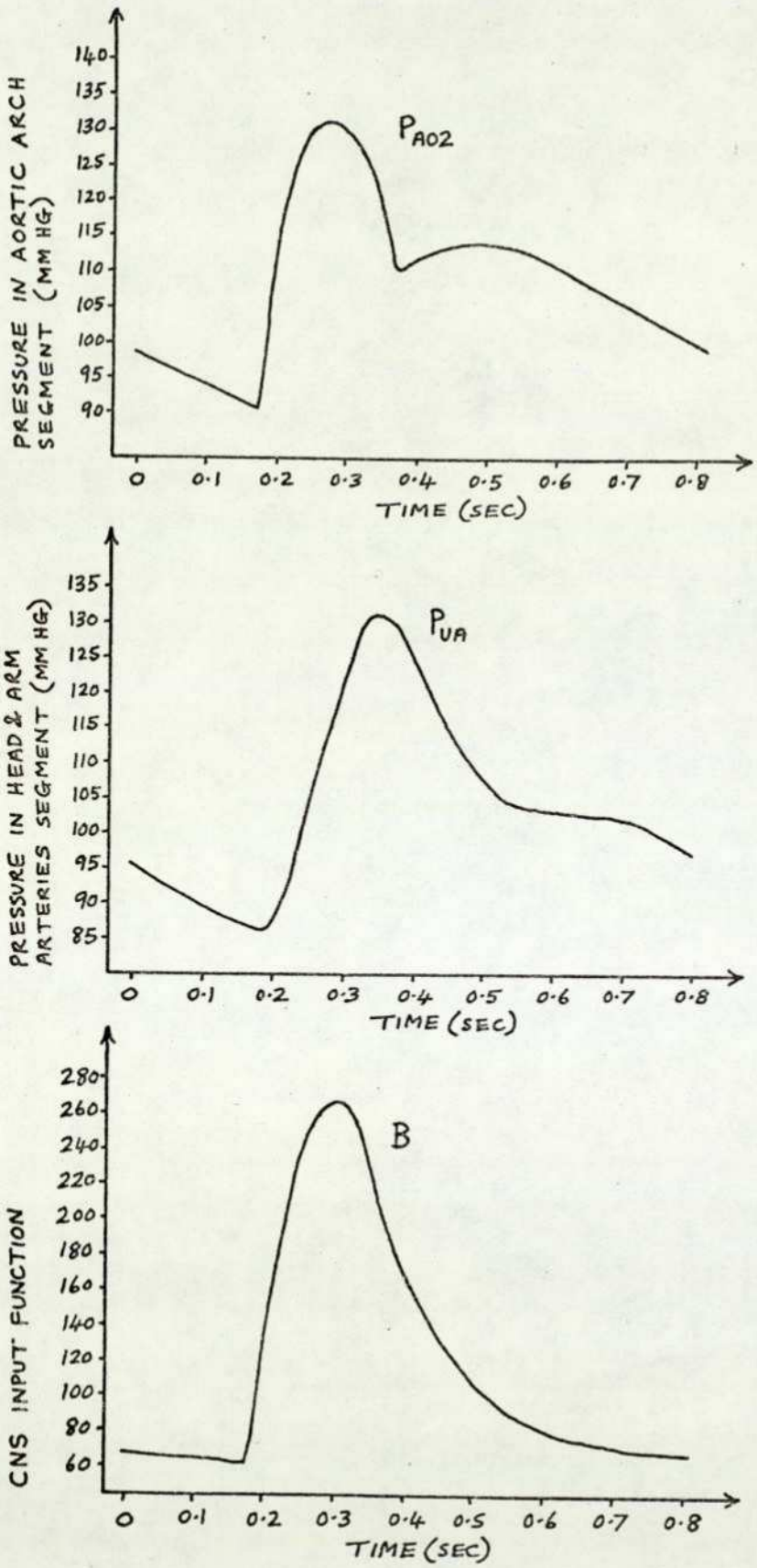

FIG. 6.4 WAVEFORMS OF PRESSURE IN THE AORTIC ARCH SEGMENT (P_{A02}), PRESSURE IN THE HEAD & ARMS ARTERIES SEGMENT (P_{UA}) AND THE C.N.S. INPUT FUNCTION (B) DURING ONE CARDIAC CYCLE IN THE STEADY STATE

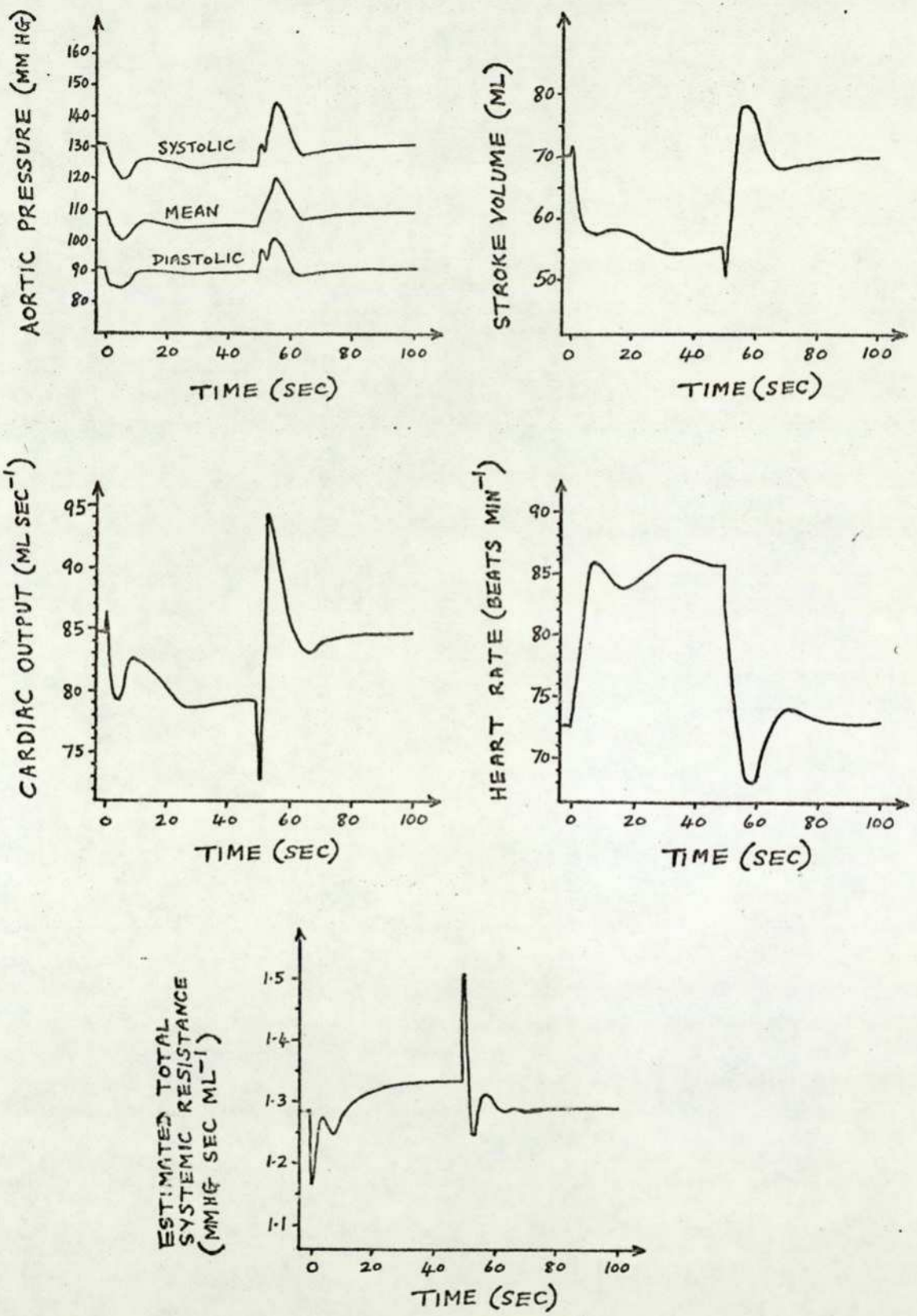

FIG. 6·5 DYNAMICS FOLLOWING A HEAD-UP TILT ($\phi = 90°$) AT $t = 0$ SEC AND A RETURN TO RECUMBENCY ($\phi = 0°$) AT $t = 50$ SEC.

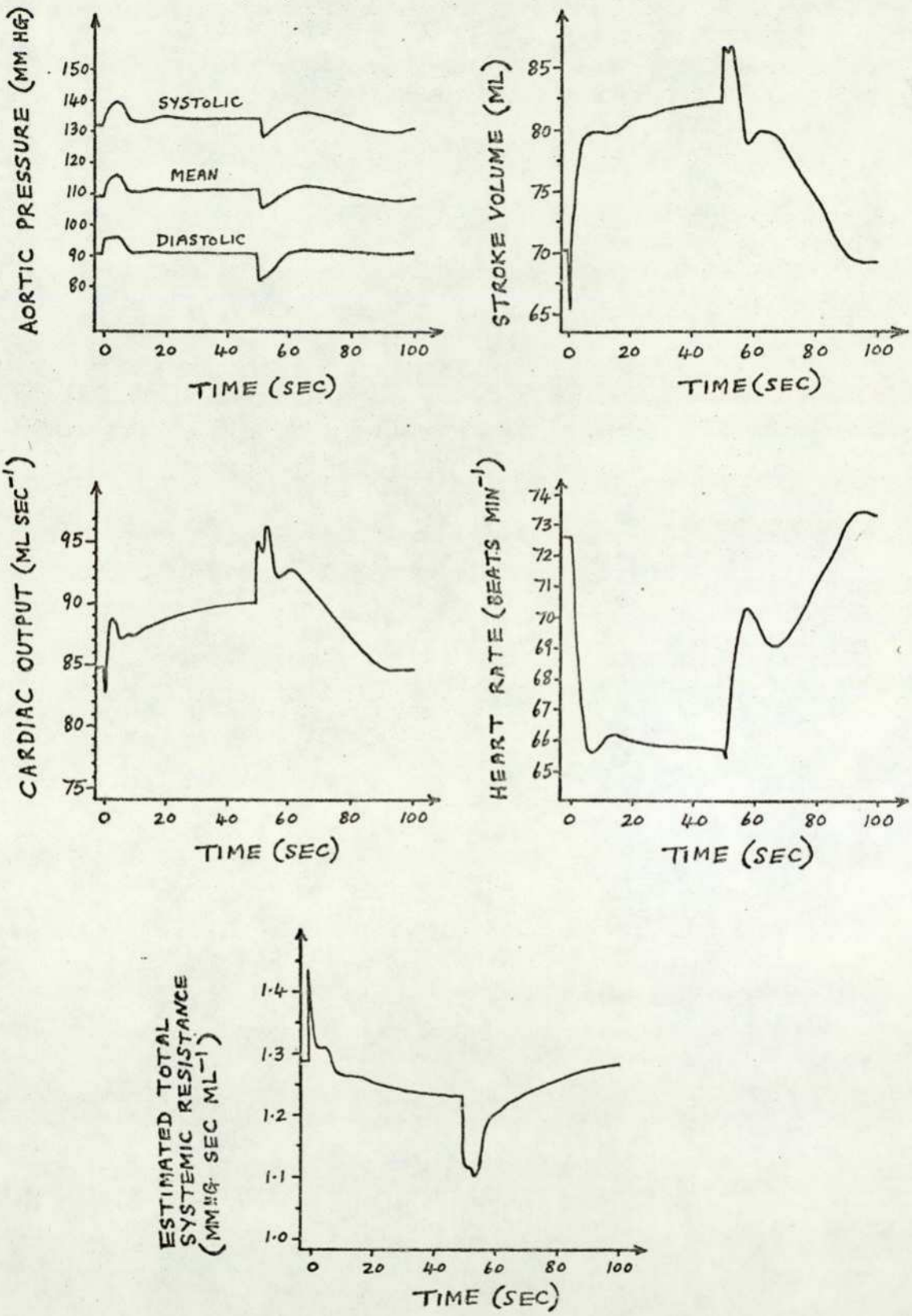

FIG. 6.6 DYNAMICS FOLLOWING A HEAD-DOWN TILT ($\phi = -90°$) AT $t = 0$ SEC AND A RETURN TO RECUMBENCY ($\phi = 0°$) AT $t = 50$ SEC

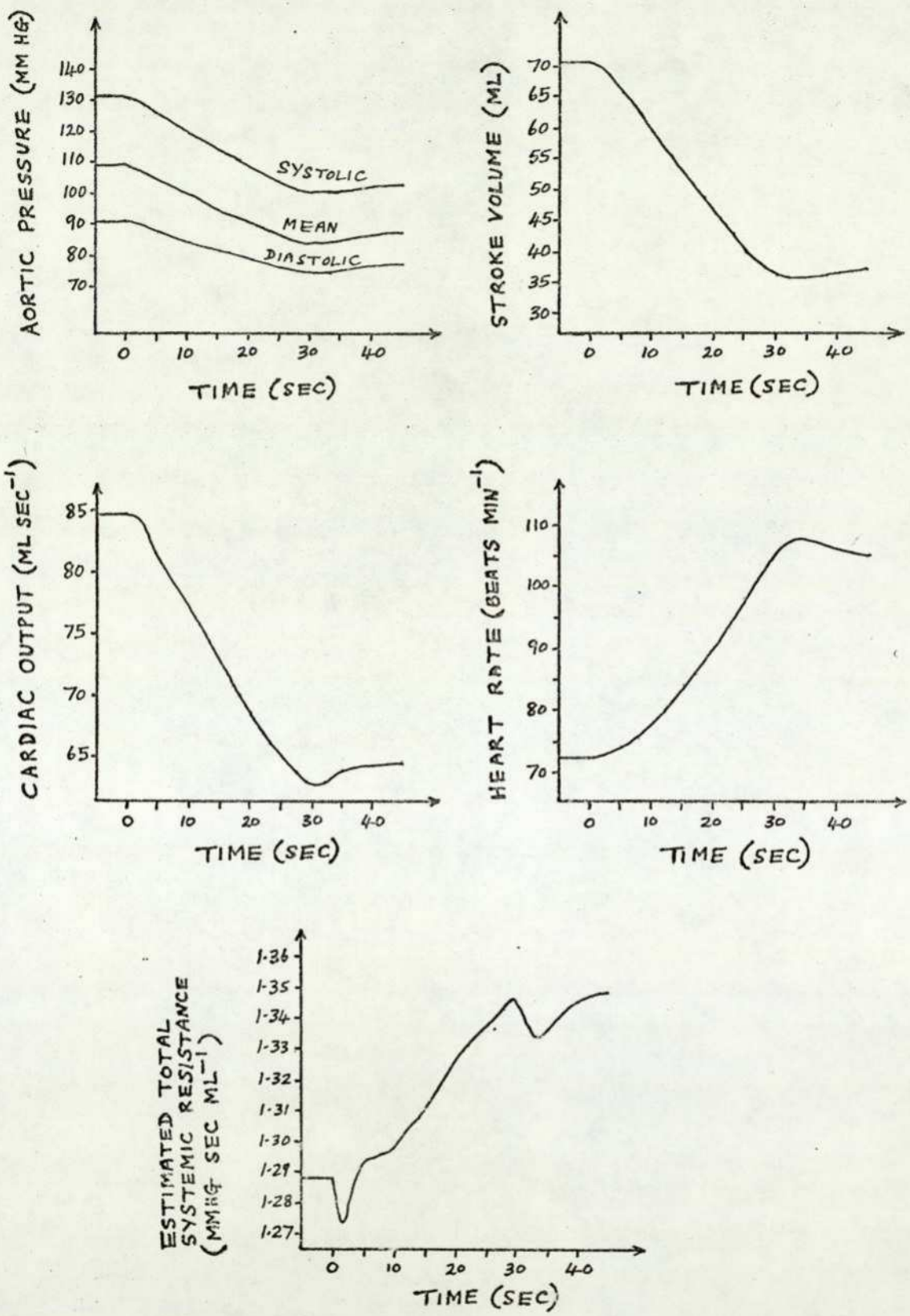

FIG. 6.7 DYNAMICS FOLLOWING THE SUDDEN REMOVAL OF 500 ML. BLOOD FROM THE SEGMENT REPRESENTING THE HEAD & ARMS VEINS AT $t=0$ sec.

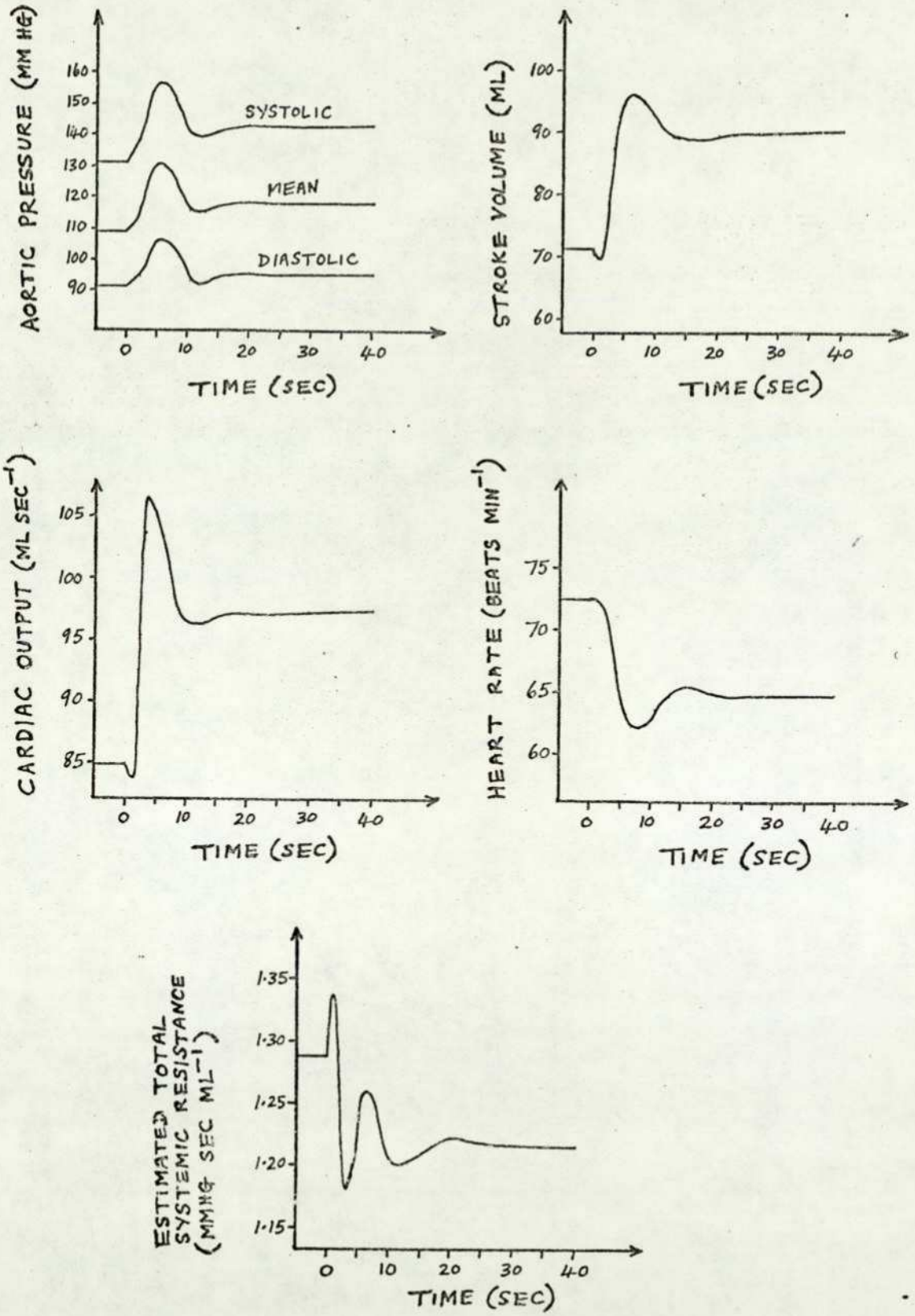

FIG. 6.8 DYNAMICS FOLLOWING THE SUDDEN INJECTION OF 500 ML. BLOOD INTO THE SEGMENT REPRESENTING THE HEAD & ARMS VEINS AT $t = 0$ sec.

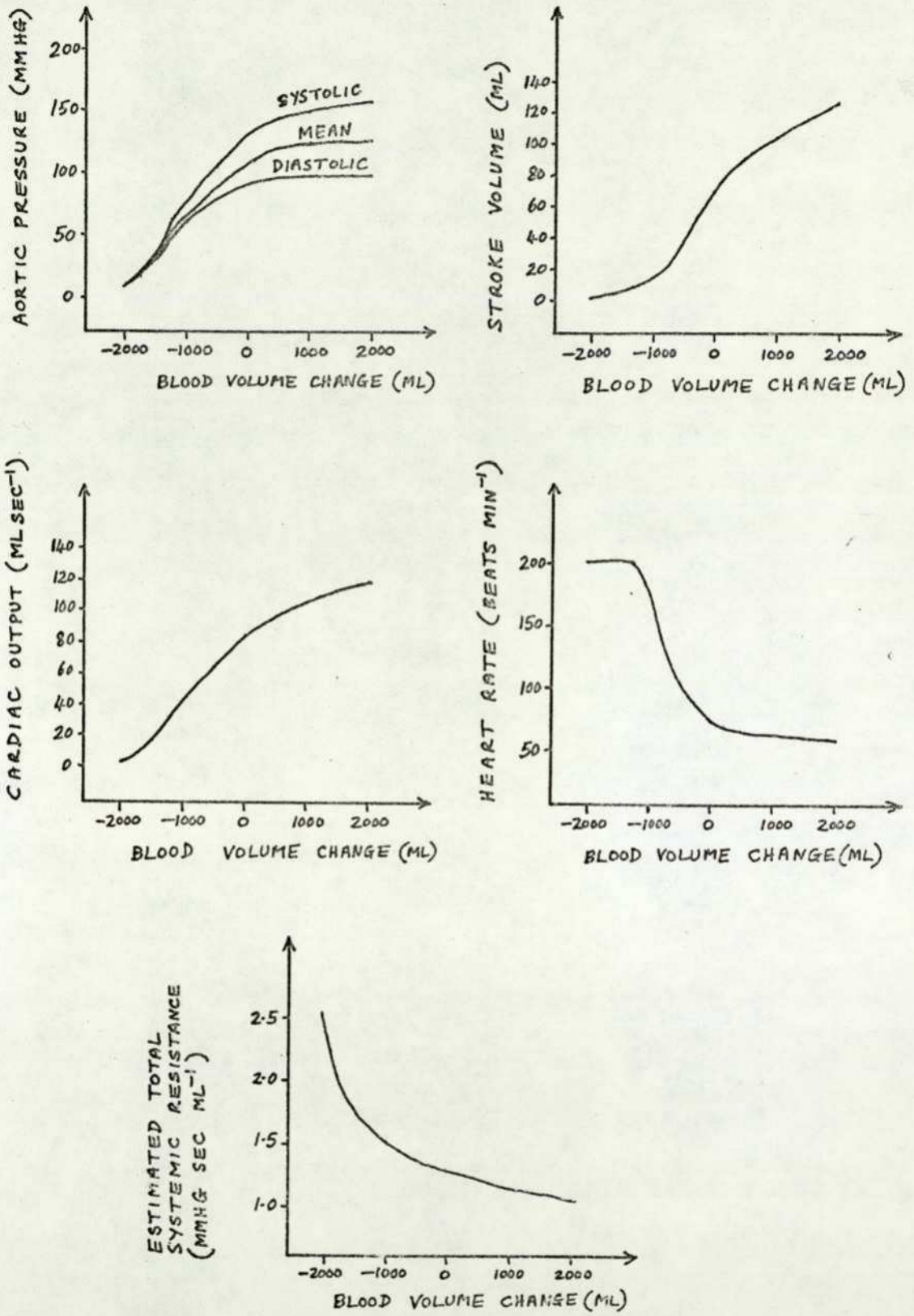

FIG. 6.9 PLOTS OF BEAT-BY-BEAT VARIABLES VERSUS BLOOD VOLUME CHANGE IN THE STEADY STATE FOLLOWING THE REMOVAL OR INJECTION OF BLOOD

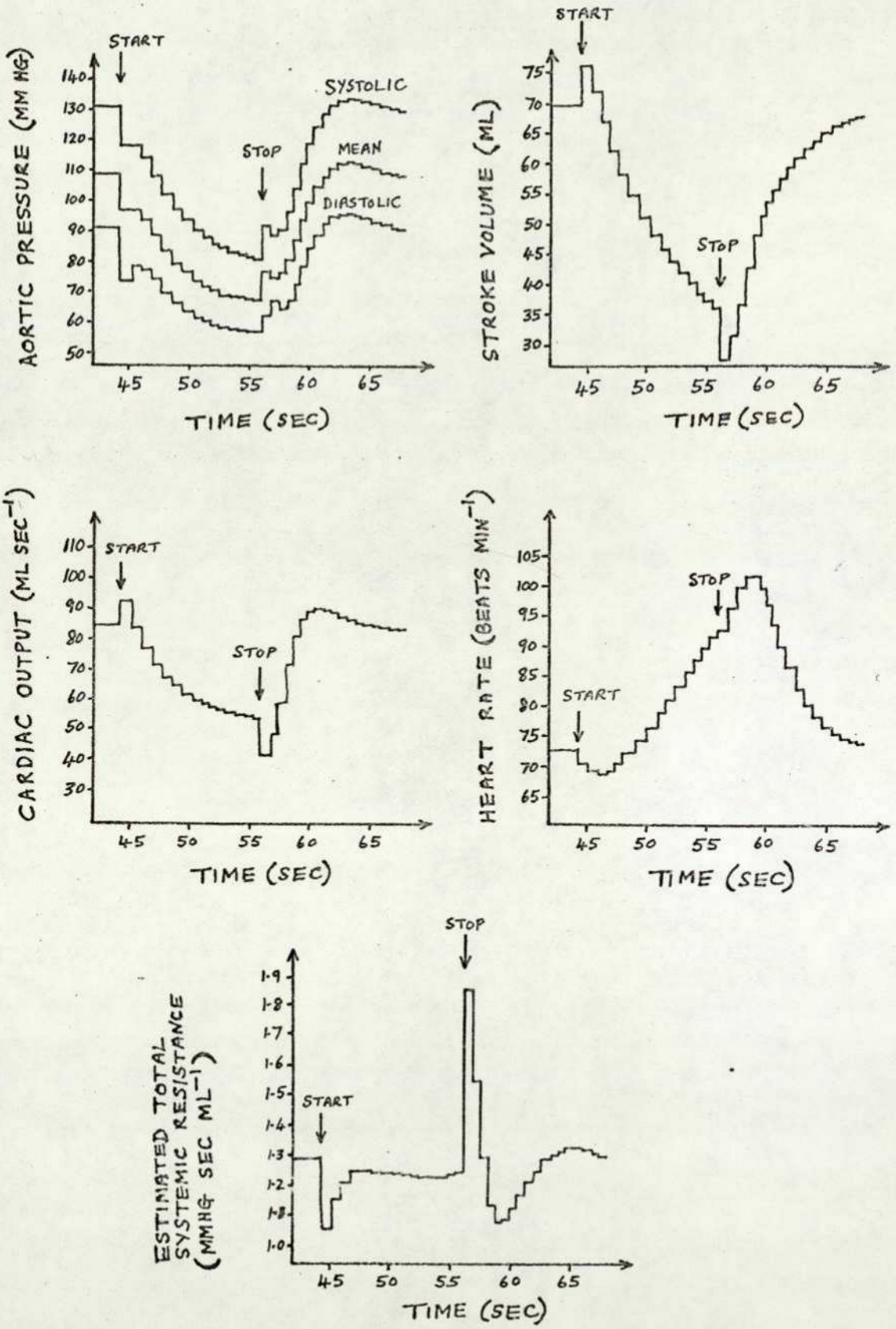

FIG. 6.10 THE DYNAMICS IN A VALSALVA MANOEUVRE. THE MANOEUVRE STARTS AT $t = 44$ sec WITH $P_{TH} = P_{ABD} = +40$ mm Hg AND STOPS AT $t = 56$ sec WITH P_{TH} AND P_{ABD} RETURNING TO NORMAL VALUES OF -4 mm Hg AND $+4$ mm Hg RESPECTIVELY.

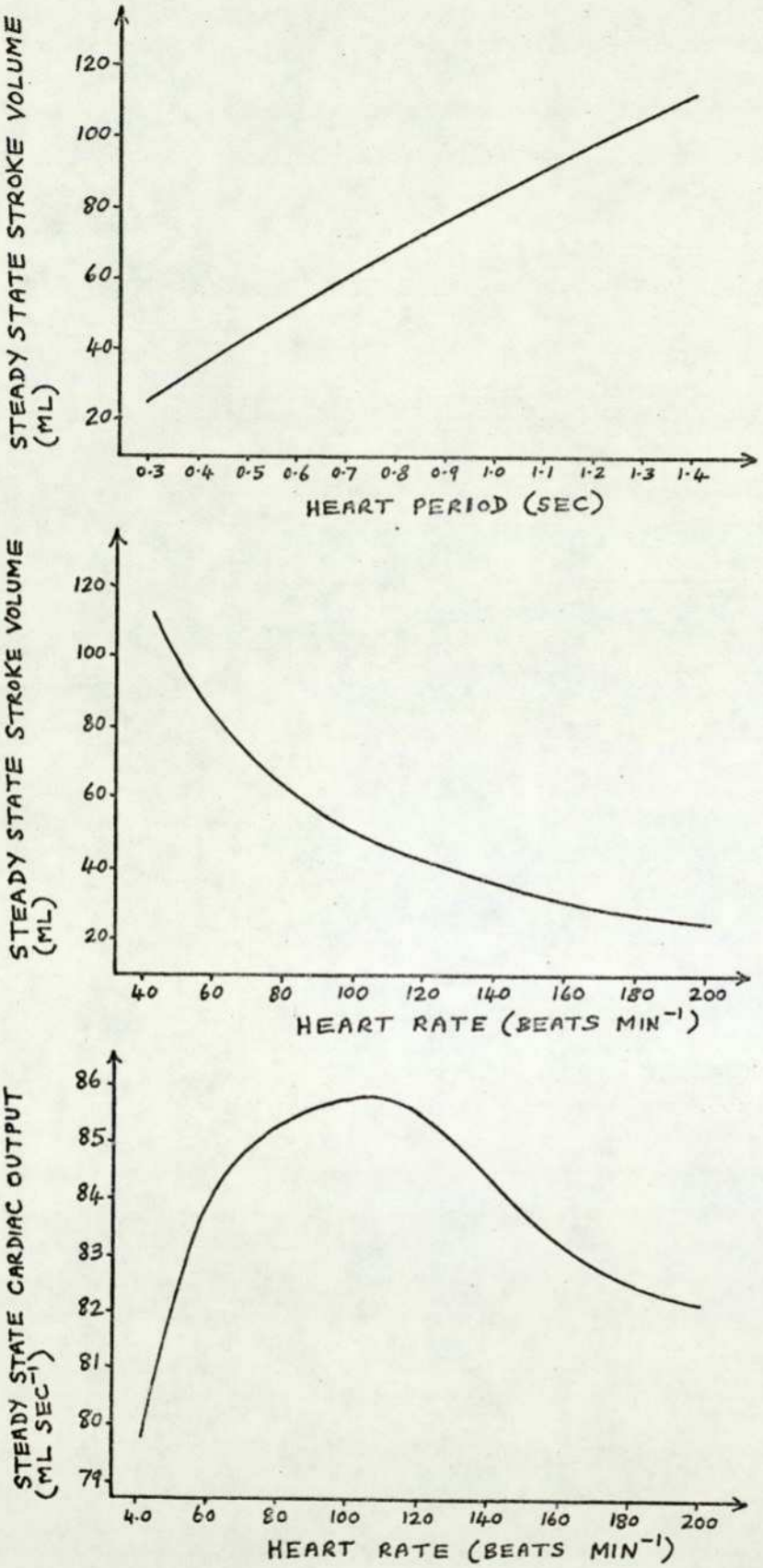

FIG. 6.11 PLOTS OF STROKE VOLUME VERSUS HEART PERIOD, STROKE VOLUME VERSUS HEART RATE AND CARDIAC OUTPUT VERSUS HEART RATE IN THE STEADY STATE. RESULTS OBTAINED FROM PACING TESTS

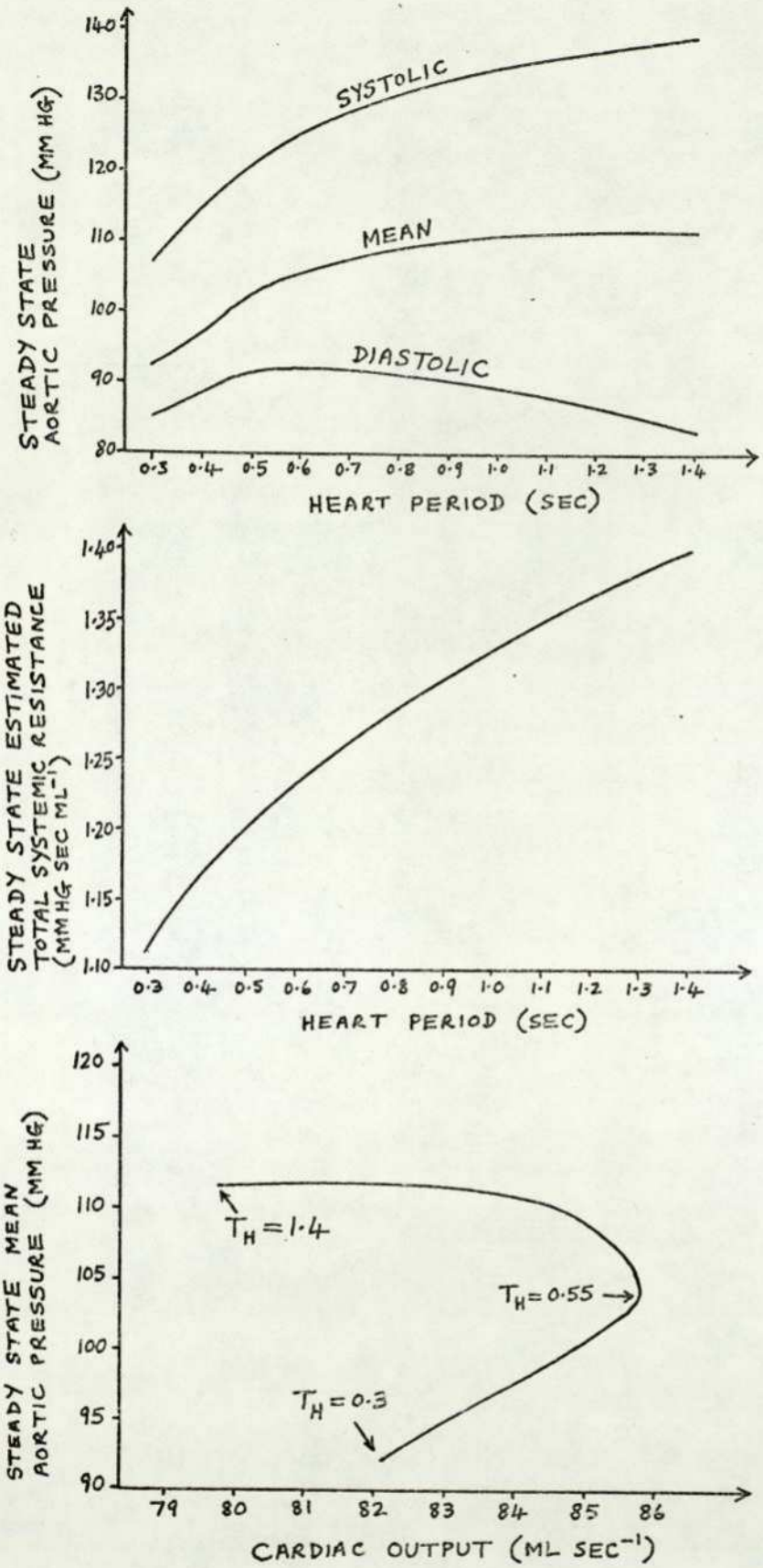

FIG. 6.12 PLOTS OF AORTIC PRESSURE VERSUS HEART PERIOD, (ETSR) VERSUS HEART PERIOD AND MEAN AORTIC PRESSURE VERSUS CARDIAC OUTPUT IN THE STEADY STATE. RESULTS OBTAINED FROM PACING TESTS.

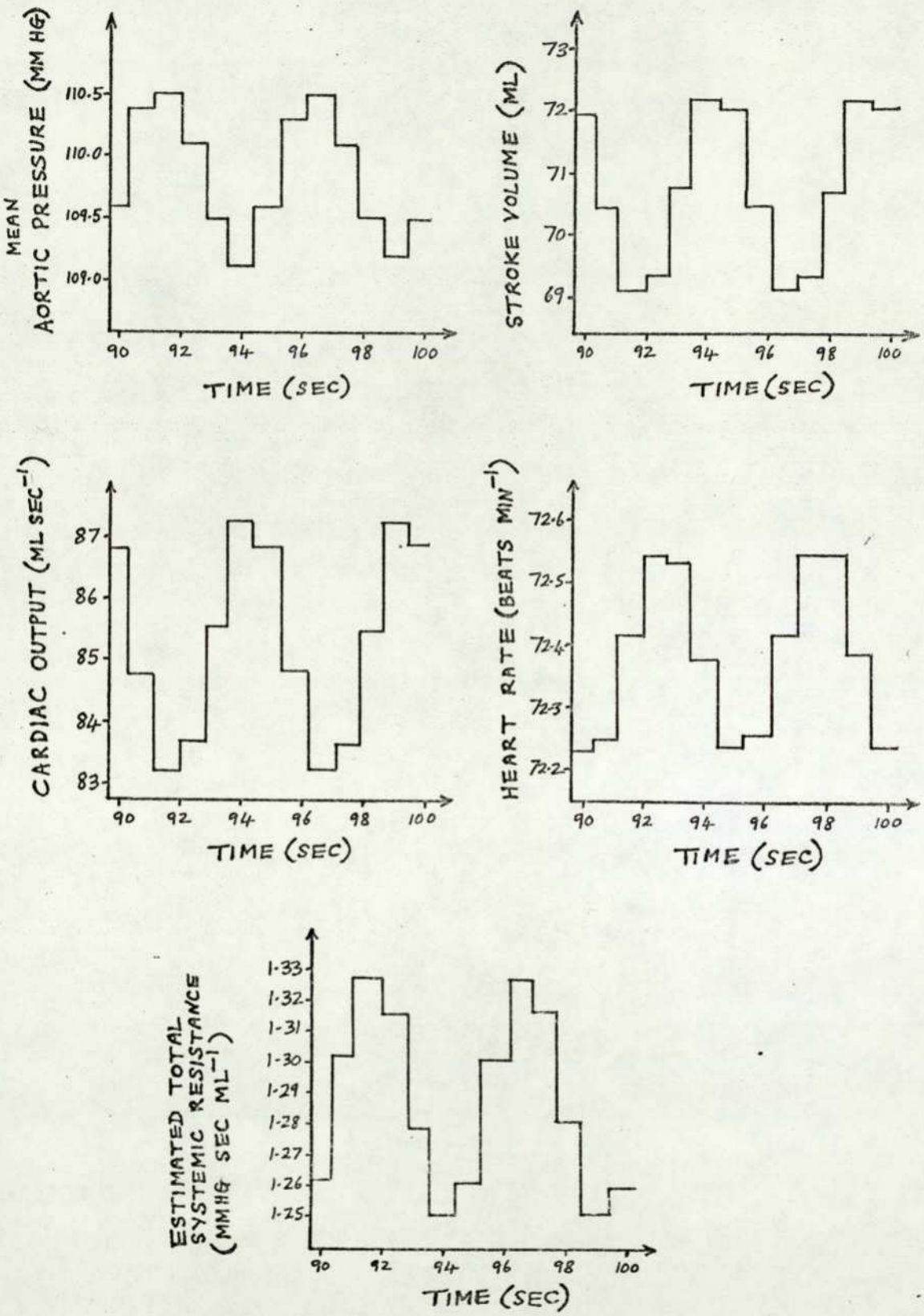

FIG. 6.13 THE EFFECT OF CYCLIC RESPIRATION (12 BREATHS PER MIN) ON THE BEAT-BY-BEAT VARIABLES IN THE STEADY STATE DURING RECUMBENCY ($\phi = 0°$)

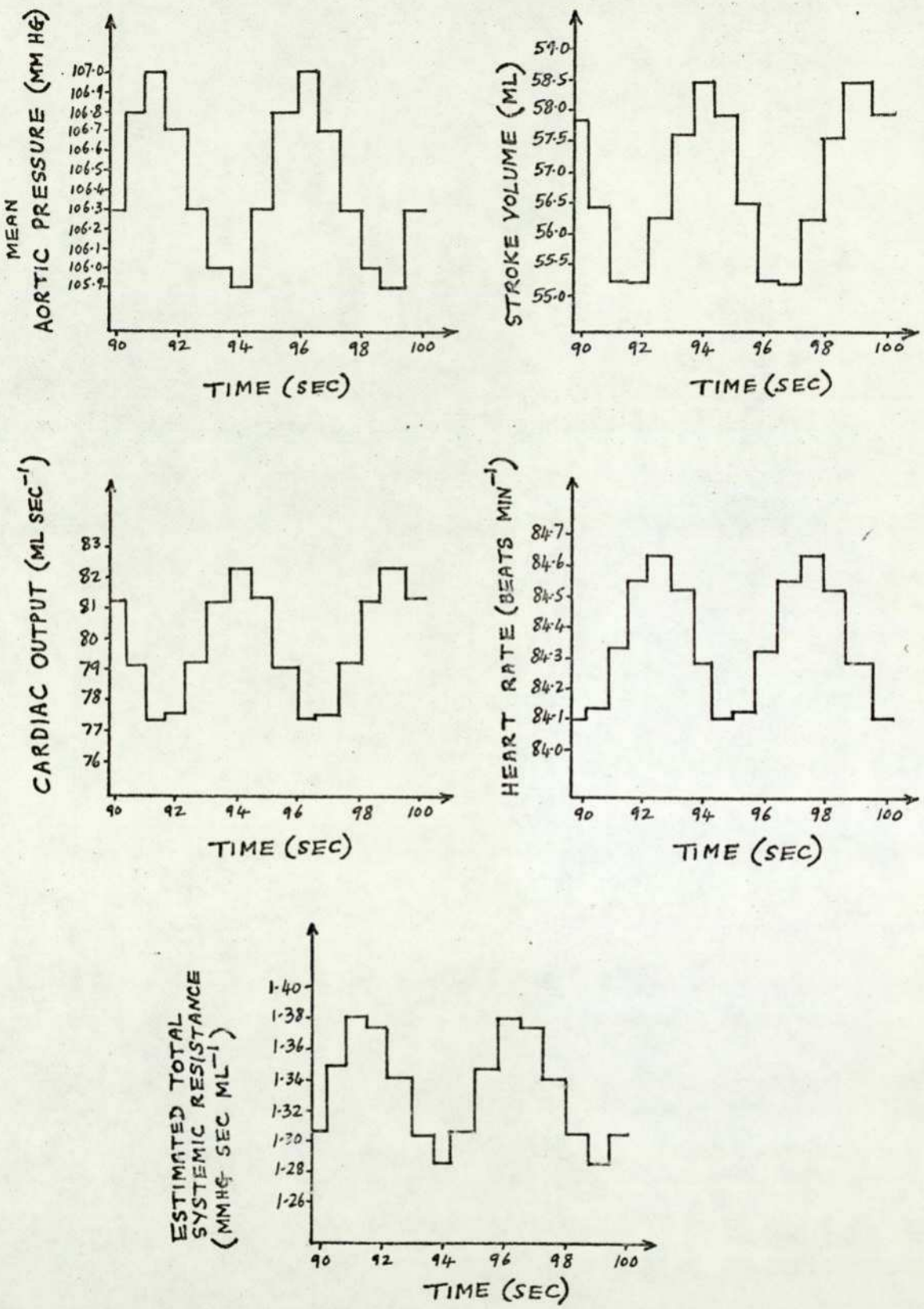

FIG. 6.14 THE EFFECT OF CYCLIC RESPIRATION (12 BREATHS PER MIN.) ON THE BEAT-BY-BEAT VARIABLES IN THE STEADY STATE FOLLOWING A HEAD-UP TILT ($\phi = 90°$)

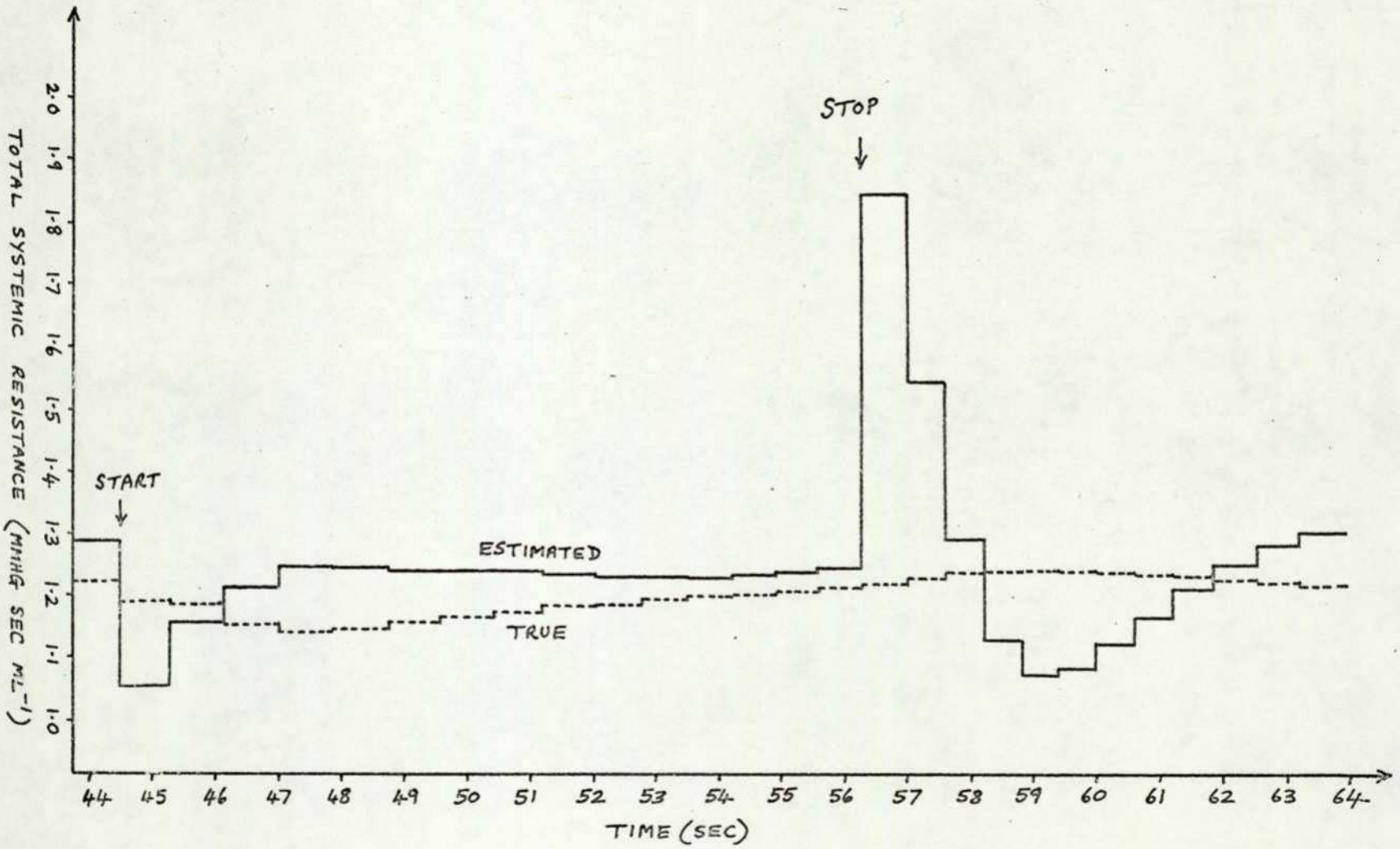

FIG. 6.15 COMPARISON OF ESTIMATED AND TRUE TOTAL SYSTEMIC RESISTANCE DURING A VALSALVA MANOEUVRE (STARTING AT $t = 44{\cdot}4$ sec AND STOPPING AT $t = 56{\cdot}2$ sec)

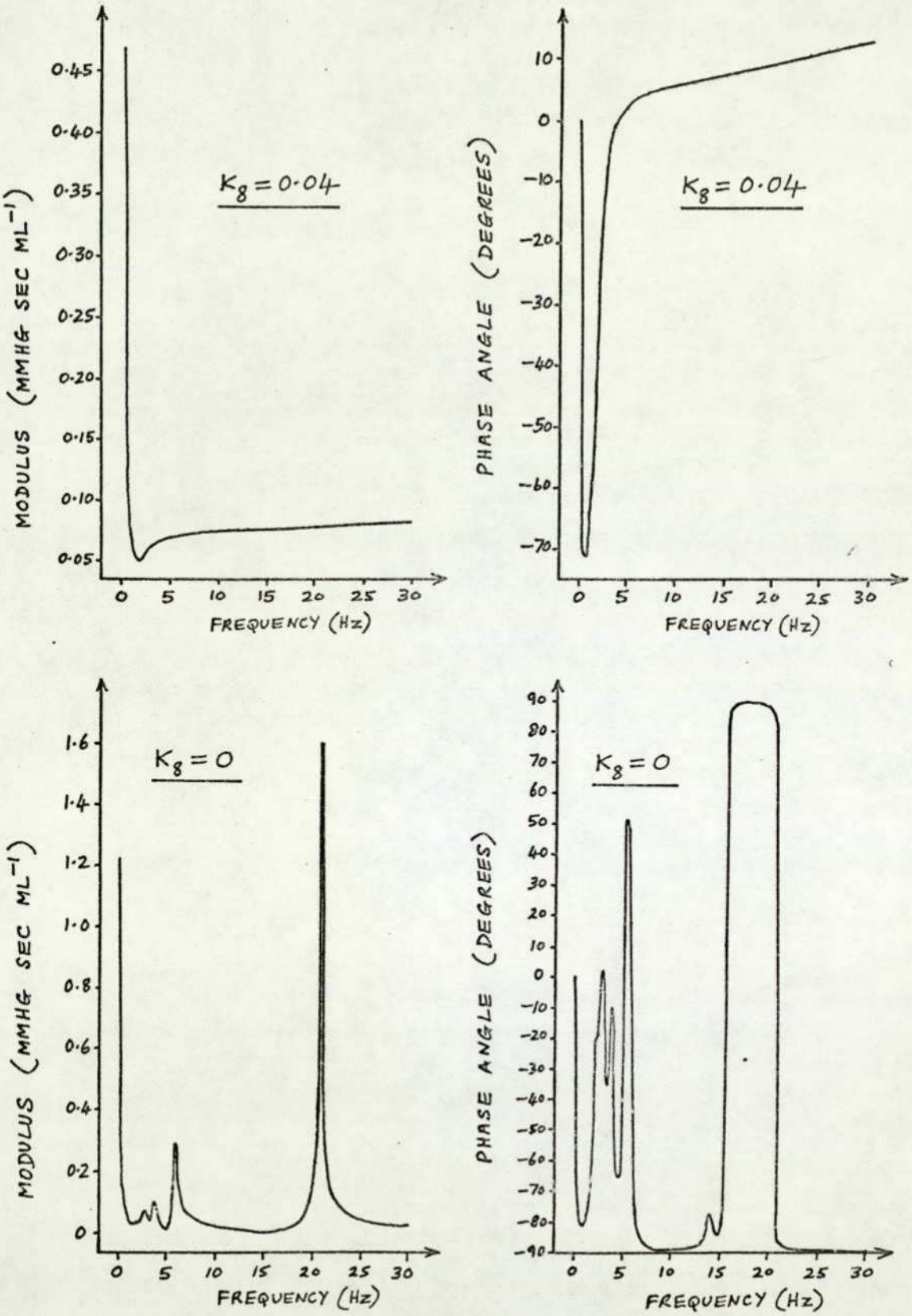

FIG. 6.16 MODULUS AND PHASE ANGLE OF THE INPUT IMPEDANCE OF THE SYSTEMIC CIRCULATION MODEL FOR $K_8 = 0.04$ (UPPER GRAPHS) AND $K_8 = 0$ (LOWER GRAPHS)

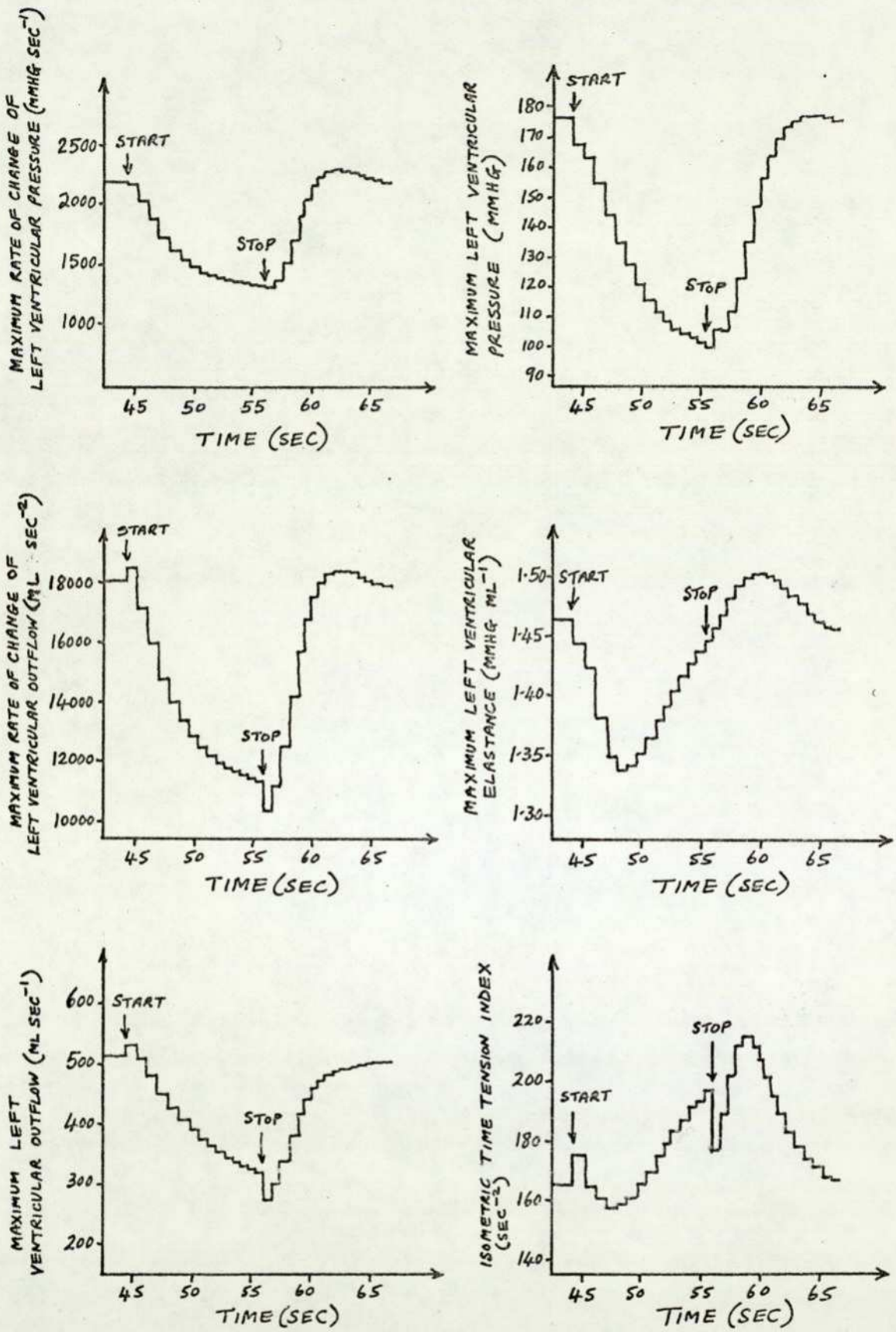

FIG. 6.17 THE COMPARISON OF VARIOUS MYOCARDIAL CONTRACTILITY MEASURES DURING A VALSALVA MANOEUVRE (STARTS AT $t = 44$ sec, STOPS AT $t = 56$ sec)

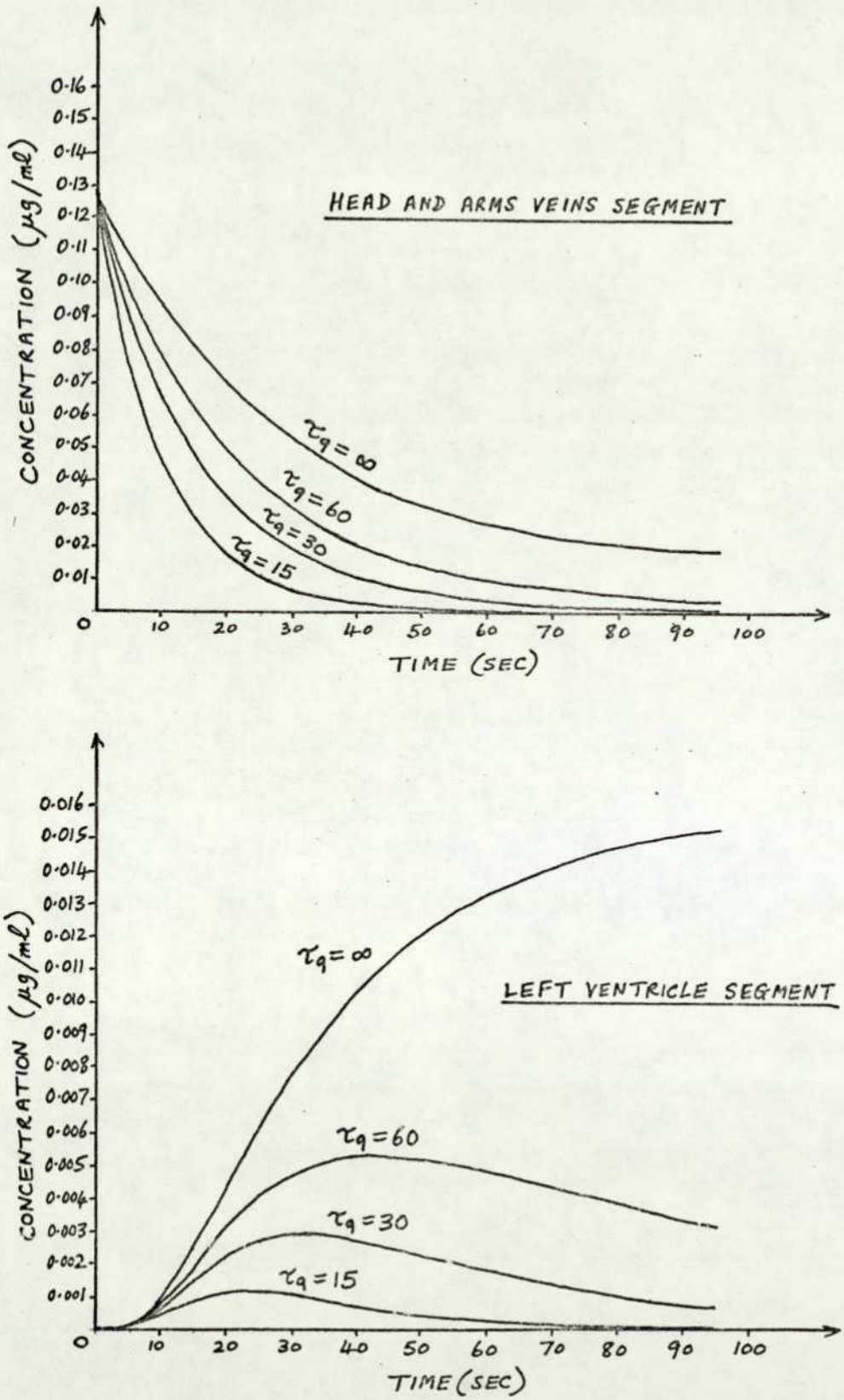

FIG. 6.18 CHANGE IN CONCENTRATION IN THE HEAD & ARMS VEINS SEGMENT AND THE LEFT VENTRICLE SEGMENT FOLLOWING AN INJECTION OF A NEUTRAL SUBSTANCE INTO THE HEAD & ARMS VEINS SEGMENT AT $t=0$ sec. FOR VARIOUS VALUES OF THE TIME CONSTANT FOR BREAKDOWN/ABSORPTION (τ_q)

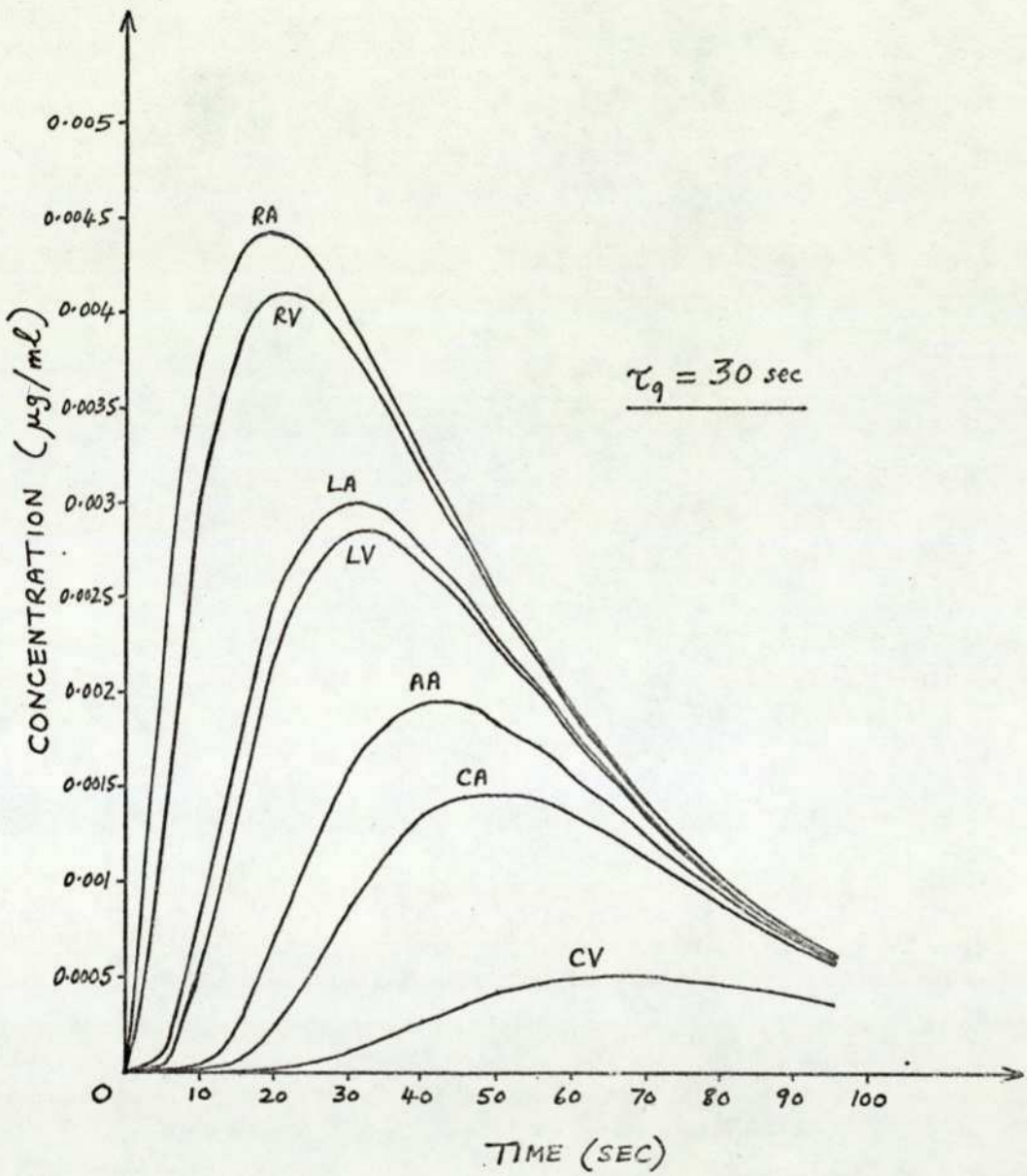

FIG. 6·19 THE DISTRIBUTION OF A NEUTRAL SUBSTANCE INJECTED INTO THE HEAD & ARMS VEINS SEGMENT AT $t=0$ sec. ASSUMING A TIME CONSTANT FOR BREAKDOWN/ABSORPTION OF 30 sec

CHAPTER 7

SIMULATED DRUG INJECTION EXPERIMENTS

This chapter describes the application of the cardiovascular model to the study of the haemodynamics following injections of cardiovascular drugs. The three sympathomimetic agents methoxamine, isoprenaline and noradrenaline (all related to adrenaline) are used in the tests because they are important cardiovascular drugs with well-known effects and these effects have been reported for conscious animals and humans in the literature.

The local direct actions of a particular drug are introduced into the model which is then used to predict the overall effects of the injected drug on the cardiovascular system of a recumbent human. Because of transport delays, the drug will arrive at different sites at different times and so the dynamics are likely to change when the site of injection is changed. For this reason, the results for two different intravenous injection locations (head and arms veins and leg veins segments) are given for each drug.

In describing drug effects, the features of responses that are frequently of interest in the pharmacological literature are the directions of change. Therefore in addition to presenting the full dynamic response of the model the general direction of change in the response is compared with results reported in the literature and is indicated in the following manner :

+	increase
0	no change
-	decrease

7.1 The selection of drug dosage and sensitivity coefficients

A drug action is implemented in the pharmacokinetics model using dimensionless factors of the form

$$\sigma_D = 1 + K\omega \qquad ---(7.1)$$

where σ_D multiplies the parameter to be influenced (vascular bed resistance, systolic elastance, etc.), K is a sensitivity coefficient and ω is the local drug concentration. Many different

combinations of K and ω can produce the same value of σ_D in eqn.(7.1). Since the concentration ω increases as the injected mass M increases, there are many different combinations of K and M that can produce the same value of σ_D and thus the same local drug action.

Hughes (1971) employed a dosage of 1 $\mu g\ kg^{-1}$ for noradrenaline and isoprenaline injections into conscious dogs. The same dosage is used in the model for a conscious human so that the results can be compared. Taking an average man as weighing 70 kg, the injected mass is set at 70 μg .

The sensitivity coefficients σ_1 , σ_2 , σ_3 and σ_4 (for effects on peripheral resistance, heart rate, myocardial contractility and venous unstressed volume respectively) are determined very approximately by the following procedure :

(1) The average values of segmental concentrations obtained in the test described in section 6.9 (injection of a neutral substance into the head & arms veins segment with τ_q = 30 sec) are used as a rough guide to the average values likely to occur in the investigation of drug effects. The average figures assumed are :

$\omega_1 = 0.0025\ \mu g\ ml^{-1}$ for the vascular beds
$\omega_2 = 0.005\ \mu g\ ml^{-1}$ for the heart
$\omega_3 = 0.025\ \mu g\ ml^{-1}$ for the venous segment into which the injection is made

(2) It is assumed that the arteriovenous resistance in a vascular bed doubles on average in drug-induced vasoconstriction so that $\sigma_1 \omega_1 = 1$ giving

$$\sigma_1 = \frac{1}{0.0025} = 400\ ml\,\mu g^{-1}$$

(3) It is assumed that heart rate on average increases by 25% in drug-induced tachycardia so that $\sigma_2 \omega_2 = 0.25$ from which

$$\sigma_2 = \frac{0.25}{0.005} = 50\ ml\,\mu g^{-1}$$

(4) It is assumed that the systolic elastance on average increases by 25% in drug-induced positive inotropy so that $\sigma_3 \omega_2 = 0.25$ giving

$$\sigma_3 = \frac{0.25}{0.005} = 50\ ml\,\mu g^{-1}$$

(5) It is assumed that the venous unstressed volume on average

decreases by 20% in drug-induced venoconstriction so that

$$\frac{1}{1+\sigma_4 w_3} = 0.8$$ giving

$$\sigma_4 = \frac{0.25}{0.025} = 10 \ ml\,\mu g^{-1}$$

The gross approximations and assumptions in this procedure are justified because there is considerable variability in the human population and, in the pharmacological literature, it is frequently only directions of change that are of interest.

The above values of σ_1 , σ_2 and σ_3 are the default values built into the simulation program. Venoconstriction is not an integral part of the simulation program but the above value of σ_4 is used when venoconstriction is introduced in the case of noradrenaline described in section 7.4.

7.2 Injection of methoxamine

Methoxamine is a sympathomimetic amine related to adrenaline and its main action is one of vasoconstriction by direct action on α-receptors in the arteriolar smooth muscle (Goodman & Gilman,1970). It has virtually no stimulant action on the heart and no β-receptor action on smooth muscle. The local action of methoxamine is therefore simulated by setting the arteriovenous resistance sensitivity coefficient (σ_1) to the normal value and setting the remaining sensitivity coefficients to zero. Vasoconstriction is "switched on" in the computer program.

The normal intravenous dosage of methoxamine would be of the order of 100 $\mu g\ kg^{-1}$ whereas the dosage here is 1 $\mu g\ kg^{-1}$. However, as explained in section 7.1, any increased dosage can be counteracted by a decreased sensitivity coefficient in the model so that the 70 μg injected mass and the value of 400 $ml\,\mu g^{-1}$ for σ_1 can be regarded as being approximately equivalent in effect to an injected mass of 7000 μg and a value of 4 $ml\,\mu g^{-1}$ for σ_1 .

The dynamics following a methoxamine injection into the head and arms veins segment are shown in fig. 7.1. The total systemic resistance rises indicating that the peripheral vasculature is constricted. The mean, systolic and diastolic pressures rise, there is reflex slowing of the heart and the cardiac output and stroke volume

fall. Similar responses are obtained when the drug is injected into the leg veins segment (fig. 7.2). This is to be expected because the relative times of arrival of the drug at the various vascular beds will be similar in the two cases. The features of these responses (shown in table 7.1) are in good agreement with those reported by Goodman & Gilman (1970).

The estimated total systemic resistance (ETSR) agrees fairly well with the true total systemic resistance (TTSR) in fig. 7.1 indicating that, for slower transient effects, (ETSR) provides a satisfactory indication of the true value.

7.3 Injection of isoprenaline

Isoprenaline is an isopropyl derivative of noradrenaline which is particularly active on the β-receptors so that its primary local actions are inhibition of smooth muscle (giving vasodilatation) and increase in the force of contraction and rate of the heart (Green, 1972 ; p.205). These local actions are simulated by setting σ_1 , σ_2 ,and σ_3 to normal values and "switching on" vasodilatation, tachycardia and positive inotropy in the computer program. A dosage of 1 $\mu g\, kg^{-1}$ is assumed so that the default values built into the program apply.

The dynamics following an injection of isoprenaline into the head and arms veins segment is shown in fig. 7.3. (ETSR) falls indicating peripheral vasodilatation. The mean, systolic and diastolic pressures fall, the heart rate rises and the cardiac output and stroke volume also increase. Similar responses are obtained when the drug is injected into the leg veins segment (fig. 7.4).

It is interesting to note that in the first 10 seconds of the response to the injection into the head and arms veins segment, a slight rise of blood pressure occurs and also a slight fall in stroke volume and a faster rate of increase of heart rate (fig. 7.3). These effects are attributed to the early arrival of the drug at a relatively high concentration in the heart and the appearance of the positive inotropic and chronotropic effects before the drug has arrived at the peripheral vasculature and before vasodilatation can dominate. This is confirmed by increasing σ_2 and σ_3 to 200 $ml\, \mu g^{-1}$ (fig. 7.5) when these initial inotropic and chronotropic actions become more noticeable.

If the increased σ_2 and σ_3 are employed with the injection into the leg veins, the concentration has decreased significantly by the time the drug arrives at the heart and so the effects are not observed (fig. 7.6).

The features of the responses obtained in all four tests given above (shown in table 7.1) correspond well with typical responses reported by Goodman & Gilman (1970) and the dynamics are in good agreement with results obtained in conscious dogs (Hughes, 1971).

As stimulation of the heart occurs with this drug, it provides an opportunity to examine the validity of systolic elastance as a myocardial contractility measure. The systolic elastance and a number of other commonly used myocardial contractility measures are recorded following the injection of isoprenaline into the head and arms veins segment (fig. 7.7). It is seen that all the measures agree well apart from maximum left ventricular pressure which decreases. The latter, however, is not a reliable indicator of contractility. This confirms the acceptability of systolic elastance as a myocardial contractility index in this model. The results also demonstrate the positive inotropic action of isoprenaline despite the decreasing blood pressure.

7.4 Injection of noradrenaline

Noradrenaline is the chemical transmitter of the sympathetic nervous system and is a hormone released by the adrenal medulla. Its effect is to constrict the arterioles by direct action and also to stimulate the heart (Green 1972 ; p.165).

The local action of noradrenaline is initially incorporated by setting σ_1 , σ_2 and σ_3 to normal values and "switching on" vasoconstriction, tachycardia and positive inotropy in the computer program. A dosage of 1 $\mu g\ kg^{-1}$ is assumed so that the default values built into the program apply.

The dynamics following an injection into the head and arms veins segment are shown in fig. 7.8. It is seen that the mean, systolic and diastolic pressures rise, (ETSR) increases (indicating vasoconstriction) and cardiac output falls which are the correct responses (Goodman & Gilman, 1970). However the heart rate rises in the model whereas the heart rate should typically fall by reflex action. Similar responses are obtained with an injection into the leg veins segment (fig. 7.9).

It is found that adjustment of the constants σ_1 , σ_2 and σ_3 cannot produce the required bradycardia response. Now Green (1972, p.165) reports that noradrenaline also constricts the veins by direct action and so drug-induced venous effects are added to the model in an attempt to reproduce the bradycardia response.

If the effect of the drug on venous compliance is incorporated (as described in section 4.2.4), it is found that there is no appreciable difference in the noradrenaline injection results even for large values of the venous compliance sensitivity coefficient. This indicates that venous compliance changes perhaps do not play an important part in cardiovascular regulation. However, when the effect of the drug on venous unstressed volume is included in all systemic venous segments, the effect is very large. The dynamics following an injection into the head and arms veins (with $\sigma_4 = 10$) is shown in fig. 7.10. The heart rate now decreases significantly.

The considerable initial rise in arterial pressure is due to a combination of positive inotropic action and increased cardiac output as a result of the improved venous return following venoconstriction and this causes the marked reflex bradycardia. As the peripheral vasoconstrictive effects begin to dominate and the venoconstriction wanes, the responses become more like those obtained in the previous case (without venoconstriction). Similar responses are obtained when the drug is injected into the leg veins segment (fig. 7.11).

The features of the responses obtained when venoconstriction is included (shown in table 7.1) correspond with the typical responses reported by Goodman & Gilman (1970) and the dynamics are in good agreement with results obtained in conscious dogs by Hughes (1971).

7.5 Conclusion

Simulated injections of cardiovascular agents have been described in this chapter. The local direct actions of the drugs methoxamine, isoprenaline and noradrenaline have been incorporated and in each case the model has been shown to produce realistic overall responses in good agreement with results reported in the literature. The results obtained with noradrenaline suggested that venoconstriction may play an important part in producing the bradycardia commonly observed in practice. The simulated injection experiments have demonstrated that

the model has an explanatory usefulness and also potential in the prediction of overall cardiovascular responses when a number of local direct actions are assumed.

DRUG	HUMAN OR MODEL	SYSTOLIC ARTERIAL PRESSURE	MEAN ARTERIAL PRESSURE	DIASTOLIC ARTERIAL PRESSURE	CARDIAC OUTPUT	HEART RATE	TOTAL PERIPHERAL RESISTANCE
METHOXAMINE	HUMAN	+	+	+	0 OR −	−	+
	MODEL	+	+	+	−	−	+
ISOPRENALINE	HUMAN	−	−	−	+	+	−
	MODEL	−	−	−	+	+	−
NORADRENALINE	HUMAN	+	+	+	0 OR −	−	+
	MODEL WITHOUT VENOCONSTRICTION	+	+	+	−	+	+
	MODEL WITH VENOCONSTRICTION	+	+	+	−	−	+

TABLE 7.1 GENERAL FEATURES OF THE RESPONSES IN THE MODEL AND THE HUMAN TO INTRAVENOUS INJECTIONS OF METHOXAMINE, ISOPRENALINE AND NORADRENALINE

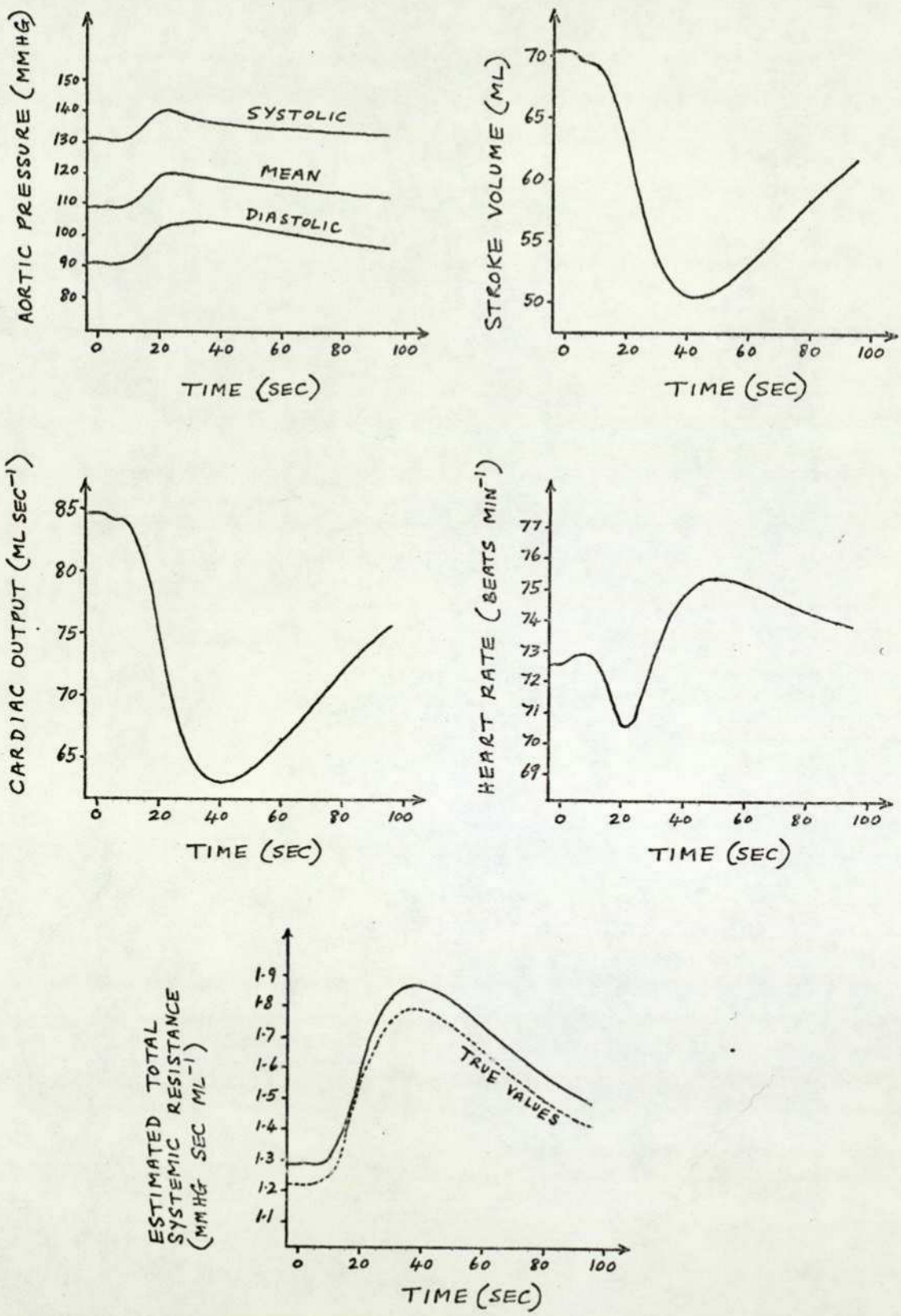

FIG. 7.1 INJECTION OF METHOXAMINE INTO THE HEAD AND ARMS VEINS SEGMENT AT $t = 0$ sec. ($\sigma_1 = 400$, $\sigma_2 = 0$, $\sigma_3 = 0$)

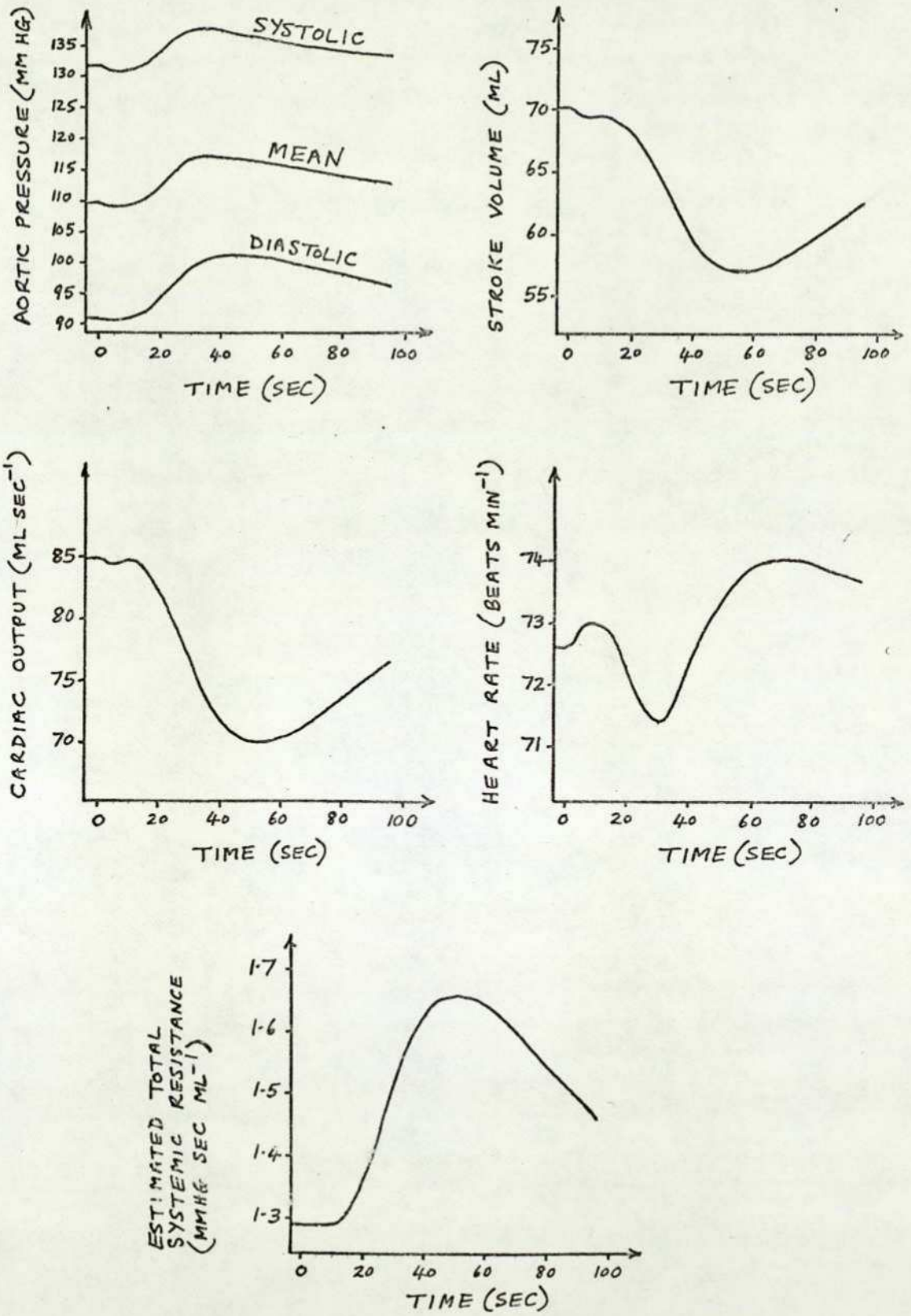

FIG. 7.2 INJECTION OF METHOXAMINE INTO THE LEG VEINS SEGMENT AT $t = 0$ sec $(\sigma_1 = 400, \sigma_2 = 0, \sigma_3 = 0)$

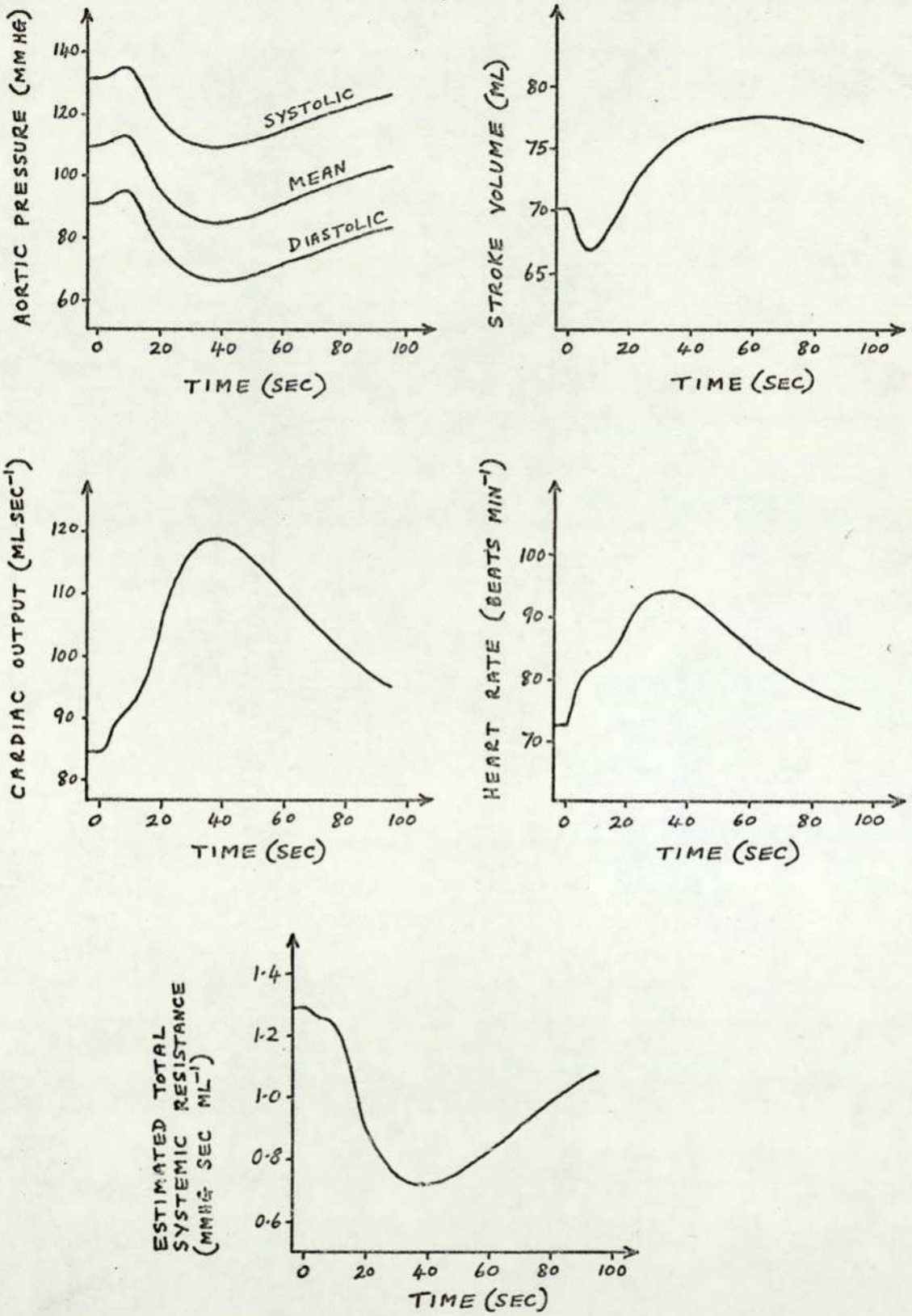

FIG. 7.3 INJECTION OF ISOPRENALINE INTO THE HEAD AND ARMS VEINS SEGMENT ($\sigma_1 = 400$, $\sigma_2 = 50$, $\sigma_3 = 50$) AT $t = 0$ sec.

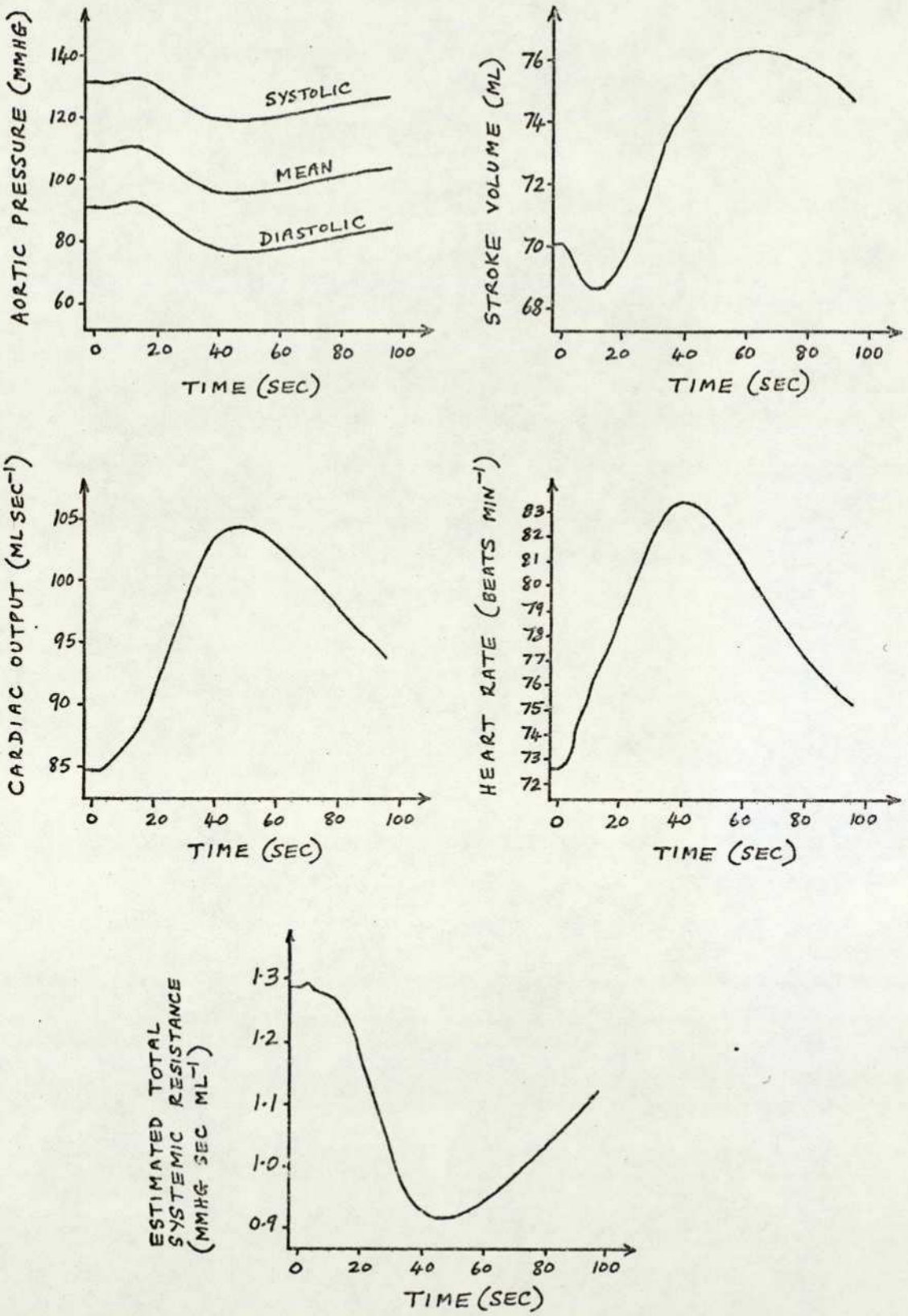

FIG. 7.4 INJECTION OF ISOPRENALINE INTO THE LEG VEINS

SEGMENT AT $t=0$ $(\sigma_1 = 400, \sigma_2 = 50, \sigma_3 = 50)$

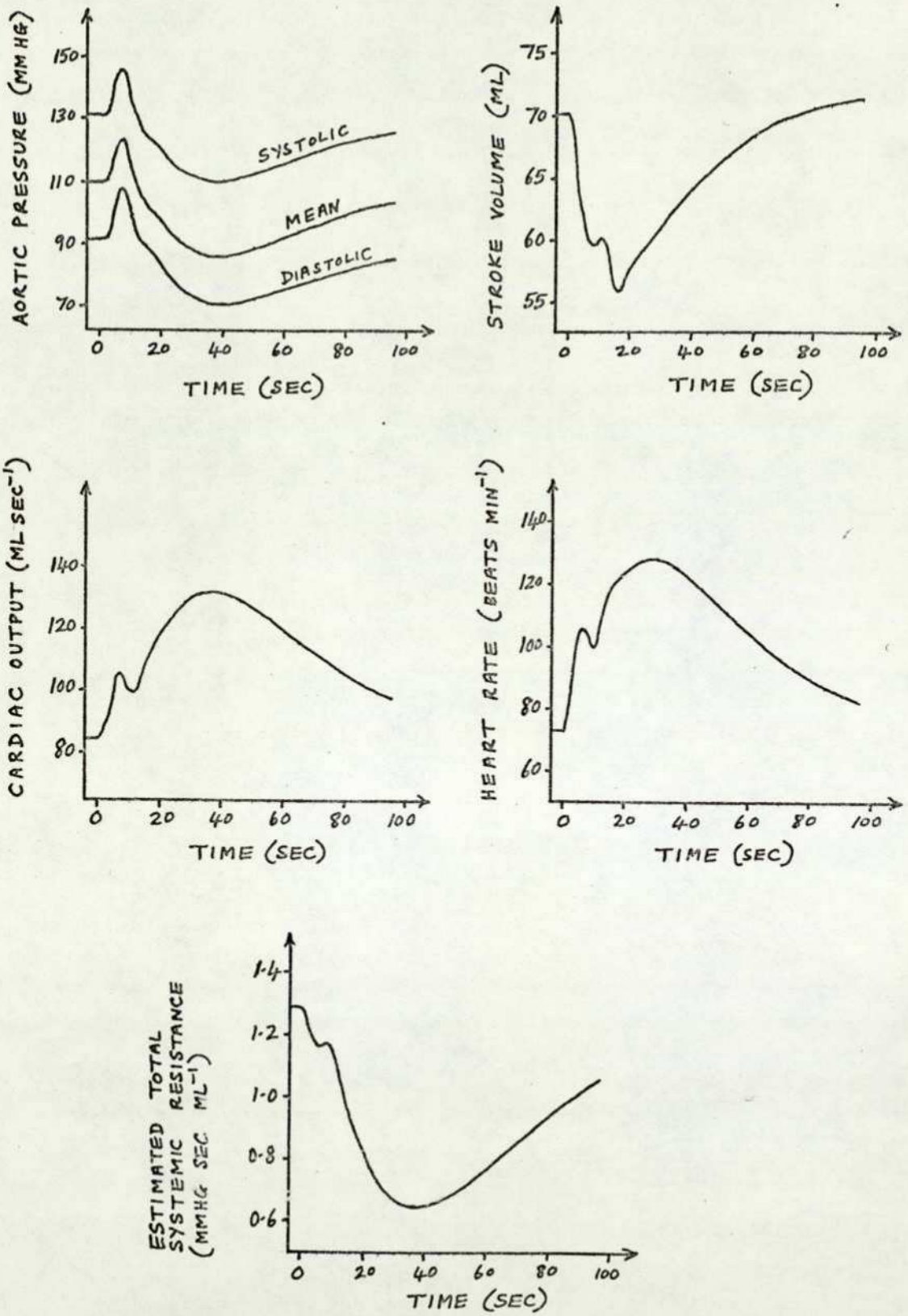

FIG. 7·5 ISOPRENALINE INJECTION INTO THE HEAD AND ARMS VEINS SEGMENT AT $t = 0$ ($\sigma_1 = 400$, $\sigma_2 = 200$, $\sigma_3 = 200$)

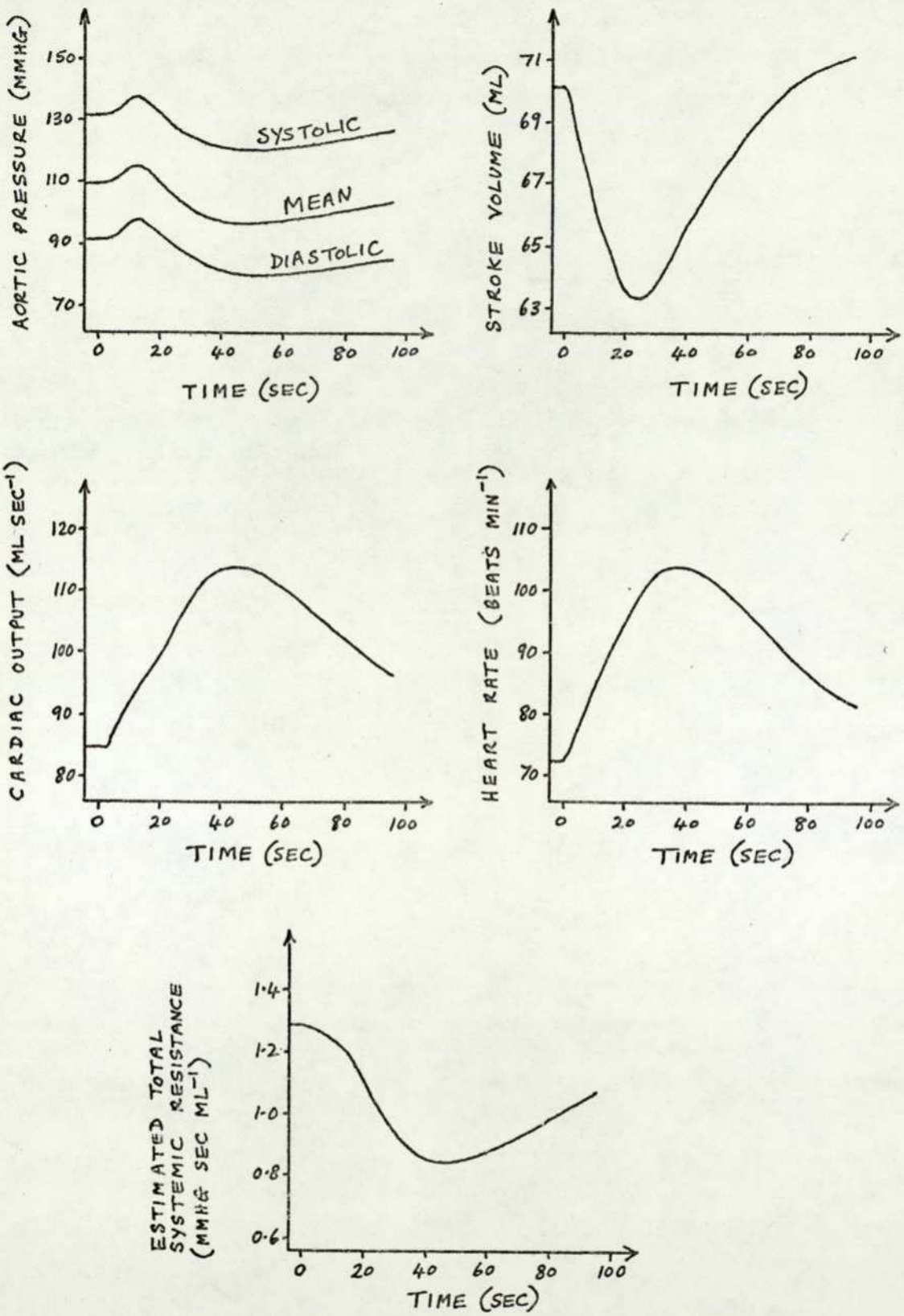

FIG. 7.6 ISOPRENALINE INJECTION INTO THE LEG VEINS SEGMENT AT $t = 0$ ($\sigma_1 = 400$, $\sigma_2 = 200$, $\sigma_3 = 200$)

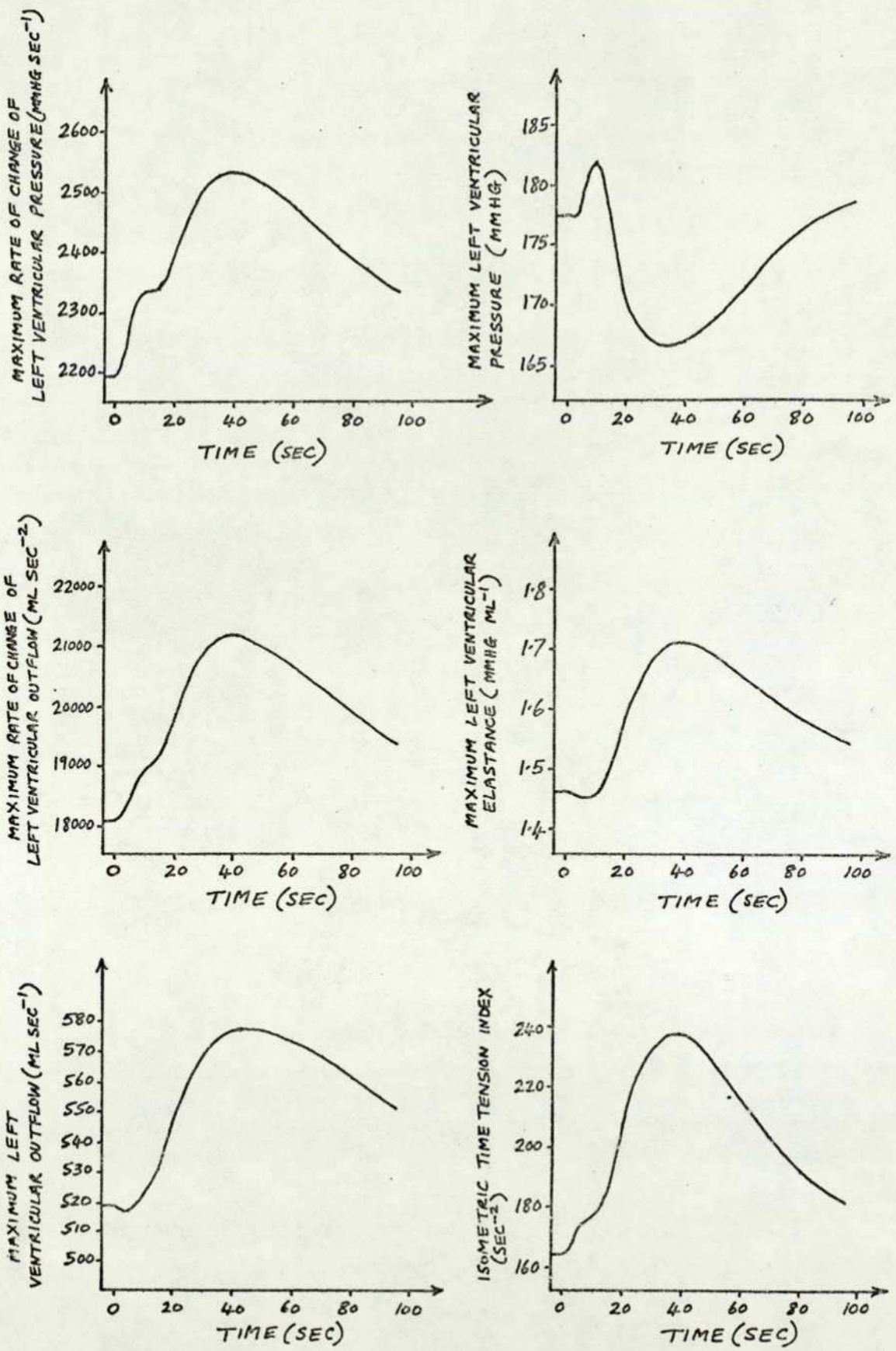

FIG. 7.7 THE COMPARISON OF VARIOUS MYOCARDIAL CONTRACTILITY MEASURES FOLLOWING THE INJECTION OF ISOPRENALINE INTO THE HEAD & ARMS VEINS SEGMENT AT $t=0$ ($\sigma_1=400$, $\sigma_2=50$, $\sigma_3=50$)

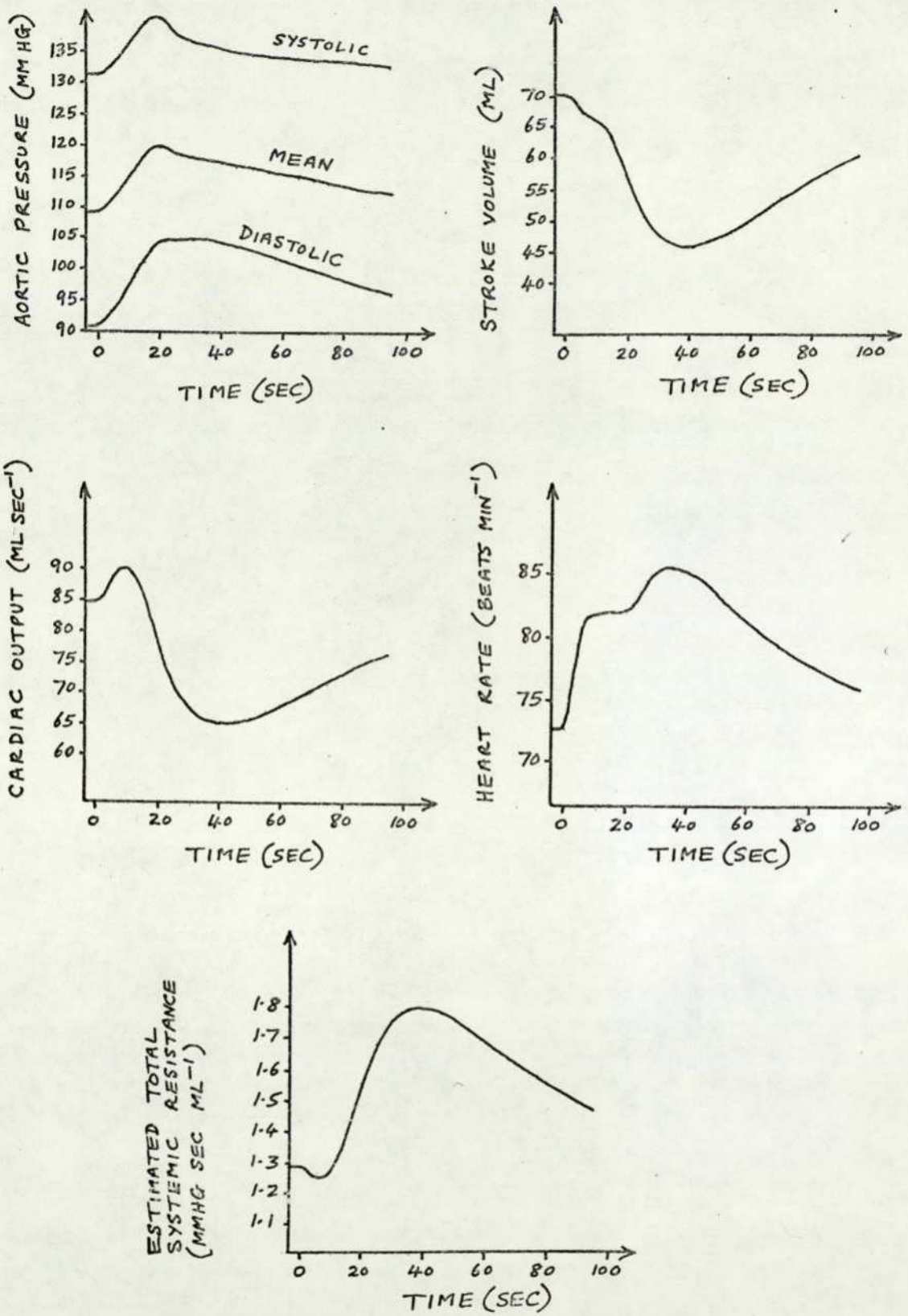

FIG. 7.8 NORADRENALINE INJECTION INTO THE HEAD & ARMS VEINS SEGMENT AT $t=0$ $(\sigma_1 = 400, \sigma_2 = 50, \sigma_3 = 50, \sigma_4 = 0)$

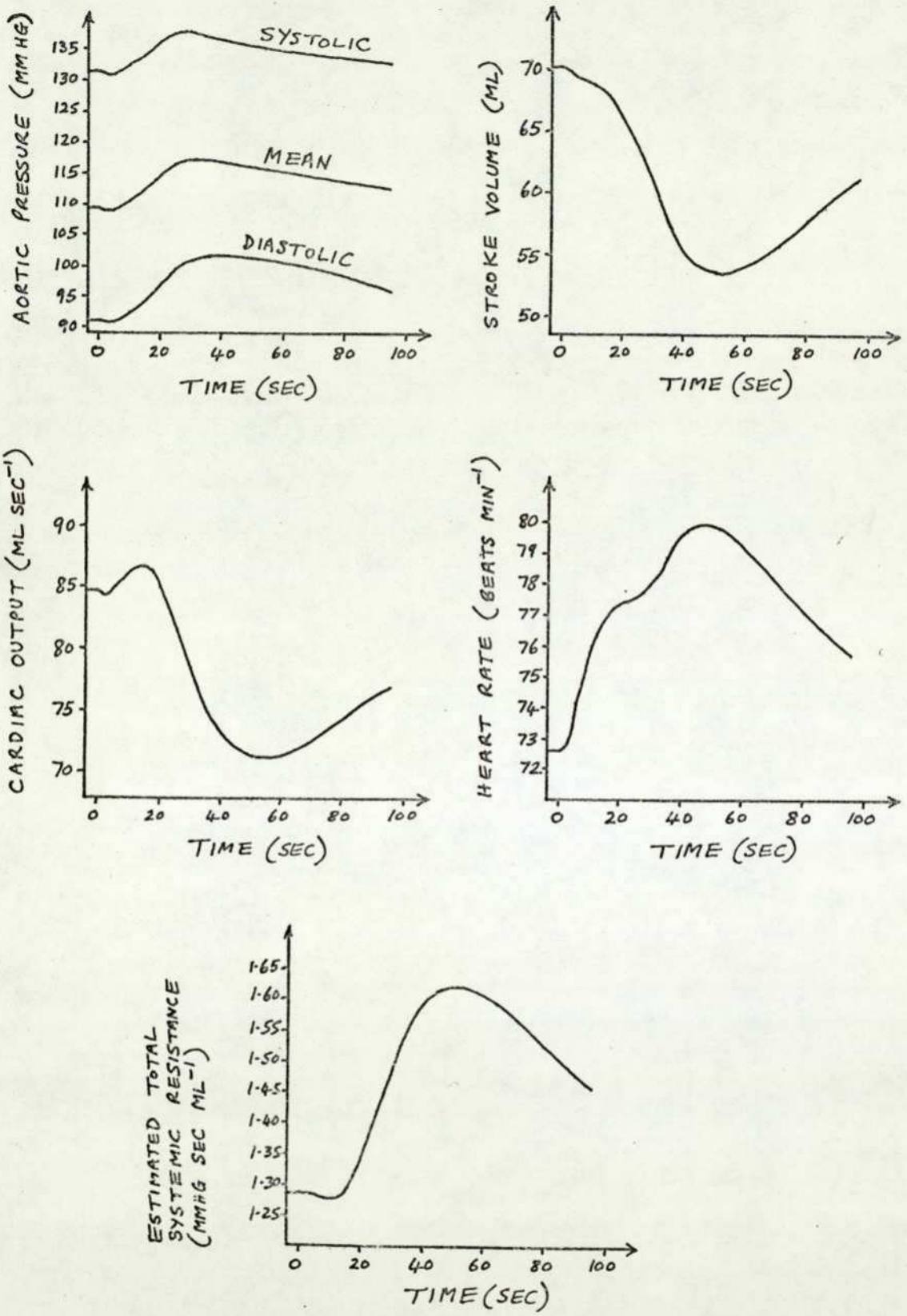

FIG. 7.9 NORADRENALINE INJECTION INTO THE LEG VEINS SEGMENT AT $t=0$ ($\sigma_1 = 400$, $\sigma_2 = 50$, $\sigma_3 = 50$, $\sigma_4 = 0$)

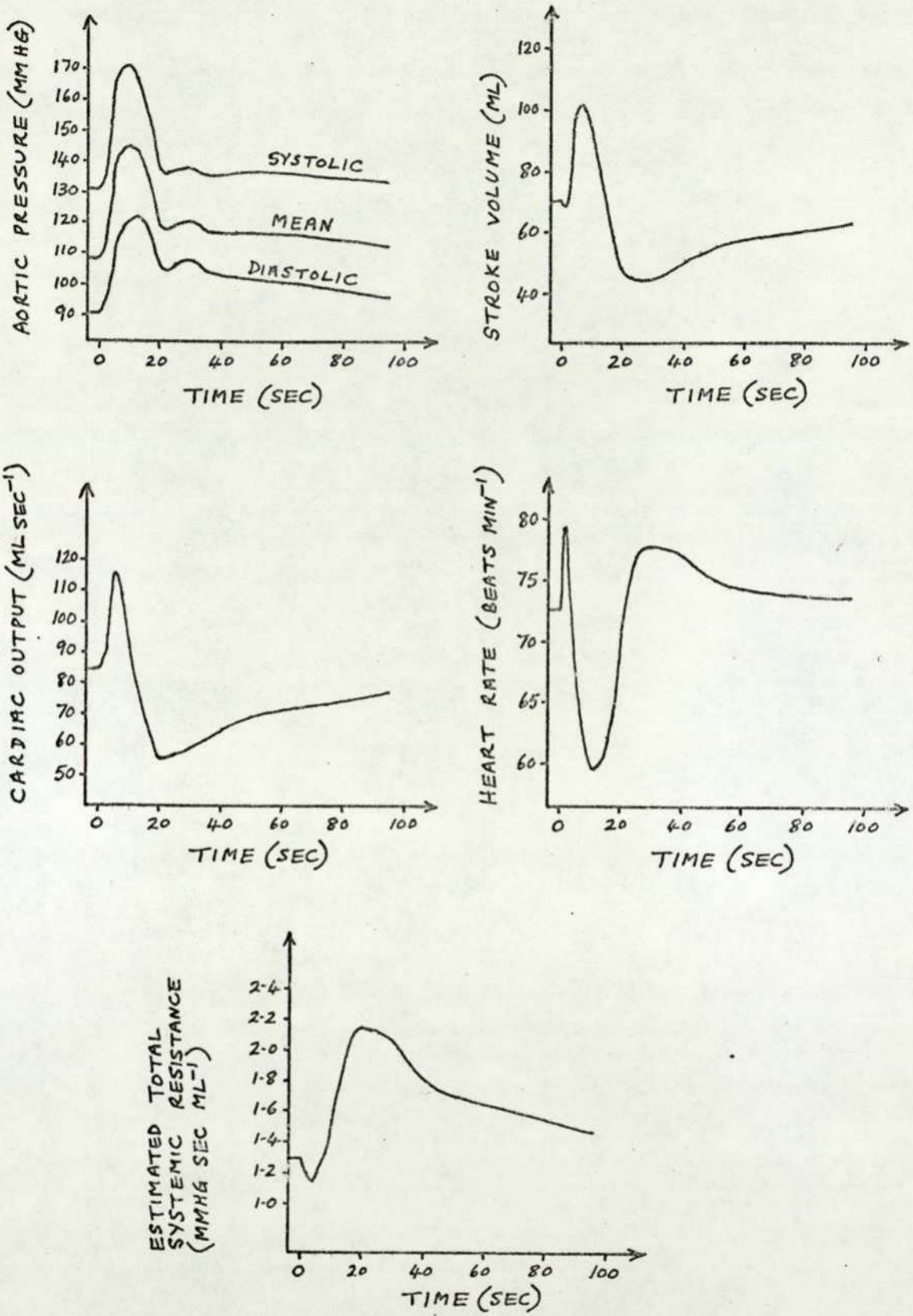

FIG. 7.10 NORADRENALINE INJECTION INTO THE HEAD AND ARMS VEINS SEGMENT AT $t=0$ ($\sigma_1=400$, $\sigma_2=10$, $\sigma_3=50$, $\sigma_4=10$)

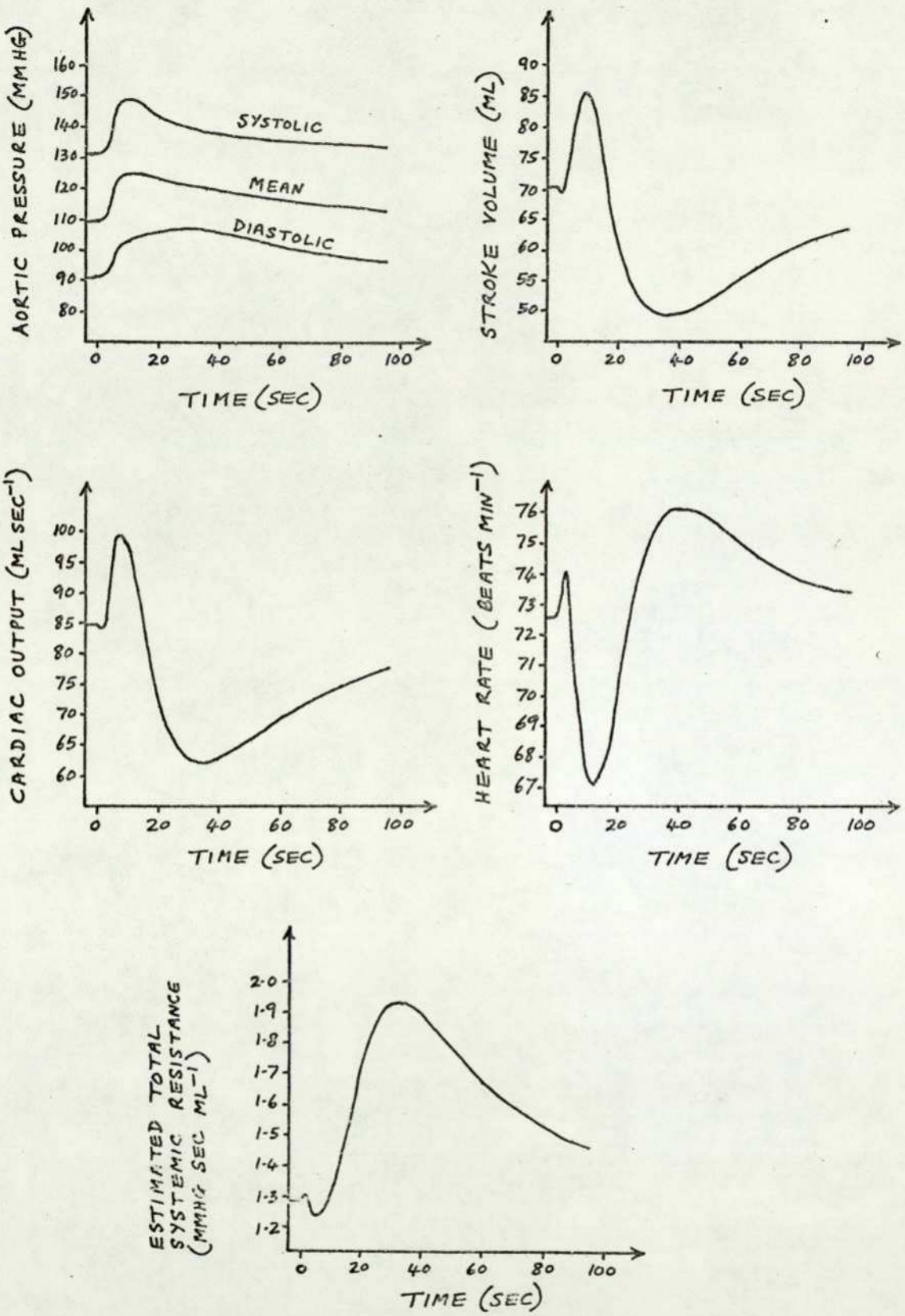

FIG. 7.11 NORADRENALINE INJECTION INTO THE LEG VEINS SEGMENT AT $t=0$ $(\sigma_1=400, \sigma_2=10, \sigma_3=50, \sigma_4=10)$

CHAPTER 8

SUGGESTIONS FOR FUTURE WORK

The results obtained in the validation tests and the simulated drug injection experiments suggest that the digital simulation of the mathematical model can serve as a flexible computerised test-bed for a variety of future investigations.

8.1 Further work using the present model

(1) In sections 6.7.7 and 7.3, systolic elastance was compared with some commonly used myocardial contractility measures to show its validity as an index of myocardial contractility in the model. This suggests that the model could be used to study commonly used myocardial contractility indices in more detail to assess their reliability in a wide range of experiments. The model could aid the design of improved indices and suggest improved measurement techniques for obtaining such indices.

(2) In section 6.7.2, it was shown that the estimated total systemic resistance (ETSR) computed from the mean arterial pressure and cardiac output in one cardiac cycle was an unreliable indicator of the true total systemic resistance during rapid transients. For slow transients, (ETSR) was more reliable (as shown in section 7.2). For investigations in animals and humans, the beat-by-beat estimation of total peripheral resistance is highly desirable if an indication of rapid changes in the peripheral vasculature is required. Further work using the model could therefore be done to devise new methods for beat-by-beat estimation which are both simple and accurate during rapid transients.

(3) The model could assist in the evaluation of present methods and the development of new methods for estimating the stroke volume and other circulatory variables by minimally invasive or non-invasive techniques.

(4) A study of the systemic circulation energy input and its variation with heart rate and other parameter changes could be studied in the present model by simply adding an extra integrator to compute

$$E = \int_{t_1}^{t_2} P_{AOI}\, F_{LVAOI}\, dt$$

The model could then be used to test the applicability of the "Principle of Adequate Design" suggested by Rashevsky (Rosen, 1973 ; p.146) :

> "The design of an organism is such that the organism performs its necessary functions adequately and with a minimal expenditure of energy and material both in the performance of the functions and in the construction of the organism"

It would be interesting to investigate whether a minimum systemic energy input occurs at or around normal heart rate.

(5) In section 6.4, it was shown that the model exhibited adequate compensation in response to the addition or removal of small volumes of blood. It was not necessary to resort to hypothetical volume receptors which are supposed to exist in the thorax (Green, 1972 ; p.48). The clarification of the mechanisms involved in compensation for blood volume changes could be investigated and the significance of venoconstriction in the present model could be assessed.

(6) Certain variables have mathematical discontinuities in the model e.g. the compliance of a venous segment at the point of collapse. Discontinuities are highly unlikely to occur in the real system and the effect of smoothing these sudden changes can be studied. A subroutine for algebraic smoothing of step changes which may be useful in this connection is given in appendix 7.

(7) The section of the model that requires the greatest attention in future work is the neural control model because of its completely empirical nature. The first step could be a detailed study of the effects of varying the parameters in the present nonlinear neural controller.

(8) Hyndman (1970,1971) suggested that very slow spontaneous oscillations at a frequency unrelated to that of respiration can appear in the blood pressure waveform in orthostasis when the respiratory rate is sufficiently low. These were not observed in the present work. The model here is more detailed than that used by Hyndman and the effects of varying the gains of the central nervous controllers and the magnitude and frequency of the

respiratory disturbance could be investigated in order to duplicate Hyndman's results. At the subnormal respiratory rates required to produce the spontaneous oscillations, there is a possibility that the change of oxygen tension in arterial blood may stimulate the chemoreceptors which then may play a part in the maintenance of the oscillations. This needs to be investigated further.

(9) The same threshold has been assumed for all the central nervous controllers (following Hyndman, 1970) in the present model. There is no reason why this should be so and the effects of introducing different thresholds for each controller could be studied. Also, a single central nervous input function (B) has been used for all controllers and there is no reason why the relative contribution of the aortic arch and carotid sinus baroreceptors should be the same in the different central nervous control mechanisms. A simple change to the model will enable this to be investigated. For the heart rate controller (HRC), peripheral resistance controller (PRC), myocardial contractility controller (MCC) and venous tone controller (VTC), suitable input functions would be

$$B_{HRC} = \alpha_1 B_{UA} + (1-\alpha_1) B_{AO2}$$

$$B_{PRC} = \alpha_2 B_{UA} + (1-\alpha_2) B_{AO2}$$

$$B_{MCC} = \alpha_3 B_{UA} + (1-\alpha_3) B_{AO2}$$

$$B_{VTC} = \alpha_4 B_{UA} + (1-\alpha_4) B_{AO2}$$

with $\alpha_1, \alpha_2, \alpha_3, \alpha_4 \in [0, 1]$

The constants α_1, α_2, α_3 and α_4 could be estimated from a study of the literature on baroreceptor reflexes. The currently used value of $\alpha = 0.7$ in the model actually corresponds to α_2 above because this figure was based on reflex effects on hindlimb vascular resistance obtained by Dampney et al.(1971).

(10) The cardiovascular system functions very effectively in a changing environment and a study of the significance of the special types of nonlinearity that have been detected (e.g. in baroreceptors and central nervous control) could be undertaken. Possible engineering applications could result from such a study. Phenomena such as the direction-dependent dynamic responses occurring in the baroreceptors (unidirectional rate sensitivity) have been observed in industrial and

engineering processes (Godfrey & Briggs, 1972).

(11) The present model has been constructed for a calm resting human in which the effects of higher centres have been ignored. The effect of introducing low or high frequency noise into the central nervous controllers to represent disturbances from the cerebral cortex could be studied (using pseudorandom number generators and filtering algorithms in the digital program). As the baroreceptors are unidirectionally rate sensitive, the effects could be significant because differentiation tends to magnify high frequency noise.

(12) The simulated drug injection experiments described in chapter 7 show that the model has potential in predictive pharmacokinetic work. A number of assumptions concerning the direct actions of drugs at specific sites can be incorporated and the overall behaviour of the cardiovascular system can be assessed on the basis of these assumptions. This suggests that the model can function as an aid for pharmacologists in the design of new fast-acting cardiovascular agents because these agents to a limited extent can be tailored chemically to produce a combination of specific local direct actions.

(13) While the main advantage of the model is its predictive capability, it can also be useful to explain observed phenomena e.g. to determine the relative contributions of various local direct actions to the overall response observed. By the use of optimisation techniques, the model could be used to determine the sensitivity coefficients (σ_1 , σ_2 , σ_3 , σ_4) in the equations which give the best match between the model response and the response obtained from the real system. This would have to be done using a hybrid computer in view of the size of the present model and the number of computer runs required.

(14) The time constant for breakdown or absorption was assumed to be the same in all segments in the work described. Breakdown or absorption may well occur more rapidly in some tissues than others and this could be easily incorporated in the model using different time constants for each segment. A similar consideration applies to the sensitivity coefficients which could be different in each segment. However both of these changes would introduce many extra parameters and make optimisation considerably more time-consuming.

8.2 The assessment of model adequacy

An important aspect of all mathematical modelling is the validation of the model that has been developed. When the model is to be used predictively, it is essential that the model should be thoroughly validated and its adequacy and credibility confirmed.

The validation of a large - scale nonlinear dynamic model of the cardiovascular system can never be totally satisfactory because :

(1) only a finite number of validation tests can be conducted.
(2) the experimental data from a given source used in the model formulation and model validation are subject to considerable variability and noise.
(3) certain results are available only from experiments on animals and there may be significant errors in extrapolating from animals to humans.
(4) many results are available only from anaesthetised animals and humans which may be in error when applied to conscious humans.
(5) there can be errors in extrapolating from the in vitro to the in vivo situation when in vitro results are employed.
(6) many experimental results used in the validation tests are derived from invasive measurements which may significantly disturb the system and its control mechanisms. Also surgically prepared experimental animals or humans do not remain in an acceptable biological condition over long observation periods.

In all future work, these considerations must be taken into account and validation must be based on the most reliable data.

In the tests conducted in the present model, both quantitative and qualitative assessments of validity have been employed. Future work on cardiovascular modelling needs to be based on objective quantitative measures of adequacy. It was suggested in section 6.1 that comparison of response features is the most satisfactory method of assessing validity of cardiovascular models and so the quantification of features is an important part of future work. Also, adequacy measures can be based on the distances between response features of the model and the real system. Possible constructions for adequacy measures are suggested in appendix 9.

In the drug injection results of the present work, a feature of the responses used was the direction of change. This could be

quantified as

$$F = \begin{cases} +1, & \text{increase} \\ 0, & \text{no change} \\ -1, & \text{decrease} \end{cases}$$

and then conventional distance measures between two such features (F_1 , F_2) could be used e.g.

$$d_1(F_1, F_2) = |F_1 - F_2|$$
$$d_2(F_1, F_2) = (F_1 - F_2)^2$$

8.3 Reduction of the cardiovascular model

Beneken (1970) has suggested the matching of computerised models to individual human subjects to "follow" that individual's cardiovascular system e.g. in clinical or surgical applications, patient monitoring, etc. This would require appropriate measurement techniques, interface hardware and an optimisation algorithm (for performing the actual matching) and could give :

(1) estimates of inaccessible internal variables of the patient and information on the present circulatory condition.
(2) prediction of likely future cardiovascular states.
(3) a safe test-bed to evaluate alternative treatments for the individual patient.

It is not practical to use the present cardiovascular simulation in such applications because of the computing time or equipment requirements so the model would have to be reduced substantially with the following factors in mind :

(1) The computer simulation should be cheaply implemented and operate faster than real time (analog computing techniques using cheap integrated circuit operational amplifiers may be appropriate here)
(2) The model should have physiologically meaningful parameters and yield immediately useful information for physicians or surgeons.
(3) The model must be simple enough to enable the optimisation algorithm to match the model to the patient extremely rapidly if the model is required to "follow" the patient.
(4) The model structure and parameters must be appropriate to the

information that can be derived from the patient. Thus in a clinical situation it is desirable that the model is matched to information from the electrocardiogram, phonocardiogram, external pressure transducers, ultrasound measurements, the ballistocardiogram or other non-invasive measurements.

In the present model, the essentially linear sections can be reduced. For example the systemic circulation model can be replaced by the simplified second order model given in appendix 8 if the only function required of the systemic model is to offer the correct impedance to the heart. Nonlinearities, however, are difficult to simplify and may have to be retained to give an adequate reduced model of the complete cardiovascular system (e.g. heart valves)

8.4 Expansion of the cardiovascular model

An alternative direction for future work is the expansion of the present model to include more detail and to deal with longer term effects. This is essential if the model is to be used predictively over a time scale greater than about 2 minutes which is approximately the limit of the current short-term model.

Some of the following mechanisms could be included in an expanded model of the cardiovascular system of a conscious human :

(1) The internal production, transport, action and breakdown or uptake of the catecholamines adrenaline and noradrenaline which augment the sympathetic nervous system activity.

(2) A simplified model of the kidney (linked to the abdominal arteries and inferior vena cava segments in the present model). together with a model of the renin-angiotensin-aldosterone-ADH system to test hypotheses concerning blood volume regulation and the role of the kidney in blood pressure regulation.

(3) The release, action and breakdown of prostaglandins. There has been considerable interest recently in the prostaglandins (Hinman, 1967 ; Pike, 1971) which are produced by many tissues of the body. These substances are very potent, have a wide diversity of biological effects and breakdown rapidly after production. A detailed model could be useful to test hypotheses concerning the action of these substances on the cardiovascular system.

(4) More detailed models of the baroreceptor system (e.g. using the

recent nonlinear model of Koushanpour & Spickler, 1975) and the central nervous control systems. To improve credibility, the neural control models could be based more on the physiology, biochemistry and known structure of the central nervous system than on a purely empirical approach.

(5) The transport and action of oxygen and carbon dioxide together with models of chemoreceptors and respiratory regulation. The latter can easily be connected to the present cyclic respiration model to control the rate and magnitude of intrathoracic pressure changes.

(6) The influence of coronary flow on heart performance. This would require additional models of oxygen transport, coronary autoregulation, myocardial oxygen consumption and compression of the coronary vessels by myocardial contraction. The expanded model could then be used to elucidate the phenomena occurring in shock.

(7) Delays in the onset of drug actions at particular sites. Drug action is instantaneous in the present model and delays could be approximated by the addition of first order lags.

In some of the above suggestions there is a requirement for the simultaneous transport of several substances. With the multiple modelling approach used in the present model, each extra substance would require an additional 19 first order differential equations and 43 algebraic equations together with extra equations for the actions of the substance at specific sites. Consequently the model size and digital simulation execution time would increase rapidly with the number of substances simultaneously transported. Additionally, the estimation of parameters in the expanded nonlinear model would cause severe computing problems. Thus an important aspect of future work on digitally simulated expanded models could be the study of mathematical and computational techniques which can result in considerably reduced execution times. The present work has not revealed any suitable techniques.

To achieve the necessary speed of solution for very large models, it may be more desirable to use analog computing methods. The very large number of integrators in an expanded model means that a special purpose analog computer constructed from cheap integrated circuit operational amplifiers (suggested by Grewe et al., 1969) may have to be used instead of the general purpose analog computer which usually has only a limited number of integrators. However, with the rapid

advances in digital computer technology (e.g. the availability of cheap microprocessors) and the developments in parallel processing digital systems (Slotnick, 1971 ; Korn, 1973), it is likely that very fast digital computers suitable for research on expanded cardiovascular models will be available in the near future.

8.5 Conclusion

Various directions in which future work should progress have been suggested in this chapter. The present model can serve as a convenient and flexible test-bed for the testing of hypotheses. The predictive capability of the model may be of use in the design of new cardiovascular agents.

Reduction of the model could lead to useful on-line real-time clinical applications while expansion of the model could enable long-term cardiovascular effects to be studied and better predictions to be made.

CHAPTER 9
CONCLUSIONS

A detailed pulsatile mathematical model of the cardiovascular system of a resting conscious human suitable for the study of short-term haemodynamics and pharmacokinetics has been developed.

A number of existing subsystem models have been integrated to form a large comprehensive cardiovascular model. The special requirements of short-term pharmacokinetics studies called for essential modifications of previous models and also the incorporation of new mathematical descriptions by the author including pulsatile baroreceptor dynamics, separate aortic arch and carotid sinus baroreceptors and algebraic models of drug-induced changes in circulatory parameters.

The problems of amalgamation of the subsystem models and the computing problems arising from the size and characteristics of the complete model have been overcome. The digital implementation performs well in a variety of tests designed to assess its validity.

When the local direct actions of the drugs methoxamine, isoprenaline and noradrenaline are incorporated, the model produces realistic haemodynamics following simulated injections of these cardiovascular agents. The results obtained with noradrenaline suggest that venoconstriction may play an important part in producing the bradycardia commonly observed in practice.

The simulated drug injection experiments demonstrate the explanatory usefulness of the model and indicate a predictive capability that may aid the design of new cardiovascular agents.

APPENDIX 1

THE COMPLETE MATHEMATICAL MODEL

A1.1 The circulatory fluid mechanics model

RIGHT ATRIUM :

$$\frac{dV_{RA}}{dt} = F_1 - F_{RARV} \quad , \quad V_{RA} \geq 0 \qquad \text{-----(A1.1)}$$

$$P_{RA} = a_{RA}(V_{RA} - V_{URA}) \qquad \text{-----(A1.2)}$$

$$F_{RARV} = \begin{cases} F_2 \, , & F_2 > 0 \\ 0 \, , & F_2 \leq 0 \end{cases} \qquad \text{-----(A1.3)}$$

$$F_1 = F_{SVCRA} + F_{IVCRA} + F_{BRONC} + F_{COR} \qquad \text{-----(A1.4)}$$

$$F_2 = \frac{P_{RA} - P_{RV}}{R_{RARV}} \qquad \text{-----(A1.5)}$$

RIGHT VENTRICLE:

$$\frac{dV_{RV}}{dt} = F_{RARV} - F_{RVPA} \quad , \quad V_{RV} \geq 0 \qquad \text{-----(A1.6)}$$

$$\frac{dF_{RVPA}}{dt} = \frac{P_{RA} - P_{PA} - R_{RVPA} F_{RVPA} - \left(\frac{\rho}{2A_{PA}^2}\right) F_{RVPA}^2}{L_{RV}} \quad , \quad F_{RVPA} \geq 0 \qquad \text{--(A1.7)}$$

$$P_{RV} = a_{RV}(V_{RV} - V_{URV}) \qquad \text{----(A1.8)}$$

PULMONARY ARTERIES :

$$\frac{dV_{PA}}{dt} = F_{RVPA} - F_{PAPV} \quad , \quad V_{PA} \geq 0 \qquad \text{-----(A1.9)}$$

$$P_{PA} = \frac{V_{PA} - V_{UPA}}{C_{PA}} \qquad \text{----(A1.10)}$$

$$F_{PAPV} = \begin{cases} \frac{P_{PA} - P_{PV}}{R_{LUNG}} \, , & P_{PV} > P_{CC} \\ \frac{P_{PA} - P_{CC}}{R_{LUNG}} \, , & P_{PV} \leq P_{CC} \end{cases} \qquad \text{----(A1.11)}$$

PULMONARY VEINS :

$$\frac{dV_{PV}}{dt} = F_{PAPV} - F_{PVLA} \;,\; V_{PV} \geq 0 \qquad \text{-----(A1.12)}$$

$$P_{PV} = \frac{V_{PV} - V_{UPV}}{C_{PV}} \qquad \text{-----(A1.13)}$$

$$C_{PV} = \begin{cases} C_{PVN} \;,\; V_{PV} > V_{UPV} \\ K_6 C_{PVN} \;,\; V_{PV} \leq V_{UPV} \end{cases} \qquad \text{-----(A1.14)}$$

$$F_3 = \frac{(P_{PV} - P_{LA}) V_{PV}^2}{R_{PVLA} V_{UPV}^2} \qquad \text{-----(A1.15)}$$

$$F_{PVLA} = \begin{cases} F_3 \;,\; F_3 > 0 \\ K_7 F_3 \;,\; F_3 \leq 0 \end{cases} \qquad \text{-----(A1.16)}$$

LEFT ATRIUM :

$$\frac{dV_{LA}}{dt} = F_{PVLA} - F_{LALV} \;,\; V_{LA} \geq 0 \qquad \text{-----(A1.17)}$$

$$P_{LA} = a_{LA} (V_{LA} - V_{ULA}) \qquad \text{-----(A1.18)}$$

$$F_4 = \frac{P_{LA} - P_{LV}}{R_{LALV}} \qquad \text{-----(A1.19)}$$

$$F_{LALV} = \begin{cases} F_4 \;,\; F_4 > 0 \\ 0 \;,\; F_4 \leq 0 \end{cases} \qquad \text{-----(A1.20)}$$

LEFT VENTRICLE :

$$\frac{dV_{LV}}{dt} = F_{LALV} - F_{LVAOI} \;,\; V_{LV} \geq 0 \qquad \text{-----(A1.21)}$$

$$\frac{dF_{LVAOI}}{dt} = \frac{P_{LV} - P_{AOI} - R_{LVAOI} F_{LVAOI} - \left(\frac{\rho}{2A_{AOI}^2}\right) F_{LVAOI}^2}{L_{LV}} \;,\; F_{LVAOI} \geq 0 \qquad \text{--(A1.22)}$$

$$P_{LV} = a_{LV} (V_{LV} - V_{ULV}) \qquad \text{-----(A1.23)}$$

ASCENDING AORTA:

$$\frac{dV_{AO1}}{dt} = F_{LVAO1} - F_{AO1AO2} - F_{COR}\ ,\ V_{AO1} \geq 0 \qquad \text{----(A1.24)}$$

$$\frac{dF_{AO1AO2}}{dt} = \frac{P_{AO1} - P_{AO2} - R_{AO2} F_{AO1AO2}}{L_{AO2}} \qquad \text{----(A1.25)}$$

$$P_{AO1} = \frac{1}{C_{AO1}} (V_{AO1} - V_{UAO1}) + \frac{K_g}{C_{AO1}} \left(\frac{dV_{AO1}}{dt}\right) \qquad \text{----(A1.26)}$$

$$F_{COR} = \frac{P_{AO1} - P_{RA}}{R_{COR}} \qquad \text{----(A1.27)}$$

AORTIC ARCH:

$$\frac{dV_{AO2}}{dt} = F_{AO1AO2} - F_{AO2UA} - F_{AO2AO3}\ ,\ V_{AO2} \geq 0 \qquad \text{---(A1.28)}$$

$$\frac{dF_{AO2UA}}{dt} = \frac{P_{AO2} + P_{TH} - P_{UA} - R_{UA} F_{AO2UA} - G_{AO2UA}}{L_{UA}} \qquad \text{---(A1.29)}$$

$$\frac{dF_{AO2AO3}}{dt} = \frac{P_{AO2} - P_{AO3} - R_{AO3} F_{AO2AO3} + G_{AO2AO3}}{L_{AO3}} \qquad \text{---(A1.30)}$$

$$P_{AO2} = \frac{1}{C_{AO2}} (V_{AO2} - V_{UAO2}) + \frac{K_g}{C_{AO2}} \left(\frac{dV_{AO2}}{dt}\right) \qquad \text{----(A1.31)}$$

HEAD & ARMS ARTERIES:

$$\frac{dV_{UA}}{dt} = F_{AO2UA} - F_{UAUV}\ ,\ V_{UA} \geq 0 \qquad \text{----(A1.32)}$$

$$P_{UA} = \frac{1}{C_{UA}} (V_{UA} - V_{UUA}) + \frac{K_g}{C_{UA}} \left(\frac{dV_{UA}}{dt}\right) \qquad \text{----(A1.33)}$$

$$F_{UAUV} = \frac{P_{UA} - P_{UV}}{R_{HEAD}\, \sigma_{HEAD}} \qquad \text{----(A1.34)}$$

HEAD & ARMS VEINS:

$$\frac{dV_{UV}}{dt} = F_{UAUV} - F_{UVSVC}\ ,\ V_{UV} \geq 0 \qquad \text{----(A1.35)}$$

HEAD & ARMS VEINS (CONTINUED):

$$P_{UV} = \frac{d_3}{C_{UV}} \left(V_{UV} - V_{uuV}\right) \qquad \text{---(A1-36)}$$

$$C_{UV} = \begin{cases} C_{UVN}, & V_{UV} > V_{uuV} \\ K_6 C_{UVN}, & V_{UV} \leq V_{uuV} \end{cases} \qquad \text{---(A1-37)}$$

$$V_{uuV} = \frac{V_{uuVN}}{d_4} \qquad \text{---(A1-38)}$$

$$F_5 = \frac{\left(P_{UV} - P_{SVC} - P_{TH} + G_{UVSVC}\right) V_{UV}^2}{R_{UV} V_{uuVN}^2} \qquad \text{---(A1-39)}$$

$$F_{UVSVC} = \begin{cases} F_5, & F_5 > 0 \\ K_9 F_5, & F_5 \leq 0 \end{cases} \qquad \text{---(A1-40)}$$

THORACIC AORTA:

$$\frac{dV_{AO3}}{dt} = F_{AO2AO3} - F_{BRONC} - F_{AO3IA} - F_{AO3AA}, \; V_{AO3} \geq 0 \qquad \text{---(A1-41)}$$

$$\frac{dF_{AO3IA}}{dt} = \frac{P_{AO3} + P_{TH} - P_{IA} - P_{ABD} - R_{IA} F_{AO3IA} + G_{AO3IA}}{L_{IA}} \qquad \text{---(A1-42)}$$

$$\frac{dF_{AO3AA}}{dt} = \frac{P_{AO3} + P_{TH} - P_{AA} - P_{ABD} - R_{AA} F_{AO3AA} + G_{AO3AA}}{L_{AA}} \qquad \text{---(A1-43)}$$

$$P_{AO3} = \frac{1}{C_{AO3}} \left(V_{AO3} - V_{UAO3}\right) + \frac{K_8}{C_{AO3}} \left(\frac{dV_{AO3}}{dt}\right) \qquad \text{---(A1-44)}$$

$$F_{BRONC} = \frac{\left(P_{AO3} - P_{RA} - G_{AO3RA}\right)}{R_{BRONC} \, {}^{a}V_4 \, {}^{\sigma}_{BRONC}} \qquad \text{---(A1-45)}$$

INTESTINAL ARTERIES:

$$\frac{dV_{IA}}{dt} = F_{AO3IA} - F_{IAIV}, \; V_{IA} \geq 0 \qquad \text{---(A1-46)}$$

$$P_{IA} = \frac{1}{C_{IA}} \left(V_{IA} - V_{UIA}\right) + \frac{K_8}{C_{IA}} \left(\frac{dV_{IA}}{dt}\right) \qquad \text{---(A1-47)}$$

INTESTINAL ARTERIES (CONTINUED):

$$F_{IAIV} = \frac{P_{IA} - P_{IV}}{R_{INT}\, q_4\, \sigma_{INT}} \qquad \text{----(A1-48)}$$

INTESTINAL VEINS:

$$\frac{dV_{IV}}{dt} = F_{IAIV} - F_{IVIVC} \;,\; V_{IV} \geq 0 \qquad \text{----(A1-49)}$$

$$P_{IV} = \frac{d_3}{C_{IV}} \left(V_{IV} - V_{uIV}\right) \qquad \text{----(A1-50)}$$

$$C_{IV} = \begin{cases} C_{IVN} \;,\; V_{IV} > V_{uIV} \\ K_6 C_{IVN} \;,\; V_{IV} \leq V_{uIV} \end{cases} \qquad \text{----(A1-51)}$$

$$V_{uIV} = \frac{V_{uIVN}}{d_4} \qquad \text{----(A1-52)}$$

$$F_6 = \frac{(P_{IV} - P_{IVC} + P_{ABD} - P_{TH} - G_{IVCIV})\, V_{IV}^2}{R_{IV}\, V_{uIVN}^2} \qquad \text{----(A1-53)}$$

$$F_{IVIVC} = \begin{cases} F_6 \;,\; F_6 > 0 \\ K_{10} F_6 \;,\; F_6 \leq 0 \end{cases} \qquad \text{----(A1-54)}$$

ABDOMINAL ARTERIES:

$$\frac{dV_{AA}}{dt} = F_{AO3AA} - F_{AAAV} - F_{AACA} \;,\; V_{AA} \geq 0 \qquad \text{----(A1-55)}$$

$$\frac{dF_{AACA}}{dt} = \frac{P_{AA} - P_{CA} + P_{ABD} - R_{CA} F_{AACA} + G_{AACA}}{L_{CA}} \qquad \text{----(A1-56)}$$

$$P_{AA} = \frac{1}{C_{AA}} \left(V_{AA} - V_{UAA}\right) + \frac{K_8}{C_{AA}} \left(\frac{dV_{AA}}{dt}\right) \qquad \text{----(A1-57)}$$

$$F_{AAAV} = \frac{P_{AA} - P_{AV}}{R_{ABD}\, q_4\, \sigma_{ABD}} \qquad \text{----(A1-58)}$$

ABDOMINAL VEINS:

$$\frac{dV_{AV}}{dt} = F_{AAAV} + F_{CVAV} - F_{AVIVC} \;,\; V_{AV} \geq 0 \qquad \text{----(A1-59)}$$

ABDOMINAL VEINS (CONTINUED):

$$P_{AV} = \frac{d_3}{C_{AV}} \left(V_{AV} - V_{uAV} \right) \qquad \text{----(A1.60)}$$

$$C_{AV} = \begin{cases} C_{AVN} \;, & V_{AV} > V_{uAV} \\ K_6 C_{AVN} \;, & V_{AV} \leq V_{uAV} \end{cases} \qquad \text{----(A1.61)}$$

$$V_{uAV} = \frac{V_{uAVN}}{d_4} \qquad \text{----(A1.62)}$$

$$F_7 = \frac{\left(P_{AV} - P_{IVC} + P_{ABD} - P_{TH} - G_{IVCAV} \right) V_{AV}^2}{R_{AV} V_{uAVN}^2} \qquad \text{----(A1.63)}$$

$$F_{AVIVC} = \begin{cases} F_7 \;, & F_7 > 0 \\ K_{11} F_7 \;, & F_7 \leq 0 \end{cases} \qquad \text{----(A1.64)}$$

LEG ARTERIES:

$$\frac{dV_{CA}}{dt} = F_{AACA} - F_{CACV} \;, \quad V_{CA} \geq 0 \qquad \text{----(A1.65)}$$

$$P_{CA} = \frac{1}{C_{CA}} \left(V_{CA} - V_{uCA} \right) + \frac{K_8}{C_{CA}} \left(\frac{dV_{CA}}{dt} \right) \qquad \text{----(A1.66)}$$

$$F_{CACV} = \frac{P_{CA} - P_{CV}}{R_{LEG} q_4 \sigma_{LEG}} \qquad \text{----(A1.67)}$$

LEG VEINS:

$$\frac{dV_{CV}}{dt} = F_{CACV} - F_{CVAV} \;, \quad V_{CV} \geq 0 \qquad \text{----(A1.68)}$$

$$P_{CV} = \frac{d_3}{C_{CV}} \left(V_{CV} - V_{uCV} \right) \qquad \text{----(A1.69)}$$

$$C_{CV} = \begin{cases} C_{CVN} \;, & V_{CV} > V_{uCV} \\ K_6 C_{CVN} \;, & V_{CV} \leq V_{uCV} \end{cases} \qquad \text{----(A1.70)}$$

$$V_{uCV} = \frac{V_{uCVN}}{d_4} \qquad \text{----(A1.71)}$$

LEG VEINS (CONTINUED):

$$F_8 = \frac{(P_{CV} - P_{AV} - P_{ABD} - G_{AVCV}) V_{CV}^2}{R_{CV} V_{uCVN}^2} \quad \text{----(A1.72)}$$

$$F_{CVAV} = \begin{cases} F_8, & F_8 \geq 0 \\ K_{12} F_8, & F_8 < 0 \end{cases} \quad \text{----(A1.73)}$$

INFERIOR VENA CAVA:

$$\frac{dV_{IVC}}{dt} = F_{AVIVC} + F_{IVIVC} - F_{IVCRA}, \; V_{IVC} \geq 0 \quad \text{----(A1.74)}$$

$$P_{IVC} = \frac{1}{C_{IVC}} (V_{IVC} - V_{uIVC}) \quad \text{----(A1.75)}$$

$$C_{IVC} = \begin{cases} C_{IVCN}, & V_{IVC} > V_{uIVC} \\ K_6 C_{IVCN}, & V_{IVC} \leq V_{uIVC} \end{cases} \quad \text{----(A1.76)}$$

$$F_9 = \frac{(P_{IVC} - P_{RA} - G_{IVCRA}) V_{IVC}^2}{R_{IVC} V_{uIVC}^2} \quad \text{----(A1.77)}$$

$$F_{IVCRA} = \begin{cases} F_9, & F_9 > 0 \\ K_5 F_9, & F_9 \leq 0 \end{cases} \quad \text{----(A1.78)}$$

SUPERIOR VENA CAVA:

$$\frac{dV_{SVC}}{dt} = F_{UVSVC} - F_{SVCRA}, \; V_{SVC} \geq 0 \quad \text{----(A1.79)}$$

$$P_{SVC} = \frac{1}{C_{SVC}} (V_{SVC} - V_{uSVC}) \quad \text{----(A1.80)}$$

$$C_{SVC} = \begin{cases} C_{SVCN}, & V_{SVC} > V_{uSVC} \\ K_6 C_{SVCN}, & V_{SVC} \leq V_{uSVC} \end{cases} \quad \text{----(A1.81)}$$

$$F_{10} = \frac{(P_{SVC} - P_{RA} + G_{SVCRA}) V_{SVC}^2}{R_{SVC} V_{uSVC}^2} \quad \text{----(A1.82)}$$

$$F_{SVCRA} = \begin{cases} F_{10}, & F_{10} > 0 \\ K_5 F_{10}, & F_{10} \leq 0 \end{cases} \quad \text{----(A1.83)}$$

TIME-VARYING COMPLIANCES OF ATRIA AND VENTRICLES:

$$\frac{du_{10}}{dt} = 1.0 \quad (u_{10} \text{ set to zero at end of cardiac cycle}) \qquad \text{---(A1-84)}$$

$$T_{AS} = K_{22} + K_{23} T_H \qquad \text{----(A1-85)}$$

$$T_{AV} = T_{AS} - K_{24} \qquad \text{----(A1-86)}$$

$$T_{VS} = K_{25} + K_{26} T_H \qquad \text{----(A1-87)}$$

$$x_1 = \frac{\pi}{T_{AS}} \qquad \text{----(A1-88)}$$

$$x_2 = \frac{\pi}{T_{VS}} \qquad \text{----(A1-89)}$$

$$x_3 = \begin{cases} 0, & u_{10} > T_{AS} \\ \sin(x_1 u_{10}), & u_{10} \leq T_{AS} \end{cases} \qquad \text{----(A1-90)}$$

$$x_4 = \begin{cases} u_{10} - T_{AV}, & u_{10} > T_{AV} \\ 0, & u_{10} \leq T_{AV} \end{cases} \qquad \text{----(A1-91)}$$

$$x_5 = \begin{cases} 0, & x_4 > T_{VS} \\ \sin(x_2 x_4), & x_4 \leq T_{VS} \end{cases} \qquad \text{----(A1-92)}$$

$$a_{LA} = x_3 \left[b_2 \sigma_{LA} a_{LAS} - a_{LAD} \right] + a_{LAD} \qquad \text{----(A1-93)}$$

$$a_{LV} = x_5 \left[b_2 \sigma_{LV} a_{LVS} - a_{LVD} \right] + a_{LVD} \qquad \text{----(A1-94)}$$

$$a_{RA} = x_3 \left[b_2 \sigma_{RA} a_{RAS} - a_{RAD} \right] + a_{RAD} \qquad \text{----(A1-95)}$$

TIME-VARYING COMPLIANCES OF ATRIA & VENTRICLES (CONTINUED):

$$a_{RV} = x_5\left[b_2 \bar{\sigma}_{RV} a_{RVS} - a_{RVD}\right] + a_{RVD} \qquad \text{---(A1-96)}$$

RESPIRATION:

$$\frac{dy_2}{dt} = 1.0 \quad (y_2 \text{ set to zero at end of respiratory cycle}) \qquad \text{---(A1-97)}$$

$$y_1 = \begin{cases} y_2, & y_2 \leq T_{IE} \\ 0, & y_2 > T_{IE} \end{cases} \qquad \text{---(A1-98)}$$

$$P_{TH} = K_1 + (K_2 - K_1)\sin\left(\frac{\pi y_1}{T_{IE}}\right) \qquad \text{---(A1-99)}$$

$$P_{ABD} = K_3 + (K_4 - K_3)\sin\left(\frac{\pi y_1}{T_{IE}}\right) \qquad \text{---(A1-100)}$$

CALCULATION OF (MAP), (SV), (CO), (ETSR):

$$(MAP) = \frac{1}{T_H}\int_{t_1}^{t_1+T_H} P_{AOI}\, dt \quad (t_1 = \text{start of a cardiac cycle}) \qquad \text{---(A1-101)}$$

$$(SV) = \int_{t_1}^{t_1+T_H} F_{LVAOI}\, dt \qquad \text{---(A1-102)}$$

$$(CO) = \frac{(SV)}{T_H} \qquad \text{---(A1-103)}$$

$$(ETSR) = \frac{(MAP)}{(CO)} \qquad \text{---(A1-104)}$$

CALCULATION OF TRUE TOTAL SYSTEMIC RESISTANCE:

$$R_A = R_{UA} + R_{HEAD}\bar{\sigma}_{HEAD} + \frac{R_{UV} V_{UUVN}^2}{V_{UV}^2} + \frac{R_{SVC} V_{USVC}^2}{V_{SVC}^2} \qquad \text{---(A1-105)}$$

$$R_B = q_{V4}\, \bar{\sigma}_{BRONC} R_{BRONC} \qquad \text{---(A1-106)}$$

$$R_C = R_{CA} + q_4 R_{LEG}\bar{\sigma}_{LEG} + \frac{R_{CV} V_{UCVN}^2}{V_{CV}^2} \qquad \text{---(A1-107)}$$

CALCULATION OF TRUE TOTAL SYSTEMIC RESISTANCE (CONTINUED):

$$R_D = q_4 R_{ABD} \sigma_{ABD} \qquad \text{----(A1.108)}$$

$$R_E = \frac{R_C R_D}{(R_C + R_D)} + R_{AA} + \frac{R_{AV} V_{UAVN}^2}{V_{AV}^2} \qquad \text{----(A1.109)}$$

$$R_F = R_{IA} + q_4 \sigma_{INT} R_{INT} + \frac{R_{IV} V_{UIVN}^2}{V_{IV}^2} \qquad \text{----(A1.110)}$$

$$R_G = \frac{R_E R_F}{(R_E + R_F)} + \frac{R_{IVC} V_{UIVC}^2}{V_{IVC}^2} \qquad \text{----(A1.111)}$$

$$R_H = R_{AO3} + \frac{R_B R_G}{(R_B + R_G)} \qquad \text{----(A1.112)}$$

$$R_I = R_{AO2} + \frac{R_A R_H}{(R_A + R_H)} \qquad \text{----(A1.113)}$$

$$(TTSR) = \frac{R_{COR} R_I}{(R_{COR} + R_I)} \qquad \text{----(A1.114)}$$

A1.2 The neural control model

AORTIC ARCH BARORECEPTORS:

$$\frac{dS_3}{dt} = \frac{P_{AO2} - S_3}{\tau_1} \qquad \text{----(A1.115)}$$

$$\frac{dS_4}{dt} = \frac{S_2 - S_4}{\tau_2} \qquad \text{----(A1.116)}$$

$$S_1 = \frac{dP_{AO2}}{dt} \qquad \text{----(A1.117)}$$

$$S_2 = \begin{cases} S_1, & S_1 > 0 \\ 0, & S_1 \leq 0 \end{cases} \qquad \text{----(A1.118)}$$

AORTIC ARCH BARORECEPTORS (CONTINUED):

$$S_5 = K_{13}\left(S_3 + K_{14} S_4 - K_{15}\right) \qquad \text{---(A1.119)}$$

$$B_{AO2} = \begin{cases} S_5 , & S_5 > 0 \\ 0 , & S_5 \leq 0 \end{cases} \qquad \text{---(A1.120)}$$

CAROTID SINUS BARORECEPTORS:

$$\frac{dS_8}{dt} = \frac{P_{UA} - S_8}{\tau_1} \qquad \text{---(A1.121)}$$

$$\frac{dS_9}{dt} = \frac{S_7 - S_9}{\tau_2} \qquad \text{---(A1.122)}$$

$$S_6 = \frac{dP_{UA}}{dt} \qquad \text{---(A1.123)}$$

$$S_7 = \begin{cases} S_6 , & S_6 > 0 \\ 0 , & S_6 \leq 0 \end{cases} \qquad \text{---(A1.124)}$$

$$S_{10} = K_{13}\left(S_8 + K_{14} S_9 - K_{15}\right) \qquad \text{---(A1.125)}$$

$$B_{UA} = \begin{cases} S_{10} , & S_{10} > 0 \\ 0 , & S_{10} \leq 0 \end{cases} \qquad \text{---(A1.126)}$$

C.N.S. INPUT FUNCTION:

$$B = (1 - K_{16})\, B_{AO2} + K_{16}\, B_{UA} \qquad \text{---(A1.127)}$$

C.N.S. CONTROL OF HEART RATE:

$$\frac{du_4}{dt} = \frac{u_1 - u_4}{u_3} \qquad \text{---(A1.128)}$$

$$\frac{du_6}{dt} = \frac{u_5 - u_6}{\tau_3} \qquad \text{---(A1.129)}$$

$$\frac{du_7}{dt} = \frac{u_6 - u_7}{\tau_4} \qquad \text{---(A1.130)}$$

C.N.S. CONTROL OF HEART RATE (CONTINUED):

$$u_1 = \begin{cases} K_{17}(B - K_{18}), & B > K_{18} \\ 0, & B \leq K_{18} \end{cases} \quad \text{---(A1-131)}$$

$$u_2 = \frac{du_1}{dt} \quad \text{---(A1-132)}$$

$$u_3 = \begin{cases} K_{19}, & u_2 > 0 \\ K_{20}, & u_2 \leq 0 \end{cases} \quad \text{---(A1-133)}$$

$$u_5 = \begin{cases} K_{18}, & B > K_{18} \\ B, & B \leq K_{18} \end{cases} \quad \text{---(A1-134)}$$

$$u_8 = K_{21}\,\sigma_H\,(u_4 + u_7) \quad \text{---(A1-135)}$$

$$u_9 = \begin{cases} 2.0, & u_8 \geq 2.0 \\ u_8, & 0.3 < u_8 < 2.0 \\ 0.3, & u_8 \leq 0.3 \end{cases} \quad \text{---(A1-136)}$$

T_H is set to the value of u_9 at the end of the cardiac cycle.

C.N.S. CONTROL OF PERIPHERAL RESISTANCE:

$$\frac{dq_2}{dt} = \frac{q_1 - q_2}{\tau_5} \quad \text{---(A1-137)}$$

$$\frac{dq_3}{dt} = \frac{q_1 - q_3}{\tau_6} \quad \text{---(A1-138)}$$

$$q_4 = K_{29}\,q_3 + (1 - K_{29})\,q_2 \quad \text{---(A1-139)}$$

$$q_1 = \begin{cases} K_{27}, & B > K_{18} \\ K_{28}, & B \leq K_{18} \end{cases} \quad \text{---(A1-140)}$$

C.N.S. CONTROL OF MYOCARDIAL CONTRACTILITY:

$$\frac{db_2}{dt} = \frac{b_1 - b_2}{\tau_8} \quad \text{---(A1-141)}$$

C.N.S. CONTROL OF MYOCARDIAL CONTRACTILITY (CONTINUED):

$$b_1 = \begin{cases} K_{34}, & B > K_{18} \\ K_{35}, & B \leq K_{18} \end{cases} \qquad \text{---(A1.142)}$$

C.N.S. CONTROL OF VENOUS TONE:

$$\frac{dd_2}{dt} = \frac{d_1 - d_2}{\tau_7} \qquad \text{---(A1.143)}$$

$$d_1 = \begin{cases} K_{30}, & B > K_{18} \\ K_{31}, & B \leq K_{18} \end{cases} \qquad \text{---(A1.144)}$$

$$d_3 = 1 + K_{32}(d_2 - 1) \qquad \text{---(A1.145)}$$

$$d_4 = 1 + K_{33}(d_2 - 1) \qquad \text{---(A1.146)}$$

A1.3 <u>The pharmacokinetics model</u>

RIGHT ATRIUM:

$$\frac{dm_{RA}}{dt} = w_{SVCRA} F_{SVCRA} + w_{COR} F_{COR} + w_{BRONC} F_{BRONC} + w_{IVCRA} F_{IVCRA} - w_{RARV} F_{RARV} - \frac{m_{RA}}{\tau_9} \qquad \text{---(A1.147)}$$

$$w_{RA} = \frac{m_{RA}}{V_{RA}} \qquad \text{---(A1.148)}$$

RIGHT VENTRICLE:

$$\frac{dm_{RV}}{dt} = w_{RARV} F_{RARV} - w_{RVPA} F_{RVPA} - \frac{m_{RV}}{\tau_9} \qquad \text{---(A1.149)}$$

$$w_{RV} = \frac{m_{RV}}{V_{RV}} \qquad \text{---(A1.150)}$$

PULMONARY ARTERIES:

$$\frac{dm_{PA}}{dt} = w_{RVPA} F_{RVPA} - w_{PAPV} F_{PAPV} - \frac{m_{PA}}{\tau_9} \qquad \text{---(A1.151)}$$

$$w_{PA} = \frac{m_{PA}}{V_{PA}} \qquad \text{---(A1.152)}$$

PULMONARY VEINS:

$$\frac{dm_{PV}}{dt} = w_{PAPV} F_{PAPV} - w_{PVLA} F_{PVLA} - \frac{m_{PV}}{\tau_q} \quad \text{---(A1-153)}$$

$$w_{PV} = \frac{m_{PV}}{V_{PV}} \quad \text{---(A1-154)}$$

LEFT ATRIUM:

$$\frac{dm_{LA}}{dt} = w_{PVLA} F_{PVLA} - w_{LALV} F_{LALV} - \frac{m_{LA}}{\tau_q} \quad \text{---(A1-155)}$$

$$w_{LA} = \frac{m_{LA}}{V_{LA}} \quad \text{---(A1-156)}$$

LEFT VENTRICLE:

$$\frac{dm_{LV}}{dt} = w_{LALV} F_{LALV} - w_{LVAO1} F_{LVAO1} - \frac{m_{LV}}{\tau_q} \quad \text{---(A1-157)}$$

$$w_{LV} = \frac{m_{LV}}{V_{LV}} \quad \text{---(A1-158)}$$

ASCENDING AORTA:

$$\frac{dm_{AO1}}{dt} = w_{LVAO1} F_{LVAO1} - w_{AO1AO2} F_{AO1AO2} - w_{COR} F_{COR} - \frac{m_{AO1}}{\tau_q} \quad \text{---(A1-159)}$$

$$w_{AO1} = \frac{m_{AO1}}{V_{AO1}} \quad \text{---(A1-160)}$$

AORTIC ARCH:

$$\frac{dm_{AO2}}{dt} = w_{AO1AO2} F_{AO1AO2} - w_{AO2UA} F_{AO2UA} - w_{AO2AO3} F_{AO2AO3} - \frac{m_{AO2}}{\tau_q} \quad \text{---(A1-161)}$$

$$w_{AO2} = \frac{m_{AO2}}{V_{AO2}} \quad \text{---(A1-162)}$$

HEAD & ARMS ARTERIES:

$$\frac{dm_{UA}}{dt} = w_{AO2UA} F_{AO2UA} - w_{UAUV} F_{UAUV} - \frac{m_{UA}}{\tau_q} \quad \text{---(A1-163)}$$

$$w_{UA} = \frac{m_{UA}}{V_{UA}} \quad \text{---(A1-164)}$$

HEAD & ARMS VEINS :

$$\frac{dm_{UV}}{dt} = w_{UAUV} F_{UAUV} - w_{UVSVC} F_{UVSVC} - \frac{m_{UV}}{\tau_q} + M\delta(t) \qquad \text{---(A1-165)}$$

(assuming mass M injected at time t=0)

$$w_{UV} = \frac{m_{UV}}{V_{UV}} \qquad \text{---(A1-166)}$$

THORACIC AORTA :

$$\frac{dm_{AO3}}{dt} = w_{AO2AO3} F_{AO2AO3} - w_{BRONC} F_{BRONC} - w_{AO3IA} F_{AO3IA} - w_{AO3AA} F_{AO3AA} - \frac{m_{AO3}}{\tau_q} \qquad \text{---(A1-167)}$$

$$w_{AO3} = \frac{m_{AO3}}{V_{AO3}} \qquad \text{---(A1-168)}$$

INTESTINAL ARTERIES :

$$\frac{dm_{IA}}{dt} = w_{AO3IA} F_{AO3IA} - w_{IAIV} F_{IAIV} - \frac{m_{IA}}{\tau_q} \qquad \text{---(A1-169)}$$

$$w_{IA} = \frac{m_{IA}}{V_{IA}} \qquad \text{---(A1-170)}$$

INTESTINAL VEINS :

$$\frac{dm_{IV}}{dt} = w_{IAIV} F_{IAIV} - w_{IVIVC} F_{IVIVC} - \frac{m_{IV}}{\tau_q} \qquad \text{---(A1-171)}$$

$$w_{IV} = \frac{m_{IV}}{V_{IV}} \qquad \text{---(A1-172)}$$

ABDOMINAL ARTERIES :

$$\frac{dm_{AA}}{dt} = w_{AO3AA} F_{AO3AA} - w_{AAAV} F_{AAAV} - w_{AACA} F_{AACA} - \frac{m_{AA}}{\tau_q} \qquad \text{---(A1-173)}$$

$$w_{AA} = \frac{m_{AA}}{V_{AA}} \qquad \text{---(A1-174)}$$

ABDOMINAL VEINS :

$$\frac{dm_{AV}}{dt} = w_{AAAV} F_{AAAV} + w_{CVAV} F_{CVAV} - w_{AVIVC} F_{AVIVC} - \frac{m_{AV}}{\tau_q} \qquad \text{---(A1-175)}$$

$$w_{AV} = \frac{m_{AV}}{V_{AV}} \qquad \text{---(A1-176)}$$

LEG ARTERIES:

$$\frac{dm_{CA}}{dt} = w_{AACA} F_{AACA} - w_{CACV} F_{CACV} - \frac{m_{CA}}{\tau_q} \qquad \text{---(A1-177)}$$

$$w_{CA} = \frac{m_{CA}}{V_{CA}} \qquad \text{---(A1-178)}$$

LEG VEINS:

$$\frac{dm_{CV}}{dt} = w_{CACV} F_{CACV} - w_{CVAV} F_{CVAV} - \frac{m_{CV}}{\tau_q} \qquad \text{---(A1-179)}$$

$$w_{CV} = \frac{m_{CV}}{V_{CV}} \qquad \text{---(A1-180)}$$

INFERIOR VENA CAVA:

$$\frac{dm_{IVC}}{dt} = w_{AVIVC} F_{AVIVC} + w_{IVIVC} F_{IVIVC} - w_{IVCRA} F_{IVCRA} - \frac{m_{IVC}}{\tau_q} \qquad \text{---(A1-181)}$$

$$w_{IVC} = \frac{m_{IVC}}{V_{IVC}} \qquad \text{---(A1-182)}$$

SUPERIOR VENA CAVA:

$$\frac{dm_{SVC}}{dt} = w_{UVSVC} F_{UVSVC} - w_{SVCRA} F_{SVCRA} - \frac{m_{SVC}}{\tau_q} \qquad \text{---(A1-183)}$$

$$w_{SVC} = \frac{m_{SVC}}{V_{SVC}} \qquad \text{---(A1-184)}$$

CONCENTRATIONS APPROPRIATE TO DIRECTIONS OF FLOW:

$$w_{SVCRA} = \begin{cases} w_{SVC}, & F_{SVCRA} > 0 \\ w_{RA}, & F_{SVCRA} \leq 0 \end{cases} \qquad \text{---(A1-185)}$$

$$w_{COR} = \begin{cases} w_{AOI}, & F_{COR} > 0 \\ w_{RA}, & F_{COR} \leq 0 \end{cases} \qquad \text{---(A1-186)}$$

$$w_{BRONC} = \begin{cases} w_{AO3}, & F_{BRONC} > 0 \\ w_{RA}, & F_{BRONC} \leq 0 \end{cases} \qquad \text{---(A1-187)}$$

$$w_{IVCRA} = \begin{cases} w_{IVC}, & F_{IVCRA} > 0 \\ w_{RA}, & F_{IVCRA} \leq 0 \end{cases} \qquad \text{---(A1-188)}$$

CONCENTRATIONS APPROPRIATE TO DIRECTIONS OF FLOW (CONTINUED):

$$\omega_{RARV} = \begin{cases} \omega_{RA}, & F_{RARV} > 0 \\ \omega_{RV}, & F_{RARV} \leq 0 \end{cases} \quad \text{---(A1-189)}$$

$$\omega_{RVPA} = \begin{cases} \omega_{RV}, & F_{RVPA} > 0 \\ \omega_{PA}, & F_{RVPA} \leq 0 \end{cases} \quad \text{---(A1-190)}$$

$$\omega_{PAPV} = \begin{cases} \omega_{PA}, & F_{PAPV} > 0 \\ \omega_{PV}, & F_{PAPV} \leq 0 \end{cases} \quad \text{---(A1-191)}$$

$$\omega_{PVLA} = \begin{cases} \omega_{PV}, & F_{PVLA} > 0 \\ \omega_{LA}, & F_{PVLA} \leq 0 \end{cases} \quad \text{---(A1-192)}$$

$$\omega_{LALV} = \begin{cases} \omega_{LA}, & F_{LALV} > 0 \\ \omega_{LV}, & F_{LALV} \leq 0 \end{cases} \quad \text{---(A1-193)}$$

$$\omega_{LVAO1} = \begin{cases} \omega_{LV}, & F_{LVAO1} > 0 \\ \omega_{AO1}, & F_{LVAO1} \leq 0 \end{cases} \quad \text{---(A1-194)}$$

$$\omega_{AO1AO2} = \begin{cases} \omega_{AO1}, & F_{AO1AO2} > 0 \\ \omega_{AO2}, & F_{AO1AO2} \leq 0 \end{cases} \quad \text{---(A1-195)}$$

$$\omega_{AO2UA} = \begin{cases} \omega_{AO2}, & F_{AO2UA} > 0 \\ \omega_{UA}, & F_{AO2UA} \leq 0 \end{cases} \quad \text{---(A1-196)}$$

$$\omega_{AO2AO3} = \begin{cases} \omega_{AO2}, & F_{AO2AO3} > 0 \\ \omega_{AO3}, & F_{AO2AO3} \leq 0 \end{cases} \quad \text{---(A1-197)}$$

$$\omega_{UAUV} = \begin{cases} \omega_{UA}, & F_{UAUV} > 0 \\ \omega_{UV}, & F_{UAUV} \leq 0 \end{cases} \quad \text{---(A1-198)}$$

$$\omega_{UVSVC} = \begin{cases} \omega_{UV}, & F_{UVSVC} > 0 \\ \omega_{SVC}, & F_{UVSVC} \leq 0 \end{cases} \quad \text{---(A1-199)}$$

$$\omega_{AO3IA} = \begin{cases} \omega_{AO3}, & F_{AO3IA} > 0 \\ \omega_{IA}, & F_{AO3IA} \leq 0 \end{cases} \quad \text{---(A1-200)}$$

CONCENTRATIONS APPROPRIATE TO DIRECTIONS OF FLOW (CONTINVED):

$$\omega_{AO3AA} = \begin{cases} \omega_{AO3}, F_{AO3AA} > 0 \\ \omega_{AA}, F_{AO3AA} \leq 0 \end{cases} \quad \text{---(A1.201)}$$

$$\omega_{IAIV} = \begin{cases} \omega_{IA}, F_{IAIV} > 0 \\ \omega_{IV}, F_{IAIV} \leq 0 \end{cases} \quad \text{---(A1.202)}$$

$$\omega_{IVIVC} = \begin{cases} \omega_{IV}, F_{IVIVC} > 0 \\ \omega_{IVC}, F_{IVIVC} \leq 0 \end{cases} \quad \text{---(A1.203)}$$

$$\omega_{AAAV} = \begin{cases} \omega_{AA}, F_{AAAV} > 0 \\ \omega_{AV}, F_{AAAV} \leq 0 \end{cases} \quad \text{---(A1.204)}$$

$$\omega_{AACA} = \begin{cases} \omega_{AA}, F_{AACA} > 0 \\ \omega_{CA}, F_{AACA} \leq 0 \end{cases} \quad \text{---(A1.205)}$$

$$\omega_{CVAV} = \begin{cases} \omega_{CV}, F_{CVAV} > 0 \\ \omega_{AV}, F_{CVAV} \leq 0 \end{cases} \quad \text{---(A1.206)}$$

$$\omega_{AVIVC} = \begin{cases} \omega_{AV}, F_{AVIVC} > 0 \\ \omega_{IVC}, F_{AVIVC} \leq 0 \end{cases} \quad \text{---(A1.207)}$$

$$\omega_{CACV} = \begin{cases} \omega_{CA}, F_{CACV} > 0 \\ \omega_{CV}, F_{CACV} \leq 0 \end{cases} \quad \text{---(A1.208)}$$

EFFECT OF DRUG ON HEART RATE:

$$\sigma_H = \begin{cases} 1 + \sigma_2 \omega_{RA}, & \text{BRADYCARDIA} \\ \dfrac{1}{1 + \sigma_2 \omega_{RA}}, & \text{TACHYCARDIA} \end{cases} \quad \text{---(A1.209)}$$

EFFECT OF DRUG ON PERIPHERAL RESISTANCE:

$$\sigma_{BRONC} = \begin{cases} 1 + \sigma_1 \omega_{AO3}, & \text{VASOCONSTRICTION} \\ \dfrac{1}{1 + \sigma_1 \omega_{AO3}}, & \text{VASODILATATION} \end{cases} \quad \text{---(A1.210)}$$

$$\sigma_{INT} = \begin{cases} 1 + \sigma_1 \omega_{IA}, & \text{VASOCONSTRICTION} \\ \dfrac{1}{1 + \sigma_1 \omega_{IA}}, & \text{VASODILATATION} \end{cases} \quad \text{---(A1.211)}$$

EFFECT OF DRUG ON PERIPHERAL RESISTANCE (CONTINUED):

$$\sigma_{ABD} = \begin{cases} 1 + \sigma_1 w_{AA}, & \text{VASOCONSTRICTION} \\ \dfrac{1}{1 + \sigma_1 w_{AA}}, & \text{VASODILATATION} \end{cases} \quad \text{--- (A1.212)}$$

$$\sigma_{LEG} = \begin{cases} 1 + \sigma_1 w_{CA}, & \text{VASOCONSTRICTION} \\ \dfrac{1}{1 + \sigma_1 w_{CA}}, & \text{VASODILATATION} \end{cases} \quad \text{--- (A1.213)}$$

$$\sigma_{HEAD} = \begin{cases} 1 + \sigma_1 w_{UA}, & \text{VASOCONSTRICTION} \\ \dfrac{1}{1 + \sigma_1 w_{UA}}, & \text{VASODILATATION} \end{cases} \quad \text{--- (A1.214)}$$

EFFECT OF DRUG ON MYOCARDIAL CONTRACTILITY:

$$\sigma_{RA} = \begin{cases} 1 + \sigma_3 w_{RA}, & \text{POSITIVE INOTROPY} \\ \dfrac{1}{1 + \sigma_3 w_{RA}}, & \text{NEGATIVE INOTROPY} \end{cases} \quad \text{--- (A1.215)}$$

$$\sigma_{RV} = \begin{cases} 1 + \sigma_3 w_{RV}, & \text{POSITIVE INOTROPY} \\ \dfrac{1}{1 + \sigma_3 w_{RV}}, & \text{NEGATIVE INOTROPY} \end{cases} \quad \text{--- (A1.216)}$$

$$\sigma_{LA} = \begin{cases} 1 + \sigma_3 w_{LA}, & \text{POSITIVE INOTROPY} \\ \dfrac{1}{1 + \sigma_3 w_{LA}}, & \text{NEGATIVE INOTROPY} \end{cases} \quad \text{--- (A1.217)}$$

$$\sigma_{LV} = \begin{cases} 1 + \sigma_3 w_{LV}, & \text{POSITIVE INOTROPY} \\ \dfrac{1}{1 + \sigma_3 w_{LV}}, & \text{NEGATIVE INOTROPY} \end{cases} \quad \text{--- (A1.218)}$$

NOTE

(1) The derivatives required in equations (A1.117),(A1.123) and (A1.132) are evaluated using the expressions given in section 5.6.

(2) Due to the presence of algebraic loops (discussed in section 5.7), the following variables are evaluated using rearranged expressions given in Appendix 4 :

P_{AO1} in equation (A1.26), P_{UA} in equation (A1.33),

P_{AO3} in equation (A1.44), P_{IA} in equation (A1.47),

P_{AA} in equation (A1.57), P_{CA} in equation (A1.66).

APPENDIX 2

VARIABLES AND CONSTANTS USED IN THE COMPUTER PROGRAM

The variables and constants given in the tables below are those referred to in the mathematical model of Appendix 1 and the simulation program of Appendix 3.

A2.1 State variables

STATE VARIABLE IN COMPUTER PROGRAM	STATE VARIABLE IN MATHEMATICAL MODEL	INITIAL VALUE OF STATE VARIABLE	STATE VARIABLE IN COMPUTER PROGRAM	STATE VARIABLE IN MATHEMATICAL MODEL	INITIAL VALUE OF STATE VARIABLE
X(1)	V_{RA}	153·63	X(32)	S_9	1·7048
X(2)	V_{RV}	132·32	X(33)	u_4	62·617
X(3)	V_{PA}	114·86	X(34)	u_6	75·268
X(4)	V_{PV}	536·52	X(35)	u_7	75·115
X(5)	V_{LA}	104·02	X(36)	u_{10}	0·0
X(6)	V_{LV}	131·27	X(37)	q_2	0·97272
X(7)	V_{AO1}	81·233	X(38)	q_3	0·97109
X(8)	V_{AO2}	90·243	X(39)	d_2	1·1178
X(9)	V_{UA}	146·39	X(40)	b_2	0·97153
X(10)	V_{UV}	546·85	X(41)	$\int P_{AO1}\,dt$	0·0
X(11)	V_{AO3}	88·157	X(42)	$\int F_{LVAO1}\,dt$	0·0
X(12)	V_{IA}	22·552	X(43)	m_{RA}	0·0
X(13)	V_{IV}	597·54	X(44)	m_{RV}	0·0
X(14)	V_{AA}	77·249	X(45)	m_{PA}	0·0
X(15)	V_{AV}	290·32	X(46)	m_{PV}	0·0
X(16)	V_{CA}	74·33	X(47)	m_{LA}	0·0
X(17)	V_{CV}	271·05	X(48)	m_{LV}	0·0
X(18)	V_{IVC}	534·04	X(49)	m_{AO1}	0·0
X(19)	V_{SVC}	542·37	X(50)	m_{AO2}	0·0
X(20)	F_{RVPA}	0·0	X(51)	m_{UA}	0·0
X(21)	F_{LVAO1}	0·0	X(52)	m_{UV}	0·0
X(22)	F_{AO1AO2}	6·8039	X(53)	m_{AO3}	0·0
X(23)	F_{AO2UA}	−3·8444	X(54)	m_{IA}	0·0
X(24)	F_{AO2AO3}	25·669	X(55)	m_{IV}	0·0
X(25)	F_{AO3IA}	35·075	X(56)	m_{AA}	0·0
X(26)	F_{AO3AA}	−3·3266	X(57)	m_{AV}	0·0
X(27)	F_{AACA}	2·6994	X(58)	m_{CA}	0·0
X(28)	y_2	0·0	X(59)	m_{CV}	0·0
X(29)	S_3	109·26	X(60)	m_{IVC}	0·0
X(30)	S_4	1·4146	X(61)	m_{SVC}	0·0
X(31)	S_8	104·93			

A2.2 Other numerical variables

VARIABLE IN COMPUTER PROGRAM	VARIABLE IN MATHEMATICAL MODEL	VARIABLE IN COMPUTER PROGRAM	VARIABLE IN MATHEMATICAL MODEL	VARIABLE IN COMPUTER PROGRAM	VARIABLE IN MATHEMATICAL MODEL
V(1)	P_{RA}	V(42)	P_{CV}	V(83)	(CO)
V(2)	a_{RA}	V(43)	F_8	V(84)	(ETSR)
V(3)	dB_{AO2}/dt	V(44)	F_{CVAV}	V(85)	(TTSR)
V(4)	F_1	V(45)	P_{IVC}	V(86)	V_T
V(5)	F_2	V(46)	F_9	V(87)	(SV)
V(6)	F_{RARV}	V(47)	F_{IVCRA}	V(88)	y_1
V(7)	P_{RV}	V(48)	P_{SVC}	V(89)	P_{TH}
V(8)	a_{RV}	V(49)	F_{10}	V(90)	P_{ABD}
V(9)	P_{PA}	V(50)	F_{SVCRA}	V(91)	dB_{UA}/dt
V(10)	F_{PAPV}	V(51)	S_1	V(92)	w_{RA}
V(11)	P_{PV}	V(52)	S_2	V(93)	w_{RV}
V(12)	F_3	V(53)	S_5	V(94)	w_{PA}
V(13)	F_{PVLA}	V(54)	B_{AO2}	V(95)	w_{PV}
V(14)	P_{LA}	V(55)	S_6	V(96)	w_{LA}
V(15)	a_{LA}	V(56)	S_7	V(97)	w_{LV}
V(16)	F_4	V(57)	S_{10}	V(98)	w_{AO1}
V(17)	F_{LALV}	V(58)	B_{UA}	V(99)	w_{AO2}
V(18)	P_{LV}	V(59)	B	V(100)	w_{UA}
V(19)	a_{LV}	V(60)	u_1	V(101)	w_{UV}
V(20)	P_{AO1}	V(61)	u_2	V(102)	w_{AO3}
V(21)	F_{COR}	V(62)	u_3	V(103)	w_{IA}
V(22)	P_{AO2}	V(63)	u_5	V(104)	w_{IV}
V(23)	P_{UA}	V(64)	u_8	V(105)	w_{AA}
V(24)	F_{UAUV}	V(65)	u_9	V(106)	w_{AV}
V(25)	P_{UV}	V(66)	T_H	V(107)	w_{CA}
V(26)	F_5	V(67)	f_H	V(108)	w_{CV}
V(27)	F_{UVSVC}	V(68)	T_{AS}	V(109)	w_{IVC}
V(28)	P_{AO3}	V(69)	T_{AV}	V(110)	w_{SVC}
V(29)	F_{BRONC}	V(70)	T_{VS}	V(111)	$(P_{AO1})_{MAX}$
V(30)	P_{IA}	V(71)	x_1	V(112)	$(P_{AO1})_{MIN}$
V(31)	F_{IAIV}	V(72)	x_2	SRA	σ_{RA}
V(32)	P_{IV}	V(73)	x_3	SRV	σ_{RV}
V(33)	F_6	V(74)	x_4	SLA	σ_{LA}
V(34)	F_{IVIVC}	V(75)	x_5	SLV	σ_{LV}
V(35)	P_{AA}	V(76)	q_1	SHEAD	σ_{HEAD}
V(36)	F_{AAAV}	V(77)	q_4	SBRONC	σ_{BRONC}
V(37)	P_{AV}	V(78)	d_1	SINT	σ_{INT}
V(38)	F_7	V(79)	d_3	SABD	σ_{ABD}
V(39)	F_{AVIVC}	V(80)	d_4	SLEG	σ_{LEG}
V(40)	P_{CA}	V(81)	b_1	SHR	σ_H
V(41)	F_{CACV}	V(82)	(MAP)	PHI	ϕ

A2.3 Numerical constants

All constants are given in medical units (mmHg, ml, sec) unless otherwise stated.

CONSTANT IN COMPUTER PROGRAM	CONSTANT IN MATHEMATICAL MODEL	VALUE	CONSTANT IN COMPUTER PROGRAM	CONSTANT IN MATHEMATICAL MODEL	VALUE
P(1)	$C_{PVN} K_6$	COMPUTED	P(32)	R_{RARV}	0.003
P(2)	$R_{PVLA} V_{UPV}^2$	COMPUTED	P(33)	K_5	0.1
P(3)	$C_{AOI} + \frac{K_8}{R_{COR}}$	COMPUTED	P(34)	a_{RVS}	0.3
P(4)	$C_{UVN} K_6$	COMPUTED	P(35)	a_{RVD}	0.046
P(5)	$C_{SVCN} K_6$	COMPUTED	P(36)	V_{URV}	0.0
P(6)	$R_{SVC} V_{USVC}^2$	COMPUTED	P(37)	R_{RVPA}	0.003
P(7)	P_{THN}	−4.0	P(38)	A_{PA}	1.539 cm^2
P(8)	P_{ABDN}	+4.0	P(39)	L_{RV}	0.00018
P(9)	K_1	−3.0	P(40)	C_{PA}	4.3
P(10)	K_2	−6.0	P(41)	V_{UPA}	50.0
P(11)	K_3	+3.0	P(42)	P_{CC}	7.0
P(12)	K_4	+6.0	P(43)	R_{LUNG}	0.11
P(13)	T_{IE}	4.0	P(44)	C_{PVN}	8.4
P(14)	T_R	5.0	P(45)	V_{UPV}	460.0
P(15)	n	1.0	P(46)	K_6	20.0
P(16)	ϕ_N	90.0 degrees	P(47)	R_{PVLA}	0.007
P(17)	ℓ_{AO2UA}	19.5 cm	P(48)	K_7	0.1
P(18)	ℓ_{AO2AO3}	10.0 cm	P(49)	a_{LAS}	0.28
P(19)	ℓ_{UVSVC}	18.0 cm	P(50)	a_{LAD}	0.12
P(20)	ℓ_{AO3IA}	8.0 cm	P(51)	V_{ULA}	30.0
P(21)	ℓ_{AO3AA}	16.0 cm	P(52)	R_{LALV}	0.003
P(22)	ℓ_{IVCIV}	8.0 cm	P(53)	a_{LVS}	1.5
P(23)	ℓ_{AACA}	48.0 cm	P(54)	a_{LVD}	0.067
P(24)	ℓ_{IVCAV}	16.0 cm	P(55)	V_{ULV}	0.0
P(25)	ℓ_{AVCV}	48.0 cm	P(56)	R_{LVAOI}	0.003
P(26)	ℓ_{IVCRA}	10.0 cm	P(57)	A_{AOI}	1.539 cm^2
P(27)	ℓ_{SVCRA}	1.5 cm	P(58)	L_{LV}	0.00022
P(28)	ℓ_{AO3RA}	10.0 cm	P(59)	C_{AOI}	0.28
P(29)	a_{RAS}	0.15	P(60)	V_{UAOI}	53.0
P(30)	a_{RAD}	0.05	P(61)	K_8	0.04
P(31)	V_{URA}	30.0	P(62)	R_{COR}	12.0

Numerical constants (continued)

CONSTANT IN COMPUTER PROGRAM	CONSTANT IN MATHEMATICAL MODEL	VALUE	CONSTANT IN COMPUTER PROGRAM	CONSTANT IN MATHEMATICAL MODEL	VALUE
P(63)	R_{AO2}	3.0×10^{-5}	P(94)	C_{IVN}	10.6
P(64)	L_{AO2}	0.00043	P(95)	V_{UIVN}	607.0
P(65)	C_{AO2}	0.29	P(96)	G_{IVCIV}	COMPUTED
P(66)	V_{UAO2}	61.0	P(97)	R_{IV}	0.166
P(67)	R_{UA}	0.047	P(98)	K_{10}	1.0
P(68)	L_{UA}	0.014	P(99)	C_{AA}	0.21
P(69)	R_{AO3}	0.0009	P(100)	V_{UAA}	58.0
P(70)	L_{AO3}	0.0038	P(101)	R_{ABD}	57.0
P(71)	G_{AO2UA}	COMPUTED	P(102)	R_{CA}	0.18
P(72)	G_{AO2AO3}	COMPUTED	P(103)	L_{CA}	0.031
P(73)	C_{UA}	0.33	P(104)	G_{AACA}	COMPUTED
P(74)	V_{UUA}	114.0	P(105)	C_{AVN}	5.1
P(75)	R_{HEAD}	6.0	P(106)	V_{UAVN}	305.0
P(76)	C_{UVN}	9.4	P(107)	G_{IVCAV}	COMPUTED
P(77)	V_{UUVN}	552.0	P(108)	R_{AV}	0.595
P(78)	G_{UVSVC}	COMPUTED	P(109)	K_{11}	1.0
P(79)	R_{UV}	0.226	P(110)	C_{CA}	0.12
P(80)	K_9	0.667	P(111)	V_{UCA}	63.0
P(81)	C_{AO3}	0.29	P(112)	R_{LEG}	15.0
P(82)	V_{UAO3}	59.0	P(113)	C_{CVN}	4.8
P(83)	G_{AO3RA}	COMPUTED	P(114)	V_{UCVN}	257.0
P(84)	R_{BRONC}	12.0	P(115)	G_{AVCV}	COMPUTED
P(85)	R_{IA}	0.0014	P(116)	R_{CV}	0.3
P(86)	L_{IA}	0.0027	P(117)	K_{12}	0.0
P(87)	G_{AO3IA}	COMPUTED	P(118)	C_{IVCN}	8.3
P(88)	R_{AA}	0.012	P(119)	V_{UIVC}	488.0
P(89)	L_{AA}	0.014	P(120)	G_{IVCRA}	COMPUTED
P(90)	G_{AO3AA}	COMPUTED	P(121)	R_{IVC}	0.015
P(91)	C_{IA}	0.06	P(122)	$C_{IVCN}\,K_6$	COMPUTED
P(92)	V_{UIA}	17.0	P(123)	C_{SVCN}	8.3
P(93)	R_{INT}	2.3	P(124)	V_{USVC}	488.0

Numerical constants (continued)

CONSTANT IN COMPUTER PROGRAM	CONSTANT IN MATHEMATICAL MODEL	VALUE	CONSTANT IN COMPUTER PROGRAM	CONSTANT IN MATHEMATICAL MODEL	VALUE
P(125)	G_{SVCRA}	COMPUTED	P(156)	K_{30}	0.7
P(126)	R_{SVC}	0.06	P(157)	K_{31}	1.6
P(127)	$R_{IVC}\ V^2_{UIVC}$	COMPUTED	P(158)	τ_7	14.0
P(128)	τ_1	0.8	P(159)	K_{32}	1.0
P(129)	τ_2	0.1	P(160)	K_{33}	1.0
P(130)	K_{13}	1.0	P(161)	K_{34}	0.6
P(131)	K_{14}	1.0	P(162)	K_{35}	1.4
P(132)	K_{15}	40.0	P(163)	τ_8	10.0
P(133)	K_{16}	0.7	P(164)	$C_{AVN}\ K_6$	COMPUTED
P(134)	$R_{UV}\ V^2_{UUVN}$	COMPUTED	P(165)	h	0.0005
P(135)	$C_{IVN}\ K_6$	COMPUTED	P(166)	$R_{AV}\ V^2_{UAVN}$	COMPUTED
P(136)	K_{17}	1.0	P(167)	$C_{CVN}\ K_6$	COMPUTED
P(137)	K_{18}	80.0	P(168)	$R_{CV}\ V^2_{UCVN}$	COMPUTED
P(138)	$R_{IV}\ V^2_{UIVN}$	COMPUTED	P(169)	τ_9	30.0
P(139)	K_{19}	1.5	P(170)	$\varrho/(2A^2_{PA})$	COMPUTED
P(140)	K_{20}	4.5	P(171)	$\varrho/(2A^2_{AOI})$	COMPUTED
P(141)	τ_3	1.0	P(172)	π/T_{IE}	COMPUTED
P(142)	τ_4	2.0	P(173)	$K_2 - K_1$	COMPUTED
P(143)	K_{21}	0.006	P(174)	M	70.0 μg
P(144)	$T_H(0)$	0.8264	P(175)	σ_1	400.0 $ml\,\mu g^{-1}$
P(145)	K_{22}	0.1	P(176)	σ_2	50.0 $ml\,\mu g^{-1}$
P(146)	K_{23}	0.09	P(177)	σ_3	50.0 $ml\,\mu g^{-1}$
P(147)	K_{24}	0.04	P(178)	$K_4 - K_3$	COMPUTED
P(148)	K_{25}	0.16	PI	π	3.14159
P(149)	K_{26}	0.2	ØRIF	$\varrho/2$	0.0003978
P(150)	K_{27}	0.6	RHØG	ϱg	0.7807
P(151)	K_{28}	1.4	DEGRAD	$\pi/180$	0.01745
P(152)	τ_5	4.0	NS	SIZE OF X-VECTOR	61
P(153)	τ_6	20.0	NP	SIZE OF P-VECTOR	178
P(154)	K_{29}	0.75	NV	SIZE OF V-VECTOR	112
P(155)	T_{HN}	0.8	INJLØC	INJECTION LOCATION	52

A2.4 Logical variables

Logical variables are used to control the simulation.
'TRUE' is equivalent to 'ON' and 'FALSE' is equivalent to 'OFF'.

Logical variable in computer program	Initial Value	Comments
L(1)	TRUE	'ON' at t=0 ; 'OFF' for t>0
L(2)	FALSE	'ON' at the end of each cardiac cycle
L(3)	FALSE	Drug Injection
L(4)	FALSE	Respiration
L(5)	FALSE	Orthostasis
L(6)	TRUE	Heart rate control
L(7)	TRUE	Peripheral resistance control
L(8)	TRUE	Venous tone control
L(9)	TRUE	Myocardial contractility control
L(10)	TRUE	'ON' = Tachycardia ; 'OFF' = Bradycardia
L(11)	TRUE	'ON'=Vasoconstriction 'OFF'=Vasodilatation
L(12)	TRUE	'ON' = Positive Inotropy 'OFF' = Negative Inotropy
L(13)	FALSE	Drug transport
L(14)	FALSE	Drug action

APPENDIX 3

THE CARDIOVASCULAR SIMULATION PROGRAM

A3.1 Summary of the program structure

The program listed in section A3.2 uses facilities available in most versions of FORTRAN IV to ensure portability. Free formats, mixed mode arithmetic and other features of extended FORTRAN IV are not used. In the program listing, the letter O is distinguished from the number 0 by placing a line through the letter thus : $\emptyset$.

The principal arrays in the program are :

(1) X(61) - vector of state variables
(2) D(61) - vector of derivatives of state variables
(3) V(112) - other numerical variables
(4) P(178) - numerical constants
(5) L(14) - logical variables (for control of the simulation)

The variables in the mathematical model corresponding to the program variables are given in Appendix 2.

Following the Executive Control Segment, the subprograms in order are :

(1) SUBROUTINE INTEG(D,X,T) - computes a new state vector after one integration step using Euler's method.
(2) SUBROUTINE MODEL(D,X,T) - computes the derivative of the current state vector from the mathematical model.
(3) SUBROUTINE ODDJOB(D,X,T) - performs miscellaneous tasks at t=0 and once every cardiac cycle.
(4) SUBROUTINE CYCLE(D,X,T) - deals with respiration at each integration step, detects the end of the cardiac cycle and performs miscellaneous tasks at the end of the cardiac cycle.
(5) SUBROUTINE RESULT(D,X,T) - prints heading and results.
(6) SUBROUTINE PRELIM - preliminary calculation of frequently used constants.
(7) SUBROUTINE TTSR(X) - computes the true total systemic resistance.
(8) BLOCK DATA - initialises the arrays and variables in labelled COMMON blocks.

A3.2 The program listing

```
C
C   EXECUTIVE CØNTRØL SEGMENT
C
      LØGICAL L(14)
      DIMENSIØN X(61),D(61)
      CØMMØN /MISC/ NS,NP,NV,INJLØC,PMIN,PMAX
      CØMMØN /LØGIC/ L
      CØMMØN /PV/ P(178),V(112)
      CØMMØN /XIC/ XD(61)
C
C   SECØND PART ØF INITIALISATIØN (1ST PART IN BLØCK DATA SUBPRØGRAM)
C
      T=0.0
      DØ 1 I=1,NS
      D(I)=0.0
    1 X(I)=XD(I)
C
C-----------------------------------------------------------------
C   ANY REQUIRED CHANGES IN STATE VARIABLES ØR NØN-CØMPUTED
C   CØNSTANTS BEFØRE THE RUN MAY BE INTRØDUCED AT THIS PØINT
C-----------------------------------------------------------------
C
      CALL PRELIM
      CALL ØDDJØB(D,X,T)
      CALL MØDEL(D,X,T)
      CALL CYCLE(D,X,T)
      CALL RESULT(D,X,T)
C
C   DYNAMIC SECTIØN
C
      L(1)=.FALSE.
    2 CØNTINUE
      CALL INTEG(D,X,T)
      CALL CYCLE(D,X,T)
      IF(.NØT.L(2))GØ TØ 2
      CALL ØDDJØB(D,X,T)
      CALL RESULT(D,X,T)
      IF(T.GT.100.0)STØP
      L(2)=.FALSE.
      GØ TØ 2
      END
```

```
      SUBRØUTINE INTEG(D,X,T)
C
C   CØMPUTES NEW STATE VECTØR AFTER ØNE INTEGRATIØN
C   STEP USING EULER'S METHØD
C
      DIMENSIØN X(61),D(61)
      CØMMØN /PV/ P(178),V(112)
      CØMMØN /MISC/ NS,NP,NV,INJLØC,PMIN,PMAX
      H=P(165)
      DØ 1 I=1,NS
      X(I)=X(I)+H*D(I)
    1 CØNTINUE
      CALL MØDEL(D,X,T)
      T=T+H
      RETURN
      END
```

```
      SUBRØUTINE MØDEL(D,X,T)
C
C     CØMPUTES THE DERIVATIVE ØF THE STATE VECTØR FRØM THE
C     MATHEMATICAL MØDEL ØF THE HUMAN CARDIØVASCULAR SYSTEM
C
      LØGICAL L(14)
      DIMENSIØN X(61),D(61)
      CØMMØN /PV/ P(178),V(112)
      CØMMØN /MISC/ NS,NP,NV,INJLØC,PMIN,PMAX
      CØMMØN /LØGIC/ L
      CØMMØN /SIGMA/ SRA,SRV,SLA,SLV,SHEAD,SBRØNC,SINT,SABD,SLEG,SHR
      DATA PI/3.1415926536/
C
C     DECIDE IF DRUG ACTIØN IS REQUIRED
C
      IF(.NØT.L(14))GØ TØ 5
C
C     DIMENSIØNLESS FACTØRS FØR DRUG ACTIØN
C
      SIG1=P(175)
      SIG3=P(177)
      URA=1.0+SIG3*V(92)
      URV=1.0+SIG3*V(93)
      ULA=1.0+SIG3*V(96)
      ULV=1.0+SIG3*V(97)
      UHEAD=1.0+SIG1*V(100)
      UBRØNC=1.0+SIG1*V(102)
      UINT=1.0+SIG1*V(103)
      UABD=1.0+SIG1*V(105)
      ULEG=1.0+SIG1*V(107)
      UHR=1.0+P(176)*V(92)
      IF(.NØT.L(12))GØ TØ 1
C
C     PØSITIVE INØTRØPY
C
      SRA=URA
      SRV=URV
      SLA=ULA
      SLV=ULV
      GØ TØ 2
C
C     NEGATIVE INØTRØPY
C
1     SRA=1.0/URA
      SRV=1.0/URV
      SLA=1.0/ULA
      SLV=1.0/ULV
2     IF(.NØT.L(11))GØ TØ 3
C
C     VASØCØNSTRICTIØN
C
      SHEAD=UHEAD
      SBRØNC=UBRØNC
      SINT=UINT
      SABD=UABD
      SLEG=ULEG
      GØ TØ 4
C
C     VASØDILATATIØN
C
```

```
  3   SHEAD=1.0/UHEAD
      SBRØNC=1.0/UBRØNC
      SINT=1.0/UINT
      SABD=1.0/UABD
      SLEG=1.0/ULEG
C
C   BRADYCARDIA
C
  4   SHR=UHR
C
C   TACHYCARDIA
C
      IF(L(10))SHR=1.0/UHR
  5   CØNTINUE
C
C   SET INITIAL VALUE ØF HEART PERIØD
C
      IF(L(1))V(66)=P(144)
C
C   SET FIXED HEART PERIØD IF HEART RATE CØNTRØL ØFF
C
      IF(.NØT.L(6))V(66)=P(155)
C
C   TIME-VARYING CØMPLIANCE GENERATIØN.
C
      V(68)=P(145)+P(146)*V(66)
      V(69)=V(68)-P(147)
      V(70)=P(148)+P(149)*V(66)
      V(71)=PI/V(68)
      V(72)=PI/V(70)
      V(73)=0.0
      IF(X(36).LE.V(68))V(73)=SIN(V(71)*X(36))
      V(74)=0.0
      IF(X(36).GT.V(69))V(74)=X(36)-V(69)
      V(75)=0.0
      IF(V(74).LE.V(70))V(75)=SIN(V(72)*V(74))
      V(2)=V(73)*(P(29)*X(40)*SRA-P(30))+P(30)
      V(8)=V(75)*(P(34)*X(40)*SRV-P(35))+P(35)
      V(15)=V(73)*(P(49)*X(40)*SLA-P(50))+P(50)
      V(19)=V(75)*(P(53)*X(40)*SLV-P(54))+P(54)
C
C   START ØF CIRCULATØRY FLUID MECHANICS AND NEURAL CØNTRØL MØDELS
C
      V(53)=P(130)*(X(29)+P(131)*X(30)-P(132))
      V(64)=P(143)*(X(33)+X(35))*SHR
      V(77)=P(154)*X(38)+(1.0-P(154))*X(37)
      IF(.NØT.L(7))V(77)=1.0
      V(79)=1.0+P(159)*(X(39)-1.0)
      V(80)=1.0+P(160)*(X(39)-1.0)
      V(1)=V(2)*(X(1)-P(31))
      V(7)=V(8)*(X(2)-P(36))
      V(5)=(V(1)-V(7))/P(32)
      V(6)=V(5)
      IF(V(5).LT.0.0)V(6)=0.0
      V(9)=(X(3)-P(41))/P(40)
      CPV=P(44)
      IF(X(4).LT.P(45))CPV=P(1)
      V(11)=(X(4)-P(45))/CPV
      V(10)=(V(9)-V(11))/P(43)
      IF(V(11).LT.P(42))V(10)=(V(9)-P(42))/P(43)
```

```
V(14)=V(15)*(X(5)-P(51))
V(12)=(V(11)-V(14))*X(4)*X(4)/P(2)
V(13)=V(12)
IF(V(12).LT.0.0)V(13)=V(12)*P(48)
V(18)=V(19)*(X(6)-P(55))
V(16)=(V(14)-V(18))/P(52)
V(17)=V(16)
IF(V(16).LT.0.0)V(17)=0.0
QA=X(7)-P(60)+P(61)*(X(21)-X(22)+V(1)/P(62))
V(20)=QA/P(3)
IF(V(20).GT.PMAX)PMAX=V(20)
IF(V(20).LT.PMIN)PMIN=V(20)
V(21)=(V(20)-V(1))/P(62)
QB=X(8)-P(66)+P(61)*(X(22)-X(23)-X(24))
V(22)=QB/P(65)
QC=X(10)-P(77)/V(80)
CUV=P(76)
IF(QC.LT.0.0)CUV=P(4)
V(25)=QC*V(79)/CUV
QHD=P(75)*SHEAD
QD=X(9)-P(74)+P(61)*(X(23)+V(25)/QHD)
DHD=P(73)+P(61)/QHD
V(23)=QD/DHD
V(24)=(V(23)-V(25))/QHD
QE=X(19)-P(124)
CSVC=P(123)
IF(QE.LT.0.0)CSVC=P(5)
V(48)=QE/CSVC
QF=(V(48)-V(1)+P(125))*X(19)*X(19)
V(49)=QF/P(6)
V(50)=V(49)
IF(V(49).LT.0.0)V(50)=V(49)*P(33)
QG=X(18)-P(119)
CIVC=P(118)
IF(QG.LT.0.0)CIVC=P(122)
V(45)=QG/CIVC
QH=(V(45)-V(1)-P(120))*X(18)*X(18)
V(46)=QH/P(127)
V(47)=V(46)
IF(V(46).LT.0.0)V(47)=V(46)*P(33)
QI=(V(25)-V(48)-V(89)+P(78))*X(10)*X(10)
V(26)=QI/P(134)
V(27)=V(26)
IF(V(26).LT.0.0)V(27)=V(26)*P(80)
QJ=V(77)*P(84)*SBRØNC
QK=X(11)-P(82)+P(61)*(X(24)-X(25)-X(26)+V(1)/QJ)
V(28)=QK/(P(81)+P(61)/QJ)
V(29)=(V(28)-V(1)-P(83))/QJ
QL=X(13)-P(95)/V(80)
CIV=P(94)
IF(QL.LT.0.0)CIV=P(135)
V(32)=QL*V(79)/CIV
QM=(V(32)-V(45)+V(90)-V(89)-P(96))*X(13)*X(13)
V(33)=QM/P(138)
V(34)=V(33)
IF(V(33).LT.0.0)V(34)=V(33)*P(98)
QN=V(77)*P(93)*SINT
QØ=X(12)-P(92)+P(61)*(X(25)+V(32)/QN)
V(30)=QØ/(P(91)+P(61)/QN)
```

```
      V(31)=(V(30)-V(32))/QN
      QP=X(15)-P(106)/V(80)
      CAV=P(105)
      IF(QP.LT.0.0)CAV=P(164)
      V(37)=QP*V(79)/CAV
      QQ=(V(37)-V(45)+V(90)-V(89)-P(107))*X(15)*X(15)
      V(38)=QQ/P(166)
      V(39)=V(38)
      IF(V(38).LT.0.0)V(39)=V(38)*P(109)
      QR=V(77)*P(101)*SABD
      QS=X(14)-P(100)+P(61)*(X(26)-X(27)+V(37)/QR)
      V(35)=QS/(P(99)+P(61)/QR)
      V(36)=(V(35)-V(37))/QR
      QT=X(17)-P(114)/V(80)
      CCV=P(113)
      IF(QT.LT.0.0)CCV=P(167)
      V(42)=QT*V(79)/CCV
      QU=(V(42)-V(37)-V(90)-P(115))*X(17)*X(17)
      V(43)=QU/P(168)
      V(44)=V(43)
      IF(V(43).LT.0.0)V(44)=V(43)*P(117)
      QV=V(77)*P(112)*SLEG
      QW=X(16)-P(111)+P(61)*(X(27)+V(42)/QV)
      V(40)=QW/(P(110)+P(61)/QV)
      V(41)=(V(40)-V(42))/QV
      V(4)=V(50)+V(47)+V(29)+V(21)
C
C     DECIDE IF DRUG TRANSPØRT IS REQUIRED
C
      IF(.NØT.L(13))GØ TØ 8
C
C     CØMPUTE DRUG CØNCENTRATIØNS IN EACH SEGMENT AND
C     SELECT CØNCENTRATIØNS APPRØPRIATE TØ DIRECTIØNS ØF FLØW
C
      DØ 6 I=1,19
      V(I+91)=X(I+42)/X(I)
    6 CØNTINUE
      GSVCRA=V(110)
      IF(V(50).LE.0.0)GSVCRA=V(92)
      GCØR=V(98)
      IF(V(21).LE.0.0)GCØR=V(92)
      GBRØNC=V(102)
      IF(V(29).LE.0.0)GBRØNC=V(92)
      GIVCRA=V(109)
      IF(V(47).LE.0.0)GIVCRA=V(92)
      GRARV=V(92)
      IF(V(6).LE.0.0)GRARV=V(93)
      GRVPA=V(93)
      IF(X(20).LE.0.0)GRVPA=V(94)
      GPAPV=V(94)
      IF(V(10).LE.0.0)GPAPV=V(95)
      GPVLA=V(95)
      IF(V(13).LE.0.0)GPVLA=V(96)
      GLALV=V(96)
      IF(V(17).LE.0.0)GLALV=V(97)
      GLVAØ1=V(97)
      IF(X(21).LE.0.0)GLVAØ1=V(98)
      GAØ12=V(98)
      IF(X(22).LE.0.0)GAØ12=V(99)
```

```
      GAØ2UA=V(99)
      IF(X(23).LE.0.0)GAØ2UA=V(100)
      GAØ23=V(99)
      IF(X(24).LE.0.0)GAØ23=V(102)
      GUAUV=V(100)
      IF(V(24).LE.0.0)GUAUV=V(101)
      GUVSVC=V(101)
      IF(V(27).LE.0.0)GUVSVC=V(110)
      GAØ3IA=V(102)
      IF(X(25).LE.0.0)GAØ3IA=V(103)
      GAØ3AA=V(102)
      IF(X(26).LE.0.0)GAØ3AA=V(105)
      GIAIV=V(103)
      IF(V(31).LE.0.0)GIAIV=V(104)
      GIVIVC=V(104)
      IF(V(34).LE.0.0)GIVIVC=V(109)
      GAAAV=V(105)
      IF(V(36).LE.0.0)GAAAV=V(106)
      GAACA=V(105)
      IF(X(27).LE.0.0)GAACA=V(107)
      GCVAV=V(108)
      IF(V(44).LE.0.0)GCVAV=V(106)
      GAVIVC=V(106)
      IF(V(39).LE.0.0)GAVIVC=V(109)
      GCACV=V(107)
      IF(V(41).LE.0.0)GCACV=V(108)
      HSVCRA=GSVCRA*V(50)
      HCØR=GCØR*V(21)
      HBRØNC=GBRØNC*V(29)
      HIVCRA=GIVCRA*V(47)
      HRARV=GRARV*V(6)
      HRVPA=GRVPA*X(20)
      HPAPV=GPAPV*V(10)
      HPVLA=GPVLA*V(13)
      HLALV=GLALV*V(17)
      HLVAØ1=GLVAØ1*X(21)
      HAØ12=GAØ12*X(22)
      HAØ2UA=GAØ2UA*X(23)
      HAØ23=GAØ23*X(24)
      HUAUV=GUAUV*V(24)
      HUVSVC=GUVSVC*V(27)
      HAØ3IA=GAØ3IA*X(25)
      HAØ3AA=GAØ3AA*X(26)
      HIAIV=GIAIV*V(31)
      HIVIVC=GIVIVC*V(34)
      HAAAV=GAAAV*V(36)
      HAACA=GAACA*X(27)
      HCVAV=GCVAV*V(44)
      HAVIVC=GAVIVC*V(39)
      HCACV=GCACV*V(41)
C
C     DRUG MASS DERIVATIVES IN PHARMACØKINETICS MØDEL
C
      D(43)=HSVCRA+HCØR+HBRØNC+HIVCRA-HRARV
      D(44)=HRARV-HRVPA
      D(45)=HRVPA-HPAPV
      D(46)=HPAPV-HPVLA
      D(47)=HPVLA-HLALV
      D(48)=HLALV-HLVAØ1
      D(49)=HLVAØ1-HAØ12-HCØR
```

```
      D(50)=HAØ12-HAØ2UA-HAØ23
      D(51)=HAØ2UA-HUAUV
      D(52)=HUAUV-HUVSVC
      D(53)=HAØ23-HBRØNC-HAØ3IA-HAØ3AA
      D(54)=HAØ3IA-HIAIV
      D(55)=HIAIV-HIVIVC
      D(56)=HAØ3AA-HAAAV-HAACA
      D(57)=HAAAV+HCVAV-HAVIVC
      D(58)=HAACA-HCACV
      D(59)=HCACV-HCVAV
      D(60)=HAVIVC+HIVIVC-HIVCRA
      D(61)=HUVSVC-HSVCRA
      DØ 7 I=43,61
C
C     INCLUSIØN ØF DRUG BREAKDØWN/ABSØRPTIØN
C
      D(I)=D(I)-X(I)/P(169)
C
C     ENSURES PØSITIVE DRUG MASSES IN VARIABLE STEP INTEGRATIØN RØUTINES
C
      IF(D(I).GT.0.0)GØ TØ 7
      SLØPE=-200.0*X(I)
      IF(D(I).LT.SLØPE)D(I)=SLØPE
7     CØNTINUE
8     CØNTINUE
      D(1)=V(4)-V(6)
      D(2)=V(6)-X(20)
      D(3)=X(20)-V(10)
      D(4)=V(10)-V(13)
      D(5)=V(13)-V(17)
      D(6)=V(17)-X(21)
      D(7)=X(21)-X(22)-V(21)
      D(8)=X(22)-X(23)-X(24)
      D(9)=X(23)-V(24)
      D(10)=V(24)-V(27)
      D(11)=X(24)-V(29)-X(25)-X(26)
      D(12)=X(25)-V(31)
      D(13)=V(31)-V(34)
      D(14)=X(26)-V(36)-X(27)
      D(15)=V(36)+V(44)-V(39)
      D(16)=X(27)-V(41)
      D(17)=V(41)-V(44)
      D(18)=V(39)+V(34)-V(47)
      D(19)=V(27)-V(50)
      D(20)=(V(7)-V(9)-X(20)*(P(37)+P(170)*X(20)))/P(39)
      D(21)=(V(18)-V(20)-X(21)*(P(56)+P(171)*X(21)))/P(58)
      DØ 9 I=1,21
C
C     ENSURES PØSITIVE VØLUMES AND PØSITIVE VENTRICULAR
C     ØUTFLØWS IN VARIABLE STEP INTEGRATIØN RØUTINES
C
      IF(D(I).GT.0.0)GØ TØ 9
      SLØPE=-200.0*X(I)
      IF(D(I).LT.SLØPE)D(I)=SLØPE
9     CØNTINUE
      D(22)=(V(20)-V(22)-X(22)*P(63))/P(64)
      D(23)=(V(22)+V(89)-V(23)-X(23)*P(67)-P(71))/P(68)
      D(24)=(V(22)-V(28)-X(24)*P(69)+P(72))/P(70)
      D(25)=(V(28)+V(89)-V(30)-V(90)-X(25)*P(85)+P(87))/P(86)
      D(26)=(V(28)+V(89)-V(35)-V(90)-X(26)*P(88)+P(90))/P(89)
```

```
      D(27)=(V(35)-V(40)+V(90)-X(27)*P(102)+P(104))/P(103)
      D(28)=1.0
C
C   NEURAL CØNTRØL SECTIØN
C
      D(29)=(V(22)-X(29))/P(128)
      V(51)=(D(8)+P(61)*(D(22)-D(23)-D(24)))/P(65)
      V(52)=V(51)
      IF(V(51).LT.0.0)V(52)=0.0
      V(55)=(D(9)+P(61)*(D(23)+V(79)*D(10)/(CUV*QHD)))/DHD
      V(56)=V(55)
      IF(V(55).LT.0.0)V(56)=0.0
      D(30)=(V(52)-X(30))/P(129)
      D(31)=(V(23)-X(31))/P(128)
      D(32)=(V(56)-X(32))/P(129)
      IF(V(53).LE.0.0)GØ TØ 10
      V(3)=P(130)*(D(29)+P(131)*D(30))
      V(54)=V(53)
      GØ TØ 11
10    V(54)=0.0
      V(3)=0.0
11    CØNTINUE
      V(57)=P(130)*(X(31)+P(131)*X(32)-P(132))
      IF(V(57).LE.0.0)GØ TØ 12
      V(91)=P(130)*(D(31)+P(131)*D(32))
      V(58)=V(57)
      GØ TØ 13
12    V(58)=0.0
      V(91)=0.0
13    CØNTINUE
      V(59)=(1.0-P(133))*V(54)+P(133)*V(58)
C
C   CØMPARE BARØRECEPTØR SYSTEM ØUTPUT WITH THRESHØLD
C   FØR BANG-BANG ACTIØN IN NEURAL CØNTRØLLERS
C
      IF(V(59).LE.P(137))GØ TØ 14
      V(60)=P(136)*(V(59)-P(137))
      V(63)=P(137)
      V(76)=P(150)
      V(78)=P(156)
      V(81)=P(161)
      V(61)=P(136)*((1.0-P(133))*V(3)+P(133)*V(91))
      GØ TØ 15
14    V(60)=0.0
      V(63)=V(59)
      V(76)=P(151)
      V(78)=P(157)
      V(81)=P(162)
      V(61)=0.0
15    CØNTINUE
      V(62)=P(139)
      IF(V(61).LE.0.0)V(62)=P(140)
      D(33)=(V(60)-X(33))/V(62)
      D(34)=(V(63)-X(34))/P(141)
      D(35)=(X(34)-X(35))/P(142)
      D(36)=1.0
      D(37)=(V(76)-X(37))/P(152)
      D(38)=(V(76)-X(38))/P(153)
      D(39)=(V(78)-X(39))/P(158)
      D(40)=(V(81)-X(40))/P(163)
```

```
C
C   IF VENØUS TØNE ØR MYØCARDIAL CØNTRACTILITY CØNTRØL NØT REQUIRED,
C   SET DERIVATIVES ØF CØRRESPØNDING STATE VARIABLES TØ ZERØ
C
      IF(.NØT.L(8))D(39)=0.0
      IF(.NØT.L(9))D(40)=0.0
C
C   PART ØF MAP AND SV CALCULATIØN
C
      D(41)=V(20)
      D(42)=X(21)
      RETURN
      END
```

```
      SUBRØUTINE ØDDJØB(D,X,T)
C
C   MISCELLANEØUS TASKS AT T=0 AND ØNCE EVERY CARDIAC CYCLE
C
      LØGICAL L(14)
      DIMENSIØN X(61),D(61)
      CØMMØN /PV/ P(178),V(112)
      CØMMØN /MISC/ NS,NP,NV,INJLØC,PMIN,PMAX
      CØMMØN /LØGIC/ L
      DATA RHØG,DEGRAD/0.7807,0.01745/
C
C   ØRTHØSTASIS
C
      PHI=0.0
      IF(L(5))PHI=P(16)
      TILT=P(15)*RHØG*SIN(DEGRAD*PHI)
      P(71)=TILT*P(17)
      P(72)=TILT*P(18)
      P(78)=TILT*P(19)
      P(87)=TILT*P(20)
      P(90)=TILT*P(21)
      P(96)=TILT*P(22)
      P(104)=TILT*P(23)
      P(107)=TILT*P(24)
      P(115)=TILT*P(25)
      P(120)=TILT*P(26)
      P(125)=TILT*P(27)
      P(83)=TILT*P(28)
C
C   DRUG INJECTIØN
C
      IF(.NØT.L(3))GØ TØ 1
      X(INJLØC)=P(174)
      L(3)=.FALSE.
1     CØNTINUE
C
C   IF VENØUS TØNE ØR MYØCARDIAL CØNTRACTILITY CØNTRØL NØT REQUIRED,
C   SET CØRRESPØNDING STATE VARIABLES TØ UNITY
C
      IF(.NØT.L(8))X(39)=1.0
      IF(.NØT.L(9))X(40)=1.0
C
C   CØMPUTE TØTAL BLØØD VØLUME
C
      VSUM=0.0
      DØ 2 I=1,19
```

```
2       VSUM=VSUM+X(I)
        V(86)=VSUM
        RETURN
        END
```

```
        SUBRØUTINE CYCLE(D,X,T)
C
C   DEALS WITH RESPIRATIØN AT EACH INTEGRATIØN STEP
C   DETECTS END ØF CARDIAC CYCLE AND PERFØRMS
C   MISCELLANEØUS TASKS AT END ØF CARDIAC CYCLE
C
        LØGICAL L(14)
        DIMENSIØN X(61),D(61)
        CØMMØN /PV/ P(178),V(112)
        CØMMØN /MISC/ NS,NP,NV,INJLØC,PMIN,PMAX
        CØMMØN /LØGIC/ L
C
C   RESPIRATIØN
C
        IF(L(4))GØ TØ 1
        X(28)=0.0
        V(89)=P(7)
        V(90)=P(8)
        GØ TØ 2
  1     IF(X(28).GT.P(14))X(28)=0.0
        V(88)=X(28)
        IF(X(28).GT.P(13))V(88)=0.0
        Q=SIN(P(172)*V(88))
        V(89)=P(9)+P(173)*Q
        V(90)=P(11)+P(178)*Q
  2     CØNTINUE
C
C   TEST FØR END ØF CARDIAC CYCLE
C
        IF(X(36).LT.V(66))RETURN
C
C   VARIØUS CALCULATIØNS AT THE END ØF THE CARDIAC CYCLE
C
        L(2)=.TRUE.
        V(111)=PMAX
        V(112)=PMIN
        PMAX=-1.0E20
        PMIN=1.0E20
        V(87)=X(42)
        V(82)=X(41)/V(66)
        V(83)=V(87)/V(66)
        V(84)=V(82)/V(83)
        CALL TTSR(X)
C
C   UPDATE HEART PERIØD
C
        V(65)=V(64)
        IF(V(64).GT.2.0)V(65)=2.0
        IF(V(64).LT.0.3)V(65)=0.3
        IF(L(6))V(66)=V(65)
        V(67)=60.0/V(66)
        X(36)=0.0
        X(41)=0.0
        X(42)=0.0
        RETURN
        END
```

```
      SUBRØUTINE RESULT(D,X,T)
C
C   PRINT HEADING AND TABULATED RESULTS
C
      LØGICAL L(14)
      DIMENSIØN X(61),D(61)
      CØMMØN /PV/ P(178),V(112)
      CØMMØN /MISC/ NS,NP,NV,INJLØC,PMIN,PMAX
      CØMMØN /LØGIC/ L
      IF(.NØT.L(1))GØ TØ 1
      WRITE(2,100)
    1 WRITE(2,101)T,V(82),V(87),V(83),V(66),V(67),V(84),V(111),V(112)
      RETURN
  100 FØRMAT(1H1,6X,1HT,11X,3HMAP,9X,2HSV,10X,2HCØ,10X,
     A2HTH,10X,2HFH,10X,4HETSR,8X,4HPMAX,8X,4HPMIN/)
  101 FØRMAT(1H ,10E12.4)
      END
```

```
      SUBRØUTINE PRELIM
C
C   PRELIMINARY CALCULATIØN ØF FREQUENTLY USED CØNSTANTS
C
      CØMMØN /PV/ P(178),V(112)
      DATA PI,ØRIF/3.14159,0.0003978/
      P(1)=P(44)*P(46)
      P(2)=P(47)*P(45)*P(45)
      P(3)=P(59)+P(61)/P(62)
      P(4)=P(76)*P(46)
      P(5)=P(123)*P(46)
      P(6)=P(126)*P(124)*P(124)
      P(122)=P(118)*P(46)
      P(127)=P(121)*P(119)*P(119)
      P(134)=P(79)*P(77)*P(77)
      P(135)=P(94)*P(46)
      P(138)=P(97)*P(95)*P(95)
      P(164)=P(105)*P(46)
      P(166)=P(108)*P(106)*P(106)
      P(167)=P(113)*P(46)
      P(168)=P(116)*P(114)*P(114)
      P(170)=ØRIF/(P(38)*P(38))
      P(171)=ØRIF/(P(57)*P(57))
      P(172)=PI/P(13)
      P(173)=P(10)-P(9)
      P(178)=P(12)-P(11)
      RETURN
      END
```

```
      SUBRØUTINE TTSR(X)
C
C   CØMPUTES TRUE TØTAL SYSTEMIC RESISTANCE
C
      DIMENSIØN X(61)
      CØMMØN /PV/ P(178),V(112)
      CØMMØN /SIGMA/ SRA,SRV,SLA,SLV,SHEAD,SBRØNC,SINT,SABD,SLEG,SHR
      RA=P(67)+P(75)*SHEAD+P(134)/(X(10)*X(10))+P(6)/(X(19)*X(19))
      RB=V(77)*SBRØNC*P(84)
      RC=P(102)+V(77)*P(112)*SLEG+P(168)/(X(17)*X(17))
      RD=V(77)*P(101)*SABD
      RE=RC*RD/(RC+RD)+P(88)+P(166)/(X(15)*X(15))
      RF=P(85)+V(77)*SINT*P(93)+P(138)/(X(13)*X(13))
```

```
      RG=RE*RF/(RE+RF)+P(127)/(X(18)*X(18))
      RH=P(69)+RB*RG/(RB+RG)
      RI=P(63)+RA*RH/(RA+RH)
      V(85)=P(62)*RI/(P(62)+RI)
      RETURN
      END
```

```
      BLØCK DATA
C
C     FIRST PART ØF INITIALISATIØN
C
      LØGICAL L(14)
      CØMMØN /PV/ P(178),V(112)
      CØMMØN /XIC/ X(61)
      CØMMØN /MISC/ NS,NP,NV,INJLØC,PMIN,PMAX
      CØMMØN /LØGIC/ L
      CØMMØN /SIGMA/ SRA,SRV,SLA,SLV,SHEAD,SBRØNC,SINT,SABD,SLEG,SHR
      DATA P /0.0,0.0,0.0,0.0,0.0,0.0,-4.0,4.0,-3.0,
     A-6.0,3.0,6.0,4.0,5.0,1.0,90.0,19.5,10.0,18.0,
     B8.0,16.0,8.0,48.0,16.0,48.0,10.0,1.5,10.0,0.15,
     C0.05,30.0,0.003,0.1,0.3,0.046,0.0,0.003,1.539,0.00018,
     D4.3,50.0,7.0,0.11,8.4,460.0,20.0,0.007,0.1,0.28,
     E0.12,30.0,0.003,1.5,0.067,0.0,0.003,1.539,0.00022,0.28,
     F53.0,0.04,12.0,3.0E-5,0.00043,0.29,61.0,0.047,0.014,0.0009,
     G0.0038,0.0,0.0,0.33,114.0,6.0,9.4,552.0,0.0,0.226,
     H0.667,0.29,59.0,0.0,12.0,0.0014,0.0027,0.0,0.012,0.014,
     I0.0,0.06,17.0,2.3,10.6,607.0,0.0,0.166,1.0,0.21,
     J58.0,57.0,0.18,0.031,0.0,5.1,305.0,0.0,0.595,1.0,
     K0.12,63.0,15.0,4.8,257.0,0.0,0.3,0.0,8.3,488.0,
     L0.0,0.015,0.0,8.3,488.0,0.0,0.06,0.0,0.8,0.1,
     M1.0,1.0,40.0,0.7,0.0,0.0,1.0,80.0,0.0,1.5,
     N4.5,1.0,2.0,0.006,0.8264,0.1,0.09,0.04,0.16,0.2,
     Ø0.6,1.4,4.0,20.0,0.75,0.8,0.7,1.6,14.0,1.0,
     P1.0,0.6,1.4,10.0,0.0,0.0005,0.0,0.0,0.0,30.0,
     Q0.0,0.0,0.0,0.0,70.0,400.0,50.0,50.0,0.0/
      DATA V /112*0.0/
      DATA X /153.63,132.32,114.86,536.52,
     A104.02,131.27,81.233,90.243,146.39,
     B546.85,88.157,22.552,597.54,77.249,
     C290.32,74.33,271.05,534.04,542.37,
     D0.0,0.0,6.8039,-3.8444,25.669,
     E35.075,-3.3266,2.6994,0.0,109.26,
     F1.4146,104.93,1.7048,62.617,75.268,
     G75.115,0.0,0.97272,0.97109,1.1178,
     H0.97153,0.0,0.0,0.0,0.0,0.0,0.0,0.0,0.0,0.0,0.0,0.0,
     I0.0,0.0,0.0,0.0,0.0,0.0,0.0,0.0,0.0,0.0,0.0,0.0,
     J0.0,0.0/
      DATA NS,NP,NV,INJLØC,PMIN,PMAX/61,178,112,52,1.0E20,-1.0E20/
      DATA L/.TRUE.,.FALSE.,.FALSE.,.FALSE.,.FALSE.,.TRUE.,.TRUE.,
     A.TRUE.,.TRUE.,.TRUE.,.TRUE.,.TRUE.,.FALSE.,.FALSE./
      DATA SRA,SRV,SLA,SLV,SHEAD,SBRØNC,SINT,SABD,SLEG,SHR/10*1.0/
      END
```

APPENDIX 4

REARRANGEMENT OF THE SYSTEMIC ARTERIAL EQUATIONS TO ELIMINATE ALGEBRAIC LOOPS

Algebraic loops (discussed in section 5.7) cause problems in the digital simulation and are eliminated by manual rearrangement of the equations involving loop variables.

(a) Substituting for $\frac{dV_{AO1}}{dt}$ in eqn.(A1.26) from eqn.(A1.24) gives :

$$P_{AO1} = \frac{1}{C_{AO1}}(V_{AO1} - V_{UAO1}) + \frac{K_8}{C_{AO1}}\left(F_{LVAO1} - F_{AO1AO2} - F_{COR}\right) \qquad ---(A4.1)$$

Substituting for F_{COR} in eqn.(A4.1) from eqn.(A1.27) and rearranging gives :

$$P_{AO1} = \frac{V_{AO1} - V_{UAO1} + K_8\left(F_{LVAO1} - F_{AO1AO2} + \frac{P_{RA}}{R_{COR}}\right)}{C_{AO1} + \frac{K_8}{R_{COR}}} \qquad ---(A4.2)$$

(b) Substituting for $\frac{dV_{UA}}{dt}$ in eqn.(A1.33) from eqn.(A1.32) gives :

$$P_{UA} = \frac{1}{C_{UA}}(V_{UA} - V_{UUA}) + \frac{K_8}{C_{UA}}\left(F_{AO2UA} - F_{UAUV}\right) \qquad ---(A4.3)$$

Substituting for F_{UAUV} in eqn.(A4.3) from eqn.(A1.34) and rearranging gives :

$$P_{UA} = \frac{V_{UA} - V_{UUA} + K_8\left(F_{AO2UA} + \frac{P_{UV}}{R_{HEAD}\,\sigma_{HEAD}}\right)}{C_{UA} + \frac{K_8}{R_{HEAD}\,\sigma_{HEAD}}} \qquad ---(A4.4)$$

(c) Substituting for $\frac{dV_{AO3}}{dt}$ in eqn.(A1.44) from eqn.(A1.41) gives :

$$P_{AO3} = \frac{1}{C_{AO3}}(V_{AO3} - V_{UAO3}) + \frac{K_8}{C_{AO3}}\left(F_{AO2AO3} - F_{BRONC} - F_{AO31A} - F_{AO3AA}\right) \qquad ---(A4.5)$$

Substituting for F_{BRONC} in eqn.(A4.5) from eqn.(A1.45) and rearranging gives :

$$P_{AO3} = \frac{V_{AO3} - V_{UAO3} + K_8\left(F_{AO2AO3} - F_{AO31A} - F_{AO3AA} + \frac{P_{RA}}{R_{BRONC}\,\sigma_{BRONC}\,q_{14}}\right)}{C_{AO3} + \frac{K_8}{R_{BRONC}\,\sigma_{BRONC}\,q_{14}}} \qquad ---(A4.6)$$

(d) Substituting for $\frac{dV_{IA}}{dt}$ in eqn.(A1.47) from eqn.(A1.46) gives :

$$P_{IA} = \frac{1}{C_{IA}}(V_{IA} - V_{UIA}) + \frac{K_8}{C_{IA}}\left(F_{AO3IA} - F_{IAIV}\right) \qquad ---(A4.7)$$

Substituting for F_{IAIV} in eqn.(A4.7) from eqn.(A1.48) and rearranging gives :

$$P_{IA} = \frac{V_{IA} - V_{UIA} + K_8\left(F_{AO3IA} + \frac{P_{IV}}{R_{INT}\,\sigma_{INT}\,q_4}\right)}{C_{IA} + \frac{K_8}{R_{INT}\,\sigma_{INT}\,q_4}} \qquad ---(A4.8)$$

(e) Substituting for $\frac{dV_{AA}}{dt}$ in eqn.(A1.57) from eqn.(A1.55) gives :

$$P_{AA} = \frac{1}{C_{AA}}(V_{AA} - V_{UAA}) + \frac{K_8}{C_{AA}}\left(F_{AO3AA} - F_{AAAV} - F_{AACA}\right) \qquad ---(A4.9)$$

Substituting for F_{AAAV} in eqn.(A4.9) from eqn.(A1.58) and rearranging gives :

$$P_{AA} = \frac{V_{AA} - V_{UAA} + K_8\left(F_{AO3AA} - F_{AACA} + \frac{P_{AV}}{R_{ABD}\,\sigma_{ABD}\,q_4}\right)}{C_{AA} + \frac{K_8}{R_{ABD}\,\sigma_{ABD}\,q_4}} \qquad ---(A4.10)$$

(f) Substituting for $\frac{dV_{CA}}{dt}$ in eqn.(A1.66) from eqn.(A1.65) gives :

$$P_{CA} = \frac{1}{C_{CA}}(V_{CA} - V_{UCA}) + \frac{K_8}{C_{CA}}\left(F_{AACA} - F_{CACV}\right) \qquad ---(A4.11)$$

Substituting for F_{CACV} in eqn.(A4.11) from eqn.(A1.67) and rearranging gives :

$$P_{CA} = \frac{V_{CA} - V_{UCA} + K_8\left(F_{AACA} + \frac{P_{CV}}{R_{LEG}\,\sigma_{LEG}\,q_4}\right)}{C_{CA} + \frac{K_8}{R_{LEG}\,\sigma_{LEG}\,q_4}} \qquad ---(A4.12)$$

APPENDIX 5

CALCULATION OF THE EFFECTIVE CROSS-SECTIONAL AREAS OF THE SEGMENTS REPRESENTING THE ASCENDING AORTA AND PULMONARY ARTERIES FOR THE APPLICATION OF BERNOULLI'S THEOREM

In the modelling of the ejection of blood at high velocity from the right and left ventricles, Bernoulli's theorem is applied (eqns. 2.34 & 2.35). A complication arises in applying this theorem because the blood is constrained to flow in a curved elastic artery. It is therefore necessary to determine the effective cross-sectional areas of the ascending aorta and pulmonary arteries segments which will take into account this constraint.

Consider a curved section of blood vessel having a radius of curvature R and internal radius r as in fig. A5.1 . A ventricular valve orifice is assumed to be located at one end of the vessel (CD). Blood ejected at high velocity from the ventricle will tend to continue moving in a straight line by Newton's first law of motion. The presence of the curved constraining vessel will result in an increased pressure on one side of the vessel. The assumption is made that the effective cross-sectional area as "seen" from the valve orifice reduces with increasing distance from the orifice.

At a distance z measured along the vessel axis distal to the orifice, the effective viewed area may be approximated by a circle with diameter

$$d(z) = AB = OB - OA$$

$$\therefore \quad d(z) = (R+r) - (R-r)\sec\left(\frac{z}{R}\right) \qquad ---(A5.1)$$

The length of vessel L at which d(L) just reduces to zero is given by

$$0 = (R+r) - (R-r)\sec\left(\frac{L}{R}\right)$$

$$\therefore \quad L = R\cos^{-1}\left(\frac{R-r}{R+r}\right) \qquad ---(A5.2)$$

The average viewed area over a length ℓ of the vessel is given by

$$A(\ell) = \frac{1}{\ell}\int_0^{\ell} \frac{\pi\{d(z)\}^2}{4}\, dz$$

Substituting for d(z) from eqn.(A5.1) gives

$$A(\ell) = \frac{\pi}{4\ell}\int_0^{\ell}\left[(R+r)^2 + (R-r)^2\sec^2\left(\frac{z}{R}\right) - 2(R+r)(R-r)\sec\left(\frac{z}{R}\right)\right] dz$$

which on integration leads to

$$A(\ell) = \frac{\pi}{4\ell}\left[(R+r)^2\ell + R(R-r)^2\tan\left(\frac{\ell}{R}\right) - 2R(R+r)(R-r)\ln\left\{\sec\left(\frac{\ell}{R}\right)+\tan\left(\frac{\ell}{R}\right)\right\}\right] \qquad ---(A5.3)$$

Now from eqn.(A5.2) :

$$\sec\left(\frac{L}{R}\right) = \frac{R+r}{R-r} \qquad ---(A5.4)$$

and

$$\tan\left(\frac{L}{R}\right) = \frac{2\sqrt{Rr}}{R-r} \qquad ---(A5.5)$$

Putting $\ell = L$ in eqn.(A5.3) and substituting for $\sec\left(\frac{L}{R}\right)$ and $\tan\left(\frac{L}{R}\right)$, the average viewed area over the length L of the vessel is

$$A(L) = \frac{\pi}{4L}\left[L(R+r)^2 + 2R(R-r)\sqrt{Rr} - 2R(R+r)(R-r)\ln\left\{\frac{R+r+2\sqrt{Rr}}{R-r}\right\}\right] \qquad ---(A5.6)$$

This area is assumed to be the effective value required for the application of Bernoulli's theorem. The corresponding effective diameter will be given by

$$D = 2\sqrt{\frac{A(L)}{\pi}} \qquad ---(A5.7)$$

In section 2.2.4, the orifice diameter for the aortic and pulmonary valves is taken as 1.9 cm so the orifice radius is r = 0.95 cm. Assuming a radius of curvature of, say, 25 cm and substituting these values in eqn.(A5.6), the effective cross-sectional area is calculated to be 1.539 cm^2 corresponding to an effective diameter of 1.4 cm. The effective vessel length calculated from eqn.(A5.2) is 9.626 cm which is an acceptable value.

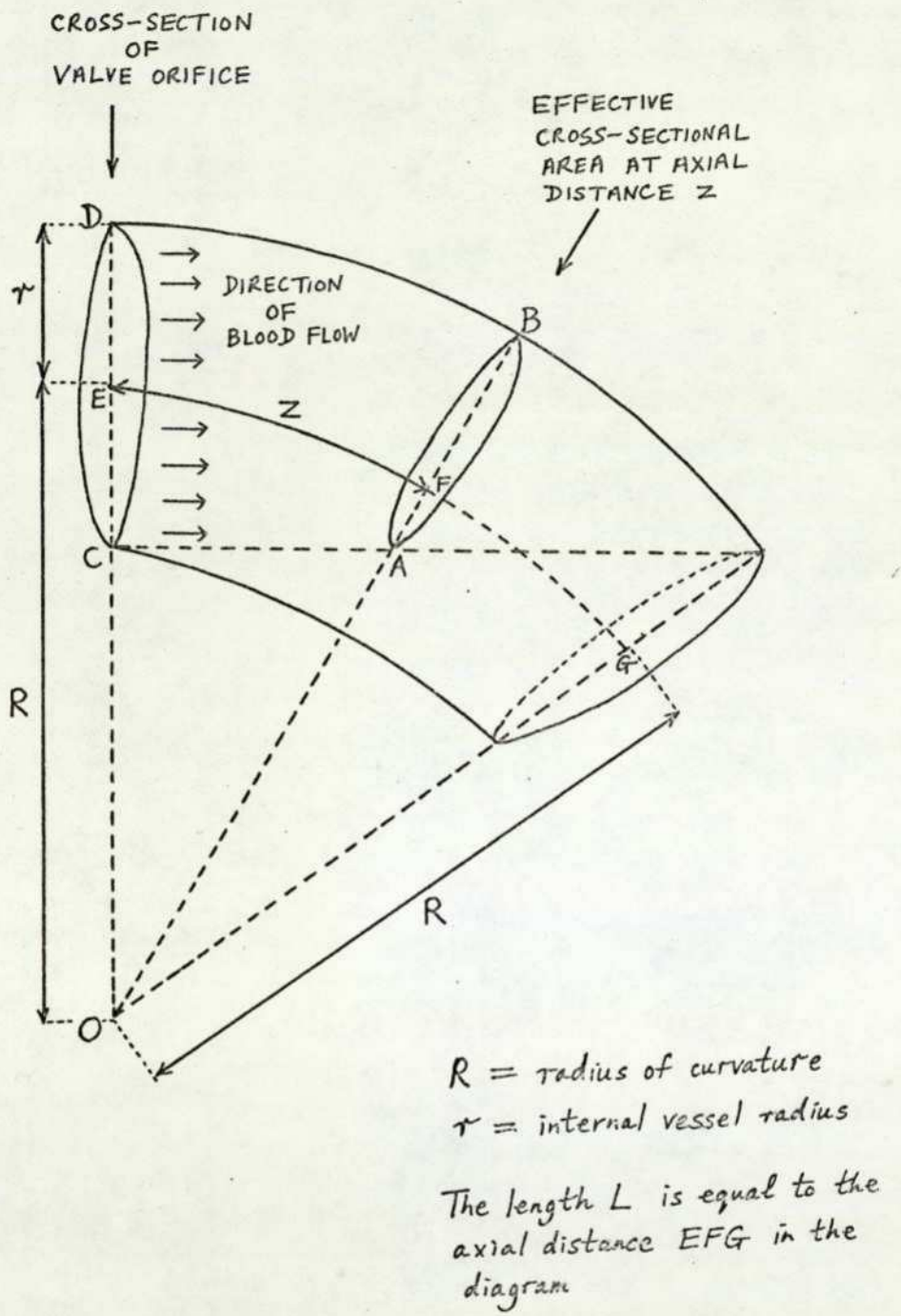

FIG. A5.1 DIAGRAM SHOWING A SECTION OF BLOOD VESSEL (HIGHLY EXAGGERATED) FOR THE CALCULATION OF EFFECTIVE CROSS-SECTIONAL AREAS OF THE SEGMENTS REPRESENTING THE ASCENDING AORTA AND PULMONARY ARTERIES (TO BE USED IN THE APPLICATION OF BERNOULLI'S THEOREM)

APPENDIX 6

CALCULATION OF THE INPUT IMPEDANCE OF THE SYSTEMIC CIRCULATION MODEL

The equations of the systemic circulation model are used to prepare a linear electrical analog shown in fig. 2.5 using the analogies mentioned in section 2.3. This electrical analog is used in one of the preliminary validation tests described in chapter 6 to check that the systemic circulation model has a realistic input impedance.

As frequency response is being considered, the steady or very low frequency intrathoracic and intra-abdominal pressures are ignored. The systemic venous circulation contributes very little to the overall input impedance at the ascending aorta and so each nonlinear venous segment is replaced by a linear approximation with a constant uncollapsed compliance and a linear pressure-flow relation. The arteriovenous resistances in the systemic vascular beds are set to their normal values.

The input impedance of the electrical analog is obtained by successive reduction to a single complex impedance value using combinations of impedances in series, impedances in parallel, star-delta and delta-star transformations.

A FORTRAN IV subroutine for computing the input impedance is given in section A6.1 . The subroutine employs COMPLEX variables and, as presented, is designed to investigate the variation of input impedance with K_8 (the arterial viscoelastic time constant). The subroutine may be changed easily if the effect of varying another parameter is required.

The subroutine arguments in order are as follows :

Inputs : FREQ - frequency (Hz)
AK8 - arterial viscoelastic time constant (sec)

Outputs : ZM - magnitude of input impedance (mmHg sec ml^{-1})
ZP - phase angle of input impedance (degrees)
ZR - real part of input impedance (mmHg sec ml^{-1})
ZI - imaginary part of input impedance (mmHg sec ml^{-1})

In the subroutine listing, the letter O is distinguished from the number 0 by placing a line through the letter thus : $\emptyset$.

A6.1 The subroutine listing

```
      SUBRØUTINE IMP(FREQ,AK8,ZM,ZP,ZR,ZI)
C
C   CØMPUTES INPUT IMPEDANCE ØF SYSTEMIC CIRCULATIØN MØDEL
C
      REAL LAØ2,LUA,LAØ3,LIA,LAA,LCA
      CØMPLEX ZY,ZZ,ZAA,ZAB,ZAC,ZAD,ZAE,ZAF,ZAG,ZAH,ZAI,ZAJ,ZAK,ZAL
      CØMPLEX ZAM,ZAN,ZAØ,ZAP,ZAQ,ZAR,ZAS,ZBA,ZBB,ZBC,ZBD,ZBE,ZBF
      CØMPLEX ZBG,ZBH,ZBI,ZBJ,ZBK,ZBL,ZBM,ZBN,ZBØ,ZBP,ZBQ,ZBR,ZBS
      CØMPLEX ZBT,ZBU,ZBV,ZBW,ZBX,ZBY,ZBZ,ZCA,ZCB,ZCC,ZCD,ZCE,ZCF
      CØMPLEX ZCG,ZCH,ZCI,ZCJ,ZCK,ZCL,ZCM,ZCN,ZCØ,ZIN
      DATA PI,CAØ1,LAØ2,RCØR,CAØ2,LUA,RAØ2,RAØ3,LAØ3,
     1CUA,RHEAD,CUV,RUV,CAØ3,RBRØNC,RIA,LIA,RAA,LAA,
     2CIA,RINT,CIV,RIV,CAA,RABD,RCA,LCA,CAV,RAV,
     3CCA,RLEG,CCV,RCV,CIVC,RIVC,CSVC,RSVC,RUA
     A/3.14159,0.28,0.00043,12.0,0.29,0.014,0.00003,0.0009,0.0038,
     B0.33,6.0,9.4,0.226,0.29,12.0,0.0014,0.0027,0.012,0.014,
     C0.06,2.3,10.6,0.166,0.21,57.0,0.18,0.031,5.1,0.595,
     D0.12,15.0,4.8,0.3,8.3,0.015,8.3,0.06,0.047/
      W=2.0*PI*FREQ
      WA=-1.0/W
      ZY=CMPLX(0.0,WA)
      ZZ=CMPLX(AK8,WA)
      ZAA=ZZ/CAØ1
      ZAB=CMPLX(RAØ2,W*LAØ2)
      ZAC=ZZ/CAØ2
      ZAD=CMPLX(RAØ3,W*LAØ3)
      ZAE=ZZ/CAØ3
      ZAF=CMPLX(RIA,W*LIA)
      ZAG=ZZ/CIA
      ZAH=ZY/CIV
      ZAI=ZY/CIVC
      ZAJ=CMPLX(RAA,W*LAA)
      ZAK=ZZ/CAA
      ZAL=CMPLX(RCA,W*LCA)
      ZAM=ZZ/CCA
      ZAN=ZY/CCV
      ZAØ=ZY/CAV
      ZAP=CMPLX(RUA,W*LUA)
      ZAQ=ZZ/CUA
      ZAR=ZY/CUV
      ZAS=ZY/CSVC
      ZBA=RUV+ZAS*RSVC/(ZAS+RSVC)
      ZBB=RHEAD+ZAR*ZBA/(ZAR+ZBA)
      ZBC=ZAP+ZAQ*ZBB/(ZAQ+ZBB)
      ZBD=ZAL*ZAM+(ZAL+ZAM)*RLEG
      ZBE=ZBD/ZAL
      ZBF=ZBD/RLEG
      ZBG=ZBD/ZAM
      ZBH=ZBG+RCV+RABD
      ZBI=RABD*ZBG/ZBH
      ZBJ=RCV*ZBG/ZBH
      ZBK=RABD*RCV/ZBH
      ZBL=ZBJ+ZBE*ZAN/(ZBE+ZAN)
      ZBM=ZBK*(ZAØ+RAV)+RAV*ZAØ
      ZBN=ZBM/ZAØ
```

```
ZBØ=ZBM/RAV
ZBP=ZBM/ZBK
ZBQ=ZBL*ZBØ/(ZBL+ZBØ)
ZBR=ZAK*ZBF/(ZAK+ZBF)
ZBS=ZAJ*(ZBI+ZBR)+ZBI*ZBR
ZBT=ZBS/ZBR
ZBU=ZBS/ZBI
ZBV=ZBS/ZAJ
ZBW=ZBV*ZBQ/(ZBV+ZBQ)
ZBX=ZBT*(ZBN+ZBW)+ZBN*ZBW
ZBY=ZBX/ZBW
ZBZ=ZBX/ZBN
ZCA=ZBX/ZBT
ZCB=ZCA*ZBP/(ZCA+ZBP)
ZCC=RIV*ZAH+(RIV+ZAH)*RINT
ZCD=ZCC/ZAH
ZCE=ZCC/RIV
ZCF=ZCC/RINT
ZCG=ZAG*ZCE/(ZAG+ZCE)
ZCH=ZAF*(ZCD+ZCG)+ZCD*ZCG
ZCI=ZCH/ZCG
ZCJ=ZCH/ZCD
ZCK=ZCH/ZAF
ZCL=ZCI*ZBY/(ZCI+ZBY)
ZCM=1.0/(1.0/ZAI+1.0/RIVC+1.0/ZCB+1.0/ZCF+1.0/ZCK)+ZCL
ZCN=1.0/(1.0/ZBZ+1.0/ZAE+1.0/ZBU+1.0/ZCJ+1.0/ZCM+1.0/RBRØNC)+ZAD
ZCØ=1.0/(1.0/ZAC+1.0/ZBC+1.0/ZCN)+ZAB
ZIN=1.0/(1.0/RCØR+1.0/ZAA+1.0/ZCØ)
ZR=REAL(ZIN)
ZI=AIMAG(ZIN)
ZM=SQRT(ZR*ZR+ZI*ZI)
ZP=ATAN(ZI/ZR)*180.0/PI
RETURN
END
```

APPENDIX 7

A SUBROUTINE FOR THE CUBIC SMOOTHING OF STEP CHANGES

Step changes occur in certain variables in the present model e.g.

(a) the sudden change of venous compliance when a venous segment collapses.

(b) bang-bang action in the peripheral resistance, myocardial contractility and venous tone controllers.

Truly instantaneous changes of level are highly unlikely to occur in the cardiovascular system or in real biological systems in general. Therefore, in future work, it is desirable to introduce a more realistic smoothing of step changes. One method for achieving this smoothing is to approximate the step function in the vicinity of the discontinuity by a cubic curve as shown in fig. A7.1 .

Two points (x_1, y_1) and (x_2, y_2) are selected on each side of the discontinuity and a cubic is constructed to pass through the two points and to have zero slope at the two points. These constraints are sufficient to determine the cubic uniquely. The composite curve consists of the cubic between the two points and the original step function elsewhere and is continuous and has a finite slope everywhere. As the two points come closer to the discontinuity, the cubic becomes a better approximation to the original step function.

Suppose the cubic function is given by

$$y = ax^3 + bx^2 + cx + d \qquad ---(A7.1)$$

where a,b,c and d are constants to be determined. The cubic passes through the points (x_1, y_1) and (x_2, y_2) so that

$$y_1 = ax_1^3 + bx_1^2 + cx_1 + d \qquad ---(A7.2)$$

$$y_2 = ax_2^3 + bx_2^2 + cx_2 + d \qquad ---(A7.3)$$

The slope of the cubic is given by

$$\frac{dy}{dx} = 3ax^2 + 2bx + c \qquad ---(A7.4)$$

The slope is required to be zero at the points (x_1, y_1) and (x_2, y_2)

so that

$$3ax_1^2 + 2bx_1 + c = 0 \qquad \text{---(A7.5)}$$

$$3ax_2^2 + 2bx_2 + c = 0 \qquad \text{---(A7.6)}$$

Equations (A7.2),(A7.3),(A7.5) and (A7.6) enable a,b,c and d to be determined. It may be shown that

$$a = \frac{2(y_2 - y_1)}{(x_1 - x_2)^3} \qquad \text{---(A7.7)}$$

$$b = -\frac{3}{2}(x_1 + x_2)a \qquad \text{---(A7.8)}$$

$$c = 3x_1 x_2 a \qquad \text{---(A7.9)}$$

$$d = y_1 - ax_1^3 - bx_1^2 - cx_1 \qquad \text{---(A7.10)}$$

A FORTRAN IV subroutine for evaluating the cubic smoothing function is given in section A7.1 . The arguments of the subroutine are as follows :

Inputs : X1 - abscissa of the point to the left of the discontinuity at which the cubic is to start

Y1 - ordinate of the point to the left of the discontinuity at which the cubic is to start

X2 - abscissa of the point to the right of the discontinuity at which the cubic is to finish

Y2 - ordinate of the point to the right of the discontinuity at which the cubic is to finish

X - current value of the independent variable for which the smoothed function value is required

Output : Y - the smoothed function value

A7.1 The subroutine listing

```
      SUBRØUTINE SMØØTH(X1,Y1,X2,Y2,X,Y)
C
C   CUBIC SMØØTHING ØF STEP CHANGES
C
      IF(X.LE.X1)GØ TØ 1
      IF(X.GE.X2)GØ TØ 2
      A=2.0*(Y2-Y1)/(X1-X2)**3
      B=-1.5*(X1+X2)*A
      C=3.0*X1*X2*A
      D=Y1-((A*X1+B)*X1+C)*X1
      Y=((A*X+B)*X+C)*X+D
      RETURN
1     Y=Y1
      RETURN
2     Y=Y2
      RETURN
      END
```

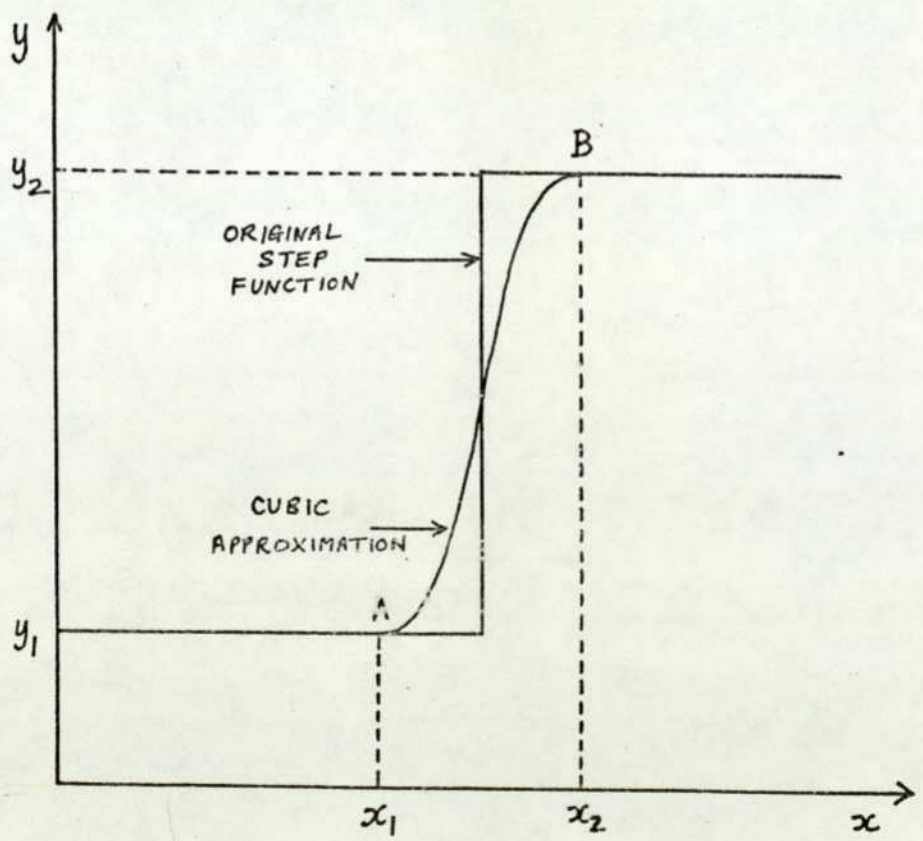

FIG. A7.1 SMOOTHING OF A STEP CHANGE USING A CUBIC FUNCTION IN THE VICINITY OF THE DISCONTINUITY.

APPENDIX 8

THE ESTIMATION OF TOTAL SYSTEMIC RESISTANCE FROM MEAN ARTERIAL PRESSURE AND CARDIAC OUTPUT

It was suggested in section 2.9 that, during transient dynamics, there may be a considerable difference between the true total systemic resistance (TTSR) and the estimated total systemic resistance (ETSR) obtained using eqn.(2.76) :

$$(ETSR) = \frac{(MAP)}{(CO)} \qquad ---(A8.1)$$

where (MAP) and (CO) are obtained on a beat-by-beat basis as follows :

$$(MAP) = \frac{1}{T_H}\int_{t_1}^{t_1+T_H} P_{AOI}\, dt \qquad ---(A8.2)$$

$$(CO) = \frac{1}{T_H}\int_{t_1}^{t_1+T_H} F_{LVAOI}\, dt \qquad ---(A8.3)$$

This assertion may be proved using a simple reduced model of the systemic circulation. In section A8.1, the reduced model and its characteristics are presented. The reliability of the estimate (ETSR) when the reduced model is in a pulsatile steady state and when the same model is exhibiting transient dynamics is assessed in sections A8.2 and A8.3 respectively.

A8.1 A simple reduced model of the systemic circulation

A gross approximation to the systemic circulation is a single lumped parameter segment described in mathematical terms by a second order differential equation. The electrical analog of this highly reduced model is shown in fig. A8.1 . The modulus and phase angle of the input impedance of the reduced model are given in fig. A8.2 and it is seen that, despite the simplicity of the model, the frequency response corresponds closely with the frequency response of the real systemic circulation e.g. as given by Mills et al.(1970).

At zero frequency, the input resistance of the model is $(R_1 + R_2)$ which represents the true total systemic resistance of this model.

Using the notation of fig. A8.1, the following equations apply to the electrical analog :

$$P_1 - P_2 = R_1 F_1 + L \frac{dF_1}{dt} \qquad ---(A8.4)$$

$$F_1 = C \frac{dP_2}{dt} + \frac{P_2}{R_2} \qquad ---(A8.5)$$

A8.2 The model in a pulsatile steady state

Consider an applied pulsatile pressure with period T_H . If the model is in a pulsatile steady state, the resultant flow F_1 and pressure P_2 will also be periodic with period T_H .

Integrate equations (A8.4) and (A8.5) between limits t_1 and $t_1 + T_H$ as follows :

$$\frac{1}{T_H}\int_{t_1}^{t_1+T_H} P_1\,dt - \frac{1}{T_H}\int_{t_1}^{t_1+T_H} P_2\,dt = R_1 \cdot \frac{1}{T_H}\int_{t_1}^{t_1+T_H} F_1\,dt + L \cdot \frac{1}{T_H}\int_{t_1}^{t_1+T_H} \frac{dF_1}{dt}\,dt \qquad ---(A8.6)$$

$$\frac{1}{T_H}\int_{t_1}^{t_1+T_H} F_1\,dt = C \cdot \frac{1}{T_H}\int_{t_1}^{t_1+T_H} \frac{dP_2}{dt}\,dt + \frac{1}{R_2} \cdot \frac{1}{T_H}\int_{t_1}^{t_1+T_H} P_2\,dt \qquad ---(A8.7)$$

Now, both F_1 and P_2 are periodic so that the integrals of the derivatives in eqns.(A8.6) and (A8.7) have zero value. Let

$$\overline{P_1} = \frac{1}{T_H}\int_{t_1}^{t_1+T_H} P_1\,dt \quad , \quad \overline{P_2} = \frac{1}{T_H}\int_{t_1}^{t_1+T_H} P_2\,dt$$

and

$$\overline{F_1} = \frac{1}{T_H}\int_{t_1}^{t_1+T_H} F_1\,dt$$

Then eqns.(A8.6) and (A8.7) become

$$\overline{P_1} - \overline{P_2} = R_1 \overline{F_1} \qquad ---(A8.8)$$

$$\overline{F_1} = \frac{1}{R_2} \cdot \overline{P_2} \qquad ---(A8.9)$$

Eliminating $\overline{P_2}$ from eqns.(A8.8) and (A8.9) gives

$$\frac{\overline{P_1}}{\overline{F_1}} = R_1 + R_2 \qquad \text{---(A8.10)}$$

Now from eqns.(A8.2) and (A8.3), $\overline{P_1}$ and $\overline{F_1}$ represent the mean arterial pressure and cardiac output respectively for this model. Thus the left hand side of eqn.(A8.10) represents the (ETSR) for the model. The right hand side of eqn.(A8.10) is the (TTSR) for the model so it is concluded that, for the simplified model presented here, the (ETSR) will be correct provided the system is in a pulsatile steady state.

A8.3 The model exhibiting a transient response

Consider a nonperiodic pressure Q such that $Q \to 0$ as $t \to \infty$. Suppose that if this is applied to the circuit independently, the resultant response is a flow G such that $G \to 0$ as $t \to \infty$.

The principle of superposition applies to a linear system so that the nonperiodic pressure Q and flow G can be superimposed on the previous pulsatile steady state pressure P_1 and flow F_1 respectively. The composite pressure P_1' and the resultant flow F_1' are then given by

$$P_1' = Q + P_1 \qquad \text{---(A8.11)}$$

$$F_1' = G + F_1 \qquad \text{---(A8.12)}$$

As $t \to \infty$, $P_1' \to P_1$ and $F_1' \to F_1$. The (ETSR) in these transient conditions will be

$$(ETSR) = \frac{\frac{1}{T_H}\int_{t_1}^{t_1+T_H} P_1'\,dt}{\frac{1}{T_H}\int_{t_1}^{t_1+T_H} F_1'\,dt} = \frac{\frac{1}{T_H}\int_{t_1}^{t_1+T_H} Q\,dt + \overline{P_1}}{\frac{1}{T_H}\int_{t_1}^{t_1+T_H} G\,dt + \overline{F_1}} \qquad \text{---(A8.13)}$$

But from eqn.(A8.10),

$$\frac{\overline{P_1}}{\overline{F_1}} = (TTSR) \qquad \text{---(A8.14)}$$

and the ratio

$$\frac{1}{T_H}\int_{t_1}^{t_1+T_H} Q\,dt \Big/ \frac{1}{T_H}\int_{t_1}^{t_1+T_H} G\,dt$$

can be varied by choosing the nonperiodic function Q suitably so that the estimate (ETSR) may differ considerably from the true value (TTSR). Clearly, (ETSR)$\to$(TTSR) as $t \to \infty$.

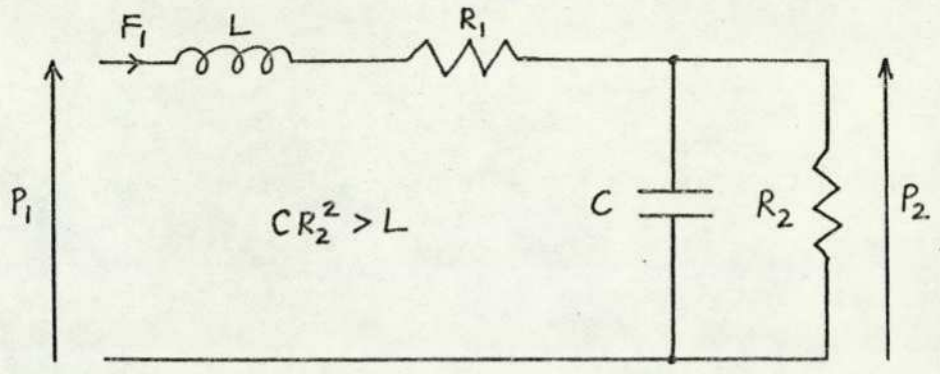

FIG. A8.1 ELECTRICAL ANALOG OF A SIMPLE REDUCED MODEL OF THE SYSTEMIC CIRCULATION

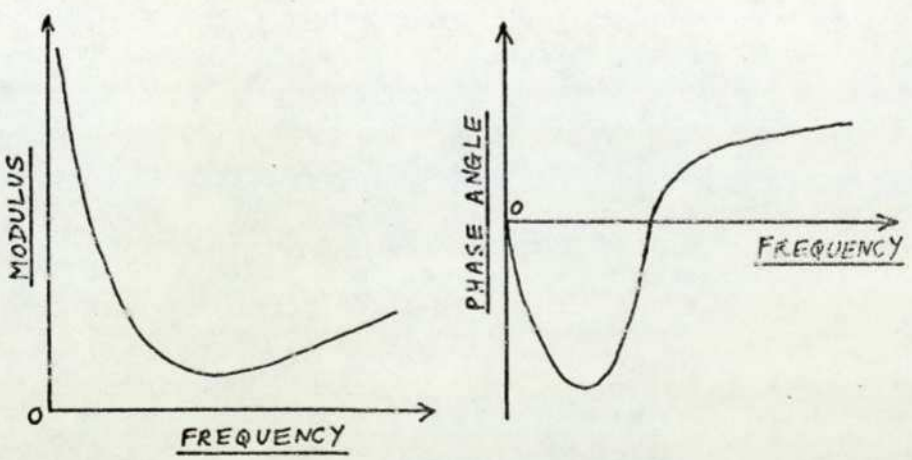

FIG. A8.2 MODULUS AND PHASE ANGLE OF THE INPUT IMPEDANCE OF THE REDUCED SYSTEMIC CIRCULATION MODEL

APPENDIX 9

AN APPROACH TO THE QUANTIFICATION OF MODEL ADEQUACY

A perfect mathematical model of a biological system would require an infinite number of tests to prove that the outputs are correct for all possible values of the inputs. Clearly a practical quantitative measure of model adequacy has to be based on the results from a limited number of comparative tests on the model and the real system.

The usual performance criteria of integral error squared, integral absolute error, etc. used in matching the responses of models and real systems are unsatisfactory in biological applications due to biological variation within a given species and an approach based on features is more appropriate. To pursue this feature approach, the following definitions are introduced (the notation is local to this appendix) :

Let U be the set of all possible tests which can be designed to compare the performance of the model and the real system. A finite subset of tests is selected :

$$T = (T_1, T_2, T_3, \ldots\ldots, T_J) \subset U$$

where J is the number of tests.

Let H be the set of all possible features which can be attributed to responses of the real system. J finite subsets of features are selected

$$G_1 \subset H,\ G_2 \subset H,\ G_3 \subset H,\ \ldots\ldots,\ G_J \subset H$$

which will be used in each of the tests $T_1, T_2, T_3, \ldots, T_J$ respectively. The set $F = (G_1, G_2, \ldots\ldots, G_J)$ contains all the features used in the tests.

Let N_K be the number of features used in the Kth test (i.e. the number of features in the subset G_K). The total number of features in F is

$$N = \sum_{K=1}^{J} N_K$$

Let $M_{K\ell}$ be the ℓth feature of the model response in the Kth test and similarly let $S_{K\ell}$ be the ℓth feature of the corresponding real system response in the Kth test.

Let $d_{k\ell}(M_{k\ell}, S_{k\ell})$ be a measure of distance between $M_{k\ell}$ and $S_{k\ell}$. $d_{k\ell}(M_{k\ell}, S_{k\ell})$ is specified in the usual way for distance functions i.e. for features A, B and C

$$\begin{cases} d_{k\ell}(A,B) \geq 0 \\ d_{k\ell}(A,B) = 0 \quad \text{iff} \quad A = B \end{cases}$$

$$d_{k\ell}(A,B) = d_{k\ell}(B,A)$$

$$d_{k\ell}(A,B) \leq d_{k\ell}(A,C) + d_{k\ell}(C,B)$$

Let $\omega_{k\ell}$ be a positive weighting factor attached to $d_{k\ell}(M_{k\ell}, S_{k\ell})$ with a value corresponding to the importance in the overall adequacy measure of the ℓth feature comparison in the Kth test.

Let D be the set of N distance functions (which may be different) and W be the set of N weighting factors used in the J tests.

If all the distance functions are unbounded then the adequacy may be defined as

$$\alpha_1(T, F, D, W) = \frac{1}{1 + \sum_{K=1}^{J} \sum_{\ell=1}^{N_K} \omega_{k\ell}\, d_{k\ell}(M_{k\ell}, S_{k\ell})}$$

If all the distance functions are bounded i.e.

$$d_{k\ell}(M_{k\ell}, S_{k\ell}) \leq \hat{d}_{k\ell}(M_{k\ell}, S_{k\ell}) < \infty$$

and the upper bounds can be computed, a definition of adequacy is

$$\alpha_2(T, F, D, W) = 1 - \frac{\sum_{K=1}^{J} \sum_{\ell=1}^{N_K} \omega_{k\ell}\, d_{k\ell}(M_{k\ell}, S_{k\ell})}{\sum_{K=1}^{J} \sum_{\ell=1}^{N_K} \omega_{k\ell}\, \hat{d}_{k\ell}(M_{k\ell}, S_{k\ell})}$$

In both cases, the adequacy value is on the closed interval $[0,1]$. A value of 1 indicates complete agreement and a value of 0 indicates complete disagreement between the model and real system responses in the tests conducted. The inadequacy may be defined as

$$\beta = 1 - \alpha$$

Clearly there are an infinite number of different adequacy functions that can be defined in this way depending on the choice of

T, F, D and W and the formulation of the adequacy function.

There could be difficulties in quantifying particular features or constructing a suitable distance function and a discrete "fuzzy" distance function using qualitative statements may have to be used e.g.

$$d = \begin{cases} 0 , & \text{Complete Agreement} \\ k_1 , & \text{Good Agreement} \\ k_2 , & \text{Moderate Agreement} \\ k_3 , & \text{Poor Agreement} \\ k_4 , & \text{Complete Disagreement} \end{cases}$$

where $0 < k_1 < k_2 < k_3 < k_4$

This can introduce a subjective variability into the adequacy measure.

REFERENCES

AUSLANDER D.M.

"Distributed system simulation with bilateral delay-line models" Transactions of A.S.M.E., Journal of Basic Engineering, vol.90, no.2, June 1968, pp. 195-200

AUSLANDER D.M., LOBDELL T.E., CHONG D.

"A large-scale model of the human cardiovascular system and its application to ballistocardiography" Transactions of A.S.M.E., Journal of Dynamic Systems, Measurement & Control, September 1972, pp. 230-236

BENEKEN J.E.W.

"A mathematical approach to cardiovascular function" Institute of Medical Physics TNO, Utrecht, Netherlands, May 1965, Report No. 2-4-5/6

BENEKEN J.E.W., DEWIT B.

"A physical approach to hemodynamic aspects of the human cardiovascular system" in Reeve E.B. & Guyton A.C. (eds.) "Physical Bases of Circulatory Transport : Regulation and Exchange", W.B.Saunders Company, Philadelphia, 1967

BENEKEN J.E.W., RIDEOUT V.C.

"The use of multiple models in cardiovascular system studies : transport and perturbation methods" I.E.E.E. Transactions on Biomedical Engineering, vol. BME-15, no.4, October 1968, pp. 281-289

BENEKEN J.E.W.

in Progress Report no.PR2, Institute of Medical Physics TNO, Utrecht, Netherlands, August 1970, p.16

BENEKEN J.E.W.

"Some computer models in cardiovascular research" in Bergel D.H. (ed.) "Cardiovascular fluid dynamics", vol.1, Academic Press, 1972

BROWER R., REDDY R., NOORDERGRAAF A.

"Difficulties in the further development of venous hemodynamics" I.E.E.E. Transactions on Biomedical Engineering, vol. BME-16, no.4, October 1969, pp. 335-338

CHU Y.

"Digital simulation of continuous systems"
McGraw-Hill, 1969

CROSBIE R.E.

"The credibility of computerised models"
Paper G1, Proceedings of the U.K. Simulation Council Conference on Computer Simulation, Bowness-on-Windermere, May 6th-8th, 1975

DAMPNEY R.A.L., TAYLOR M.G., McLACHLAN E.M.

"Reflex effects of stimulation of carotid sinus and aortic baroreceptors on hindlimb vascular resistance in dogs"
Circulation Research, vol.29, no.2, August 1971, pp. 119-127

DAVIES D.V. (ed.)

"Gray's Anatomy"
Longmans, 1967 (34th edition)

DICK D.E., KENDRICK J.E., MATSON G.L., RIDEOUT V.C.

"Measurement of nonlinearity in the arterial system of the dog by a new method"
Circulation Research, vol.22, 1968, p.101

GEAR C.W.

"Numerical initial value problems in ordinary differential equations" Prentice Hall, 1971

GODFREY K.R., BRIGGS P.A.N.

"Identification of processes with direction-dependent dynamic responses" Proceedings of the I.E.E., vol.119,no.12, December 1972, pp. 1733-1739 (paper 6821C)

GOODMAN L.S., GILMAN A. (eds.)

"The pharmacological basis of therapeutics"
Fourth edition, Macmillan, 1970

GREEN J.H.

"An introduction to human physiology"
Third edition, Oxford University Press, 1972

GREWE L., NEUSTEDTER P., RIDEOUT V., RUKAVINA D.

"Cardiovascular modeling using integrated circuit op-amps"
Simulation, August 1969, pp. 103-106

GUYTON A.C.

"A textbook of medical physiology" Saunders, 1971

GUYTON A.C., COLEMAN T.G., GRANGER H.J.
"Circulation : overall regulation"
Ann. Rev. Physiol., vol.34, 1972, pp. 13-46

HINMAN J.W.
"Prostaglandins"
Bioscience, vol.17, 1967, pp. 779-785

HUGHES R.
"Continuous measurement of peripheral vascular resistance and circulatory function"
Medical & Biological Engineering, vol.9, 1971, pp. 603-610

HYNDMAN B.W.
"A digital simulation of the human cardiovascular system and its use in the study of sinus arrhythmia"
Ph.D. thesis, Imperial College, University of London, January 1970

HYNDMAN B.W., KITNEY R.I., SAYERS B.McA.
"Spontaneous rhythms in physiological control systems"
Nature, vol.233, October 1st 1971, pp. 339-341

KATONA P.G., BARNETT O., JACKSON W.D.
"Computer simulation of the blood pressure control of heart period" in Kezdi P. (ed.) "Baroreceptors & Hypertension" , Pergamon, 1967, pp. 191-199

KORN G.A.
"Recent computer system developments and continuous system simulation"
A.I.C.A. Conference on Hybrid Computation, Prague, August 27th-31st, 1973

KOUSHANPOUR E., SPICKLER J.W.
"Effect of mean pressure levels on the dynamic response characteristics of the carotid sinus baroceptor process in dog"
I.E.E.E. Transactions on Biomedical Engineering, vol. BME-22, no.6, November 1975, pp. 502-507

MAWSON J.B.
"A continuous system simulation language for an advanced hybrid computing system (AHCSSL)"
Paper 14, A.I.C.A. Symposium on Simulation Languages for Dynamic Systems, London, England, September 8th-10th 1975

MILLS C.J., GABE I.T., et al.

"Pressure-flow relationships and vascular impedance in man"
Cardiovascular Research, vol.4, October 1970, pp. 405-417

MOORE R.E.

"Interval Analysis" Prentice Hall, 1966

NEWMAN F.H., SEARLE V.H.L.

"The general properties of matter" E. Arnold, 1952

NOBLE M.I.M., TRENCHARD D., GUZ A.

"Effect of changing heart rate on cardiovascular function in the conscious dog"
Circulation Research, vol.19, July 1966

NOBLE M.I.M., GABE I.T., TRENCHARD D., GUZ A.

"Blood pressure and flow in the ascending aorta of conscious dogs"
Cardiovascular Research, vol.1, no.1, January 1967, pp. 9-20

NOORDERGRAAF A.

"Hemodynamics" in Schwan H.P. (ed.) "Biological Engineering", McGraw-Hill, 1969

PIKE J.E.

"Prostaglandins"
Scientific American, vol.225, no.5, November 1971, pp. 84-93

PULLEN H.E.

"Cardiovascular modelling and simulation"
M.Sc. dissertation, The City University, London, September 1970

PULLEN H.E.

"A digital simulation of human haemodynamics and its use in the study of the cardiovascular effects of drugs"
Paper C3, Proceedings of the U.K. Simulation Council conference on Computer Simulation, Bowness-on-Windermere, May 6th-8th 1975

ROSEN R. (ed.)

"Foundations of mathematical biology" , vol.3 "Supercellular systems" , Academic Press, 1973

RUSHMER R.F.

"Cardiovascular dynamics" , 3rd edition, Saunders, 1970

SHANNON C.

"Communication in the presence of noise"
Proceedings of the Institute of Radio Engineers, vol.37, no.1, January 1949, pp. 10-21

SIEGEL J.H., SONNENBLICK E.H.

"Isometric time-tension relationships as an index of myocardial contractility"

Circulation Research, vol.12, 1963, p. 597

SLOTNICK D.L.

"The fastest computer"

Scientific American, February 1971, p.76

SMITH G.D.

"Numerical solution of partial differential equations"

Oxford University Press, 1969

SNYDER M.F., RIDEOUT V.C.

"Computer simulation studies of the venous circulation"

I.E.E.E. Transactions on Biomedical Engineering, vol. BME-16, no.4, October 1969, pp. 325-334

TALBOT S., GESSNER U.

"Systems Physiology" John Wiley , 1973

WESTERHOF N., NOORDERGRAAF A.

"Arterial viscoelasticity : a generalised model"

Journal of Biomechanics, vol.3, 1970, pp. 357-379